Chemistry for gene silencing:

4'-modified and 2'-fluorinated nucleosides and oligonucleotides

Jonathan K. Watts

Department of Chemistry, McGill University

Montreal, QC, Canada

April, 2008

A thesis submitted to McGill University in partial fulfillment of the requirements of the degree of Doctor of Philosophy

Dedicated to the memory of Kenneth Elliot Mitchell
December 29, 1919 – February 13, 2008

Grandpa, you inspired us all with your warmth, wisdom, creativity and integrity.

Copyright statement

Abstract

A series of studies on 2'-fluorinated and 4'-chalcogen-modified nucleic acids is described, mainly directed toward the development of better gene silencing therapeutics.

NMR/MD and osmotic stressing were used to compare the structure and hydration of 10-bp 2'F-ANA•RNA, ANA•RNA and DNA•RNA duplexes. The 2'F-ANA and ANA strands both featured sugars that pucker in the east (O4'-*endo*) conformation, as previously observed for hairpin structures containing hybrid stems. Osmotic stressing suggested that the 2'F-ANA•RNA duplex liberated fewer molecules of water upon melting than did ANA•RNA, which may give the former an entropic advantage that contributes to its far greater thermal stability.

The stability of 2'F-ANA to acid-mediated hydrolysis was compared to that of DNA and RNA. Several phosphodiester (PO) or phosphorothioate (PS) 2'F-ANA sequences were incubated at pH ~1.2, and virtually no cleavage was observed after 2 days. In contrast, rapid degradation was observed for DNA ($t_{1/2}$ = minutes) and RNA ($t_{1/2}$ = hours (PO) or days (PS)). The nuclease-catalyzed hydrolysis of 2'F-ANA was also explored in detail. One diastereomer of the PS-2'F-ANA linkage was much more vulnerable to enzymatic cleavage than the other, which is parallel to the properties observed for PS-DNA. We also show that the nuclease stability induced by 2'F-ANA depends on the oligonucleotide sequence.

An improved synthesis of 2'-deoxy-2'-fluoro-5-methyl-4'-thioarabinouridine (4'S-FMAU) is described. Participation of the 3'-*O*-benzoyl protecting group in the thiosugar precursor influenced the stereochemistry of the *N*-glycosylation reaction in nonpolar solvents, permitting a higher β:α ratio than previously observed for similar Lewis acid-catalyzed glycosylations. The nucleoside adopted a predominantly northern conformation, in contrast to 2'-deoxy-2'-fluoro-5-methylarabinouridine (FMAU), which adopts a predominantly southeast conformation.

The synthesis of oligonucleotides containing 2'-deoxy-2'-fluoro-4'-thioarabinonucleotides is then described. 18-mer antisense oligonucleotides

(AON) containing 4'S-FMAU, unlike those containing FMAU, were unable to elicit *E. coli* or human RNase H activity, thus corroborating the hypothesis that RNase H prefers duplexes containing oligonucleotides that can adopt eastern (O4'-*endo*) conformations in the antisense strand. The duplex structure and stability of these oligonucleotides was also investigated *via* circular dichroism (CD) and UV binding studies. Replacement of the 4'-oxygen by a sulfur atom resulted in a marked decrease in melting temperature of AON•RNA as well as AON•DNA duplexes. 2'-Deoxy-2'-fluoro-4'-thioarabinouridine (4'S-FAU) was incorporated into siRNA and the resulting siRNA duplexes were able to trigger RNA interference with good efficiency. Positional effects were explored, and synergy with 2'F-ANA was demonstrated. This synergy inspired us to combine other northern nucleosides with 2'F-ANA, and we discovered that combination of 2'F-RNA and 2'F-ANA leads to fully modified siRNA duplexes that are more potent than the control siRNAs. This is one of only a few chemistries allowing fully modified siRNAs with increased potency. Several related patterns of chemical modification were used to modify two siRNA sequences targeting firefly luciferase.

The first synthesis of oligonucleotides containing 4'-selenium-modified ribonucleotides (4'-Se-rN) is described. Four sequences containing the 4'-selenoribonucleotide were successfully synthesized, and compared with DNA and RNA oligonucleotides containing a dT, rT or LNA insert in place of the 4'-Se-rT. The 4'-Se-rT behaved more like rT than dT in its effects on binding affinity, despite the DNA-like structure previously observed for the nucleoside. Incorporation of 4'-Se-rT into A-RNA and hybrid duplexes led to increased binding affinity, while incorporation into B-DNA destabilized the duplex to the same extent as an rT nucleotide.

Abrégé

On a fait une série d'études sur des acides nucléiques contenant un 2'-fluor et/ou un 4'-chalcogène. Ces études visent l'amélioration de thérapeutiques basées sur le silençage des gènes.

On a utilisé la RMN/DM et le stressage osmotique pour comparer la structure et l'hydratation des duplex 2'F-AAN•ARN, AAN•ARN et ADN•ARN. Les sucres des brins de 2'F-AAN et d'AAN adoptent la forme O4'-*endo* (est), comme observé dans le passé pour des structures en épingle à cheveux contenant une tige en hybride. Le stressage osmotique a suggéré que la fusion du duplex 2'F-AAN•ARN a libéré moins de molécules d'eau que celle du duplex AAN•ARN, ce qui pourrait donner à ce premier un avantage entropique qui contribue à sa stabilité beaucoup plus élevée.

On a comparé la stabilité du 2'F-AAN envers l'hydrolyse par acide à celle de l'ADN et de l'ARN. Plusieurs oligonucléotides en PO ou PS ont été incubés à pH ~1.2, et il n'y avait pas de clivage pour le 2'F-AAN après deux jours. Par contre, on a observé une dégradation rapide pour l'ADN ($t_{1/2}$ = minutes) et l'ARN ($t_{1/2}$ = heures (PO) ou jours (PS)). On a exploré aussi l'hydrolyse du 2'F-AAN par nucléase en détail. Un diastéréoisomère de la liaison PS-2'F-AAN a été beaucoup plus vulnérable au clivage par l'enzyme que l'autre, ce qui est parallèle aux propriétés du PS-ADN. Nous démontrons aussi que la stabilité introduite par le 2'F-AAN dépend de la séquence de l'oligonucléotide.

On décrit une synthèse améliorée du 2'-désoxy-2'-fluoro-5-méthyle-4'-thioarabinouridine (4'S-FMAU). Une participation par le groupe 3'-*O*-benzoyl influence la stéréochimie de la *N*-glycosylation dans des solvants non-polaires. Ceci a permis un plus haut rapport des produits β:α que celui qui a été observé dans le passé pour des glycosylations semblables catalysés par acide Lewis. Le nucléoside adopte une forme nord, tandis que le 2'-désoxy-2'-fluoro-5-méthyle-arabinouridine (4'S-FMAU) adopte principalement une forme sud-est.

On a fait ensuite la synthèse d'oligonucléotides contenant des 2'-désoxy-2'-fluoro-4'-thioarabinonucleotides. Des oligonucléotides antisens (ONA) de 18 nt

qui contiennent le 4'S-FMAU, contrairement à ceux qui contiennent le FMAU, n'ont pas pu éliciter le clivage par la RNase H. Ceci est consistant avec l'hypothèse que la RNase H préfère les duplex où les nucléotides du brin antisens peuvent adopter la forme est (O4'-*endo*). La structure et la stabilité de ces oligonucléotides ont été étudiées par le dichroïsme circulaire (DC) et les études de fusion par UV. Remplacement du 4'-O par un S a causé une baisse importante dans la température de fusion des duplex ONA•ARN et ONA•ADN. Le 2'-désoxy-2'-fluoro-4'-thioarabinouridine (4'S-FAU) a été incorporé dans les ARNsi et les duplex modifiés ont pu déclencher l'ARNi de façon efficace. On a démontré de la synergie avec le 2'F-AAN.

Cette synergie nous a inspiré de combiner d'autres modifications qui adoptent la forme nord avec le 2'F-AAN, et nous avons découvert que la combinaison du 2'F-ARN et du 2'F-AAN donne des ARNsi entièrement modifiés qui sont plus efficaces que les ARNsi non-modifiés. Il s'agit d'une des seules façons de modifier entièrement une ARNsi qui donne une augmentation d'efficacité. On a utilisé plusieurs motifs de modification sur deux séquences ARNsi ayant pour cible la luciferase *Photinus*.

On a effectué la première synthèse des oligonucleotides qui contiennent des 4'-sélénoribonucléotides (4'-Se-rN). Quatre séquences qui contiennent un 4'-Se-rN ont été synthétisées. On les a comparées avec des oligonucléotides en ADN et en ARN qui contiennent un dT, un rT ou un ALN-T au lieu du 4'-Se-rT. Le 4'-Se-rT s'est comporté plus comme rT que dT dans son effet sur l'affinité de fixation, malgré la forme observé pour la nucléoside qui était semblable à l'ADN. L'incorporation du 4'-Se-rT dans des duplex de l'ARN (conformation A) ou hybride a causé une augmentation de l'affinité de fixation, tandis que l'incorporation dans un duplex de l'ADN (conformation B) a déstabilisé le duplex au même niveau qu'un ribonucléotide.

Acknowledgements

I am very grateful to Prof. Damha, my research supervisor, for inviting me to join his group and providing such a stimulating learning environment. He expresses a great deal of confidence in his students—allowing us a great deal of freedom to think, explore and grow—and it's been a real encouragement throughout my studies. He has given me many opportunities for development, in research, teaching and publishing.

During my time in the Damha group, I learned a huge amount from the students, postdocs and visiting professor that I worked with: Kazim, Maria, Sandra, Rami, Mohamed, Katya, Anne, Anna Lisa, Bénédicte, Robert, Chang Geng, David, Alex, Siara, Jeremy, Matt, Julia, Maxie, Pascal, Jean-Christophe, Dilip, Nuria, Adam and Glen. It has been a true pleasure to work with all of them.

From that list, however, several people have made especially big contributions to my research and my experience in the group. Robert Donga is a good friend whose admirable patience with the HPLC led to the eventual success of several of my purifications and possibly saved the instrument from destruction at my hands in the meantime. Siara Isaac and he have also made sure that I learned about a lot more than chemistry during this degree… I thank them both for conversations that will stay with me for years to come. I thank Chang Geng Peng for being a good friend and brother, and for showing us all the best Chinese restaurants. Matthew Hassler, who could cheer up a funeral, I thank for his unceasing encouragement of my choice of shirt. I'm indebted to Alex Wahba for teaching me some biology and for the RNase H assays and native gels he ran for me (Chapters 5 and 6). He is an amazingly cheerful, helpful and generous colleague and friend. Julia Viladoms, as well as giving me the chance to learn about life in Spain, synthesized the dinucleoside phosphorothioates used in Chapter 3. Finally, while everybody in the Damha group works hard, David Sabatino, Jeremy Lackey, Chang Geng Peng and Alex Wahba have consistently inspired me by going the extra mile to "get 'er done!"

Many other students and faculty in the chemistry department have contributed significantly to my experience here. I would like to particularly thank Prof. David

Harpp for his example of excellent teaching, and for giving me the opportunity to work with him in this area. I also thank Prof. Tony Mittermaier, Prof. Bruce Lennox and Prof. William Galley for their insight into the question of nucleic acid hydration.

I have benefited in a very significant way from the help of Prof. Mario Pinto (Simon Fraser University), who generously invited me to spend a summer in his lab, and has mentored me at a distance through several other collaborative projects. He has taught me a great deal about both conducting and publishing research. Thanks are also due to the members of the Pinto lab, especially Niloufar, Kashi and Blair for making compounds for me, but also to Monica and Wes for their friendship.

Other collaborators have also made a huge contribution to the research in this thesis, especially Francis Robert and Jerry Pelletier of McGill Biochemistry, who carried out the luciferase assays, Stefanie Lang and Ken Douglas of the University of Manchester, who are working on the 2'F-ANA exciplex system (Chapter 3), and Nerea Martin-Pintado and Carlos Gonzalez (CSIC, Madrid), who are working on the NMR/MD study (Chapter 2). There are also several ongoing collaborations related to siRNA and delivery which have not been included in this thesis, and I thank Ania Kalota and Alan Gewirtz (University of Pennsylvania), Mahmoud Elsahaby, Nada Wazen and Jean-Christophe Leroux (Université de Montréal), Jose Manuel Garcia Fernandez (Instituto de Investigaciones Químicas, CSIC, Universidad de Sevilla) and Jacques Defaye (Université Joseph-Fournier-Grenoble 1). It has been a pleasure to work with them all.

I'm very grateful to Prof. Cornelis Altona (Leiden University) for his help with the PSEUROT program. It was a real privilege to work with such a pioneer of the field of nucleoside conformational analysis, who remains nonetheless eminently approachable. I also appreciate the valuable advice of Prof. Eriks Rozners (Northeastern University) in the field of osmotic stressing. Thanks are due to Professors Charles Spink (SUNY – Cortland) and Jonathan Chaires (University of Mississippi Medical Center) for providing the osmolality data used in Chapter 2.

Many people have made significant contributions to this thesis through their skillful editing of manuscripts written throughout my degree. Besides my supervisor, coauthors and research group, these include Dr. Maria Mangos, Dr. John DiMaio, Dr. Serge Shehanian, Dr. Nicolay Ferrari, Prof. David Corey, Prof. Jean-Christophe Leroux, and Dr. Muthiah Manoharan.

I'm very grateful to Chantal Marotte and Colleen McNamee for their help with administrative challenges. Thanks are due to Paul Xia for his help with NMR spectroscopy and Nadim Saade for his help with MS. I would also like to specially thank Fred Kluck and Rick Rossi for literally keeping our instruments running, as well as Mr. Rebello for being the most helpful janitor I've ever met.

I'd like to thank my parents, Chris and Marny Watts, and my sisters Carolyn and Stephanie. Their influence has shaped me in more ways than I will ever know, and I am incredibly grateful for their ongoing support, encouragement and prayers.

Albert Einsten said, "There are two ways to live your life. One is as though nothing is a miracle. The other is as though everything is a miracle." I'd like to thank Liam, my precious son, for reminding us to choose the second option.

My deepest thanks are saved for my beloved Katie, my soulmate and best friend. She has somehow managed to get through childbirth *and* be a tremendous support to me during the writing of this thesis. "Many women have done wonderful things, but you surpass them all." (Proverbs 31:29).

Table of Contents

List of Figures

List of Schemes

List of Tables

Abbreviations

A	adenosine
Å	Angstrom
A_{260}	UV absorbance at 260 nm
Ac_2O	acetic anhydride
Ade	adenine
AGO2	Argonaute2, the endonuclease at the heart of human RISC
ANA	arabinonucleic acid
AON	antisense oligonucleotide
ATP	adenosine triphosphate
B	base
bc	bicyclo
Bn	benzyl
bp	base pair
Bz	benzoyl
C	cytidine
CD	circular dichroism
cDNA	complementary DNA
CE	2-cyanoethyl
CeNA	cyclohexene nucleic acid
CNE	A buffer containing sodium cacodylate, sodium chloride and EDTA. In our studies, the exact concentrations are 10 mM sodium cacodylate, 300 mM NaCl, and 0.1 mM Na_2EDTA, pH 7.2.
COSY	correlation spectroscopy, homonuclear (NMR)
Cyt	cytosine
d	doublet
DAST	diethylaminosulfur trifluoride
DCI	4,5-dicyanoimidazole
dd	doublet of doublets
DEPC	diethylpyrocarbonate
DIPEA	*N,N*-diisopropylethylamine
DMAP	4-(dimethylamino)pyridine
DMEM	Dulbecco's modified Eagle medium

DMF	*N,N*-dimethylformamide
DMSO	dimethylsulfoxide
DMT	4,4'-dimethoxytrityl
dN	2'-deoxyribonucleoside
DNA	2'-deoxyribonucleic acid
dNTP	2'-deoxyribonucleoside triphosphate
ds	double-stranded
dt	doublet of triplets
dT	2'-deoxythymidine
DTT	dithiothreitol (*threo*-1,4-dimercapto-2,3-butanediol)
EBV	Epstein-Barr virus
EGFP	enhanced green fluorescent protein (*i.e.*, GFP with codon usage optimized for mammalian cells)
ESI-MS	electrospray ionization mass spectrometry
Et	ethyl
EtOAc	ethyl acetate
EtOH	ethanol
ETT	5-ethylthiotetrazole
FACS	fluorescence-assisted cell sorting
2'F-ANA	2'-deoxy-2'-fluoroarabinonucleic acid
2'F-araN	2'-deoxy-2'-fluoroarabinonucleoside
2'F-araNTP	2'-deoxy-2'-fluoroarabinonucleoside triphosphate
FAU	2'-deoxy-2'-fluoroarabinouridine (“2'F-araU” or “2'F-ANA-U”)
FBS	fetal bovine serum
FIAC	2'-deoxy-2'-fluoro-5-iodoarabinocytidine
FIAU	2'-deoxy-2'-fluoro-5-iodoarabinouridine
FMAU	2'-deoxy-2'-fluoro-5-methylarabinouridine (“2'F-araT” or “2'F-ANA-T”)
2'F-RNA	2'-deoxy-2'-fluororibonucleic acid
G	guanosine
Gua	guanine
%H	percent hyperchromicity; $(A_{final} - A_{initial}) / A_{initial}$
HBV	hepatitis B virus

Hex	hexanes
HMQC	heteronuclear multiple quantum correlation spectroscopy (NMR)
HPLC	high performance (or high pressure) liquid chromatography
HSQC	heteronuclear single quantum correlation spectroscopy (NMR)
HSV	herpes simplex virus
J	scalar coupling contstant (in Hz)
LES	locally excited state
LNA	locked nucleic acid, *i.e.* containing 2'-*O*,4'-*C*-methylene-bicyclo nucleotides
MALDI	matrix-assisted laser desorption/ionization (mass spectrometry)
Me	methyl
MeCN	acetonitrile
MeOH	methanol
miRNA	micro RNA
mRNA	messenger RNA
MMT	4-monomethoxytrityl
NMP	*N*-methylpyrrolidinone (*i.e.*, 1-methyl-2-pyrrolidinone)
NMR	nuclear magnetic resonance spectroscopy
NOE	nuclear Overhauser enhancement
NOESY	nuclear Overhauser effect spectroscopy (a 2D NOE experiment)
ODU	optical density units, defined as the hypothetical A_{260} of a solution of the sample of interest in 1 mL water, in a 1-cm path cuvette.
PAGE	polyacrylamide gel electrophoresis
PCR	polymerase chain reaction
PET	positron emission tomography
PO	phosphodiester (linkage)
PS	phosphorothioate (linkage)
Pu	purine
Py	pyrimidine
RISC	RNA-induced silencing complex, the effector complex of RNA interference
rN	ribonucleoside
RNA	ribonucleic acid
RNAi	RNA interference

rNTP	ribonucleoside triphosphate
r.t.	room temperature
R_f	retention factor (in TLC, the ratio of the distance traveled by the center of a spot to the distance from the baseline to the solvent front)
s	singlet
SELEX	systematic evolution of ligands by exponential enrichment
SGF	simulated gastric fluid; in this thesis a pepsin-free SGF is used containing 0.20 g NaCl and 0.70 mL HCl in 100 mL sterile water (pH ~1.2).
shRNA	short hairpin RNA
siRNA	small interfering RNA
SNP	single-nucleotide polymorphism
ss	single-stranded
SVPDE	snake venom phosphodiesterase, a 3'-exonuclease
t	triplet
T	thymidine
TBAF	tetrabutylammonium fluoride
TBE	a buffer containing tris, boric acid and EDTA, very commonly used for gel electrophoresis.
TCA	trichloroacetic acid
TEA	triethylamine
TEAA	triethylammonium acetate
TFE	2,2,2-trifluoroethanol
THF	tetrahydrofuran
Thy	thymine
TLC	thin-layer chromatography
T_m	melting temperature, the temperature at which (for a simple two-state transtition) both the mole fraction of nucleic acid in the duplex form and the mole fraction of denatured nucleic acid are 0.5.
TRBP	HIV1 TAR RNA-binding protein, a component of RISC
U	uridine
Ura	uracil
UV	ultraviolet (spectroscopy)

Chapter 1. Introduction

1.1 Nucleic acids and their fundamental role

1.1.1 The genome

Hidden in the nucleus of every human cell is a miracle of design: fine-tuned over millions of years of evolution, six billion base pairs of DNA make up the blueprints for everything else. Every structural protein, every enzyme, every piece of RNA, all are determined by the sequence of bases A, G, C and T, making the genome a story of mind-boggling complexity written with a four letter alphabet. Smaller molecules are, in turn, dependent on the structure of the enzymes that synthesize them. Not only protein structure and function, but also levels of protein expression, are precisely regulated.

For years RNA was considered a passive participant, a rather uninteresting junior partner in the business of gene expression.[1] RNA relayed messages (mRNA), fetched building blocks (tRNA) and helped provide factories for protein assembly (ribosomes) – blue collar jobs at best. But over the past two decades, it has become clear that RNA plays a much more complex role.

1.1.2 Recently discovered roles of RNA

1.1.2.1 Catalytic RNA

For years, proteins were thought to be the only biomolecules with catalytic activity. However, in a series of studies in the early 1980s, the groups of Tom Cech (University of Colorado)[2-4] and Sidney Altman (Yale)[5,6] demonstrated that RNA can also have catalytic activity (these species are termed "ribozymes"). Cech and Altman were awarded the 1989 Nobel Prize in Chemistry for this work. In the years to follow, many other groups have worked to unravel the details of RNA-based catalysis.[7] (While no examples of catalytic DNA have been found in nature, it is also possible to evolve so-called "deoxyribozymes" *in vitro*.[8]) The ribosome, a complex of three RNA molecules and more than 50 proteins, is now understood to be a ribozyme, the proteins essentially providing a scaffold for the catalytic RNA molecules.[9,10]

The fact that RNA is an information-rich, replicable molecule that can also have catalytic activity is the inspiration for the "RNA world" hypothesis, which holds

that before DNA and proteins existed, RNA carried out both genetic and catalytic functions. Among the most significant recent discoveries in support of this hypothesis was the development, by David Bartel (MIT) and colleagues, of an RNA polymerase made of RNA.[11]

Another new class of functional RNAs contains both a recognition/binding domain and a catalytic/functional domain – these so-called riboswitches have catalytic activity that changes in the presence of a ligand, and they often serve to regulate gene expression.[12]

1.1.2.2 RNA splicing

Except in the simplest organisms, RNA must undergo significant processing in order to provide a useful protein coding sequence. This process is called splicing, and involves the removal of sequences called "introns," and the concurrent joining together of the remaining "exon" sequences into a functional mRNA. The discovery of RNA splicing was the subject of the 1993 Nobel Prize in Physiology or Medicine, to Richard Roberts (New England Biolabs) and Phillip Sharp (MIT).

In many cases, multiple proteins can be produced by including or excluding introns and exons from the final mRNA. This "alternative splicing," once thought to be a rare anomaly, is now thought to be a feature of 40-60% of human genes.[13] In an extreme case, a Drosophila gene called Dscam can be spliced into more than 38 000 variants.[14]

1.1.2.3 Post-transcriptional gene regulation (siRNA, miRNA, piRNA)

In 1998, a study was carried out on the use of antisense RNA in gene repression in the nematode worm *C. elegans*.[15] Double-stranded RNA was used as a negative control. However, to the surprise of the researchers, this dsRNA was far more potent than either strand individually.[15] This process became known as RNA interference (RNAi), caused a paradigm shift in biochemistry and genetics, and earned the 2006 Nobel Prize in Physiology or Medicine for these researchers, Andrew Fire (Stanford) and Craig Mello (UMass Medical School).

The process of RNAi is described in detail in Section 1.2.2. Fire and Mello had introduced long dsRNA into cells,[15] but it was later determined that this long dsRNA was cleaved into short (19-21 bp) duplexes called small interfering RNA (siRNA),[16] and that these duplexes themselves are sufficient to cause RNAi.[17,18]

These short duplexes are similar in structure to another class of small RNAs, called microRNAs (miRNAs). The first miRNA was observed in 1993,[19,20] but it was not until the dawn of the genomic era that miRNAs were recognized to be involved in the regulation of thousands of human genes.[21,22] Furthermore, after the discovery of siRNA, it was observed that there is significant overlap between the miRNA and siRNA regulatory pathways.[23] However, siRNA normally causes mRNA cleavage, while miRNA leads to translational repression and/or mRNA destabilization.[22,24,25]

Other classes of small RNAs continue to be discovered. In mammals, the PIWI-interacting RNAs (piRNAs) are a class of 26-31 nt ssRNAs that are important for spermatogenesis.[26-28] In other species, at least three other classes of small RNAs have been identified.[23]

1.1.2.4 Transcriptional regulation and the genome as an RNA machine

The involvement of small RNAs in post-transcriptional gene regulation has been the major paradigm shift of the past decade, in the field of genetics. However, it seems that small RNAs may not content themselves with post-transcriptional regulation. Indeed, recent studies have found that small RNAs can be involved in activation or repression at the transcriptional level.[29-33] This process appears to be related to the presence of longer noncoding RNAs associated with chromosomal DNA.[34]

Indeed, while only about 2% of the human genome is transcribed into mRNA, it has become clear through several recent studies that the vast majority of the genome is transcribed.[35-37] Furthermore, much of this RNA may be functional, in contrast to long-held scientific opinion.[38] The idea that most of the genome may be transcribed into a hidden RNA regulatory system has led some to speak of the human genome as an "RNA machine."[39]

1.1.3 Structure and conformation of nucleic acids

1.1.3.1 Primary structure

DNA and RNA consist of heterocyclic bases built on a sugar–phosphate backbone (Figure 1.1). At neutral pH, the phosphates are constitutively charged.

The main difference between DNA and RNA is the 2'-hydroxyl group. This small difference leads to very different conformational properties through stereoelectronic and steric effects.

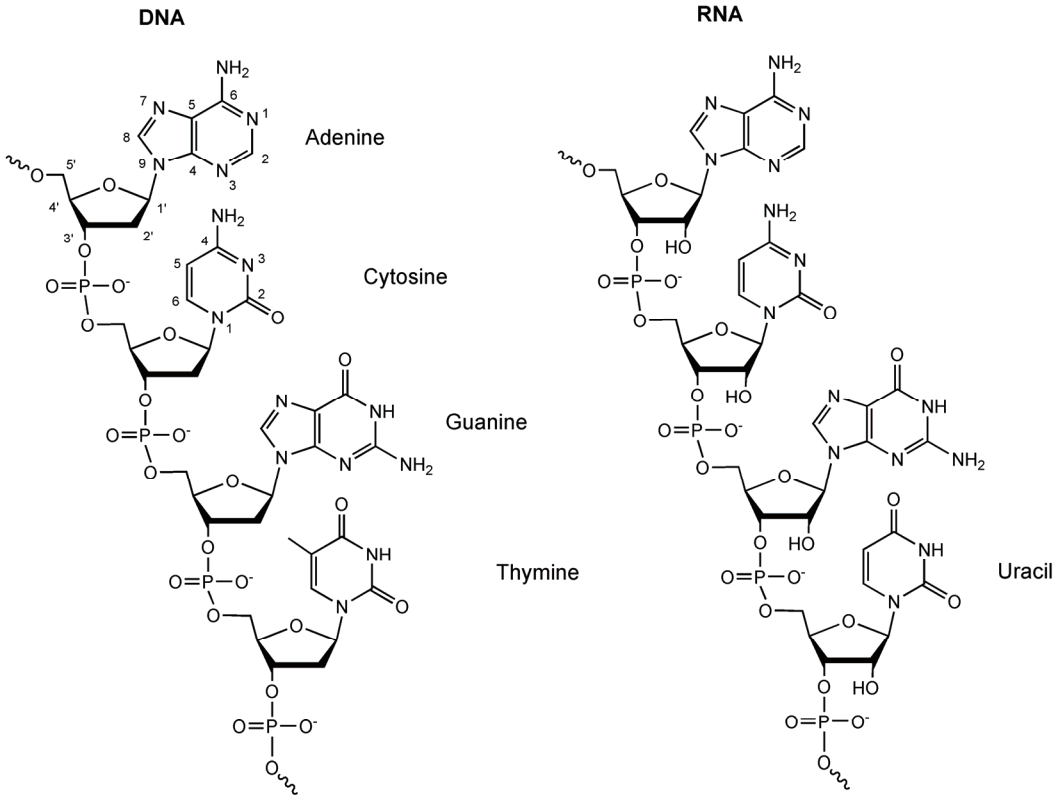

Figure 1.1. Primary structure of DNA and RNA. Note that RNA contains uracil instead of thymine, lacking the 5-methyl group. Purine, pyrimidine and sugar numbering are shown at top left.

1.1.3.2 Nucleoside conformation

The conformational parameters of a nucleoside or other furanoside can be described using two parameters, namely the phase angle P and degree of maximum puckering ϕ_{max}, which are in turn derived from the torsion angles of the sugar ring.[40] The value of P takes on an intuitive meaning when it is represented on a "pseudorotational wheel" as shown in Figure 1.2.[40]

Unmodified DNA and RNA nucleotides have two major conformational minima, in the north (0º – 36º) and south (144º – 180º), and rapid interconversion occurs preferentially via the east (90º) pseudorotamer. The conformational equilibrium of 2'-deoxyribonucleotides favors the south (about 65% is the southern conformer), while ribonucleotides exist as a fairly even distribution of the northern and southern conformers.[41]

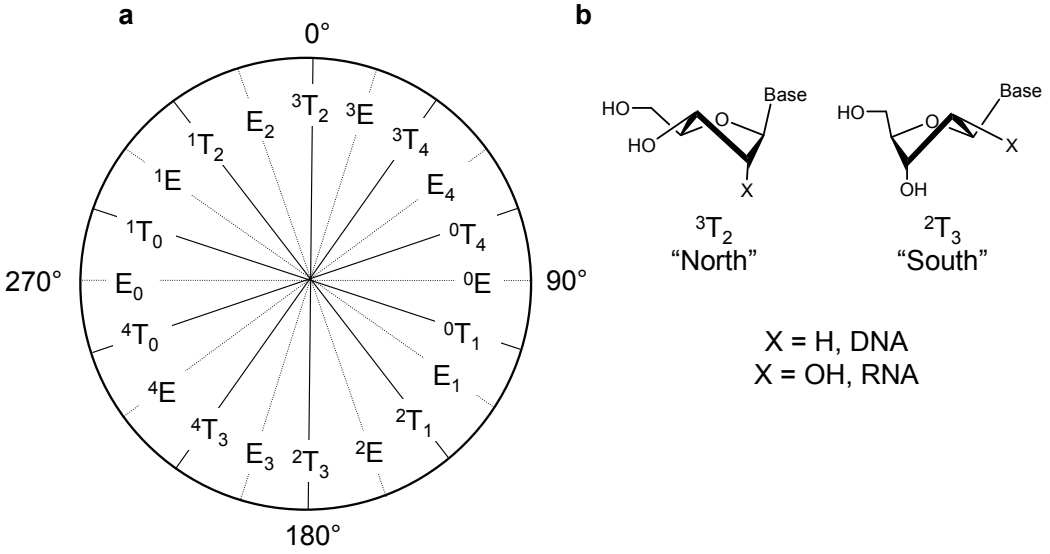

Figure 1.2. Nucleoside conformations. (a) The pseudorotational wheel describing the sugar conformations of nucleosides; E = envelope, T = twist. (b) Natural nucleosides have characteristic minima in the north (0º – 36º) and south (144º – 180º) regions (pictured at right).

1.1.3.3 Helical structure

Double-stranded nucleic acids typically adopt one of two right-handed helical conformations. The helical structure DNA is most commonly found in the B-form, but can adopt the A-form under conditions of low hydration. A rare left-handed helical conformation, called Z-form, is also possible for DNA, as are even less-well known structures called C-form, D-form and T-form.[42] RNA, in contrast to DNA, exists almost entirely in the A-form: it cannot exist in the B-form,[43] but it has been observed in the Z-form in rare circumstances.[44] Helical structures and average parameters are shown in Figure 1.3. The sugars of nucleotides in A-form

helices pucker in northern conformations, while those in B-form helices pucker in southern conformations.

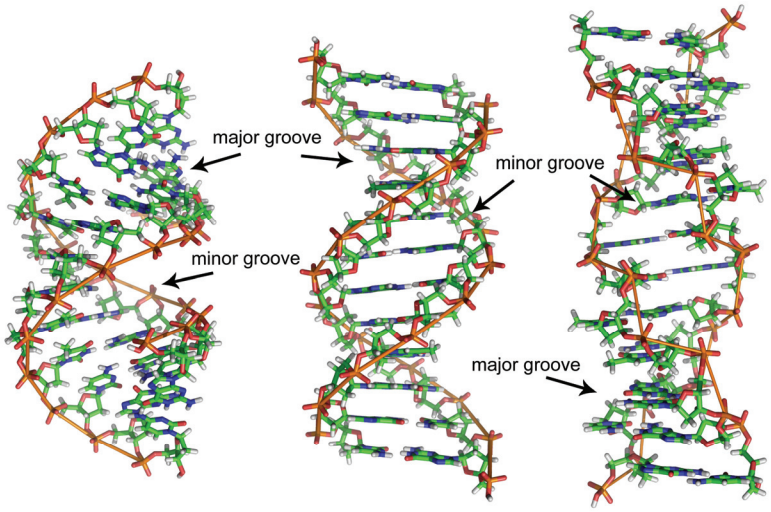

	A-DNA	B-DNA	Z-DNA
Helix sense	Right	Right	Left
Sugar pucker	C3'-*endo*	C2'-*endo*	C3'-*endo* (syn)
Residues per turn	11	10	12
Twist per bp	32.7 °	36 °	–9, –51 °
Displacement per bp	4.5 Å	–0.2 to –1.8 Å	–2 to –3 Å
Rise per bp	2.56 Å	3.3–3.4 Å	3.7 Å
Base tilt	20 °	–6 °	–7 °
Major groove: width	2.7 Å	11.7 Å	8.8 Å
depth	13.5 Å	8.8 Å	3.7 Å
Minor groove: width	11.0 Å	5.7 Å	2.0 Å
depth	2.8 Å	7.5 Å	13.8 Å

Figure 1.3. Helical conformations of A-DNA, B-DNA and Z-DNA. The structure of A-RNA closely resembles that of A-DNA. Structures shown are based on an image taken from the Wikimedia Commons and used by permission, see page iv. Data taken from ref.[42]

1.1.4 The importance of nucleic acid hydration

Nucleic acids are heavily hydrated. Water molecules coordinate to the charged phosphates, and an ordered water structure lines the grooves of nucleic acid helices. At least 25 molecules of water per base pair are tightly bound to DNA.[45] A spine of water molecules in the minor groove of B-DNA or the major groove of A-DNA has been observed,[46] but the ordered water structure of DNA is most

concentrated around its phosphates.[47] In the case of RNA, more extensive hydration is observed in both grooves, partly because of the hydrophilic 2'-hydroxyl group.[48]

Hydration plays a determining role in many of the properties of nucleic acids, including duplex stability[48,49] and protein recognition,[45,50] and may even explain some of the sequence specificity of protein-nucleic acid interactions.[45,51,52]

1.2 Targeting RNA

Most traditional drugs bind to proteins. However, the prevalence of RNA in the cell, in both familiar and recently discovered roles, makes it clear that targeting RNA could be a powerful strategy. Indeed, RNA itself can be targeted in various ways, and with applications in both therapeutics and research. This section describes classic and novel methods of targeting RNA.

1.2.1 Antisense oligonucleotides (AON)

In 1978, Zamecnik and Stephenson demonstrated that a 13-mer unmodified oligodeoxynucleotide could inhibit replication of Rous sarcoma virus in cell culture.[53,54] However, it was not until automated oligonucleotide synthesis[55] became routine in the following decade that the potential for gene knockdown using AONs was fully understood. For that potential to be reached took many more years again, including the development of chemically modified analogues which are more stable under physiological conditions. Finally in 1998, the first antisense drug (Vitravene®, ISIS) received FDA approval; but its field of application is very limited and no others have yet followed.

Over the thirty years since the initial discovery by Zamecnik and Stephenson, the field of AONs has undergone significant development.[56-58] AONs fall into two classes. The first is capable only of attaching itself to complementary mRNA, then acting as a steric block to reduce translation (or redirect splicing, see below). The second class achieves destruction of its mRNA target by recruitment of the enzyme RNase H, which cleaves the RNA strand of a DNA•RNA hybrid duplex.[59,60]

1.2.2 Small interfering RNA (siRNA)

While the AON strategy is still an attractive therapeutic option, RNA interference (RNAi) is the gene silencing strategy that has attracted the most attention in recent years, including the 2006 Nobel Prize in physiology or medicine. The two strategies have been compared in various studies[61-63] and reviews,[57,64] and some work has even been done on the use of both strategies together.[65]

Both approaches involve the cleavage of mRNA by an endonuclease, guided by an exogenous oligonucleotide strand. However, there are several important differences, summarized in Table 1.1.

Antisense	RNAi
Catalytic enzyme is RNase H	Catalytic enzyme is an Argonaute enzyme, part of the RNA-Induced Silencing Complex (RISC).
RNA•DNA duplexes recognized	siRNA (short, double-stranded RNA) recognized
Exogenous oligonucleotide introduced as a single strand	Exogenous oligonucleotides introduced as an siRNA duplex, one strand subsequently incorporated into RISC.
DNA-like modifications required for RNase H activity	RNA-like modifications required for RISC activity

Table 1.1. Differences between antisense and RNAi strategies.

Much excellent work has led to significant growth in understanding of the mechanism of RNAi[23,66,67] (Figure 1.4). When an exogenous 19-21 bp siRNA is introduced into a mammalian cell, the 5'-end is phosphorylated. The duplex is then assembled into the RNA-induced silencing complex (RISC), a multiprotein complex including Argonaute2 (AGO2) and Dicer, as well as other proteins, some of which are yet unknown.[23,68,69] The strand with lower binding affinity at its 5'-end becomes the antisense (guide) strand,[66] and the other strand (known as the sense or passenger strand) is cleaved and unwound, to leave a single-stranded RNA associated with AGO2, an endonuclease at the heart of RISC that promotes location of complementary mRNA, hybridization, and cleavage of the mRNA target.[70] When modifying an siRNA duplex (discussed in detail in Section 1.3), it is important to remember that different modification approaches are required for the sense and antisense strands, because of their very different roles.[71,72]

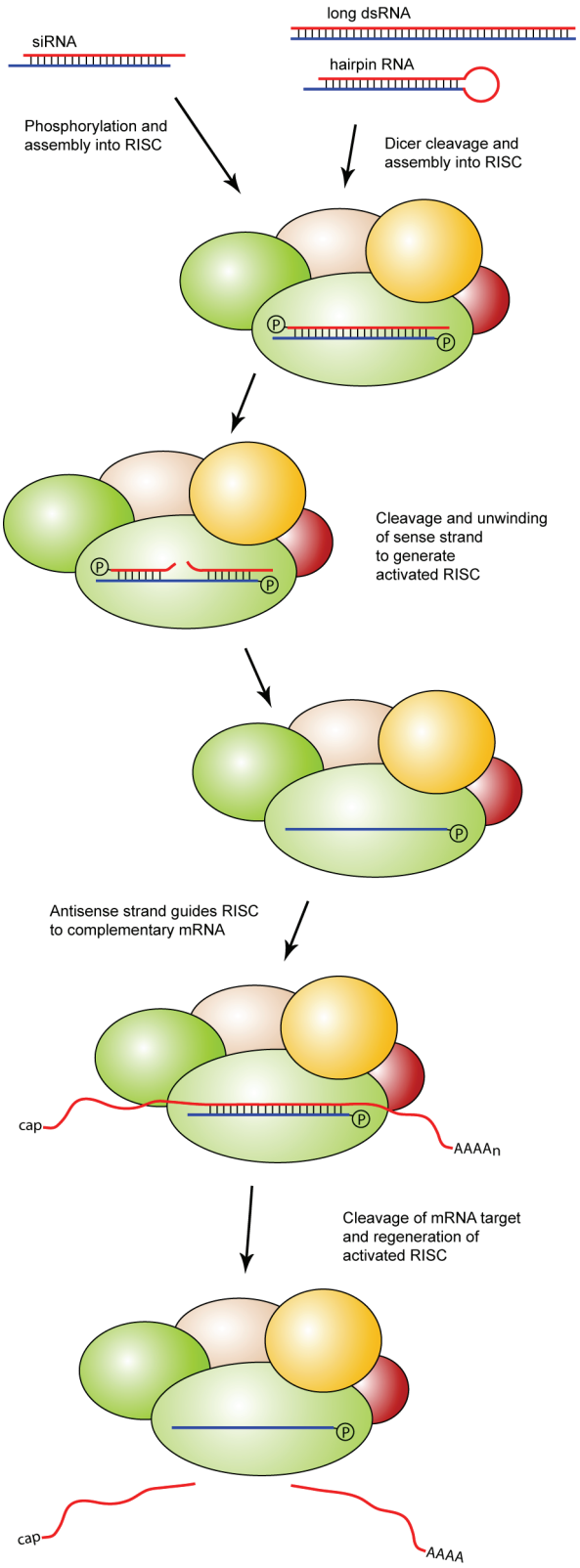

Figure 1.4. The mechanism of RNAi in human cells. The largest of the ellipses signifies AGO2, the catalytic engine of RISC.

AGO2 contains two main domains. The N-terminal PAZ domain binds primarily to the 3'-overhang.[73-77] The C-terminal PIWI domain contains a region with an RNase-H-like fold,[78,79] which catalyzes the cleavage of complementary RNA.[80-82] Other portions of the PIWI domain interact with the 5'-phosphate of the antisense strand,[83,84] with proteins containing an "Argonaute hook" domain,[85] and with Dicer.[86,87]

1.2.3 Ribozymes

The methods described above require proteins to cleave the target mRNA. However, since RNA itself can have catalytic activity (Section 1.1.2.1), it can be used to effect mRNA cleavage in a protein-independent manner,[88,89] or even to repair aberrant mRNA through *trans*-splicing.[90] Ribozymes can be optimized for therapeutic purposes through careful use of chemical modification.[91]

1.2.4 Other RNA targets

The three methods discussed above have been used primarily to downregulate mRNA. However, the recently discovered roles of RNA discussed in Section 1.1.2, besides allowing a new method of targeting mRNA (namely siRNA), also open the door to new and creative RNA targets for both research and therapeutics.

For example, "antagomirs"[92] or "anti-miRNA AONs"[93] are ~20mer oligonucleotides complementary to the guide strand of miRNA. They are thought to bind to the complex containing the miRNA associated with the RISC complex.[93] Surprisingly, however, targeting miRNAs can lead to either upregulation or downregulation of mRNAs targeted by the miRNAs.[92] Thus gene regulation by miRNAs is more complex than our current understanding allows. However, even with our current imperfect understanding, therapeutically relevant results have already been obtained *in vivo*.[92,94]

As mentioned above, alternative splicing occurs in many human genes, in different tissues or at various stages of development.[95] In some cases, however, aberrant splicing can lead to dysfunctional protein. In these cases, the splice sites (intron/exon junctions) of pre-mRNA can also be targeted using synthetic oligonucleotides.[95,96] Steric block antisense oligonucleotides have been used to redirect the splicing of several genes of therapeutic interest, including Bcl-X[97] and dystrophin.[98]

Finally, the long untranslated RNAs associated with chromosomal DNA can be targeted.[34] siRNA duplexes targeting the promoter regions of genes interact with these mysterious transcripts and can either upregulate or downregulate gene expression, depending on a series of factors still poorly understood.[29-33] The position of the targeted site relative to the transcriptional start site is one determining factor. This may therefore allow another method to control gene expression.

1.2.5 The importance of chemical modifications for targeting RNA

Some methods of gene silencing were discovered initially with natural oligonucleotides, either DNA (in the case of AON) or RNA (in the case of RNAi). However, since cells contain nucleases, unmodified DNA and RNA do not last long. Furthermore, unmodified nucleic acids can cause a variety of unwanted effects, as discussed below. Other strategies, such as targeting miRNA, simply cannot make use of unmodified RNA, since an RNA antagomir would simply be cleaved by the activated RISC it is trying to block.[93]

This thesis is based on the importance of chemistry in bringing to fruition the therapeutic potential of oligonucleotides. The rest of this introduction will focus on three areas. We will first explore in more detail the importance of chemical modifications in the siRNA gene regulation pathway (Section 1.3), since this is the method of gene silencing used in my studies. We will then examine the history and properties of one modification in detail (2'F-ANA, Section 1.4), since most of my research has made use of 2'F-ANA or 2'F-ANA analogues. Finally, we will briefly examine the techniques involved in nucleic acids research (Section 1.5) before examining the objectives of this thesis (Section 1.6).

1.3 Chemical modifications of siRNA

1.3.1 Introduction to siRNA

1.3.1.1 Brief background

It has been ten years since the publication of the seminal paper demonstrating the high potency of long double-stranded RNA in gene knockdown.[15] Shortly thereafter, it was discovered that the same effect could be produced in mammalian cells using synthetic short RNA duplexes.[18] The relatively few years since then have seen an explosion of research into therapeutic applications of RNAi. Several companies have been formed to pursue the technology, and transactions involving these companies have recently been measured in the billions of dollars.

The reason for the excitement is that RNAi allows potent gene knockdown of virtually any gene. This in turn allows rapid progression from target selection to preclinical trials. siRNA has become the most common tool in functional genomics, and therefore can often also help at the target identification stage. Furthermore, some targets that are not druggable by traditional methods can be targeted by gene knockdown.

1.3.1.2 Need for chemical modification

In spite of the immense attractiveness of gene knockdown as a therapeutic strategy, siRNA duplexes are not optimal drug-like molecules. RNA is highly vulnerable to serum exo- and endonucleases, leading to a short half-life in serum. siRNA duplexes are composed of two strands that can drift apart in a dilute environment like serum. And because oligonucleotides are polyanions, they do not easily cross cell membranes, and because this charge density leads to extensive hydration, they do not easily interact with albumin and other serum proteins, leading to rapid elimination. Unmodified oligonucleotides have limited tissue distribution. And finally, oligonucleotides can have off-target effects, either through stimulation of the immune system or by entering other endogenous gene regulation pathways.

A wide variety of chemical modifications have been proposed to address these issues. In this section, we examine the principles of chemical modification of siRNA duplexes. We will briefly look into the toolbox, that is, summarize the possible ways that siRNA duplexes can be modified. Following this, we will

review the ways these tools have been applied to move siRNA toward the clinic, including the use of chemical modifications to improve potency, serum stability, specificity and delivery. We will point out the most useful and universal modifications as well as some of the most creative modifications and applications, which stretch our paradigms and open new avenues of research into RNAi-based drugs.

1.3.1.3 Selection of siRNA sequences

siRNA sequence selection is key to effective gene silencing. To select an siRNA sequence, one of various algorithms can be used, based on the mechanism of RNAi.[99] For example, duplexes are chosen such that their lower affinity end corresponds to the 5'-end of the antisense strand (to ensure effective loading of the antisense strand, see Section 1.3.3.2), and such that homology between the 5'-end of the antisense strand and other mRNA targets is minimized (to reduce off-target effects, see Section 1.3.3.4).

Some of these algorithms are available on the web. For example, BIOPREDsi (www.biopredsi.org) is a site developed by the Novartis Institutes for BioMedical Research,[100] which features a very simple input and output (input is a gene accession number or gene sequence, output is a user-defined number of optimized siRNA sequences). Another popular website for sequence selection is the Whitehead Institute siRNA Selection Web Server (jura.wi.mit.edu/bioc/siRNAext).[101] Developed and hosted by the Whitehead Institute, this site is somewhat more complex, giving a large number of possible duplexes ranked according to their thermodynamic properties. An off-target search (*i.e.* checking for other mRNAs that could unintentionally be silenced by the siRNA, see Section 1.3.3.4), can be done for each duplex, within the site but in a separate step.

Even after using a sequence selection algorithm, it is best to test several duplexes against the same gene. In fact, if resources are available, the most thorough way to find highly active siRNA sequences is to test as many as 100-200 sequences against a given mRNA.[102,103] By careful choice of siRNA sequence, high potency and minimum off-target and immunostimulatory effects can be

achieved even with native RNA. These siRNAs can then be further optimized through chemical modification(s).

1.3.2 Toolbox for siRNA modification

siRNA duplexes have been chemically modified in a wide variety of ways. However, some of the results in the literature seem to contradict each other, or to work on one system but not another. This field is still very young, and it will take time for the more robust and universal modifications to be recognized as such. In the meantime, it is useful to have many options, so that at least one of the chemistries can be used to modify an siRNA without compromising its potency.

In this section, we will briefly review the most significant siRNA modifications in the literature, drawing attention to those which have proven most useful and robust up to now. The goal of this section is not to explore the advantages of each modification in detail, but simply to present all the known possibilities in a straightforward way (in Section 1.3.3, we will explore how these modifications can help move siRNA toward the clinic).

In most cases it is simply assumed that the RNAi mechanism is unaffected by chemical modification of siRNA duplexes. A few studies using modified siRNA have confirmed this by showing that the cleavage of complementary mRNA occurs between bases 10 and 11, counting from the 5'-end of the guide strand, as is the case for unmodified duplexes.[104-106] However, in principle, this should be verified for each new pattern of modification.

1.3.2.1 Sugar modifications

The most widely-used siRNA modifications are on the sugar moiety (Figure 1.5). One of the earliest studies on chemically-modified siRNA showed that while A-form duplex structure is important, the 2'-OH is not required for active siRNA.[107] Therefore, the 2' position has been extensively modified.

2'-*O*-methylation of RNA increases binding affinity and nuclease stability, and the resulting 2'-*O*-Me-RNA can be well-tolerated throughout the duplex, making it one of the most popular and versatile siRNA modifications. Many groups have found that large numbers of 2'-*O*-Me modifications (in either strand) decrease

siRNA activity,[107-110] but others have found that fully modified 2'-*O*-Me sense strands are functional.[103,105] Kraynack and Baker attribute these differences to their finding that 2'-*O*-Me modifications work best in blunt-ended duplexes,[105] but at least one group found that even in this context, activity is greatly reduced by heavy 2'-*O*-Me modification.[110]

In general, bulkier 2'-modifications are not well-tolerated in siRNA duplexes, except small numbers of modifications on the termini. Davis *et al*. demonstrated that bulky 2'-substituents correlate with poor activity as siRNA sense strands and, for the same reasons, excellent activity as "antagomirs" (to block miRNAs).[93]

Thus, the 2'-*O*-methoxyethyl (2'-*O*-MOE) modification has been used in the 3'-overhangs of an siRNA targeting the pain-related cation-channel $P2X_3$, and resulted in successful gene targeting *in vivo*.[111] Another group found that 2'-*O*-MOE modifications could be included the sense strand, especially at the termini, but not in the antisense strand.[112] Similarly, 2'-*O*-allyl-modifications caused a reduction in activity at most positions in the duplex, but can be used in the 3'-overhangs.[113]

siRNAs in which 70% of the 2'-OH groups are converted at random into 2,4-dinitrophenyl ethers (2'-*O*-DNP) show a variety of improved properties, including higher binding affinity, nuclease resistance and potency.[114]

Instead of a hydroxyl, alkoxy, or aryloxy substituent, functional siRNAs can contain fluorine at the 2'-position. 2'F-RNA is one of the best-known siRNA modifications, and partial 2'F-RNA modification is tolerated throughout both the sense and antisense strands,[107,108,115] and some fully-modified 2'F-RNA siRNAs are also active.[116] 2'F-RNA-modified siRNA duplexes have significantly increased serum stability.[117] 2'F-RNA also increases the binding affinity of the duplex.

Changing the stereochemistry of the fluorine of 2'F-RNA gives 2'F-ANA, described in detail in Section 1.4. 2'F-ANA was originally developed as a DNA mimic,[118,119] and so it is somewhat surprising that 2'F-ANA is also well-tolerated in siRNA duplexes, including fully-modified sense strands and partial modification of the antisense strand.[120,121] Like its epimer 2'F-RNA, it binds RNA

with high affinity and increases nuclease stability. Further research on 2'F-ANA modification of siRNA is described in Chapter 5.

DNA itself, a "modification" containing no electronegative substituent at 2', can also be accepted within siRNA duplexes. For example, use of DNA in the 3'-overhangs has been well-known since the earliest days of synthetic siRNA,[18] and DNA can also be tolerated, in small numbers, within the base-paired region of an siRNA duplex.[72,109] An antisense strand made entirely of DNA purines and 2'F-RNA pyrimidines is functional,[107] since 2'F-RNA strongly favors a northern sugar pucker and A-form helical structure, and presumably directs the conformation of the more flexible deoxynucleotides. Substitution with dsDNA in the 8-bp region at the 5'-end of the guide strand gives active duplexes with reduced off-target effects.[106]

The ring oxygen has also been modified: 4'S-RNA is a high-affinity modification that gives a significant advantage in nuclease stability. 4'S-RNA is very well tolerated near the termini of siRNA duplexes.[122-124] In the antisense strand, some loss of potency was observed, but not as much as with 2'-*O*-Me-RNA at the same positions.[122] The 5'-end of the antisense strand could be modified with a few 4'S-RNA inserts without significant loss of potency.[123] The center of the antisense strand cannot be modified with 4'S-RNA without significant loss of potency.[122,123] A strand architecture consisting of four 4'-thioribonucleotides on each end of the sense strand and four at the 3'-end of the antisense strand worked consistently well against two target genes in three cell lines.[124] Combinations of 4'S-RNA with 2'-*O*-Me and 2'-*O*-MOE modifications at the termini of both strands showed excellent potency and serum stability.[123] Development and siRNA activity of another 4'S-substituted modification, 4'S-FANA, is described in Chapters 4 and 5.

The conformationally-constrained nucleotide LNA[125] has also been included in siRNA.[108,126-129] Its conformational rigidity leads to significant increases in binding affinity. Careful placement of LNA in siRNA duplexes has led to functional duplexes of various types. The most common sites of modification are the termini of the sense strand[129] and the 3'-overhang of the antisense strand.[126,128] Minimal modification of most internal positions of the antisense strand is also

tolerated,[108,126] but heavier modification of the antisense strand is tolerated only in combination with a segmented sense strand (described in more detail below).[127]

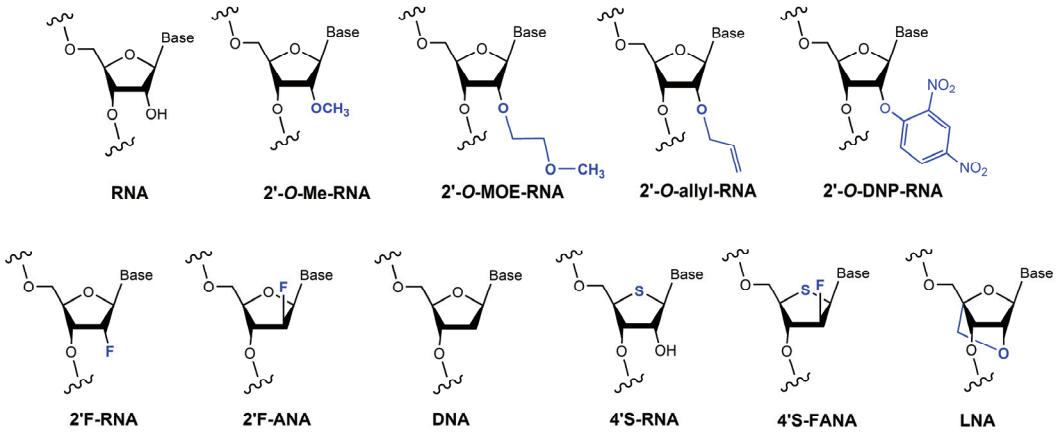

Figure 1.5. Sugar units that have been successfully used to modify siRNA duplexes. Top row, 2'-*O*-alkyl (2'-*O*-Me, 2'-*O*-MOE, 2'-*O*-allyl) and 2'-*O*-aryl (2'-*O*-DNP) modifications, bottom row, from left to right, other 2'-modifications (2'F-RNA, 2'F-ANA, DNA), 4'-modifications (4'S-RNA, 4'S-FANA), and a conformationally constrained modification (LNA).

1.3.2.2 Phosphate linkage modifications

Several variations on the phosphodiester linkage are also accepted by the RNAi machinery (Figure 1.6). Phosphorothioate (PS) linkages can be used, with comparable[113,115] or lower potency[107,130] to that of native siRNA. Some groups have found that PS linkages are not accepted at the center of the duplex, especially at the scissile phosphate.[131] However, the ability to accept fully-modified PS strands may depend on strand architecture.[105] Some cytotoxicity has been observed with extensive PS modification.[113] PS modifications do not appear to have a major effect on biodistribution of siRNA.[132]

siRNAs with boronophosphate linkages are functional and show increased potency relative to PS-modified siRNAs and often to native siRNAs as well, but to maximize potency, the center of the antisense strand should be unmodified.[130] Boranophosphate siRNAs provide a significant increase in nuclease stability over native RNA.[130]

A 2',5'-linkage (either 2',5'-DNA or 2',5'-RNA) can substitute for the native 3',5' linkage, but only in the sense strand of the duplex, and with some reduction in potency.[133] A nonionic amide linkage has been used in the 3'-overhangs of siRNA duplexes.[134]

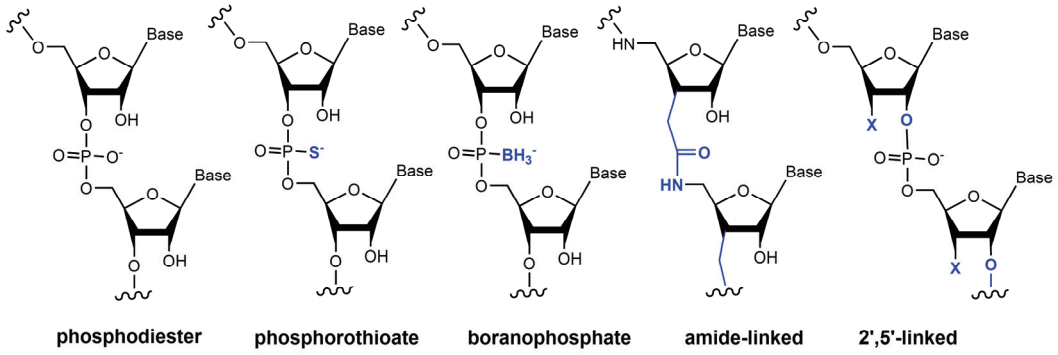

Figure 1.6. Internucleotide linkages used in siRNA. The phosphodiester linkage can be modified as a phosphorothioate or boranophosphate, which retain the negative charge of a phosphate, or a neutral amide-linked RNA can be used at select positions. Either 2',5'-linked DNA (X=H) or RNA (X=OH) can be used in the sense strand.

1.3.2.3 Base modifications

Use of modified bases in siRNA has been somewhat more limited, but there have been several examples (Figure 1.7). Modified bases that stabilize A-U base pairs (5-Br-Ura and 5-I-Ura instead of uracil, and diaminopurine instead of adenine) were tolerated in siRNA duplexes, although their activity was somewhat reduced.[107] 4-Thiouracil has also been used.[72] 2-Thiouracil[135,136] and the C-linked nucleobase pseudouracil[135,136] increase binding affinity and can be used to increase potency and specificity if placed appropriately within the duplex (see Sections 1.3.3.2 and 1.3.3.3). 5-Methylation of pyrimidines (i.e. use of T and 5-Me-C instead of U and C) is common in conjunction with sugar modifications such as DNA, 2'F-ANA and LNA.

Some surprisingly atypical base structures have been used in siRNA. A difluorotoluyl base, which has the same shape as thymine but cannot form hydrogen bonds, can replace uracil at single positions throughout an siRNA duplex, without significantly decreasing the potency or changing the mechanism

of cleavage.[137] A nonaromatic base, dihydrouracil, can also be used, but because it cannot contribute to base stacking, it lowers the binding affinity of the duplex and is best placed at the 5'-end of the duplex, as defined by the antisense strand.[135] Bulky or cationic base modifications have not been well-tolerated.[72]

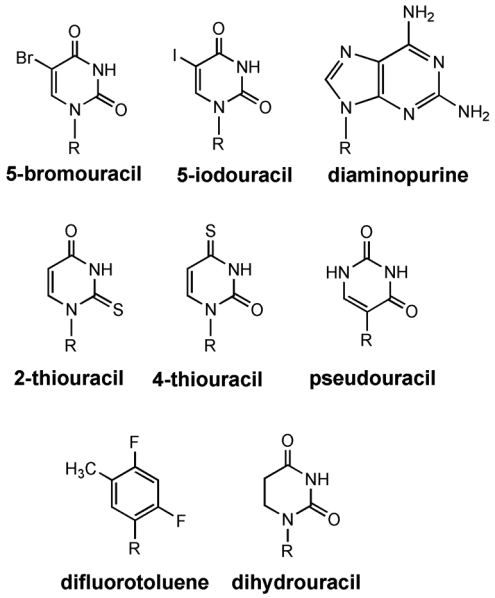

Figure 1.7. Base-modified nucleotides used in siRNA. R represents the ribose – phosphate backbone.

1.3.2.4 Modifications to the overhangs and termini

Early studies showed that the ideal siRNA consisted of 21 nt in both strands, including 2-nt 3'-overhangs.[109] These overhangs can be modified in various ways: from the beginning, deoxy units have often been used in the 3' overhangs, to reduce costs and possibly increase resistance to 3'-exoribonucleases.[18] However, RNA units also work well,[138] most of the chemistries reviewed above work well in the overhangs, and blunt-ended siRNAs have also been used.[110] Blunt-ended duplexes are more resistant to 3'-exonucleases, and one study reported a greater tolerance to chemical modifications in combination with blunt-ended duplexes.[105] However, they are more immunogenic than duplexes with 3'-overhangs.[139]

The termini of the strands can also be modified. Chemical phosphorylation of the 5'-end of the antisense strand helps ensure high potency, and is often necessary when the strand is modified. On the other hand, 5'-phosphorylation of

the sense strand can be blocked without loss of activity,[110,140] and can in fact be beneficial.[141]

Furthermore, various groups can be conjugated to the ends of siRNA duplexes, especially the termini of the sense strand. These groups can include an inverted abasic end cap,[142,143] which helps with exonuclease stability. Conjugation of fluorescent dyes[115] or biotin[144] has allowed important biophysical/biochemical studies. Finally, conjugation of membrane-penetrating peptides[145] and lipophilic groups including steroids and lipids[104,146] has helped with delivery (see Section 1.3.3.5). An intriguing recent study showed that including 5-8 dA and dT units on the 3'-ends of the strands can lead to reversible concatemerization through these sticky ends, which in turn leads to higher efficiency delivery in complex with PEI.[147]

The general consensus is that the 5'-end of the antisense strand is the most sensitive to modifications,[110,144,148] and does not tolerate most of the above modifications. However, one group observed that fluorescein could be conjugated to any of the termini except the 3'-end of the antisense strand.[115] As long as an antisense 5'-phosphate is present, attaching a group to it does not necessarily eliminate RNAi activity.[149]

1.3.2.5 Modifications to the duplex architecture

The duplex architecture itself can be modified through chemical synthesis (Figure 1.8). While most siRNA duplexes are made up of two strands, it has been shown that an siRNA made of three strands (an intact antisense strand with two 9–13 nt sense strands) can reduce off-target effects and increase potency; the resulting duplex is termed small internally-segmented interfering RNA (sisiRNA).[127] Functional siRNA can also be made from just one strand, in one of various ways. Hairpin-type duplexes, made from a single strand, can be introduced exogenously[150] or expressed within a cell.[151,152] Closing the other end of the hairpin results in a dumbbell or nanocircle which retains RNAi activity while providing complete protection from exonucleases.[153] And finally, a single-stranded antisense RNA (which does not fold into a duplex at all) has been shown to enter the RNAi pathway, with potency approaching that of the duplex siRNA in some cases.[113,148,154]

The length of an siRNA duplex can also be changed. Most synthetic duplexes are 19-21 bp in length, mimicking the natural *products* of the Dicer enzyme. However, increasing the length of an siRNA duplex makes it a *substrate* for Dicer and has been found to increase its potency.[155] It is important to keep the length below 30 nt, to avoid triggering the interferon response.[156]

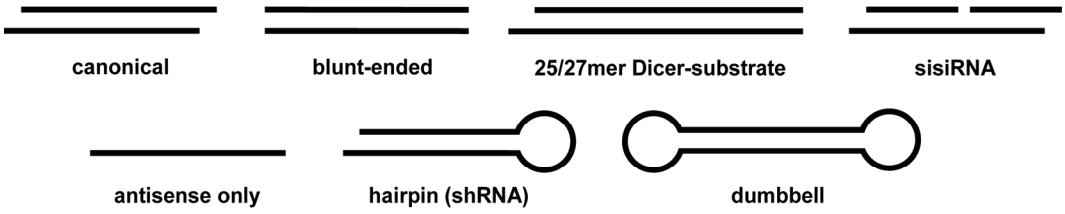

Figure 1.8. Functional siRNA architectures. The sense strand is always shown on top, in the 5' to 3' direction, and the antisense strand is on the bottom, in the 3' to 5' direction. Note that three of the structures (25/27mer, hairpin and dumbbell) require the activity of Dicer before incorporation into RISC.

1.3.3 Applications for chemically modified siRNA

1.3.3.1 Improving serum stability

Unprotected RNA is very quickly degraded in cells. The fact that siRNA is double-stranded provides it with some degree of protection, but not enough for *in vivo* use. A nuclease called *eri-1* has been found to play a key role in degradation of siRNA,[157] and expression levels of *eri-1* inversely correlate with duration of siRNA activity.[158] This and other data suggest that increasing the nuclease resistance of siRNAs can prolong their activity. Chemical modification is the principal strategy used to improve the nuclease resistance of siRNAs.

Essentially all of the modifications in the toolbox can be used to increase the serum half-life of siRNAs. Within the therapeutic siRNA community, however, two schools have emerged on the best paradigm for protecting siRNAs against nucleases. The first strategy favors extensive or entire chemical modification. This paradigm is exemplified by the research of Sirna Therapeutics (www.sirna.com) on heavily modified siRNA duplexes. For example, a fully-modified siRNA with significantly increased potency in an HBV mouse model consisted of a sense strand made of 2'F-RNA pyrimidines, DNA purines, and 5'

and 3' inverted abasic end caps. The antisense strand was made of 2'F-RNA pyrimidines, 2'-*O*-Me purines, and a single phosphorothioate linkage at the 3'-terminus.[143] This fully modified duplex had a half-life in serum of 2-3 days, as compared with 3-5 min for the unmodified duplex.[143] This improved stability translated into higher efficacy *in vivo*. Higher potency was later obtained by including 1-3 RNA inserts at the 5'-end of the antisense strand, and this heavily-modified siRNA still had a serum half-life nearly 30 times longer than that of unmodified siRNA.[142]

A few other examples of fully-modified duplexes have been reported. An siRNA made entirely of alternating 2'F-RNA and 2'-*O*-Me units was found, unsurprisingly, to have greatly increased stability in serum.[159] This architecture also maintains or improves potency, as discussed below. A functional duplex made with DNA overhangs, a 2'-*O*-Me-RNA sense strand, and a PS-RNA antisense strand was nearly all intact after 48 h in serum,[103] and a functional fully-modified 2'F-RNA siRNA has also shown excellent nuclease resistance.[116]

However, such a large degree of modification may not always be necessary. The second paradigm for creating stabilized siRNAs involves minimal, selective modification. It is exemplified in the research of, among others, Alnylam Pharmaceuticals (www.alnylam.com). Since endonuclease degradation is a major mechanism of degradation of siRNAs,[110] the endonuclease cleavage pattern of a given siRNA duplex is first characterized (this is often dominated by cleavage after a pyrimidine nucleotide, and can be readily characterized by mass spectrometry[160]). The vulnerable positions are then selectively modified, usually with 2'-*O*-Me or 2'F-RNA nucleotides, which considerably increases the stability of the siRNA with minimal modification.[161,162]

Besides these empirically-determined internal positions, key positions for modification include the termini of the strands, especially the 3'-termini, to protect the duplex from 3'-exonuclease degradation.[103]

1.3.3.2 Increasing potency

The RNAi pathway is very efficient, and unmodified siRNA is a very potent gene silencing agent, although potency does depend on cell type, target and siRNA sequence. In general, increasing potency is not considered the primary objective of chemical modification: it is sufficient to maintain the potency of unmodified siRNA while increasing its serum half-life and its specificity. However, as the requirements for effective RNAi are increasingly well understood, we can foresee an increase in the use of chemical modifications to optimize potency as well, through features such as target binding affinity (enhancing hybridization on-rates and off-rates), conformational preorganization (A-form helical structure) and flexibility.

It is very rare to find patterns of chemical modification that universally increase potency. On the other hand, there are several known modifications that increase potency, sometimes very significantly, for particular sequences or systems. One of the most dramatic increases was observed for a fully modified siRNA made of a combination of 2'-*O*-Me and 2'F-RNA modified nucleotides, which was 500 times more potent than unmodified RNA.[159] While such a high degree of improvement was not observed for other sequences, this architecture was consistently of equal or greater potency and efficacy than unmodified RNA.[163]

Part of the increase in potency observed in some studies may be due to the increased nuclease stability of the chemically modified siRNA. Beyond this, however, in most cases where increased potency is observed, it is not yet clear why. Similarly, it is not yet clear why so many patterns of chemical modification work for one system/sequence and not for another. This reflects a paucity in our understanding of the requirements of the RNAi pathway.

Rational chemical modification can, however, be used to improve potency through improving the selective loading of the antisense strand. In the normal RNAi pathway, strand incorporation into RISC is determined by the thermodynamics of the siRNA duplex. The strand with lower binding at its 5'-end is preferentially incorporated into RISC. The sequence of an siRNA should therefore be chosen to be AU-rich at the 5'-end of the antisense strand. However, chemical modifications can be used to increase the selectivity of antisense strand

incorporation, by placing high-affinity modifications like LNA at the 5'-end of the sense strand.[126] The activity of a moderately active siRNA duplex was significantly improved using the high-affinity 4'S-RNA modification in both strands.[124] On the other hand, a duplex which had optimal strand thermodynamics was not further improved by 4'S-RNA modification.[124]

Base modifications can be used to the same effect. Of a series of modified siRNA duplexes, the most potent siRNAs contained a high-affinity 2-thiouracil base at the 3'-end of the antisense strand, and a low-affinity dihydrouracil base at the 3'-end of the sense strand.[135]

1.3.3.3 Modulating immunostimulatory activity

RNAi is an evolutionarily conserved cellular mechanism believed to function as an early defense against pathogens. The presence of dsRNA in cells is often characteristic of viral infection as many viruses have a dsRNA stage in their life cycles. The cell responds to this perceived invader in several ways, including specific gene knockdown through RNAi, but also off-target effects caused by innate immune responses.[164] Side-effects from an siRNA therapeutic may result from this immune response, unless the immunogenic potential of dsRNA can be addressed.

It has long been known that dsRNAs longer than 30 bp are potent activators of immune responses.[156] This fact prevented the application of RNAi to mammalian cells until it was discovered that 21mer siRNA duplexes were capable of effecting potent and specific gene knockdown in mammalian cells, without the immunostimulation characteristic of longer dsRNAs.[18] However, the immunogenic activity of short RNA duplexes is more significant than originally thought. A growing number of recent studies report off-target effects resulting from immunostimulation caused by dsRNAs shorter than 30 bp.[129,136,142,164-168]

Immune response activation by short RNAs is a complex process, and has been reviewed elsewhere.[164,165] Briefly, RNAs are recognized by 3 main types of immunoreceptors: Toll-like receptors (specifically TLR3, TLR7 and TLR8; see Glossary), protein kinase R (PKR), and helicases like RIG-I and MDA5. Recognition by these receptors can lead to a number of cellular responses including release of cytokines and changes in gene expression.[164] The types of

immunoreceptors involved and the level of immune activation depend on a number of factors, including the length, sequence, and cellular delivery method of the RNA, as well as the type of immune cell involved. These receptors exist on cell surfaces (TLR3),[169] in endosomes (TLR3/7/8),[170-172] and in the cytoplasm (RIG-I, MDA5, PKR).[171]

The sequence dependence of immune responses is not fully understood. Judge *et al.* have identified immunostimulatory motifs in mice and *in vitro* human blood, most notably 5'-UGUGU-3' regions.[166] Hornung *et al.* demonstrated that 5'-GUCCUUCAA-3' is also a potent immunostimulatory motif.[129] In fact, any U-rich RNA sequence may be sufficient for recognition by TLR7.[173] The presence of a 5'-triphosphate or blunt end can lead to RIG-I-mediated immunostimulation.[136,139,167] Finally, duplexes between 23 and 30 bp may still induce the interferon response in a length-dependent manner, depending on cell type.[168]

Chemical modifications can be used to reduce the immunostimulatory properties of siRNAs.[171] For example, siRNA duplexes >90% modified with 2'F-RNA, 2'-*O*-Me and DNA residues were shown to cause no detectable effect on interferon levels or cytokines, while unmodified siRNA duplexes caused significant activation.[142] Because of immunostimulation, mice treated with unmodified siRNA showed increased levels of serum transaminases and signs of systemic toxicity such as decreased body weight, transient lymphopenia and thrombocytopenia, and piloerection, but these adverse effects were not evident in those mice treated with the modified siRNA.[142] More recently, it has been shown that a far smaller degree of 2'-*O*-Me modification is sufficient to eliminate immunostimulatory activity.[174] Almost any degree of modification was sufficient, with the exception that 2'-*O*-methylation of cytidine residues was ineffective in reducing immunostimulatory activity.[174] 2'F-RNA and/or 2'-*O*-Me modification of uridine resulted in elimination of immune off-target effects,[136] including both TLR-dependent and TLR-independent immune effects.[175] Strikingly, even the presence of 2'-*O*-Me modified RNAs on separate, noncomplementary strands abrogates the TLR7-dependent immunostimulatory activity of unmodified siRNAs, indicating that 2'-*O*-Me-RNA itself is a potent antagonist of TLR7.[176]

2'-*O*-Me and 2'-F modifications are not alone in reducing immunostimulation. LNA has been used to modify the ends of an siRNA sense strand containing an immunostimulatory motif, abrogating the IFN-α immunostimulatory activity of the duplex without affecting the silencing activity.[129] Base modifications, too, can help reduce immune activation: modification with pseudouracil or 2-thiouracil prevented the RIG-I-mediated immunostimulation due to a 5'-triphosphate,[136] and various base modifications abrogated immune effects mediated by TLR3, TLR7, and TLR8.[177]

Indeed, different types of chemical modifications can reduce the immune effects from different receptors. For example, of the base modifications useful for siRNA, one study found that only 2-thiouridine was able to reduce TLR3-mediated immunostimulation, but several others were able to reduce TLR7- or TLR8-mediated effects as well.[177] In another recent study, the cytokine induction profile was different upon treatment with unmodified, 2'-*O*-Me-modified, and 2'-F-modified siRNAs.[172]

Immune stimulation can have a real effect on the results of siRNA experiments. For example, use of a control siRNA that is less immunostimulatory than the experimental siRNA can lead to false positives or overestimated efficacies.[171]

Not all researchers have observed immunogenic side effects from siRNA administration. However, it is clear that when immune activation is a problem, there are many chemical modifications with immunomodulatory effects available to a nucleic acids researcher. Surely many more modifications will be tested and found successful in the years to come. Thus much work lies ahead before the full immunomodulatory potential of chemical modifications can be both realized and understood.

In closing this section, we note that the immunostimulatory activity of siRNA may actually prove useful in some cases. A recent paper showed that the therapeutic anti-angiogenesis activity of an unmodified siRNA currently in clinical trials may actually be due to TLR3-mediated immune effects.[169] Furthermore, immunostimulatory siRNAs may find use as drugs capable of facing cancer and chronic viral infections on two fronts: eliciting both gene knockdown and activation of immune responses.[164] Currently, however, immune activation is

generally considered an unwanted and potentially dangerous off-target effect.[171] Thus chemical modification provides yet another important tool for moving siRNA toward the clinic.

1.3.3.4 Reducing hybridization-dependent off-target effects

Another class of off-target effects of siRNA involves partial hybridization with the wrong mRNA.[178] This primarily occurs when siRNAs act as miRNAs, involving 6-8 nt complementarity at the 5'-end of the antisense strand,[179,180] but can also occur with a ~15 nt region of significant complementarity in the center of the antisense strand.[178] If some of the sense strand is mistakenly incorporated into RISC instead of the antisense strand, it can cause its own set of off-target effects.[178]

Thus two major strategies are used to reduce off-target effects: (1) increasing the selective uptake of the antisense strand (disfavoring incorporation of the sense strand), and (2) disfavoring the miRNA-type pathway itself.

The first of these strategies, for obvious reasons, can have the benefit of increasing potency as well as reducing off-target effects. Typically this is done by increasing the binding affinity of the 3'-end of the antisense strand and/or the 5'-end of the sense strand, as discussed in Section 1.3.3.2. However, to ensure that the sense strand makes absolutely no contribution to off-target effects, it can be further modified. The most thorough example of this is small internally segmented interfering RNA (sisiRNA), in which the sense strand is nicked to prevent it from being incorporated into RISC (see Figure 1.8).[127] To allow such a strand architecture, the high affinity of LNA modifications is required,[127] since 10-12 bp duplexes of unmodified RNA are not stable enough to be useful for gene silencing. Another method of reducing incorporation of the sense strand is to block phosphorylation of its 5'-terminus by methylation.[141] Finally, incorporation of eight DNA nucleotides at the 3'-end of the sense strand significantly reduces sense-strand mediated off-target effects.[106]

However, even if the antisense strand is incorporated into RISC with perfect selectivity, the problem remains that siRNAs can function as miRNAs[181,182] and

downregulate many genes through partial complementarity,[22,179] especially in the seed region. Furthermore, these off-target effects can cause toxicity.[183] Once again, however, chemical modification can be of significant help. Use of two 2'-*O*-Me nucleotides at the 5'-end of the antisense strand reduces miRNA-type off-target effects significantly, with little to no effect on siRNA gene silencing.[184] If the seed region is made of DNA instead of RNA, off-target effects are also significantly reduced.[106]

A third strategy for reducing off-target effects is adopted by Dharmacon RNA Technologies (www.dharmacon.com) who have championed the idea of delivering four siRNA duplexes at once, against the same gene. In this way, the desired cleavage level is maintained but the off-target effects are diluted, since they are different for each of the siRNA duplexes. Thus the overall off-target signature of a pool of siRNAs is usually less than that of any of the individual duplexes that make it up. This strategy is reflective of the natural siRNA pathway, in which long dsRNA is diced into a large number of siRNA duplexes, each targeting the same gene, but with a different off-target signature. This strategy can be combined with the chemical modification strategies described above.

To reduce or avoid both immune-mediated and hybridization-dependent off-target effects, careful sequence selection is an essential first step. Chemical modifications can then provide further protection.

1.3.3.5 Delivering siRNA

Getting siRNA into cells is one of the biggest challenges of any application of RNAi. Delivery of siRNA into cells in culture can be achieved fairly easily, usually using cationic lipids. For challenging cell types, microinjection, electroporation, and calcium phosphate precipitation have also been used.[185]

Local delivery of siRNA is somewhat more challenging, but very possible: current sites of local siRNA delivery include intravaginal,[186] intraocular, intranasal, intracerebral, intramuscular, and intratumoral examples (reviewed in [187,188]). In all of these examples, local delivery is attractive because it allows control over which tissues are exposed to the siRNA (reducing possible side

effects), and because locally delivered siRNAs are not as vulnerable to serum degradation or to hepatic or renal elimination.

Systemic delivery of siRNA *in vivo* is a greater challenge, but many targets, including most cancers and viruses, are inaccessible via local delivery.[187] To enable systemic delivery of siRNA, it can be conjugated to various ligands.[189,190] For example, conjugation to steroids or lipids[146,191] makes the siRNA more hydrophobic, helps it cross cell membranes, and increases its circulation time by allowing it to bind to circulating plasma proteins and lipoproteins.

However, the most promising delivery strategies involve formulation of siRNA into delivery vehicles. Liposome or vesicle-based siRNA delivery systems, lipid bilayers that enclose siRNA, are powerful delivery vehicles. For example, "stable nucleic acid lipid particles" (SNALPs, Figure 1.9a) are vesicles made of a mixture of lipids which allow the SNALP to enter the cell and fuse to the endosomal membrane, releasing its siRNA payload into the cytoplasm.[192] Polyethylene glycol (PEG) groups coat the outside of the particle, ensuring a long lifetime in serum. This technology has been used in key studies showing knockdown of medically relevant targets in the liver, including HBV replication in the mouse[142] and the lipoprotein ApoB in non-human primates.[193]

Another class of vesicle-type delivery agents consists of protamine-condensed siRNA surrounded by neutral phospholipids (Figure 1.9b).[194] The lipids are covalently linked to hyaluronan, which stabilizes the particle *in vivo*, and serves as a point of attachment for a monoclonal antibody (to target the particles to a desired cell type). These particles were used to slow the growth of leukocytes involved in gut inflammation after systemic administration.[194]

A cyclodextrin-based delivery system has been developed by using a cationic linker that condenses the siRNA. These can be targeted using the ability of cyclodextrins to form inclusion compounds with adamantane. Thus, adamantane-PEG-transferrin conjugates associate with siRNA-containing cyclodextrin particles (Figure 1.9c), and allow the particles to selectively enter tumor cells, which overexpress transferrin receptors.[195] This is one of the first siRNA delivery vehicles to be approved for clinical trials.

Finally, the concepts of conjugation and formulation can be combined. For example, lactose-PEG-siRNA conjugates can be combined with cationic poly-L-lysine (PLL) in a charge ratio of 1:1. This results in "polyion complex micelles" containing a dense core of siRNA and PLL, surrounded by a flexible and hydrophilic PEG shell that increases biocompatibility and protects the particles from aggregation.[196] The lactose ligand triggers receptor-mediated endocytosis, and a pH-sensitive linker facilitates dissolution of the complex once inside the cell.[196] All of these properties led to very high siRNA potency in cultured human hepatoma cells.[196]

Achieving effective delivery of siRNAs to specific cells *in vivo* is a difficult task. However, siRNA delivery technology is improving at an incredible rate, and now several approaches are in development, some of which have the potential to finally bring siRNA to the clinic.

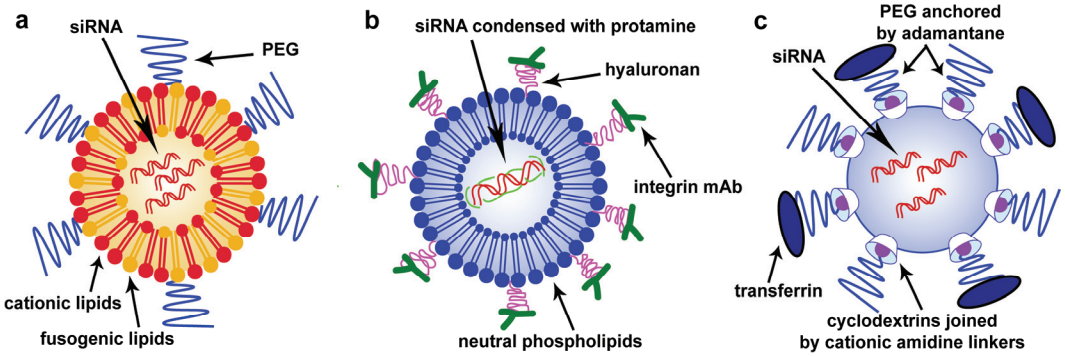

Figure 1.9. Schematics of three siRNA delivery vehicles: (a) a SNALP;[142,192,193] (b) a liposome-based β_7 integrin-targeted stabilized nanoparticle;[194] (c) a transferrin-targeted cyclodextrin nanoparticle.[195,197]

1.3.3.6 Achieving temporal or spatial control of RNAi induction

Chemical modifications can be used to turn RNAi on or off at a given time or in a specific tissue. For example, siRNA activity can be brought under the control of light by caging random phosphate groups with a photolabile group. A 4,5-dimethoxy-2-nitrophenylethyl (DMNPE) group can be linked to phosphate groups by using its diazo derivative (Figure 1.10a).[198] This reduces the activity of treated siRNAs until the photolabile groups are removed, at some point after transfection, by exposure to light.[198]

Instead of caging random phosphate groups, the antisense 5'-phosphate, which is required for activity, can be selectively caged (Figure 1.10b).[199] Use of a nitrophenylethyl caging group at the antisense 5'-phosphate was shown to reduce siRNA activity to 30-40% before irradiation, while allowing at least 80 % activity afterward.[199] The 30-40% activity before irradiation was attributed to contaminating uncaged siRNA.[199] However, it has been shown that in many cases, simply appending a group to the antisense 5'-phosphate is not sufficient to block siRNA activity completely.[149,200]

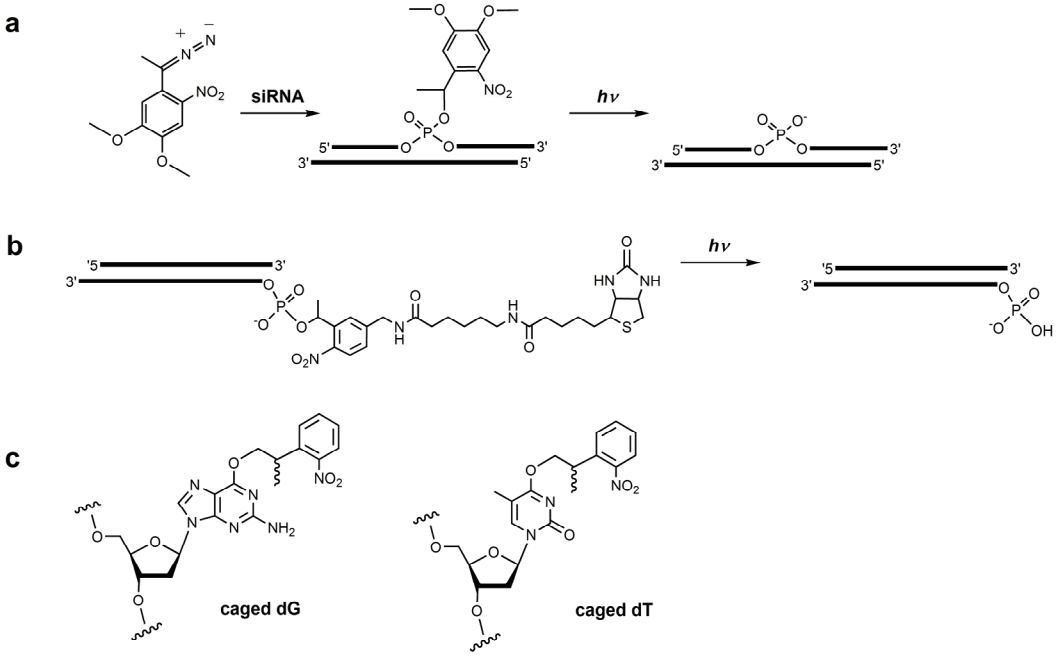

Figure 1.10. siRNA photocaging strategies: (a) random phosphate caging,[198] (b) antisense 5'-phosphate caging,[199] and (c) nucleobase caging.[201]

Instead of modifying the phosphates, it has been shown that caging of one or two antisense-strand nucleobases at positions around the cleavage site (bases 9-11) can effectively bring siRNA under the control of light (Figure 1.10c).[201] Using this strategy allows synthesis of samples containing very little uncaged siRNA, which helps ensure very low siRNA activity before UV irradiation. After irradiation, the activity was almost indistinguishable from that of unmodified siRNA.

1.3.4. Conclusions and future perspectives, siRNA modification

Appropriate chemical modifications are essential for bringing RNAi to the clinic. Although investigation was initially focused on increasing serum stability, the need for chemical modification is much broader. The areas of specificity and delivery are among the greatest challenges to RNAi therapeutics, and chemistry will certainly be a big part of the solution to both problems.

Several frontiers remain in the field of chemically modified siRNAs. Most of the currently-used strategies have significant sequence dependence; thus the remaining challenge is to find universal chemical modification strategies, or to predict reliably which modifications will be effective for a given sequence.

Many of the best modified siRNAs consist of a combination of multiple chemical modifications.[123,142,159,163] Yet most of the research being done on new chemically modified siRNA involves only one type of modification. Therefore, there is an ongoing need to combine chemistries in creative ways, if the field is to move toward universal chemical modification architectures. These modified duplexes will in turn benefit from improved delivery vehicle designs.

Many obstacles remain on the road to therapeutic siRNA, but many of them are already being removed. Creative and wise use of chemistry will continue to make a key contribution to progress in almost all of these areas.

1.4 2'F-ANA

1.4.1 Introduction

Most of the research in this thesis has had a connection with 2'-deoxy-2'-fluoroarabinonucleosides (2'F-araN) and oligonucleotides (2'F-ANA). Therefore, it is appropriate to review the history of 2'F-ANA research, mentioning various properties of 2'F-ANA as well as some new avenues of development in recent years.

The synthesis of 2'F-araN was first reported in 1969.[202,203] Since then, the study of these compounds and their oligonucleotide derivatives has remained a particularly active area of research. From the very beginning, much of the research has been aimed at therapeutic applications. At least five 2'F-araNs have reached clinical trials, of which only one has been approved for medical use (Table 1.2). The oligonucleotides (2'-deoxy-2'-fluoroarabinonucleic acids; 2'F-ANA) are now being studied for both therapeutic and non-therapeutic applications.

We will briefly summarize the history and development of 2'F-ANA, beginning with several significant 2'-deoxy-2'-fluoroarabinonucleosides. In the interests of space, only those with a true 2'-deoxy-2'-fluoroarabinose sugar will be discussed; many other modified nucleosides and derivatives containing a top-face (β) fluorine at the 2'-position have been omitted but are described elsewhere,[204] including the 2'-difluoro cancer drug gemcitabine[205] and the 2',3'-dideoxy adenosine derivative lodenosine.[206,207]

From there, we will move to a review of the properties of 2'F-ANA oligonucleotides, given in historical perspective. Finally, we will examine various other 2'-fluoroarabinooligonucleotide derivatives inspired by 2'F-ANA.

1.4.2 2'-Deoxy-2'-fluoroarabinonucleosides

1.4.2.1 Several notable 2'-deoxy-2'-fluoroarabinonucleosides

Several factors provided motivation to explore the 2'-deoxy-2'-fluoroarabinonucleosides. Fluorine has a small steric effect but a significant influence on nucleoside conformation and stability owing to its high electronegativity. For instance, the 2-deoxy-2-fluoroarabinose moiety provides

resistance to hydrolytic (acid-catalyzed) or enzymatic (phosphorylase) cleavage of the N-glycosidic bond.[208,209] Thymine and other 5-substituted pyrimidine nucleosides exhibit better antiviral activity with 2-fluoroarabinose than with 2-deoxyribose or arabinose sugars.[210] Thus FMAU (2'-fluoro-5-methyl-β-D-arabinouridine, Figure 1.11a) attracted significant attention for its antiviral activity, especially against Herpes Simplex Virus (HSV).[210-212] Despite its significant antiviral and anticancer activity,[213] FMAU caused significant neurotoxicity and myelosuppression at the doses required for activity,[214] and was found to be incorporated into DNA by eukaryotic as well as viral enzymes.[215,216] More recently it was discovered that the enantiomer L-FMAU (clevudine, Figure 1.11b) exhibits a more favorable therapeutic index than D-FMAU against Hepatitis B Virus (HBV) and Epstein-Barr Virus (EBV).[217-220]

A third nucleoside to have been tested in humans is fiacitabine (2'-fluoro-5-iodo-β-D-arabinocytidine (FIAC), Figure 1.11c). This nucleoside showed much higher activity against HSV than other drugs of its day.[221] After performing well in several Phase I and Phase I/II trials, it was eventually abandoned for reasons of toxicity. FIAC was found to be metabolized to FIAU[222] (2'-fluoro-5-iodo-β-D-arabinouridine, Figure 1.11d).[210] The latter had already demonstrated antiviral activity, and the focus of clinical work shifted to it, hoping to avoid the toxicity associated with FIAC. Indeed, it had a good short-term toxicity profile, but a longer-term, low-dose Phase II trial was cancelled after five patients died of liver failure, probably due to mitochondrial toxicity.[223] Clinical development of both FIAC and FIAU have been the subject of thorough reviews, to avoid future similar outcomes.[224] Additional details of the antiviral activities of 2'-fluorinated arabinosyl-pyrimidine nucleosides is provided elsewhere.[225]

Compound	Figure	Type	Notes
FMAU	1a	D-nucleoside	Potent antiviral and antileukemic activity. A Phase I trial for activity against solid tumors was terminated due to severe neurologic toxicity.[214]
L-FMAU (clevudine)	1b	L-nucleoside	Performed well in a 2004 Phase II clinical trial against Hepatitis B,[220] currently being developed by Pharmasset, Inc.
FIAC (fiacitabine)	1c	Base-modified D-nucleoside	Showed good antiviral activity in several Phase I trials (early 1980s) and one Phase I/II trial (against VZV in immunocompromised patients, 1986),[226] but was withdrawn after another Phase I/II trial (1989) showed significant toxicity.[224]
FIAU (fialuridine)	1d	Base-modified D-nucleoside	Showed good activity against HSV and HBV. A 1993 Phase II trial against HBV. The trial was halted on an emergency basis.[224,227]
Clofarabine	2a	Base-modified D-nucleoside	Approved by the FDA (in 2004) and the European Union (in 2006) for the treatment of pediatric patients with relapsed or refractory acute lymphoblastic leukemia (ALL).[228,229]

Table 1.2. 2'-deoxy-2'-fluoroarabinonucleosides that have entered human trials.

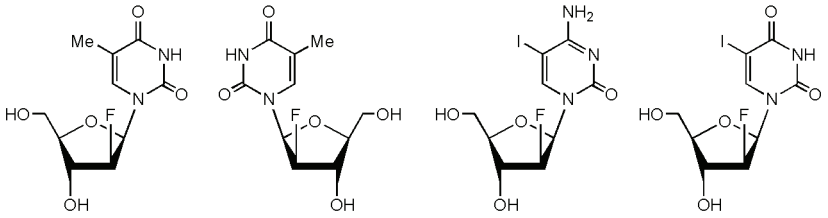

Figure 1.11. Four 2'-deoxy-2'-fluoroarabinonucleosides that have reached clinical trials.

The metabolism and DNA incorporation of other 5-modified 2'-fluoro-β-D-arabinonucleosides is significantly dependent on the 5-substituent.[215] FIAU and FEAU (2'-fluoro-5-ethyl-β-D-arabinouridine)[230,231] have recently found utility in positron emission tomography (PET)[232,233] and other imaging of experimental tumors and localized bacterial infections,[234] as a radiolabeled FIAU or FEAU molecule is preferentially phosphorylated by viral and bacterial kinases within

these systems. It is also noteworthy that FEAU is less toxic than other 2'F-araNs.[225] On the other hand, because of its greater uptake by eukaryotic DNA polymerases, ^{18}F-FMAU has been used for imaging of DNA synthesis *in vivo*.[235] Because of the very low concentrations required for PET, these nucleosides exhibit "no toxicity" when used for these imaging techniques.[234] Studies are underway to move these nucleosides toward clinical trials for this purpose.

The purine nucleosides 2'F-araA and 2'F-araG also show biological activity.[236-238] However in general, the 2'-fluoroarabino purine nucleosides have attracted less attention than their pyrimidine counterparts. The exception is clofarabine,[228,229,239] one of the most successful 2'-deoxy-2'-fluoroarabinonucleosides, which contains a modified purine, 2-chloroadenine (see Figure 1.12a). Clofarabine was developed while trying to improve upon the properties of two other adenosine-based anticancer drugs, cladribine and fludarabine (Figure 1.12).[240,241] The 2'-fluoro substitution yielded a glycosidic bond highly resistant to hydrolysis and phosphorylase cleavage.[241] Its anticancer activity results from inhibition of DNA polymerases and ribonucleotide reductase (which depletes the dNTP pool, favoring incorporation of clofarabine into DNA), and induction of apoptosis due to DNA damage after clofarabine incorporation.[239,241,242] Clofarabine was approved for treatment of pediatric acute leukemia by both the FDA (in 2004) and the European Medicines Agency (in 2006).

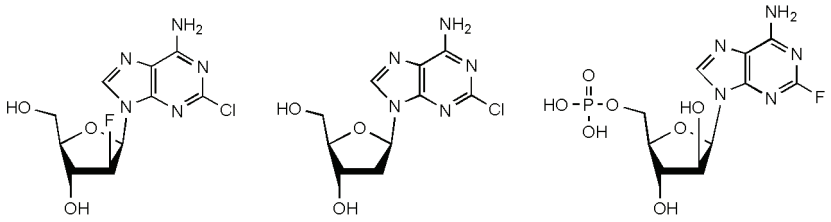

Figure 1.12. Clofarabine and the two other drugs from which it was inspired.

1.4.2.2 Synthesis of 2'-deoxy-2'-fluoroarabinonucleosides

From the earliest work on pyrimidine 2'-deoxy-2'-fluoroarabinonucleosides, the synthetic approach has been based on the coupling of the heterocyclic base to a 3,5-di-*O*-acyl-2-deoxy-2-fluoro-D-arabinosyl bromide (Scheme 1.1).[210,243] Occasionally the anomeric acetate has been used instead.[202] Direct introduction of top-face fluorine into the 2' position of a pyrimidine nucleoside by nucleophilic displacement would be very difficult because the carbonyl group at C-2 tends to displace any potential leaving group in the ribose sugar precursor before the fluorination can be carried out (Scheme 1.2).

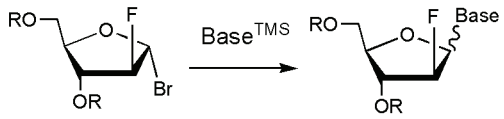

Scheme 1.1. Synthesis of 2'-fluoroarabinonucleosides is generally approached by coupling the base (normally trimethylsilylated at the carbonyl groups) to a 3,5-di-*O*-acyl-2-deoxy-2-fluoro-D-arabinosyl bromide.

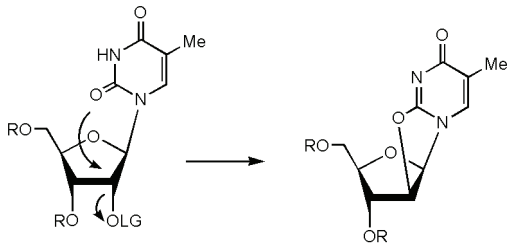

Scheme 1.2. Pyrimidine O2 rapidly displaces an alpha-face leaving group at C2', preventing direct synthesis of 2'-fluoroarabinonucleosides from ribonucleosides.

Synthesis of the requisite 3,5-di-*O*-acyl-2-deoxy-2-fluoroarabinosyl sugar has been carried out in a variety of ways (Scheme 1.3). Initial work used a methyl 2,3-anhydroribofuranoside as a key intermediate, which was in turn obtained from a protected xylofuranose (Scheme 1.3a).[202,244] Starting from a protected allofuranose reduced the number of separations required, increased the overall yield of product, and was more suitable for large scale synthesis, but required at least 8 steps (Scheme 1.3b).[243] 1,3,5-Tri-*O*-benzoylribose[245,246] is now commercially available and has been used as the starting point for most recent work, thereby simplifying the synthesis tremendously (Scheme 1.3c).[119,247]

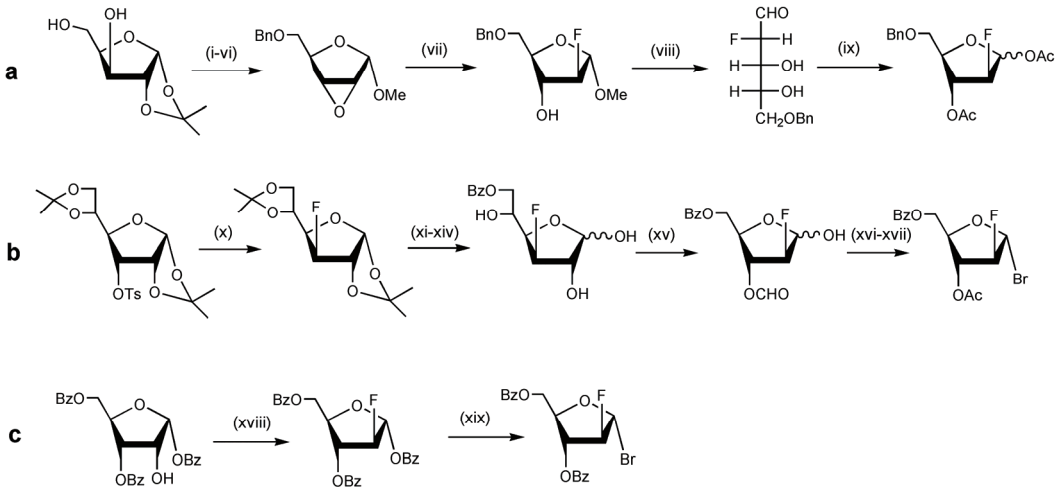

Scheme 1.3. Various synthetic routes to 1-acetyl or 1-bromo 3,5-di-*O*-acyl-2-deoxy-2-fluoroarabinose, suitable for coupling to nucleobases. Shown are (a) the first synthetic route,[202,244] (b) an early route amenable to larger scale synthesis,[243] and (c) the route used for most recent work.[119,247] Reagents and conditions: (a) (i) Methyl chloroformate in pyridine/chloroform, 0 ºC, 64h; (ii) TsCl, pyridine, 70 ºC, 6h; (iii) AcOH, Ac_2O, H_2SO_4, 19h; (iv) 1% HCl in MeOH, 19h; (v) NaOMe, MeOH, 47% over 5 steps; (vi) BnBr, Ag_2O, DMF; (vii) KHF_2, ethylene glycol, reflux, 40%; (viii) 1 N H_2SO_4 in dioxane/water, reflux, 4h, ~quant.; (ix) Ac_2O, pyridine, 18h. (b) (x) KF, acetamide, 210 ºC, 15 min, 62%; (xi) 0.35% H_2SO_4 in 1:1 methanol/water, rt, 10h; (xii) barium carbonate, reflux, 10 min; (xiii) BzCl, pyridine; (xiv) Amberlite IR-120 (H+), 78%; (xv) potassium metaperiodate, water, overnight; (xvi) NaOMe in MeOH; Ac_2O, pyridine, rt, overnight, 80%; (xvii) 30% HBr in AcOH; (c) (xviii) DAST, CH_2Cl_2, 40 ºC, 75%; (xix) 30% HBr, AcOH, CH_2Cl_2, 97%.

The fluorination step has almost invariably utilized nucleophilic displacement. The first synthesis was based on the opening of a 2',3'-α-epoxide, but this provided low yields and complex product mixtures.[202] Several authors have proposed one-pot[248] or two-step[243,245,249-252] sulfonate displacement reactions, using Bu_4NF,[243,252] KHF_2,[245,250] or $Et_3N{\bullet}3HF$[248,249,251] as the fluoride source. Diethylaminosulfur trifluoride (DAST), a mild, one-pot fluorinating reagent,[253] almost completely avoids dehydration (elimination) during the fluorination reaction. It has been used by many researcher groups.[119,208,247] One particular challenge is the scale-up of these reagents, since nucleophilic forms of fluoride such as KHF_2 or $Et_3N{\bullet}3HF$ are difficult to handle and require activation of the displaced hydroxyl group, and reagents such as DAST are too unstable to be useful on large scale. From the many options available,[254,255] Sznaidman *et al.*

have provided a possible solution in the form of a synthesis from arabinose, consisting of electrophilic addition of fluorine to a glycal moiety using the reagent Selectfluor™ (F-TEDA-BF_4).[256] Others have developed protocols that minimize the corrosiveness of the nucleophilic fluorinating agent, and have successfully reached a scale of up to 800 kg.[249]

Howell *et al.* made a major contribution to the glycosylation step by observing that the β-selectivity of the reaction could be made almost complete by carrying out the reaction in nonpolar solvents.[257] The reaction is thus forced to undergo an S_N2 mechanism from the α-bromo precursor, since the oxygen-C_1-onium ion required for an S_N1 reaction is already destabilized by the 2'-fluoro group, and cannot exist in the absence of solvent stabilization.[257] This approach results in high yields of β-nucleosides, which can be purified by crystallization. The mother liquor contains a residual mixture of α/β anomers that is very difficult to separate but can be enzymatically converted to 3'-*O*-benzoyl nucleosides that are separable by chromatography.[258]

In the case of the purine 2'-deoxy-2'-fluoroarabinonucleosides, some synthetic work has been undertaken by 2'-fluorination of ribonucleosides (reviewed by Pankiewicz,[259] another efficient route has been more recently reported by Maruyama *et al*.[260]) However, coupling to the fluorinated sugar, as described above for the pyrimidine nucleosides, has the advantage of divergence when both purine and pyrimidine nucleosides are made. In the case of guanine, the synthetic route utilizes a masked base, which is later converted into the desired guanine; initial attempts at this strategy used dichloropurine[261-264] or 2-acetamido-6-chloropurine,[236] but the synthesis can be improved and simplified using 2-chlorohypoxanthine instead.[265]

1.4.3 2'-Deoxy-2'-fluoroarabinonucleic acid (2'F-ANA)

1.4.3.1 The first 2'F-ANA oligomers

Pyrimidine 2'-deoxy-2'-fluoroarabinonucleosides (FMAU, FIAU, FAU and FAC) were first incorporated into oligonucleotides by Watanabe and co-workers in 1993 (Figure 1.13a).[266,267] Oligonucleotide synthesis using 2'-deoxy-2'-

fluoroarabino monomers was readily carried out using either phosphoramidite or H-phosphonate chemistry.[267] Another pair of studies incorporated FMAU into the self-complementary DNA Dickerson-Drew dodecamer.[268,269]

Meanwhile, quite a bit of work had been carried out on the arabinonucleic acids (ANA) (Figure 1.13b). Initial synthetic work in the Damha group[270,271] and elsewhere[272] paved the way for investigations into the hybridization and structure of ANA. As well as several hybridization studies of oligonucleotides containing one or two ANA modifications,[273-275] the hybridization of fully-modified ANA oligomers to various targets was studied.[276]

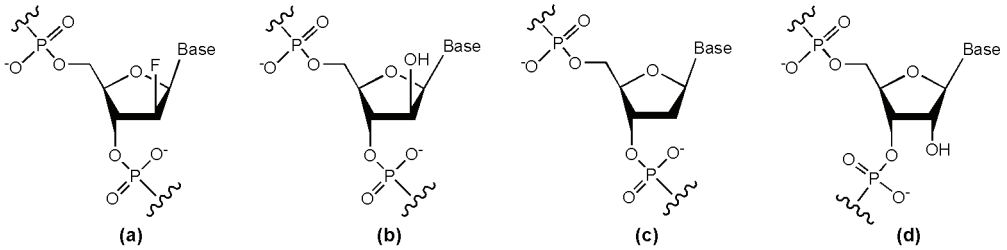

Figure 1.13. Structures of (a) 2'F-ANA and (b) ANA, in comparison with (c) DNA and (d) RNA oligomers.

In most contexts, ANA oligonucleotides bound to RNA target strands with somewhat lower affinity than DNA or RNA oligonucleotides.[276,277] The difference was even more dramatic in the case of DNA targets, to which very poor binding, or no binding at all, was observed.[276,277] It was speculated that the lower binding affinity of ANA might be due to steric hindrance of the top-face 2'-OH, perhaps lowering the efficiency of base-pairing or base-stacking.[277] In order to reduce the steric bulk of the 2' substituent, it was replaced by fluorine. This led to a study of mixed sequence, fully-modified 2'F-ANA sequences containing all four bases, using phosphoramidite chemistry.[118,119,278] As expected, the resulting 2'F-ANA•RNA and 2'F-ANA•DNA duplexes were much more stable. The reasons for this change, however, appear to be more complex than originally thought (see below).

When fully-modified ANA or 2'F-ANA strands were annealed with complementary ssRNA, their duplex conformation (as determined by circular dichroism (CD)) closely resembled that of a DNA:RNA duplex.[118] This observation prompted investigation of the recognition of the duplexes by RNase

H, a ubiquitous enzyme that cleaves the RNA strand of a DNA:RNA duplex. If an antisense oligonucleotide can induce RNase H-mediated RNA cleavage, it becomes a catalyst for the hydrolysis of multiple mRNA strands.[60]

Both ANA and 2'F-ANA were able to induce RNase H-directed cleavage of their complementary RNA strand, but the 2'F-ANA strand did so with higher efficiency.[118] ANA and 2'F-ANA represented the first examples of RNase H-competent oligomers that lacked 2-deoxy-D-ribofuranose. These findings also provided a very important advancement in understanding the catalytic mechanism and substrate selectivity of RNase H, and underscored the potential of arabinose-based oligomers as gene silencing agents. The higher efficiency of RNase H induction by 2'F-ANA, along with its higher binding affinity, made it the lead compound for further investigation into gene silencing applications.

1.4.3.2 Hydrolytic stability of 2'F-ANA to nucleases, acids and bases

Incorporation of 2'F-ANA into oligonucleotides of various types leads to improved resistance to hydrolytic cleavage by nucleases and acids. This topic is reviewed in detail in Chapter 3, where new results are also presented.

1.4.3.3 Binding affinity

When 2'F-ANA pyrimidine-modifed oligonucleotides were first synthesized, their binding to DNA was investigated and the results were somewhat mixed: 2'F-araT inserts stabilized duplexes but 2'F-araC or 2'F-araU tended to destabilize them, relative to a DNA strand.[266,267] FIAU, when incorporated into oligonucleotides, also conferred stabilization.[266] The added stabilization of FMAU and FIAU is consistent with the well-known favorable binding of 5-substituted pyrimidines.[279] It has been our experience that 2'F-ANA consistently demonstrates high binding affinity to both DNA and RNA.

A 2'F-ANA•RNA duplex is consistently more thermally stable than a DNA•RNA duplex. Depending on the sequence, the stabilization of fully modified strands ranges from 0.3 ºC/bp to 1.8 ºC/bp.[118,119,280,281] Replacing an all-purine DNA strand with 2'F-ANA (or modifying only the purines of a mixed sequence) tends to yield smaller increases than replacing an all-pyrimidine strand,[119] and in some cases no increase at all,[263] but not destabilization as was

originally predicted.[269] Interestingly, the highest stabilizations observed have been for mixed sequences (for example, up to 1.8 ºC/bp for a 10-mer mixed sequence).[281]

In some cases, 2'F-ANA•RNA duplexes are also more stable than RNA•RNA duplexes.[119,121,281,282] However, this is not always the case, and in other cases 2'F-ANA•RNA duplexes are of slightly lower stability than RNA•RNA duplexes.[119,282] Furthermore, in cases where 2'F-ANA•RNA duplexes are in fact more stable than RNA•RNA duplexes, some of the difference can be attributed to the fact that 2'F-ANA typically contains thymine bases while RNA contains uracil.[279] For example, duplexes of rT_{18} and $2'FaraT_{18}$ with rA_{18} were found to have similar melting temperatures (51 ºC and 52 ºC, respectively), but the T_m of rU_{18}•rA_{18} was 17 ºC lower.[119]

A phosphorothioate backbone reduces the binding affinity of DNA or 2'F-ANA relative to a normal phosphodiester backbone.[283] However, PS-2'F-ANA binds to RNA with higher affinity than PS-DNA (about 0.5 ºC/bp).[284]

The binding affinity of 2'F-ANA–DNA chimeras has also been studied. For example, so-called "altimers" (Figure 1.14) containing alternating stretches of 1, 2, 3 or 6 2'F-ANA nucleotides interspersed with 3 or 6 DNA units had T_m values increased by 0.6–0.8 ºC per 2'F-ANA insert (to RNA, with respect to an all-DNA strand). Fully modified 2'F-ANA strands of the same sequences caused a T_m increase of 0.75 ºC/bp.[280] Thus these architectures cause no major change in the binding affinity of 2'F-ANA on a per-insert basis. This is in contrast to a 2'-OMe-RNA–DNA chimera, for which a 1-1 altimer architecture was significantly destabilized in its binding to RNA (0.8 ºC per RNA insert) with respect to an all-DNA strand.[280] This demonstrates the compatible conformations of DNA and 2'F-ANA, but the conformational incompatibility of DNA and RNA (the latter apparently inducing multiple AB junctions within the duplex).[268] Another study has shown that these findings are also applicable to the binding affinity of 2'F-ANA–DNA chimeras with phosphorothioate backbones.[285]

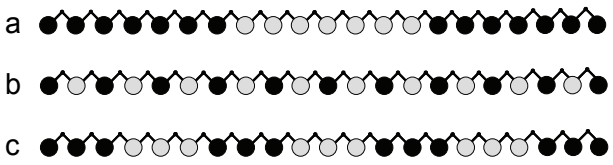

Figure 1.14. Sample architectures of chimeric strands, to illustrate terminology. (a) gapmer, (b) 1-1 altimer, (c) 3-3 altimer. In a typical 2'F-ANA–DNA chimera, the dark-colored beads would symbolize 2'F-ANA residues and the lighter beads would symbolize DNA.

The binding of 2'F-ANA–RNA chimeras is also more favorable than an all-RNA strand, whether binding to an RNA or DNA target strand.[121] However, the enhanced binding is particularly strong when the target strand is DNA. This has been shown for various architectures, including a "gapmer"-type structure (a central 2'F-ANA region with RNA wings, see Figure 1.14) and siRNA duplexes.[121]

Fully-modified 2'F-ANA strands, in contrast to ANA, also bind with high affinity to ssDNA. In one study of five 18-mer sequences, 2'F-ANA showed increased binding affinity (to DNA) ranging from 0.2 to 0.9 ºC/bp relative to DNA, and 0.4 to 1.7 ºC/bp relative to RNA.[119]

2'F-ANA also forms stable homoduplexes (that is, 2'F-ANA•2'F-ANA duplexes). While ANA•ANA duplexes tend to be highly unstable,[286] 2'F-ANA•2'F-ANA duplexes are more stable even than 2'F-ANA•RNA or RNA•RNA.[281,282]

One important finding related to binding affinity is that 2'F-ANA has a very high base pairing specificity. When a single mismatch was introduced into a DNA target strand, the T_m of the duplex dropped most sharply when the test strand was 2'F-ANA (8.0 ºC), followed by RNA (7.2 ºC), then DNA (3.9 ºC).[119] When using an RNA target strand, introduction of a single mismatch caused the T_m of the duplex to drop most sharply when the test strand was RNA (9.3 ºC), followed by 2'F-ANA (6.6 ºC), then DNA (5.4 ºC).[119] High base pairing specificity is essential for applications such as microarrays and other diagnostics, as well as for therapeutic applications.

We conclude this section by returning to the observation that the binding affinity of 2'F-ANA, to both RNA and DNA target strands, is dramatically higher

than that of the related modification ANA. This is especially true when the target strand is DNA; many ANA•DNA duplexes are so unstable that they are barely detectable. The dramatic increase in target affinity upon changing OH to F has stimulated numerous studies by our group into the structure of 2'F-ANA and its duplexes, in an attempt to understand the causes of this difference. Studies of 2'F-ANA conformation and hydration in the context of oligonucleotides are discussed in Chapter 2, and studies of the conformations of 2'F-araN (and related derivatives) are discussed in Chapter 4.

1.4.3.4 Optimization of RNase H activity and recent antisense applications

The combination of high-affinity, specific binding, nuclease stability and RNase H activation attracted significant interest 2'F-ANA, and studies were soon undertaken to characterize and optimize its antisense activity.[287]

A fully modified 2'F-ANA strand induces RNase H cleavage to a lesser extent than DNA. Lok *et al*. tested phosphorothioate gapmers (see Figure 1.14) containing 2'F-ANA wings and a central DNA gap, and showed that the combination is more active than a strand containing only DNA.[284] Furthermore, the potency of the chimera was unchanged for gap sizes ranging from 4 to 10 nucleotides. This was in sharp contrast to chimeras containing RNA wings and a central DNA gap, whose potency dropped below that of all-DNA strands when the DNA gap size dropped below 8 nucleotides.[284] It was suggested that the potency of the 2'F-ANA–DNA chimera is related to its increased flexibility with respect to an all-2'F-ANA strand. Accordingly, insertion of an acyclic nucleoside or an alkyl linker into 2'F-ANA oligonucleotides increased their ability to induce RNase H (Figure 1.15).[288] This held true even when the AON targeted a highly structured RNA.[288] The 2'F-ANA AONs containing butyl linkers comprised the first examples of high potency AONs containing unstructured elements which did not participate in base-pairing.[288] A peptide nucleic acid (PNA) insert within a 2'F-ANA strand also provided some improvement in RNase H activation, although not as much as a butyl linker.[289] Thus, either DNA–2'F-ANA chimeric constructs or flexible units within a 2'F-ANA AON provided means of improving the ability of 2'F-ANA to activate RNase H.

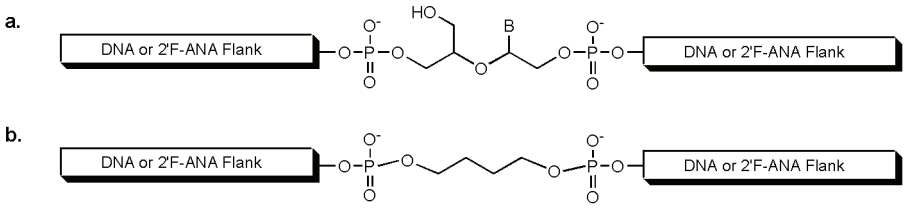

Figure 1.15. Insertion of (a) an acyclic nucleotide or (b) a butyl linker into 2'F-ANA oligonucleotides increases their ability to induce RNase H. Adapted from Mangos and Damha.[287]

The DNA–2'F-ANA chimeric constructs were also optimized. It was found that a 3-3 altimer construct (Figure 1.14) provided the highest potency RNase H-activating AON, equal to or better than a DNA gap surrounded by 2'F-ANA wings (gapmer).[280] Both the altimer and gapmer strand architectures consistently outperformed DNA itself, and were applicable to both PO and PS backbones.[63,280,284,290] A study on luciferase knockdown in HeLa cells demonstrated that PS-2'F-ANA altimers and gapmers outperform both PS-DNA and PS or mixed backbone DNA–RNA chimeras.[63] The PS-2'F-ANA gapmer gave comparable results to the better of two siRNAs targeting luciferase mRNA, in both potency and duration of action.[63]

These optimized AONs have seen several recent applications. Lacombe *et al*. showed that PS-2'F-ANA–DNA chimeras are more effective than PS-DNA AONs in reducing expression levels of Flk-1, a VEGF receptor. However, both chemistries gave comparable levels of VEGF activity.[285] Kalota *et al*. found that both altimer and gapmer architectures of PS-2'F-ANA–DNA chimeras were able to silence expression of c-MYB (a protooncogene involved in various hematologic malignancies) in human leukemia cell line K562 at 20% of the concentration of the corresponding PS-DNA AONs.[290] Furthermore, gene silencing using the 2'F-ANA-modified AONs was nearly complete, and lasted twice as long as the unmodified AONs.[290]

2'F-ANA oligomers are close to being clinically validated. TPI-1100, a PS-2'F-ANA–DNA chimera designed to treat chronic obstructive pulmonary disease (COPD), is being developed by Topigen Pharmaceuticals, Inc. Delivered *via* aerosol, TPI-1100 inhibits the expression of multiple phosphodiesterases

(PDEs) considered therapeutic targets for alleviating COPD, a deadly, debilitating disease characterized by inflammation of the airways. Local delivery of TPI-1100 has the advantage that the dose of the oligomer required for efficacy is significantly lower (μg) when delivered directly to lung tissue. Pulmonary delivery also potentially reduces undesirable systemic side effects, and overcomes the challenges of systemic delivery of oligonucleotides that target tissues within the body. Phase 1 clinical studies are planned to start within the next 12-18 months.[291]

1.4.3.5 siFANA

2'F-ANA can be used to modify siRNA, as discussed in Section 1.3.2.1. We present new results on 2'F-ANA-modified siRNA in Chapter 5.

1.4.3.6 2'F-ANA-modified triplexes, aptamers and higher-order structures

One of the earliest studies on 2'F-ANA demonstrated that it can effectively form "pyrimidine motif" triplexes where a pyrimidine-rich third strand binds parallel to the purine strand of a target duplex.[292]

Aptamers, nucleic acid species with binding or catalytic properties, have generated intense interest in recent years because they are so readily available via molecular evolution techniques, often called SELEX (Systematic Evolution of Ligands by Exponential Enrichement).[293-295] To make aptamers containing chemical modifications (to improve their properties, especially nuclease resistance), modified triphosphates can be used during the evolution process, or the unmodified aptamer can be carefully modified after determination of its sequence. The latter avenue toward modified aptamers is more challenging, since chemical modifications can affect the structure and properties of the aptamer in a way not accounted for by the selection process. However, it allows modification at selected positions and using nucleotides not amenable to the SELEX process. For example, the first aptamer-based therapeutic, Macugen® (pegaptanib sodium), was approved by the FDA in December 2004. This aptamer was discovered by the SELEX method (including use of some modified nucleoside triphosphates) but was subsequently optimized ("post-SELEX modification") to confer biostability required for *in vivo* use.[296]

1.4.3.6.1 Non-evolution-based 2'F-ANA aptamers

More recent work has shown that 2'F-ANA is suitable for use in the modification of aptamers containing G-quartets.[297] The top-face fluorine of 2'F-ANA nucleotides favors the *anti*-orientation around the glycosidic bond. Consistent with this, 2'F-ANA modification of *anti*-dG residues of three different G-quartet-containing DNA aptamers led to increased thermal stability, as well as increased nuclease resistance. Replacement of the *syn*-dGs, on the other hand, led to decreased stability or a total structural transformation. A thrombin-binding aptamer had up to 48-fold greater stability to 10% FBS when modified with 2'F-araN residues.[297] As well as the G quartets, 2'F-ANA modification of certain thymines in a loop of this aptamer caused increased thermal stability, nuclease resistance and binding to thrombin.[297]

The i-motif, a C-tetrad structure formed by C-rich DNA sequences,[298] has also been modified with 2'F-araN residues. 2'F-ANA modification of all Cs in the hexamer dTCCCCC led to an 8.5 ºC decrease in thermal stability at pH 4.5. However, the 2'F-ANA-modified structure was stable over a much wider range of pH (for example, its T_m values were 6.5 ºC higher than those of the DNA structure at pH 3.5). Since the i-motif involves C•C^+ base pairs,[298] this finding can be explained by the lower pK_a of 2'F-araC (3.88) than dC (4.5).[203] This study also demonstrated that the preorganization of 2'F-ANA led to more favorable kinetics for the modified C-tetrads. Improvements in pH range and kinetics are thus two ways in which 2'F-ANA may broaden the scope of applications of aptamers.

In another study, branched oligonucleotides made of dC or araC were shown to associate into the i-motif at acidic pH, unlike the corresponding RNA structures.[299] This occurs in spite of the fact that most of the sugar residues in i-DNA tetrads adopt the C3'-*endo* (north) sugar pucker. It was attributed to different steric effects of the 2'-substituent.[299]

1.4.3.6.2 SELEX using 2'F-ANA

For a modified nucleotide to be compatible with the SELEX process, two conditions are necessary: (1) the corresponding nucleoside 5'-triphosphates must be substrates of a polymerase enzyme, able to be incorporated with good fidelity

in a PCR-type system, and (2) the modified strand must be able to act as a template for the creation of a corresponding cDNA library. 2'F-araN 5'-triphosphates are indeed substrates of several readily available polymerase enzymes. Surprisingly, in some cases they are incorporated with higher fidelity than dNTPs.[300] The biosynthesis of pyrimidine 2'F-ANA and 2'F-RNA triphosphates was later compared using four DNA polymerases. It was found that 2'F-araTTP was significantly better incorporated than 2'F-rUTP, but 2'F-rCTP was slightly preferred over 2'F-araCTP.[301]

As for the second condition, it has been shown that a chimeric 2'F-ANA–DNA strand can act as a template for the biosynthesis of a chimeric complementary strand, and in other experiments, that a fully-modified 2'F-ANA strand can act as a template for the biosynthesis of a complementary DNA strand.[300] Thus, 2'F-ANA appears to have great potential for use within the SELEX process.

1.4.4 Other oligonucleotide derivatives based on 2'F-ANA

The attractive properties of 2'F-ANA have stimulated the development of several other 2'F-ANA-based oligonucleotide derivatives (Figure 1.16).

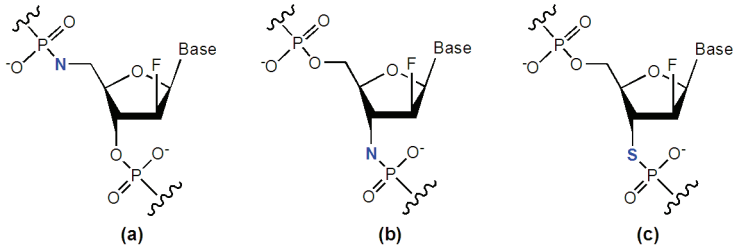

Figure 1.16. Other oligonucleotide derivatives based on 2'F-ANA. (a) 2'-fluoroarabino P3'—N5' phosphoramidates ;[302] (b) 2'-fluoroarabino N3'—P5' phosphoramidates ;[303] (c) 3'S-FANA.[304]

For example, a 2'F-ANA sugar has been tested in combination with P3'—N5'[302] and N3'—P5'[303] phosphoramidate linkages. For the P3'—N5' linkage, the resulting oligonucleotide analogue had lower binding affinity than its phosphodiester counterpart, but retained the ability to elicit RNase H activity.[302] In fact, the 2'F-ANA phosphoramidate analogue was better able to elicit RNase H activity than a corresponding DNA phosphoramidate oligomer.[302] As for the N3'—P5' phosphoramidate backbone, nucleosides introduced into this backbone appeared to pucker in the north.[303] This may be due to the stereoelectronic effect of changing the 3' group to an amine since the corresponding 2'-deoxy phosphoramidate showed a similar conformation.[303] The 2'F-ANA N3'—P5' phosphoramidate showed increased stability to base with respect to its 2'-epimer, phosphoramidate-linked 2'F-RNA, but lower binding affinity to DNA and RNA.[303]

2'F-ANA nucleosides have previously been modified with sulfur at the 3' position: Elzagheid *et al*. described the synthesis of 2'-deoxy-2'-fluoro-3'-thioarabinothymidine.[304] This synthesis has been challenging to repeat, however, since the 3'-SH group (in the precursor to the phosphoramidite) tends to displace the 2'-fluorine, resulting in a 2',3'-episulfide product.[305]

A fourth derivative based on 2'F-ANA has also recently been developed: In Chapters 4 and 5, we present the synthesis of a 2'F-ANA analogue modified with sulfur at the 4' (ring heteroatom) position, describe a conformational change observed for this 4'S-FANA analogue, and explore its biological implications.

1.4.5 Considerations for use of 2'F-ANA *in vivo*

Given the toxicity of 2'-deoxy-2'-fluoroarabinonucleosides such as FMAU and FIAU, discussed above, any potential *in vivo* use of 2'F-ANA in therapeutics must provide assurance that the catabolic metabolites (2'F-araN and their nucleotides) will not cause significant side effects. However, the success of the nucleoside analogue clofarabine, the progression toward use of 2'-fluoroarabinonucleosides as PET tracers, and the ongoing pre-clinical studies on 2'F-ANA discussed above makes it clear that 2'F-ANA remains a promising entity for therapeutic use, as long as the *in vivo* concentrations of the constituent nucleosides remain low. An

initial preclinical toxicology study has been performed in mice to compare the toxicological profile of a phosphorothioate 2'F-ANA-containing oligonucleotide (5-gap-4 configuration) and a phosphorothioate DNA oligonucleotide following repeated administrations. The sequence used in the study was that of Monia *et al.*, ISIS 5132, targeting the human c-Raf-1.[306] The oligonucleotides were administered every other day for 28 days (14 doses) at a dose up to 50 mg/kg by iv injection *via* the lateral tail vein. In line with previous reports, the toxicities observed in this study all appeared to be related to the phosphorothioate chemical class of the oligonucleotides.[307] Furthermore, no clear difference could be observed between the two chemistries, suggesting that they are not side effects of 2'F-ANA. Due to the greater efficacy and stability of 2'F-ANA oligos, it is expected that a lower or less frequent dosing will be effective, thus lowering any toxicity.

1.4.6 Summary, 2'F-ANA

2'-Fluoroarabinonucleosides are immensely versatile chemical modifications on their own or in oligonucleotides. 2'F-araNs such as clofarabine are already being used as therapeutics, and other compounds are being studied as drugs and for *in vivo* applications such as PET. While 2'F-ANA oligonucleotides form a stable duplex with RNA and these duplexes activate RNase H, additional structural alterations to the backbone further increase the capability to inhibit protein expression. This optimization can be done using gapmer or altimer chimeric constructs, or flexible linkers, according to the target sequence. Different chimeric constructs can also be used in the application of 2'F-ANA to other oligonucleotide approaches (siRNA and aptamers).

2'F-ANA oligonucleotides significantly enhance nuclease resistance, providing lower dosage requirements and the potential for improved systemic administration and safety for oligonucleotide therapeutics including antisense, aptamers, and siRNA. The increased stability exhibited by 2'F-ANA-modified oligonucleotides has the potential to increase their *in vivo* efficacy. This stability is tunable in that the half life *in vivo* can be controlled by the extent of 2'F-ANA modification. 2'F-ANA-modified oligomers allow for highly potent, long-lasting gene silencing

effects in both antisense and RNAi approaches. In a series of studies comparing available AON chemistries, 2'F-ANA oligonucleotides showed an improvement in target affinity and duration of gene response while improving efficacy.[63] The unique characteristics of 2'F-ANA could be advantageous for a wide variety of therapeutic gene or protein modifying applications, including topical and systemic administration. A drug candidate is scheduled to enter clinical trials in 2009.

1.5 Techniques used in the scientific study of oligonucleotides

This section will briefly review the techniques most essential to the research contained in this thesis.

1.5.1 Ultraviolet (UV) spectroscopy

Because of their heterocyclic bases, oligonucleotides have a strong UV absorbance signature centered at about 260 nm. UV spectroscopy is therefore a useful technique for study of nucleic acids.

The absorbance of a solution of oligonucleotide can be used to determine its concentration, since the oligonucleotide's absorption coefficient (ε) can be calculated from its base sequence. Furthermore, the shape of the absorbance curve can provide some information about the purity of the sample.

Furthermore, measuring the change in UV absorbance with changing temperature provides information about the thermal stability of the duplex. When purine and pyrimidine bases stack, the alignment of their dipoles reduces their UV absorbance (this phenomenon is called hypochromicity).[308] Thus, as a duplex denatures, stacking is reduced, and the absorbance increases. The melting temperature (T_m) is defined as the point at which half the sample is duplex and half is denatured; this is the midpoint of the baseline-corrected absorbance *vs.* temperature curve. Thermodynamic information can also be obtained by analyzing the shape of the T_m curve or the concentration dependence of the T_m.[309]

1.5.2 Gel electrophoresis[310]

Under the influence of an electric field, polyanionic oligonucleotides migrate toward the positive electrode. A matrix such as polyacrylamide acts as a sieve, separating the oligonucleotides by size and shape. Thus polyacrylamide gel electrophoresis (PAGE) is a fundamental tool in oligonucleotide research, both for analysis and purification.

The studies reported in this thesis make use of three methods of visualizing the oligonucleotide bands after electrophoresis. For purification, the bands are visualized using UV shadowing, by placing the gel above a fluorescent surface and viewing it under UV light. The band is then cut and the pure oligonucleotide eluted from the gel slice. For analytical PAGE, better results are usually obtained by staining with an intercalating reagent such as Stains-All (3,3′-diethyl-9-methyl-4,5,4′,5′-dibenzothiacarbocyanine bromide), or by autoradiography using radioactively (in our case, ^{32}P) labeled oligonucleotides.

1.5.3 High-Performance Liquid Chromatography (HPLC)[311]

HPLC is a powerful separation technique essential for much of contemporary research in chemistry and biology. Several approaches can be used for the separation of oligonucleotides. And like electrophoresis, the scale of HPLC can easily be adapted for use in analysis (of sample purity or assay progress) or purification of oligonucleotide samples.

Two types of HPLC columns are commonly used for separation of oligonucleotides. Anion-exchange HPLC makes use of a tightly packed ion-exchange resin which binds the oligonucleotides because of their polyanionic nature. By increasing the salt content of the eluent, the sample can then be eluted. Thus separation is based primarily on the ionic nature of the analyte (usually related to the number of phosphates and thus the length of an oligonucleotide).

Reverse-phase HPLC, on the other hand, is based on interactions between the oligonucleotide and a nonpolar solid support. Samples are typically loaded in buffer containing a small amount (5%) of acetonitrile or methanol, and the organic content is gradually increased to elute the sample. An ion-pairing buffer

such as triethylammonium acetate is generally used to increase the hydrophobicity of the oligonucleotide, since the alkylammonium salts pair with the phosphates.

1.5.4 Mass Spectrometry

Mass spectrometric analysis of nucleic acids is challenging because of their polarity and thermal lability.[312] However, recently developed ionization methods such as MALDI and ESI have allowed extensive work on mass spectrometry of nucleic acids to be realized.[312] Electrospray ionization can be coupled with higher accuracy mass analyzers, and also provides several ion peaks due to multiply charged species, which can be averaged to result in a more accurate mass determination.[313] This greater accuracy allows higher confidence that a synthetic oligonucleotide is correctly made and also helps in identifying minor impurities.

1.5.5 Circular dichroism (CD) spectroscopy[314]

Plane-polarized light can be considered as being made up of equal amounts of left and right circularly polarized light. In the presence of a chiral molecule, left and right circularly polarized light are absorbed to a different extent. The resulting signature can be used to characterize the chiral structure of the molecule in solution.

The CD technique is very useful to study chiral secondary structures such as nucleic acid helices, which have a characteristic signature. Thus A-form and B-form structures can be readily distinguished, and helical distortions can often be observed. While CD remains a qualitative technique, it provides useful information and is commonly used because of its ease.

1.5.6 Nuclear magnetic resonance (NMR) spectroscopy[315]

For more quantitative, detailed work on nucleic acid structure in solution, NMR is the method of choice. Various NMR techniques can be used to provide many types of information about nucleic acid structure.

Analysis of vicinal $^{1}H–^{1}H$ coupling constants provides information about the dihedral angles of the sugar ring of nucleosides and nucleotides, according to the well-known Karplus equation.[316] This in turn provides information about the sugar pucker (including the presence of multiple puckers in the conformational

equilibrium). Details on the use of coupling constants in the conformational analysis of nucleosides are provided in Section 4.3.

A great deal of information about secondary structure and conformation can be obtained by using 2D NMR methods such as NOESY, which provides information about the spatial proximity of nuclei.[315] It can be used to assign residues by connecting each nucleus in a certain region (*e.g.* imino protons) to its closest neighbor. Once the assignments are completed, NOESY spectroscopy can provide a great deal of information about secondary and tertiary structure. This technique is usually used in combination with computational methods (see below).

Finally, other NMR methods (*e.g.* based on linewidths) can be used to provide information about oligonucleotide dynamics (for example, base pair lifetimes[317]).

1.5.7 Molecular modeling[318]

Several computational techniques are useful in the study of nucleic acids. At the level of nucleosides, computationally expensive techniques such as DFT calculations are feasible and provide useful information about conformational preferences and stereoelectronic effects.

For the study of oligonucleotides, molecular mechanics methods are more feasible. Two of the best programs, with associated force fields, are AMBER[319,320] and CHARMM.[321,322] Molecular mechanics methods allow computation quickly enough that they can be used for molecular dynamics (MD) calculations, which are very useful in exploring the flexibility and conformational ensembles of oligonucleotides.[323] After all, oligonucleotides are not static: their flexibility is central to their function and recognition; however it is often overlooked by traditional methods of structure determination (*e.g.* X-ray crystallography). MD calculations involve recalculation of the structure at many very small intervals (typically on the order of a femtosecond apart, over a period of tens of nanoseconds).[42]

Molecular modeling techniques often work in tandem with NMR spectroscopy or other experimental techniques. For example, NOESY contacts can be used as distance restraints for structural minimizations.

1.5.8 Osmotic stressing[324]

Direct methods for studying the hydration of nucleic acids are few and far between. However, as discussed above, hydration (Section 1.1.4) is key to the structure, stability and molecular recognition of nucleic acids.

One method of obtaining information about hydration is to study transitions (such as duplex melting) in the presence of organic cosolutes that reduce the activity of water. This method was first applied to melting of nucleic acids by Spink and Chaires.[325] It was later demonstrated that the technique gives correct results for short oligonucleotides as well.[326] Others have used it to study the influence of hydration in DNA–protein interactions.[52]

However, in spite of the general agreement of this method with other techniques for studying hydration (*e.g.* X-ray crystallography), it remains inherently vulnerable to errors since the small molecules used to perturb water structure can in principle interact directly with the nucleic acid duplexes. Indeed, some small but significant changes in binding enthalpy have been observed in the presence of various cosolutes, indicating direct cosolute–nucleic acid interactions.[327] This technique is discussed in greater detail in Chapter 2.

1.6 Thesis objectives

1.6.1 Structure and hydration of 2'F-ANA and ANA

The dramatic difference in the binding affinities of 2'F-ANA and ANA remains a mystery, as discussed in Section 1.4.3.3. Previous structural studies by NMR spectroscopy revealed very similar conformations, and no obvious steric hindrance that would explain the low binding affinity of ANA.[328,329] In Chapter 2, two studies are described to further explore this difference. The first is an NMR/MD study of three decamer duplexes (a more realistic system than the hairpins previously used for NMR). The second is a study of duplex hydration, using the osmotic stressing technique described in Section 1.5.8.

1.6.2 Hydrolytic stability of 2'F-ANA

2'-Fluoroarabinonucleotides have demonstrated resistance to acid-catalyzed degradation.[208,330] However, nothing is known about the acid stability of 2'F-ANA oligonucleotides. In Chapter 3, a study is presented which explores the acid-

mediated cleavage of 2'F-ANA oligonucleotides. New applications of 2'F-ANA related to its exceptional acid stability are discussed.

In the past, 2'F-ANA has demonstrated improved nuclease stability relative to DNA and RNA.[120,267,277] In a second section of Chapter 3, the nucleolytic hydrolysis of 2'F-ANA is explored in greater detail. A particular area of focus is the stereochemistry of phosphorothioate-2'F-ANA cleavage by a 3'-exonuclease.

1.6.3 Novel application of 2'F-ANA to an exciplex diagnostic system

In the post-genomic era, nucleic acid biosensors will become increasingly important as medical diagnostic tools. 2'F-ANA has not yet been applied to diagnostic systems. The last section of Chapter 3 begins to address this question by presenting the application of 2'F-ANA to an exciplex-based nucleic acid biosensor.

1.6.4 Development of a 4'-thio analogue of 2'F-ANA

One of the ongoing interests of the Damha research group is the development of novel nucleic acid modifications. Several modifications based on 2'F-ANA are already known (Section 1.4.4).[302-304] In Chapter 4, the synthesis of a novel 4'-thio analogue of 2'F-ANA is described. Conformational analysis of the nucleoside indicated that this modification of the ring heteroatom caused a dramatic conformational shift. In Chapter 5, this new modification is used to modify functional siRNA duplexes. Furthermore, it is shown that this 4'S-FANA modification has a synergistic effect with 2'F-ANA modifications in the same siRNA duplex.

1.6.5 Application of 2'F-ANA to siRNA

As discussed in Section 1.3.4, very few universal patterns of chemical modification exist for siRNA. In Chapter 5, we present various studies towards meeting this need. For example, a second-generation 2'F-ANA sense strand is described that shows improved activity over fully-modified sense strands while including only a minimal number of RNA nucleotides.

The synergy between 2'F-ANA and the northern 4'S-FANA (see Section 1.6.4) inspired us to combine 2'F-ANA with other northern modifications. Thus, the second half of Chapter 5 describes a highly effective synergy between 2'F-ANA and 2'F-RNA, leading to a variety of fully modified duplexes with higher potency

than RNA itself, containing chimeric 2'F-ANA–2'F-RNA sense strands paired with a 2'F-RNA antisense strand. These duplex architectures showed excellent potency in two different duplexes targeting firefly luciferase. Studies on other mRNA targets are in progress, as we work toward universally accepted patterns of chemical modification for siRNA.

1.6.6 Development of a 4'-seleno analogue of RNA

Continuing in the theme of 4'-chalcogen-modified nucleic acids, Chapter 6 describes the first examples of oligonucleotides containing a 4'-selenoribonucleotide. The conformational behavior of 4'-selenoribonucleotides appears to be quite different in the context of oligonucleotides than as free nucleotides. This project makes a valuable contribution to the field of modified nucleic acids and their conformational behavior, and could also have useful applications in MAD phasing for X-ray crystallography.

Chapter 2. Structure and hydration of 2'F-ANA and ANA

2.1 Introduction

As discussed in Sections 1.4.3.1 and 1.4.3.3, the binding affinity of 2'F-ANA is much higher than that of ANA. Despite many conformational and computational studies on the two modifications, the origins of this difference remain a mystery.

2.1.1 Conformational studies of 2'F-ANA and ANA

2.1.1.1 Evidence from circular dichroism and thermal stability

The earliest information about the conformational properties of 2'F-ANA came by observing its effect on binding affinity (T_m) and helical structure (through CD spectroscopy). [119,268,282,331]

Two types of binding experiments can give information about conformation. The first examines the binding affinity of chimeric strands, *i.e.* those containing two types of oligonucleotides. If the binding affinity of a chimeric strand is lower than that of the modifications taken separately, it usually indicates that their conformations are not compatible. For example, when B-DNA was modified with 2'F-ANA units, the thermodynamic stability strongly increased. However, when 2'F-RNA units were used instead, the duplex was destabilized and the presence of an A-B junction was discerned by CD spectroscopy.[268] Thus, 2'F-ANA is a DNA mimic, or at least adopts a DNA-compatible conformation. The second way that binding affinity can be used to study conformation is by observing patterns in series. For example, the known order of stability of the A/T system is dA/dT > rA/dT > rA/rU > dA/rU.[331] Replacing the purine strands of 18 nt duplexes with 2'F-ANA and 2'F-RNA results in the order of stabilities 2'F-araA/dT (63.3 ºC) > 2'F-rA/dT (48.0 ºC) > 2'F-rA/rU (39.2 ºC) > 2'F-araA/rU (30.2 ºC).[282] Thus, the order is maintained, showing that 2'F-ANA and 2'F-RNA mimic the DNA and RNA structures, respectively.

Neither of these strategies has been as useful for providing information about the conformation of ANA. Fewer ANA-modified chimeric strands have been made, and patterns or series like the one above are harder to study since mixed sequences of ANA bind so weakly to DNA.[277]

General information about the conformation of oligonucleotides can be obtained from circular dichroic (CD) spectra. CD traces of 2'F-ANA•RNA and ANA•RNA duplexes are intermediate in form between DNA•RNA (A-B form) and RNA•RNA (A-form) CD traces.[119] Therefore, they have more A-form character than the DNA•RNA hybrid.

The CD spectrum of a pure 2'F-ANA•2'F-ANA duplex is also interesting in that it closely resembles the B-form signature above 250 nm, but has strong negative peaks at 207 and 245 nm that are closer to those of an RNA•RNA CD trace.[282] These two observations are consistent with 2'F-ANA's ability to mimic the DNA structure, while being compatible with RNA environments as well.

2.1.1.2 Quantitative conformational work on ANA and 2'F-ANA oligonucleotides

The first quantitative structural work on 2'F-ANA inserts in a DNA duplex was a crystallographic study which found that 2'F-ANA inserts in the Dickerson-Drew dodecamer adopted an O4'-*endo* pucker.[269] Significantly, the pucker of the neighboring nucleotides was not significantly affected.[269] Thus this rare conformation is fully compatible with the B-form helical environment.

The most significant structural study of ANA•RNA and 2'F-ANA•RNA duplexes to date examined short hairpins containing a 4 bp hybrid stem and a 4 nt DNA loop by NMR spectroscopy.[328,329] A third hairpin was studied comprising a DNA•RNA stem, for comparison. The conclusions of this study were as follows:

(1) The arabinose sugars of both 2'F-ANA•RNA and ANA•RNA duplexes are strongly preorganized into an O4'-*endo* (east) pucker.[328,329] Very strong H1'–H4' NOE crosspeaks are observed for both 2'F-ANA and ANA residues.[328,329] In contrast to the deoxyribose sugars of the DNA•RNA duplex, which are very dynamic, the ANA and 2'F-ANA sugars are quite rigid (at least 75% O4'-*endo*, with the other 0-25% made up of northern and/or southern puckers). The terminal nucleotides are exceptions, presumably because they have more conformational freedom due to end fraying. The rigidity of 2'F-ANA and ANA may explain the slower kinetics of RNase H cleavage of both modified hybrid duplexes[284] (see Section 1.4.3.4). However, since both are rigid, it cannot explain the difference in

duplex stability.[328,329] Two previous computational studies had also predicted the O4'-*endo* pucker for 2'F-ANA•RNA duplexes, but not for ANA.[332,333]

(2) The helical parameters, especially minor groove width, are similar for all three duplexes and are intermediate between A-form and B-form structures.[328,329] This may be the key to the recognition of all three duplexes by RNase H. This finding is consistent with earlier computational work on both duplexes.[332]

(3) No evidence for OH 2'–O5' hydrogen bonding was observed in the case of ANA sugars in the ANA•RNA duplex.[329] In contrast, previous computational work had attributed the predominant C2'-*endo* sugar pucker observed for ANA sugars in that study to the influence of H-bonding.[332]

(4) Very little difference was observed between the conformations of ANA and 2'F-ANA.[329] Since no steric hindrance was observed in the case of ANA, and the conformation and flexibility did not differ significantly, it was concluded that the large difference in duplex stability was likely due to differences in hydration.

It is noteworthy that both [3.3.0]bc-ANA and [3.2.0]bc-ANA (Figure 2.1) show high affinity pairing to RNA, and the latter also to DNA.[333,334] The reason most commonly advanced for this high affinity is the lack of conformational freedom of the sugar ring. The increased rigidity of the 2'F-ANA (nucleoside and oligonucleotide) means that this reasoning might help explain the increased binding affinity of 2'F-ANA as well. However, ANA oligonucleotides were also observed to be quite rigid when in duplexes with RNA. Thus there may be other reasons for the difference between ANA and its higher affinity cousins 2'F-ANA and bc-ANA. For example, the lack of a hydrogen bond donor at the 2' position would change the hydration pattern of the duplex and eliminate the possibility of OH2'-O5' H-bonding interactions.

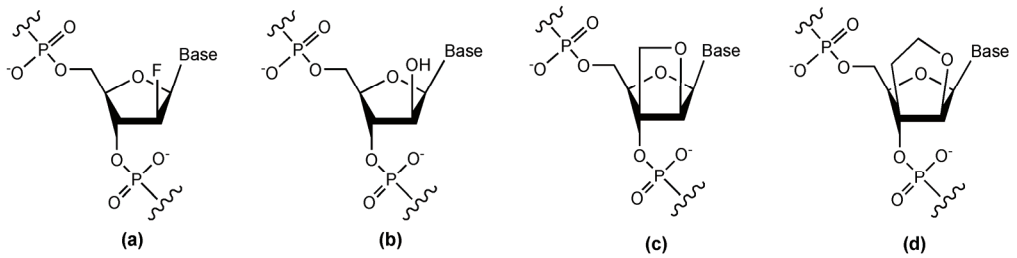

Figure 2.1. Structures of (a) 2'F-ANA, (b) ANA, (c) [3.2.0]bc-ANA and (d) [3.3.0]bc-ANA oligomers.

A very recent and thorough molecular dynamics (MD) study found that while the helical parameters (twist, roll, tilt, rise, slide, and shift) were very similar for 2'F-ANA•RNA and ANA•RNA duplexes, the force constants corresponding to twist and tilt were significantly larger for the 2'F-ANA•RNA duplex (while those corresponding to the other helical parameters were comparable between the two duplexes).[335] In fact, a crude averaging of the various helical force constants gives the order of rigidity 2'F-ANA•RNA > RNA•RNA > ANA•RNA > DNA•RNA (but note that this order is not always strictly followed for the individual helical force constants).[335] Thus, the increased rigidity of 2'F-ANA•RNA may explain some of its extra stabilization, but this order of rigidities cannot explain why ANA•RNA is less stable than DNA•RNA.

Another crystallographic study of single inserts has recently called into question some of the previous results by showing that single 2'F-ANA inserts adopt eastern puckers in the context of a B-form helix, but northern puckers when included in an A-form DNA helix.[336] In contrast, ANA inserts maintained a southeastern pucker in both helical environments. The latter result seems to contradict the earlier work on A-like 2'F-ANA•RNA hairpins, and the authors' conclusion that 2'F-ANA "disfavors the southern and south-eastern pucker ranges"[336] also seems to contradict evidence from CD and thermal stability data (see above). The differences may originate from the fact that most other ("contradictory") conformational work has examined 2'F-ANA•RNA duplexes instead of modified DNA sequences. Furthermore, we believe caution is essential when interpreting results from single inserts in an oligonucleotide, however, if this interesting result is confirmed in other contexts, it may help explain not only the high thermal

stability of 2'F-ANA•RNA duplexes, but also why 2'F-ANA–RNA chimeric structures maintain high binding affinity.

Because of the ongoing lack of a satisfactory explanation for the different binding affinities of ANA and 2'F-ANA for RNA, we undertook another NMR study in order to provide further insight into the structure and dynamics of ANA•RNA and 2'F-ANA•RNA hybrids. Preliminary results from this study are described in Section 2.2.

2.1.2 Hydration of 2'F-ANA and ANA

Berger *et al*. observed an ordered water structure around the 2'-fluorines of FMAU residues incorporated into the Dickerson-Drew dodecamer. However, the F•water contacts in this crystal structure were relatively long and argued against strongly stabilizing hydrogen bonds to fluorine.[269] More recently, Li *et al*. observed that the groove regions around 2'F-ANA residues incorporated into DNA oligomers were dry, in contrast with ANA residues which were heavily hydrated.[336]

To explore the hydration of fully-modified 2'F-ANA•RNA and ANA•RNA hybrids in solution, we undertook an osmotic stressing study (see Section 1.5.8) in tandem with the NMR/MD study described in this chapter. The results of this osmotic stressing study are described in Section 2.3.

2.2 NMR/MD study of 10mer DNA•RNA, 2'F-ANA•RNA and ANA•RNA duplexes

The structure, flexibility and hydration of 2'F-ANA•RNA and ANA•RNA duplexes are being explored through an NMR/MD study, in collaboration with Carlos Gonzalez and Nerea Martin-Pintado, of the Instituto de Química-Física Rocasolano, CSIC, Madrid. The study is still in progress, but preliminary results are presented here.

Previous NMR studies on duplexes of ANA or 2'F-ANA with RNA have made use of hairpin structures.[328,329] To avoid use of a loop structure that could in principle interfere with the results of our study, we chose to use true bimolecular 10-bp duplexes instead (Table 2.1). The DNA:RNA (**DR**) duplex has previously been used in NMR studies of hybrid duplexes.[337,338]

Furthermore, since we wanted this study to be relevant to the field of antisense oligonucleotides, we chose to study a duplex that is a substrate of RNase H. Thus, duplex **DR** was tested in an RNase H assay. As expected, the RNA strand was cleaved very rapidly (Figure 2.2).

Name	Sequences (5'-3')
DR	gct ata atgg • CCAU UAU AGC
FR	*GCT ATA ATGG* • CCAU UAU AGC
AR	*gcu aua augg* • CCAU UAU AGC

Table 2.1. Duplexes synthesized for NMR and X-ray studies. Legend: dna, RNA, *2'F-ANA*, *ana*.

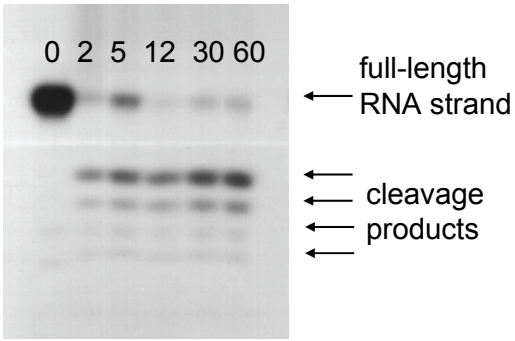

Figure 2.2. RNase H assay on the DNA•RNA duplex. A 5'-^{32}P radiolabeled RNA strand was annealed to its complementary DNA strand (to make duplex **DR**, Table 2.1). The duplex was incubated at 37 ºC with *E. coli* RNase HI. Aliquots were removed at various times as indicated (in min), quenched by heating to 95 ºC in formamide, analyzed by PAGE, and visualized by autoradiography.

2.2.1 Duplex formation and melting

In all cases, the NMR spectra are consistent with duplex formation (Figure 2.3). The imino regions (at 12–14 ppm) of the NOESY spectra are similar in the three duplexes, and their NOE cross-peak patterns are typical of Watson-Crick base pairs.

The melting of the duplexes was studied by NMR. Duplex melting can be observed by following the disappearance of signals in the imino regions as the temperature is raised. As expected, the **FR** duplex proved significantly more

stable than **DR** or **AR** (Figure 2.3; these data agree with UV thermal stability data presented in Table 2.3).

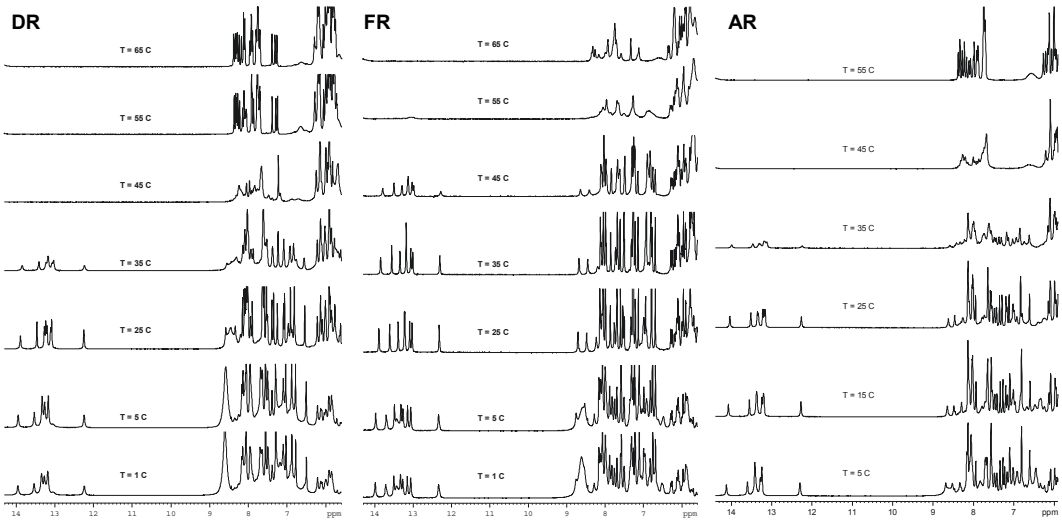

Figure 2.3. Melting of **DR**, **FR** and **AR** as observed by NMR spectroscopy.

2.2.2 Chemical shifts and coupling constants

The protons of the RNA strand resonate at very similar frequencies in all three duplexes (data not shown). This clearly indicates that the structure of the RNA strand does not change much between the three hybrids.

The vicinal ^{1}H-^{1}H coupling constants of the sugars provide information about their pucker, according to the Karplus equation. Thus, a small $^{3}J_{1'-2'}$ indicates a northern (C3'-*endo*) sugar pucker, since in this conformer the base is pseudoaxial and protons are at approximately right angles in this conformer. The $^{3}J_{1'-2'}$ values are very small in the RNA strand of all three duplexes, indicating that the riboses are in a pure north-type conformation.

Similarly, $^{3}J_{2'-3'}$ values can provide information about the population of eastern sugar puckers. Preliminary results suggest that $^{3}J_{2'-3'}$ are very small in the ANA and 2'F-ANA strands, indicating a very high population of eastern puckers.

2.2.3 NOE intensities

So far only qualitative NOE intensities have been observed for these duplexes. Quantitative distances will be calculated using a relaxation matrix approach.

In all three RNA strands, the NOE intensities are consistent with a standard A-form duplex, as expected. (The A/B-form hybrid duplex is already closer to an A-form than a B-form helix, and the RNA strand of a hybrid duplex is almost perfectly A-form.)

In both the 2'F-ANA and ANA strands, very strong H1'–H4' NOESY crosspeaks are observed (Figure 2.4), which is indicative of a major contribution from an east sugar pucker.

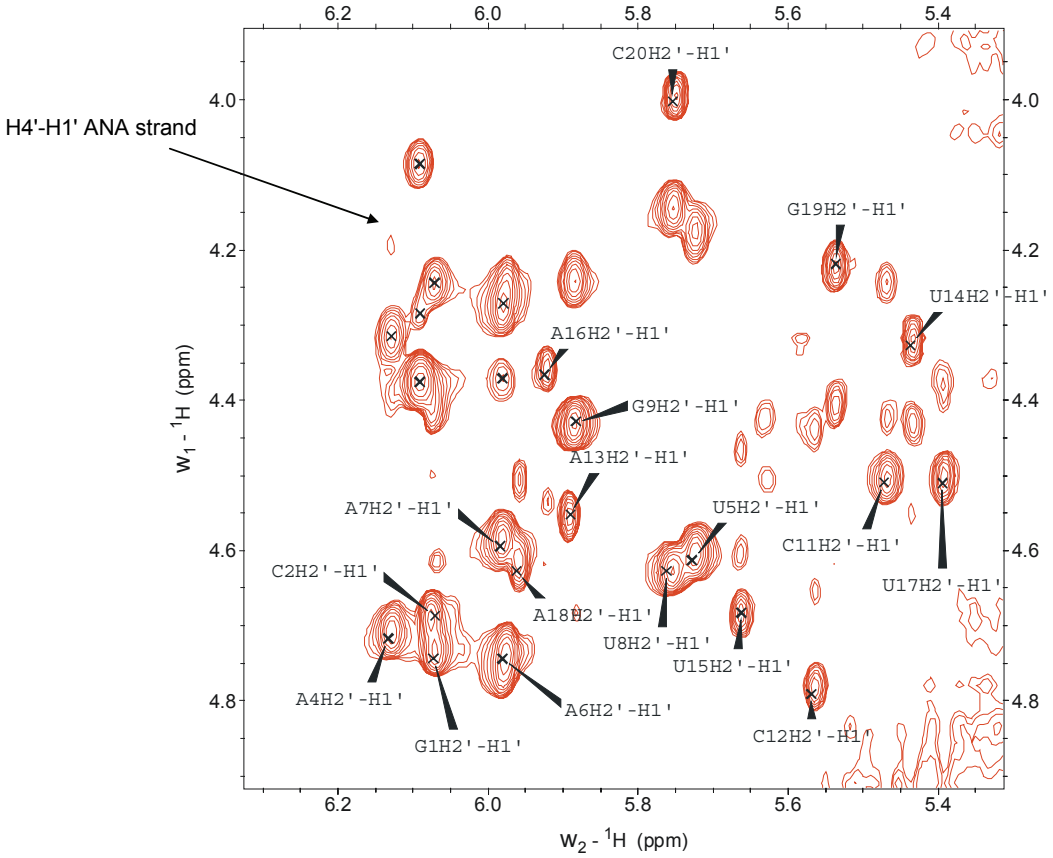

Figure 2.4. The sugar crosspeak region of the NOESY spectrum of **AR**, at T = 20 ºC and t_m = 50 ms. The H1'–H4' crosspeaks observed for the ANA strand are indicated in the box. Very strong signals such as these are also observed for duplex **FR**.

2.2.4 Structure calculations and molecular dynamics

The preliminary structural information discussed above will be confirmed and refined by MD calculations using NMR-derived constraints. The force field parameters for ANA and 2'F-ANA will be provided by Prof. Modesto Orozco, and they have already been used for a purely computational MD study of similar duplexes (mentioned in Section 2.1.1.2).[335]

This computational work will also allow a much more detailed examination of the flexibility and fine structure of the duplexes than was possible in the previous NMR studies. The flexibility of the duplexes can be explored by looking at the conformational ensembles, and solvent (or ion) interactions can be observed since explicit water and ions will be included in the MD calculation.[323] (For previous MD studies of ordered water structure around oligonucleotide duplexes, see refs.[339,340])

2.2.5 Conclusions from preliminary NMR results

The astute reader will have observed that, despite having set out to explore the differences between the **FR** and **AR** duplexes, we have up to this point discussed only the similarities. Indeed, these preliminary results from our current NMR study indicate that the structures of 2'F-ANA and ANA are very similar to each other and to structures derived from previous NMR studies on hairpins.[328,329]

The fact that these new studies seem to agree with the earlier hairpin studies is positive, but does not answer the question of the very different thermal stabilities of **FR** and **AR**. Only small structural differences exist between ANA and 2'F-ANA when in duplexes with RNA. Therefore, the differences probably result from differential flexibility or hydration. Information about both of these properties may be forthcoming, through the MD aspect of this study.

Nevertheless, we wished to explore the hydration of the duplex through empirical means as well. Our studies toward this goal are described in the next section.

2.3 Osmotic stressing

The importance of nucleic acid hydration (Section 1.1.4) motivates us to find robust experimental methods to study it. In principle, the role of hydration in any equilibrium process can be probed by changing the activity of water and observing the effect on the equilibrium. The most straightforward way to do this is by osmotic stressing (reducing the activity of water by adding a small molecule cosolute or "osmolyte"). This has been used to study melting of nucleic acid structures[325,326,341] as well as protein-DNA interactions.[51,52] We thus applied it to study the change in hydration upon melting of 2'F-ANA and ANA containing duplexes.

2.3.1 Assumptions and limitations

Osmotic stressing relies on several important assumptions, the biggest of which is that the small molecule cosolutes do not interact directly with the nucleic acid analyte. This assumption has mainly been justified by demonstrating that, irrespective of the nature of the small molecule analyte, the osmotic stress effect depends only on the activity of water.[51,52,325] However, recent work shows that the assumption does not always hold.[326,327]

If the osmolytes are not interacting with the duplexes or single strands in a direct way, the enthalpy of the melting process should be unchanged by their presence: the destabilization that results from perturbing the water structure should be purely entropic. However, a recent study demonstrated small but significant changes in enthalpies of melting in the presence of various solutes.[327] Interestingly, most of the solutes (ethylene glycol, glycerol, PEG200, urea) led to decreased enthalpy of melting, while two others (sucrose and betaine) led to increased enthalpy of melting, and one (PEG 1450) caused no significant change. These results provide evidence for the existence of direct solute–nucleic acid interactions of different types.[327] As another example, Rozners and Moulder showed that different cosolutes (ethylene glycol, glycerol, acetamide and sucrose) destabilized oligonucleotide duplexes to a different extent at the same activity of water,[326] presumably because of different direct interactions with the oligonucleotides. Nevertheless, results from all of the cosolutes agreed that

duplex RNA is more hydrated than duplex DNA.[326] Thus the technique may still be useful as a qualitative probe of relative hydration for different modifications.

A further challenge is that we wish to use the osmotic stressing technique to study new oligonucleotide modifications. The direct osmolyte–analyte interactions will almost certainly be different for different chemical modifications, and so in principle the interactions should be characterized for each one. Nevertheless, if several osmolytes of very different structures are used, and all of the experiments agree about the relative hydration of various duplexes, it would suggest that this relative hydration is real.

The osmotic stressing technique can only speak of relative hydration – that is, the change in ordered water structure upon duplex melting, not the absolute hydration of the duplex. However, since our primary goal in this study is to explore the origins of duplex thermal stability, it is precisely this change in hydration that interests us. Thus a technique such as X-ray crystallography that indicates absolute levels of duplex hydration would actually be somewhat less relevant to the problem at hand.

2.3.3 Osmotic stressing results

2.3.3.1 Preliminary experiments

To explore whether the osmotic stressing technique was appropriate for our system, we conducted preliminary experiments using glycerol as osmolyte. The buffer we chose simulates physiological salt concentrations (140 mM KCl, 5 mM Na_2HPO_4, 1 mM $MgCl_2$, pH 7.2). We did not have quantitative data on the activity of water for this buffer system, but since osmotic stressing is most useful as a qualitative technique anyway, we pursued the experiment nonetheless.

As well as the three hybrid duplexes used for the NMR study (Table 2.1), we included canonical A-form and B-form controls (duplexes **RR** and **DD**, Table 2.2). Sample T_m curves in pure buffer and 20% glycerol are shown in Figure 2.5.

Name	Sequences (5'-3')
DD	gct ata atgg • ccat tat agc
RR	GCU AUA AUGG • CCAU UAU AGC
FF	***GCT ATA ATGG*** • ***CCAT TAT AGC***

Table 2.2. Further duplexes synthesized and studied by osmotic stressing. Legend: dna, RNA, ***2'F-ANA***.

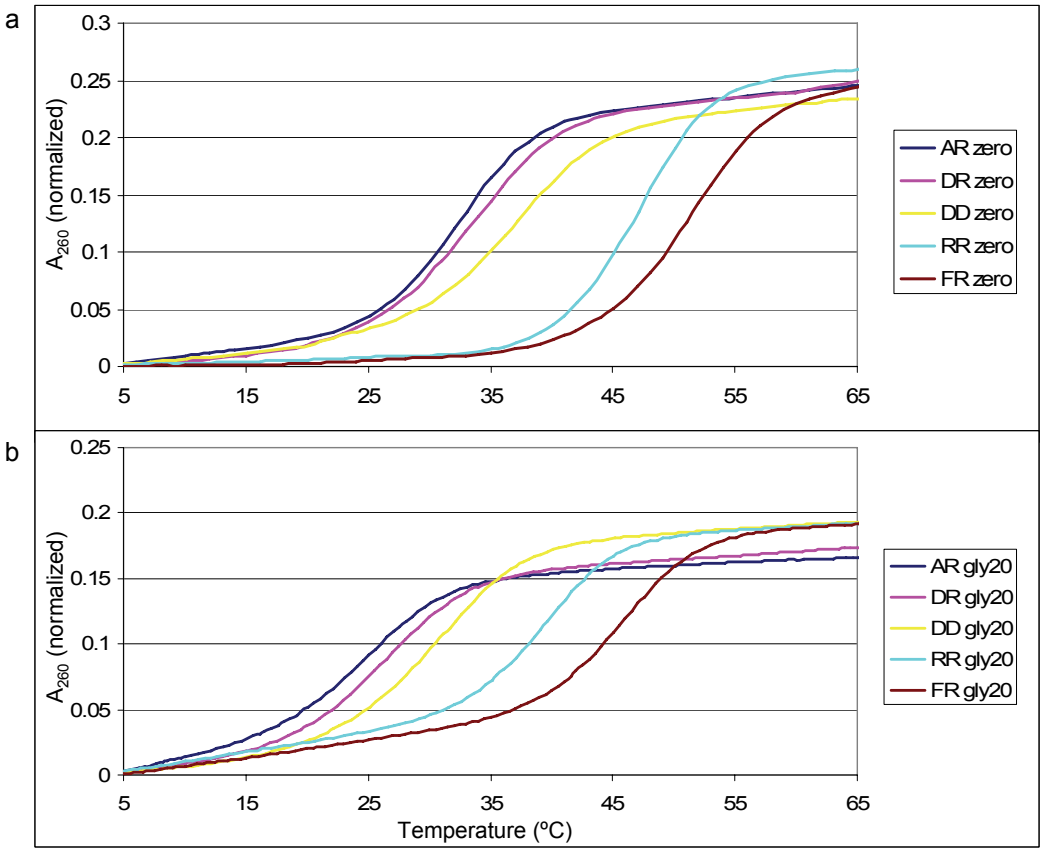

Figure 2.5. Sample T_m curves s for all duplexes in phosphate buffer containing (a) no osmolyte or (b) 20% glycerol. T_m curves were normalized by subtracting from all data points the A_{260} at the starting temperature, which ranged from A_{260} = 0.85 to 0.93.

The T_m values of the five duplexes in the buffer we used are given in Table 2.3. The strong difference in stability of the **FR** and **AR** duplexes (nearly 2 ºC per base pair) indicates that this is a good system for studying the origin of the effect.

The enthalpies of melting were obtained from the concentration dependence of the T_m, for a range of samples from 1–70 μM duplex concentration. The resulting enthalpies are consistent with the expected order for RNA_2 and DNA_2 duplexes.[326]

Extensive hydration is thought to be part of the reason why RNA_2 duplexes have such high enthalpies. Indeed, osmotic stressing with glycerol indicated that **RR** liberated significantly more water molecules upon melting than did the other duplexes. Since we did not have exact osmolality information (*i.e.,* activity of water at various concentrations of glycerol) for this buffer, we used the numbers for a CNE buffer (10 mM sodium cacodylate, 300 mM NaCl, 0.1 mM EDTA, pH 7.2) containing various percentages of glycerol (the calculations are described in detail in the experimental methods, Section 2.6). Thus these numbers are qualitative, but indicative of the relative extent of hydration of the various duplexes. These preliminary results indicate that **FR** liberates significantly fewer molecules of ordered water upon melting than does **DR** or **AR**.

Name	T_m (ºC)	ΔT_m (ºC)[a]	–ΔH (kcal/mol)[b]	Δn_w (est.)[c]
DR	33.5	-18	82.3	7.1
AR	32.6	-18.9	76.8	7.1
FR	51.5	-	84.8	5.6
DD	37.6	-13.9	71.1	5.3
RR	47.7	-3.8	101.3	9.3

Table 2.3. T_m values and enthalpies of melting in pure physiological buffer, and preliminary osmotic stressing results (with glycerol as osmolyte) of the five duplexes used for the preliminary osmotic stressing study. The buffer contained 140 mM KCl, 5 mM Na_2HPO_4, 1 mM $MgCl_2$, pH 7.2. [b]ΔT_m values are relative to FR. [b]–ΔH values were obtained from the concentration dependence of the T_m values, see Section 2.6 for details. [c]These numbers were calculated using the activity of water for glycerol in CNE buffer (described below) and should only be considered to indicate relative hydration levels. They are estimates of the number of ordered water molecules released upon melting, per base pair.

2.3.3.2 Experimental design

Encouraged by these results, we tried two other osmolytes. Since we wanted to be sure that our cosolutes were not simply replacing ordered water molecules, we tested two aprotic cosolutes. However, addition of DMSO as cosolute caused the duplexes to denature, even at low DMSO concentrations. Acetonitrile did not interfere with duplex structure like DMSO did, but it gave a totally different relative order of hydration than glycerol did: **AR** > **FR** > **DR** ≈ **DD** > **RR**. Furthermore, this order of hydration contradicts the well established fact that RNA_2 is more hydrated than DNA_2. We turned, therefore, to other osmolytes that are known in the literature: sucrose and acetamide.

A more rigorous experimental setup was required to improve the precision of the measurements and to make the final results more quantitative. Several changes were made:

(1) The preliminary experiments had been done using a small number of samples. Typically, a sample was diluted in pure buffer and a T_m experiment carried out. Some of the water was then removed under reduced pressure, a carefully measured mass of cosolute was added, and the volume brought back to 1 mL, such that the final cosolute concentration was 5%. This was repeated for 10%, 15% and 20% cosolute concentration. This procedure minimizes sample use, but is clearly vulnerable to systematic errors, so for the more rigorous experiments, each point consisted of an independently-made sample, diluted with an independently-made buffer.

(2) Only two repetitions had been used for most points in the preliminary study, but from this point forward, 5–8 experiments were carried out for most samples. As well as increasing accuracy, this allowed us to have a better sense of the errors in the various measurements. Error propagation for this study is modeled after the work by Rozners and Moulder.[326]

(3) The maximum of the derivative of the melting curve had up to this point been used to identify the T_m value, but for the new more rigorous experiments, baselines were drawn using the Cary software provided with the UV instrument, and the T_m was calculated as the point at which $\alpha = 0.5$ (where α is the mole fraction of duplex.) This significantly reduced the uncertainty of the T_m

measurements. Also, very noisy T_m experiments were not used. Thus, for the ~5–8 experiments that were run for each point, about 3–5 clean, smooth melting curves resulted, and it was these curves that were used to extract the data.

(4) A third control duplex was included (**FF**, Table 2.2) since we reasoned that if the **FR** duplex was significantly less hydrated than the others, a duplex fluorinated in both strands might show an even more dramatic effect.

(5) The buffer system was changed, to allow us to work with buffers of known osmolalities. The osmolytes were chosen to have the greatest diversity possible among commonly used osmolytes for which osmolality data were available. Thus, we chose one small polyol that was found to decrease the enthalpy of melting[327] (glycerol), one larger polyhydroxylated compound that was found to increase the enthalpy of melting[327] (sucrose) and one amide (acetamide). The activity of water in solutions of 5, 10, 15 and 20 % of these solutes (in CNE buffer, 10 mM sodium cacodylate, 300 mM NaCl, 0.1 mM EDTA, pH 7.2) was graciously provided by Prof. Charles Spink (SUNY-Cortland), who had obtained the data by vapor phase osmometry.[325]

2.3.3.3 Results

The T_m values of the samples in CNE buffer were very similar to those in the physiological buffer used above (in fact, they were within experimental error of each other; compare Tables 2.3 and 2.4). Sample T_m curves in this buffer are shown in Figure 2.6.

The thermodynamic parameters of the melting of these duplexes were derived in two ways. The Cary software enables the calculation of ΔH and ΔS through a van't Hoff plot of ln(K) vs. $1/T_m$. Therefore, these values were computed each time a T_m experiment was run in pure buffer, and all of the values were averaged. Nevertheless, this method is quite vulnerable to the choice of baseline, and a second method of calculating ΔH was used as well, which relies on the concentration dependence of the T_m: a plot of $1/T_m$ vs ln(c) for a bimolecular duplex has slope $R/\Delta H$.[309] This plot is shown in Figure 2.7 (see Section 2.6.5 for details of calculations). Both methods of calculating ΔH agreed within

experimental error, with the exception of duplex **FF**. Osmotic stressing results are shown in Table 2.5 and Figure 2.8.

Name	T_m (°C)[a]	−ΔH (van't Hoff) (kcal/mol)[a]	−ΔH (1/*T*m vs. ln(c)) (kcal/mol)[b]	−ΔS (van't Hoff) (cal/mol/K)[a]
DR	33.7 ± 0.1	76.7 ± 2.4	74.1 ± 5.9	222 ± 8
AR	32.4 ± 0.2	86.0 ± 1.8	80.9 ± 7.9	254 ± 6
FR	51.2 ± 0.4	88.7 ± 5.9	89.2 ± 3.7	246 ± 18
DD	37.1 ± 0.2	75.7 ± 1.8	72.4 ± 3.2	216 ± 6
RR	46.9 ± 0.1	86.8 ± 3.6	93 ± 14	244 ± 11
FF	60.0 ± 0.3	83.6 ± 2.2	98.1 ± 8.7	228 ± 13

Table 2.4. T_m values and thermodynamic parameters for the duplexes in pure CNE buffer. [a]Standard deviations are given. [b]Errors are estimated from the $1/T_m$ vs ln(c) plot, as described in Section 2.6.7.

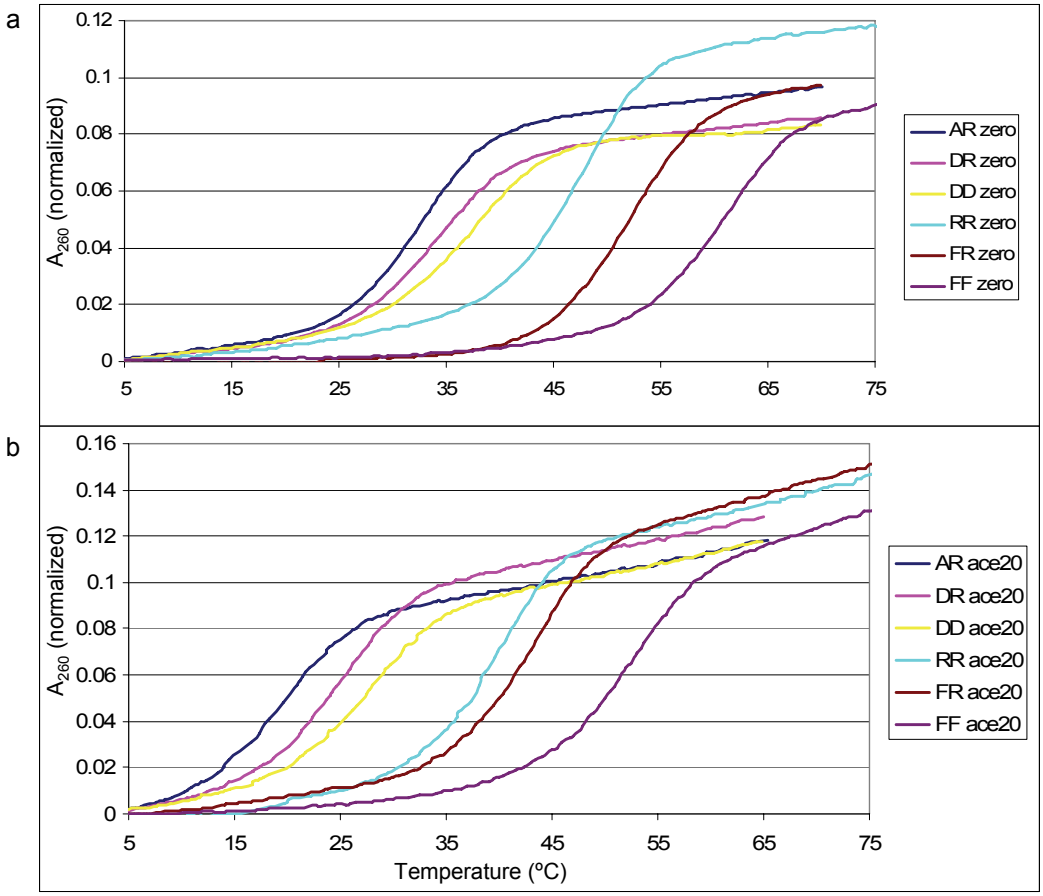

Figure 2.6. Sample T_m curves for all duplexes in CNE buffer containing (a) no osmolyte or (b) 20% acetamide. T_m curves were normalized by subtracting from all data points the A_{260} at the starting temperature, which ranged from A_{260} = 0.34 to 0.39 for part (a) and from A_{260} = 0.39 to 0.44 for part (b).

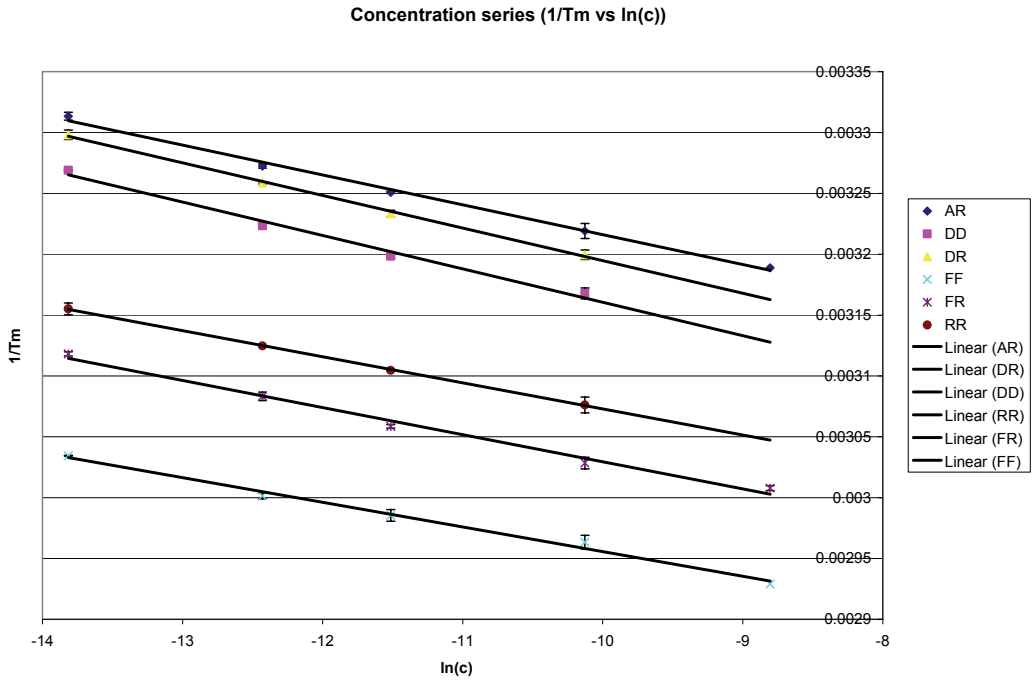

Figure 2.7. $1/T_m$ vs. ln(c) plot, used to derive ΔH values since the slope is equal to R/ΔH.[309] ΔH values derived from this plot are shown in Table 2.5.

Name	Δn_w glycerol	Δn_w sucrose	Δn_w acetamide
DR	3.2 ± 0.4	7.9 ± 1.2	6.3 ± 0.5
AR	3.4 ± 0.4	9.4 ± 1.6	9.9 ± 1.0
FR	3.3 ± 0.8	7.2 ± 2.1	6.9 ± 0.5
DD	3.3 ± 0.4	8.6 ± 1.0	6.7 ± 0.4
RR	3.7 ± 0.6	6.2 ± 1.3	6.1 ± 0.9
FF	3.1 ± 0.6	10.2 ± 2.0	7.7 ± 0.8

Table 2.5. Osmotic stressing results for all duplexes and osmolytes in CNE buffer. Details of error propagation are given in Section 2.6.7. Δn_w represents the number of ordered water molecules released upon duplex melting, per base pair.

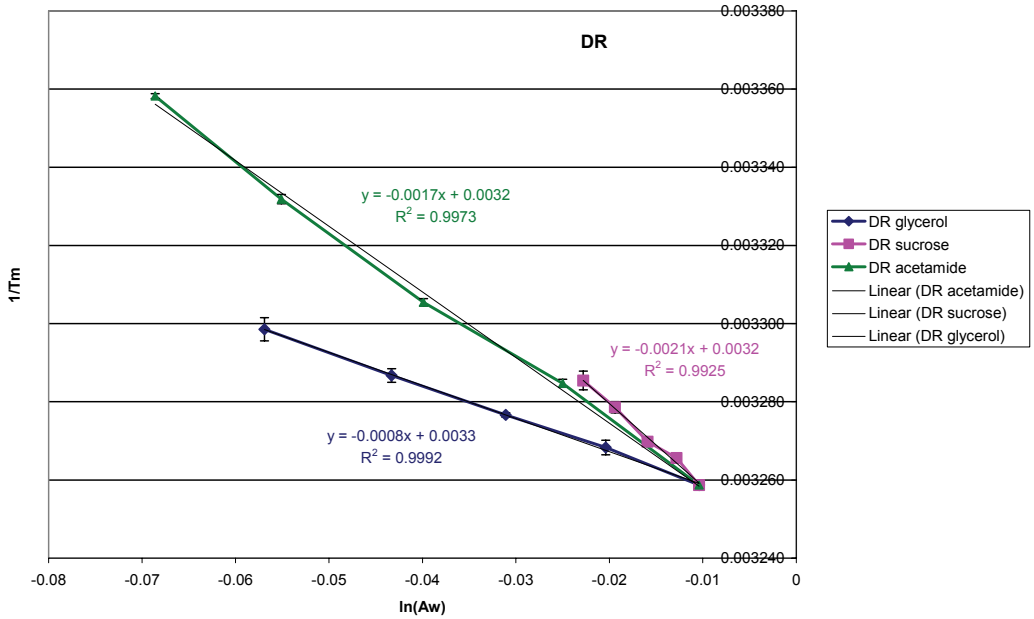

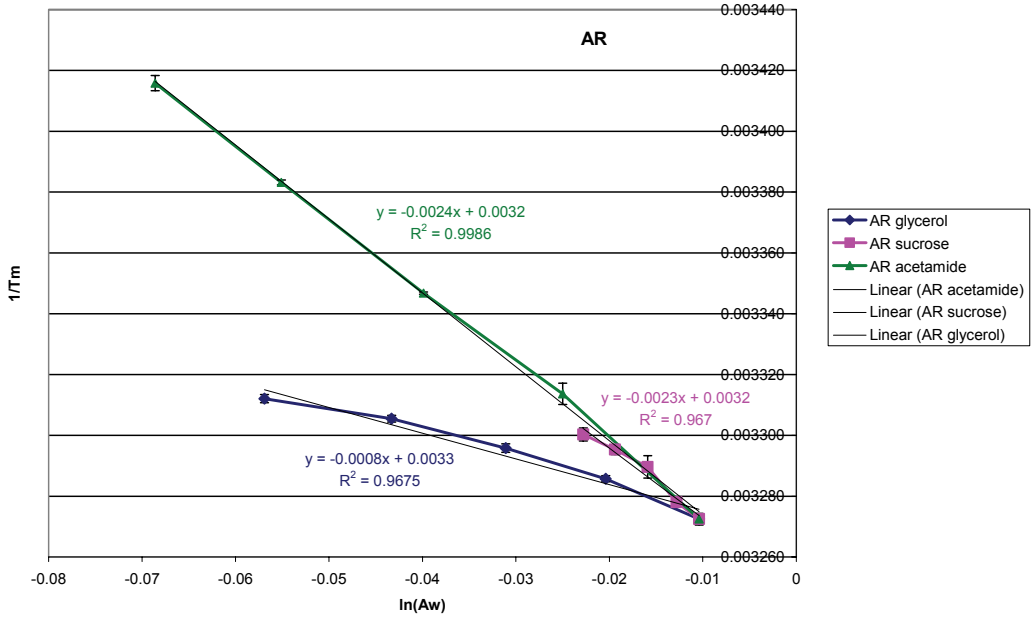

(Figure 2.8 continues next page)

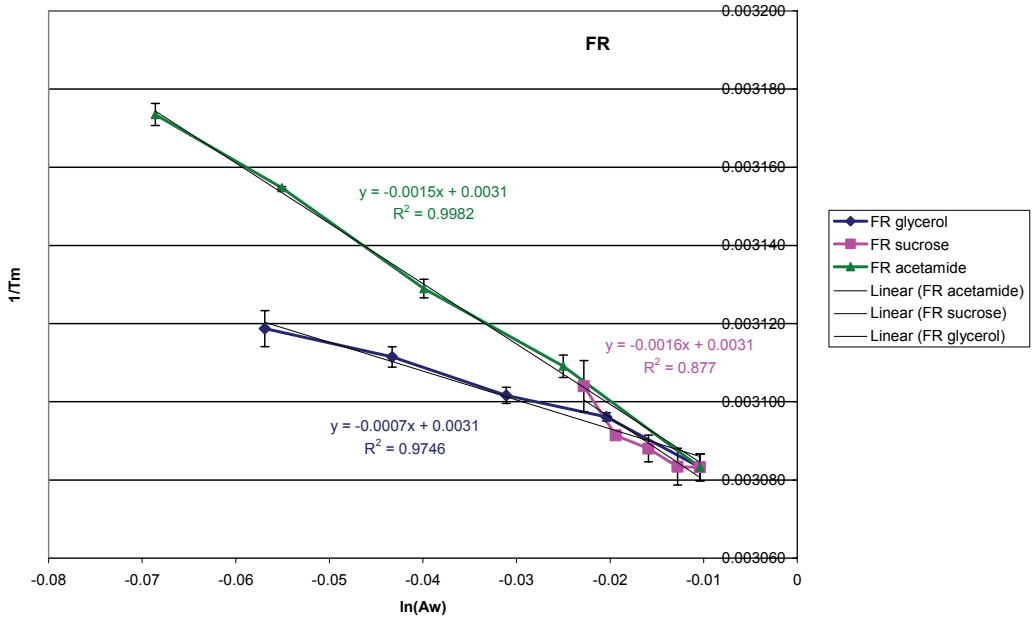

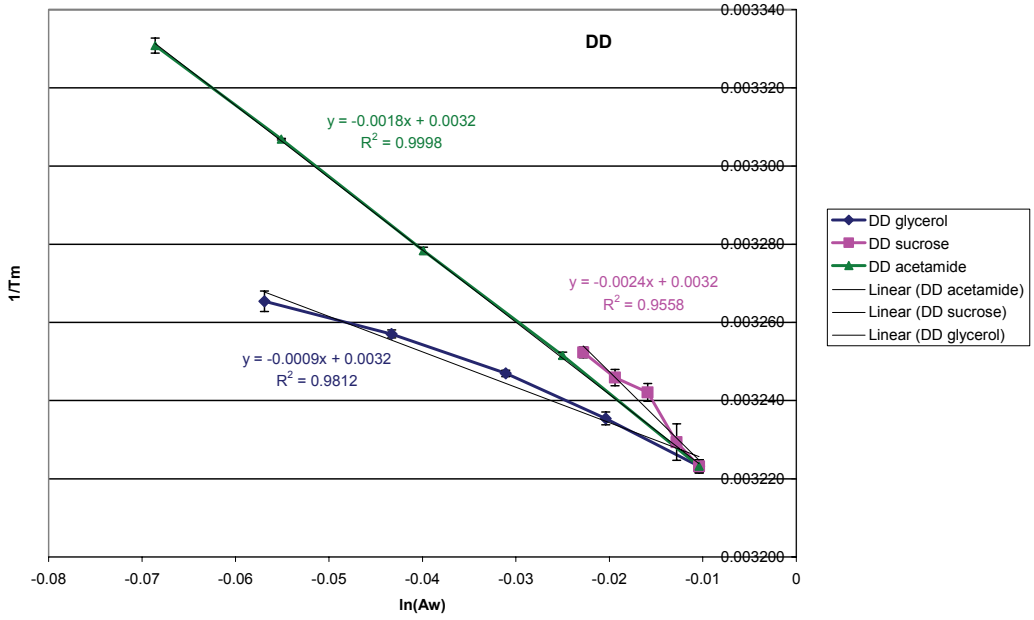

(Figure 2.8 continues next page)

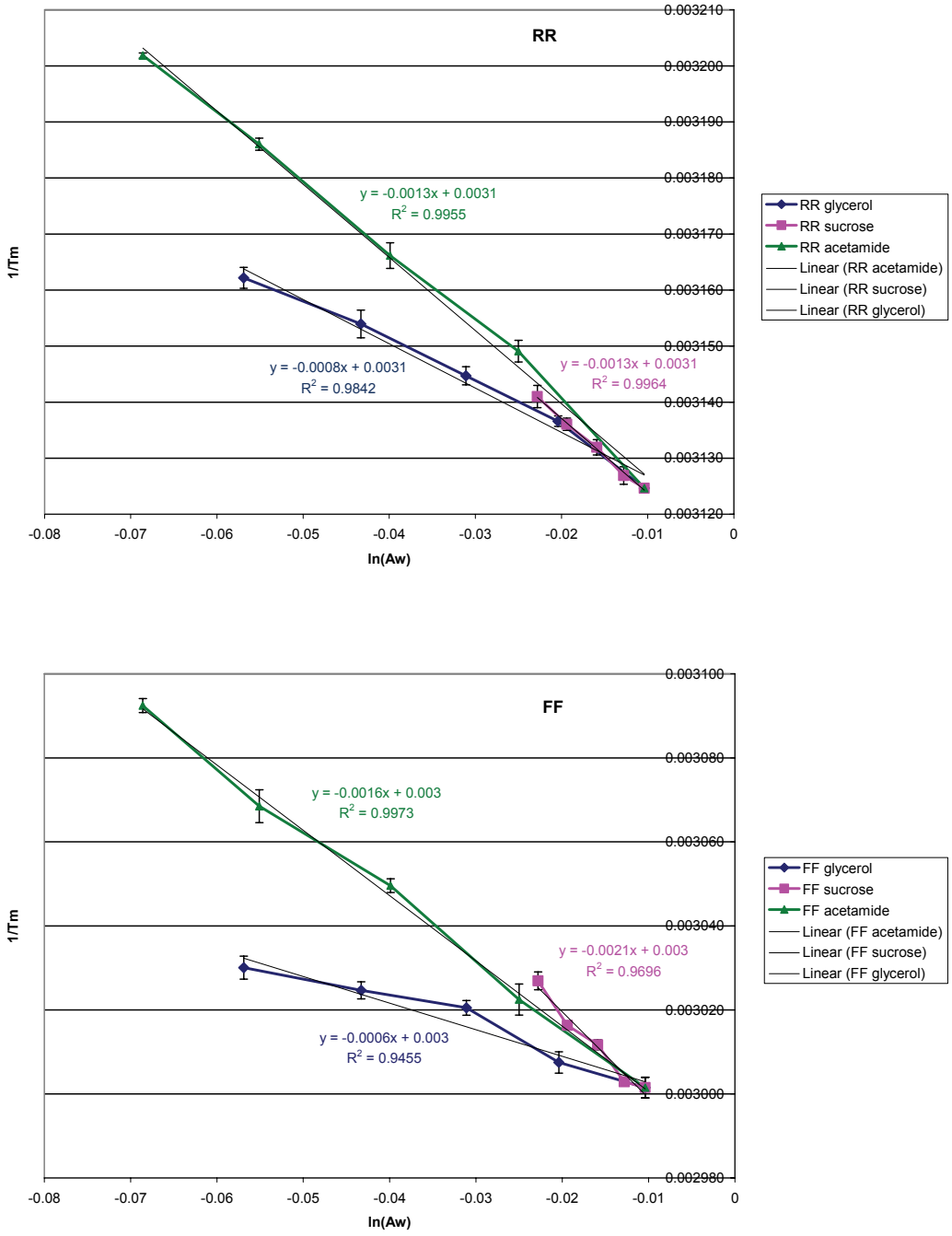

Figure 2.8. Plots showing $1/T_m$ vs $\ln(a_w)$ for all six duplexes in all three osmolytes. The calculated hydration levels according to these graphs are given in Table 2.5.

As is clear from the plots in Figure 2.8, glycerol tends to give lower values of hydration, while sucrose and acetamide give higher numbers. The apparent relative hydration of the duplexes is different according to results from the three osmolytes. In glycerol, the duplexes now appear to have very similar levels of hydration, in fact, the only thing we could say with any degree of confidence is that in terms of hydration, **RR** > **FF**, since the other differences are smaller than the errors associated with the measurements.

In the other two osmolytes, the differences are much larger compared to the errors. In sucrose the order of hydration is **FF** > **AR** > **DD** > **DR** > **FR** > **RR**, although not all of these steps are statistically significant.

Looking at Figure 2.8, it is easy to see why acetamide leads to smaller errors in Δn_w than sucrose does: at 20% concentration the molarity (and thus osmolality, which is closely related to molarity) of acetamide is much higher, leading to a lower activity of water and a greater span on the graph. Thus, although acetamide and sucrose gave comparable absolute uncertainties in T_m values, those in acetamide are smaller relative to the effect being measured. In acetamide, the clear order of hydration appears to be **AR** > **FF** > **FR** ≈ **DD** > **DR** ≈ **RR**.

In both of the latter cases, this order of hydration seems to contradict what is well established from other techniques for studying hydration, and from other reports of osmotic stressing in the literature: most strikingly, **RR** is the least hydrated duplex in both cases. However, it could be argued that because this technique examines only the change upon duplex melting, and the RNA single strands are likely more hydrated than DNA single strands, RNA is in fact more likely to release fewer molecules of water upon melting. Similarly, **FF** ranks in the top two duplexes for change in hydration in both these osmolytes, and it could be argued that at least part of the explanation is that the hydrophobic fluorinated single strands will be much less hydrated than the other single strands. Nevertheless, as mentioned, the results for **RR** *vs.* **DD** contradict even other results obtained by osmotic stressing,[325,326] so other factors may be at play.

In all cases, **AR** is shown to give up more water molecules upon melting than **FR** does. Thus, if *any* of this data is meaningful, our initial finding that **FR** is less

heavily hydrated than **AR** still stands. Nonetheless, we sought to improve these results through two further experiments.

2.3.4 pH dependence

It occurred to us that part of the discrepancy for the results using acetamide as osmolyte could be explained if acetamide was lowering the pH of the solution, thus affecting duplex stability in a way unrelated to water structure. The protocol we were following called for combining the osmolytes with a stock buffer solution, pre-adjusted to the appropriate pH; it had been assumed that the osmolytes had no effect on the pH.

Upon testing the solutions, we discovered that for higher concentrations of acetamide (15 and 20%), the pH was about a unit lower than that of the pure buffer (pH 6–6.3). Therefore, we adjusted the pH of the acetamide-containing buffers to pH 7.2 using NaOH, and carried out another series of T_m experiments (Table 2.6). However, no significant differences were observed in the T_m values, consistent with previous observations that duplex melting is pH-independent when the solution is fairly close to neutrality.[342]

It may be noteworthy, however, that the two fluorinated duplexes (**FF** and **FR**) did register a slight effect: in both cases the Δn_w value dropped by 0.7, which is on the same order as the error and may be meaningful. This would indicate that the two fluorinated duplexes are more sensitive to thermal destabilization under mildly acidic conditions. Furthermore, it may indicate that pH-uncorrected acetamide-containing solutions give an overly high value for the hydration of fluorinated strands.

In any case, the effects are very small, considering the relatively large difference in pH between the two buffers, especially at higher concentrations of acetamide. The peculiar finding that **RR** appears less hydrated than either **DD** or **FF** remains unchanged.

Name	Δn_w (acetamide)	Δn_w (pH-corrected acetamide)	$\Delta\Delta n_w$
DR	6.3 ± 0.5	6.2	–0.1
AR	9.9 ± 1.0	9.6	–0.3
FR	6.9 ± 0.5	6.2	–0.7
DD	6.7 ± 0.4	6.6	–0.1
RR	6.1 ± 0.9	6.0	–0.1
FF	7.7 ± 0.8	7.0	–0.7

Table 2.6. Calculated values of Δn_w using the original data with acetamide osmolyte, and a newer set using pH-corrected acetamide buffers.

2.3.5 Use of D_2O to study hydration

Deuterium oxide is somewhat more acidic than water. This in turn causes D_2O solutions to be more highly structured, which has macroscopic consequences including higher melting and boiling points.[343] For the same reasons, D_2O would be expected to stabilize the water structure around nucleic acid duplexes. However, it should also stabilize the H-bonding of the base pairs, and these two effects may be difficult to deconvolute. Nevertheless, we decided to attempt an experiment in buffer containing D_2O, in hopes that there would be significantly higher stabilization observed for certain duplexes. Based on the structural similarities between **DR**, **AR** and **FR** helices (including similar H-bond geometries), if one duplex were stabilized significantly more or less than the others, it would provide evidence for differential hydration.

There is one report in the literature of duplex stabilization in D_2O (~2 ºC increase in T_m upon going from 0 to 100% D_2O).[342] This effect was observed whether the sample was annealed in H_2O and diluted in D_2O, or annealed and diluted in D_2O, and it disappeared when the sample was annealed in D_2O and diluted in H_2O. Thus it was an equilibrium effect, presumably involving H-bonding and possibly water structure as well.

Our experiment was initially carried out by dissolving the oligonucleotide in 1 mL of H_2O buffer (identical to that used for the osmotic stressing experiments), evaporating to dryness, redissolving in D_2O and annealing as for the other samples. UV melting experiments on these samples did not show significant changes in T_m, relative to H_2O. To verify this finding, which seemed to contradict the large changes observed in the literature,[342] the samples were prepared in a different way: a D_2O buffer was prepared and adjusted to pD 7.2 (which corresponds to a pH meter reading of 6.8),[344] then the samples were dissolved in 1 mL of this buffer and annealed as usual. Once again, however, no significant changes were observed. Data from both experiments are given in Table 2.7.

Name	T_m (H_2O) (°C)	T_m (D_2O) method 1 (°C)	T_m (D_2O) method 2 (°C)
DR	33.7 ± 0.1	34.3 ± 0.1	33.9 ± 0.3
AR	32.4 ± 0.2	32.6 ± 0.2	32.5 ± 0.3
FR	51.2 ± 0.4	51.0 ± 0.6	51.6 ± 0.6
DD	37.1 ± 0.2	37.8 ± 0.2	36.7 ± 0.5
RR	46.9 ± 0.1	47.1 ± 0.5	47.5 ± 0.2
FF	60.0 ± 0.3	59.7 ± 0.3	60.2 ± 1.0

Table 2.7. Attempted use of D_2O to stabilize water structure. In all cases the samples contained CNE buffer. Details of D_2O buffer preparation (both methods) are described in the text.

We were surprised that no change was observed, given the literature precedent and because we were expecting both water structure and H-bonding to be stabilized in D_2O. In rare circumstances, a slight increase in T_m was observed for one of the methods (*e.g.* **DD** method 1, **DR** method 1, and **RR** method 2) but never both. Thus, this technique will not be useful for characterizing water structure.

2.3.6 X-ray crystallography

X-ray crystallography provides a quantitative picture of ordered water structure, although its applicability to solution-phase, dynamic duplexes can be called into question. In collaboration with Martin Egli (Vanderbilt University), we did try crystallizing duplexes **DR**, **AR**, and **FR**, but unfortunately they did not diffract to high resolution.

2.3.7 Discussion

It is hard to understand some of the differences, for example between the preliminary results with glycerol cosolute in a KCl-rich phosphate buffer, and the more thorough study with the same cosolute in a NaCl-rich cacodylate buffer. However, it may be that another species in solution is affected differently by the two buffers, and in turn perturbs the water structure; in this sense it would be acting as a Hofmeister salt.[345-349] These species can be quite sensitive to their environment: a Hofmeister series has been shown to act in the reverse order in cacodylate than in phosphate buffer, and furthermore, upon changing Na+ to K+ counterions, the order can be made to reverse back again![350] The differential perturbation of the water structure could well be enough to cause the dramatic differences between buffer systems, as we observed, even with the same osmolyte. One possible contaminant is some residual triethylammonium salts from the purification; even after desalting on Sephadex and repeated lyophilization, some triethylammonium signals were visible by NMR. One advantage of longer nucleic acids in osmotic stressing is that they can easily be extensively dialyzed before an experiment; here, on the other hand, we simply diluted all samples in the appropriate buffers and so any salts or other impurities present in the nucleic acid duplex are there for the whole experiment.

It is noteworthy that glycerol gave lower values for n_w than the other two osmolytes; this is consistent with previous findings.[326] This may be due to specific glycerol – nucleic acid interactions, since we could easily imagine that a small, flexible, trihydroxylated molecule like glycerol could be involved in its own ordered, H-bonded structure around a nucleic acid duplex, thus compensating

to some degree for the destabilization of the water structure upon lowering the activity of water. Glycerol has been observed to interact directly with proteins in previous osmotic stressing experiments.[351]

2.4 Future work

2.4.1 Other methods of studying hydration

Various other possibilities exist for empirical study of ordered water structure. One possibility that we have not tried is the use of Hofmeister salts to perturb water structure.[345-349] However in this approach, as for osmotic stressing, multiple effects can come into play. Recent work describes an attempt to deconvolute the Coulombic and non-specific osmotic effects from the ion-specific Hofmeister effects.[352]

NMR methods have been used to investigate directly the half-life of bound (structured) water on an NMR duplex. For example, NOE methods have been used to identify bound water molecules with a lifetime significantly greater than 1 ns, and others with lifetimes shorter than 500 ps.[353,354] Another approach used an NMR relaxation dispersion experiment to show that oligonucleotide duplexes were associated with a long-lived water structure, and then demonstrated that the water structure was in the minor groove by netropsin displacement.[355]

However, these methods may not be necessary in our case, if the NMR/MD calculations provide sufficient information about the hydration structure. The advantage of a combined NMR and computational approach is that interactions can be identified more precisely.

2.4.2 Possible differences in ion interactions

One final avenue which may be fruitful in pursuing the difference between the stabilities of **FR** and **AR** is their ion structure. The ordered water structure around nucleic acids also contains ordered cations which can also have a significant effect on duplex structure.[356-359] Because the 2'-substituents of arabinonucleic acids point into the major groove, specific ion interactions in the major groove could easily be different between ANA and 2'F-ANA. Using T_m studies at various ionic strengths, several groups have examined the ion dependence of duplex melting.[325,341] The information obtained from the MD

study may provide information about counterion structure, and this can be supplemented by similar T_m studies. Another student in the Damha group is currently undertaking studies of the thermal melting behavior of the duplexes in 10–1000 mM Na+, K+, and possibly Mg+ ions. This study might also help explain the differences we observed between the phosphate/potassium system and the cacodylate/sodium system.

2.4.3 Other methods of investigating the low binding affinity of ANA

Both this study and the previous NMR structural study of ANA[329] have made use of a complementary RNA strand. The rationale for this has been twofold: AON•RNA binding is more therapeutically relevant, and the higher stability of ANA•RNA hybrids makes them easier to study, not to mention more relevant to most applications. But precisely *because* the binding affinity of ANA is much lower to DNA than to RNA, it would be interesting to study an ANA•DNA helix by NMR spectroscopy. The substrate could be a hairpin, to stabilize the low-melting ANA•DNA duplex. Perhaps some of the same factors that contribute to the unfavorable binding of ANA to RNA are present in a more extreme way in the ANA•DNA interaction, and would thus be easier to identify.

2.5 Conclusions

We have carried out osmotic stressing experiments using two different buffers and five different osmolytes. All of the combinations gave different results, suggesting that osmotic stressing may not be appropriate for this system. Nevertheless, in all systems, **AR** released more ordered water upon melting than **FR** did.

The system that best agreed with previous findings for the control duplexes was, unfortunately, only a preliminary series of experiments, and likely contains high uncertainties. Furthermore, the fact that only one system was found to work should give us pause before relying too heavily on these data – since, as discussed in the introduction, we must see similar results from several systems if we are to have confidence that the effects arise predominantly from perturbation of water.

Nevertheless, these preliminary results indicated that **FR** liberates significantly fewer molecules of ordered water upon melting than does **DR** or **AR**. This entails

a significant entropic benefit for 2'F-ANA•RNA duplexes (no need to order water molecules around the helix) but an enthalpic penalty (since H-bonding from ordered water typically makes a significant enthalpic contribution). The low hydration of 2'F-ANA, providing a significant entropic benefit over other strands, may actually make a significant contribution to its binding affinity.

Interestingly, thermodynamic analysis of the **FR** and **AR** duplexes (Tables 2.3 and 2.4) indicated that **FR** was enthalpically favored, even with its lower levels of hydration. This indicates that hydration cannot be the only difference between the thermal stability of the two duplexes, since 2'F-ANA has an inherently higher enthalpy of binding. Thus, 2'F-ANA must have an advantage in terms of H-bonding and/or base stacking that structural studies have not yet been able to characterize.

2.6 Experimental methods

2.6.1 Strand synthesis and purification

Oligonucleotides were synthesized on solid phase using standard methods. All masses were verified by ESI-MS, by sending 0.05 to 0.1 ODU, well-desalted and dried down, to the facilities at Concordia University or the Biotechnology Research Institute (NRC). Purification of all strands was initially carried out using PAGE, and oligonucleotides were extracted from the gels by electroelution. However, some stray signals, thought to be due to soluble acrylamide byproducts, were visible in the high frequency region of the ^{1}H NMR spectra of these species, and those strands to be used for the NMR study were repurified by reverse phase HPLC using gradients of acetonitrile in water containing triethylammonium acetate buffer. However, this in turn led to a different set of foreign signals in the NMR spectrum, probably corresponding to the triethylammonium salt, even after desalting on Sephadex and repeated lyophilization. Since these peaks did not interfere with an important region of the NMR spectrum, the samples were used without further purification.

2.6.2 RNase H assay

The DNA antisense and 5'-^{32}P labeled RNA sense strands of duplex **DR** (Table 2.1) were combined in a 1.5:1 ratio and annealed by heating to 90 °C followed by

slow cooling to room temperature. The duplex (2.5 pmol) was incubated at 37 ºC with 1.5 units *E. coli* RNase HI (USB Corporation, Cleveland, OH) in 50 µL of a buffer recommended by the manufacturer (50 mM Tris-HCl, pH 7.5, 50 mM KCl, 25 mM $MgCl_2$, 0.25 mM EDTA, 0.25 mM DTT). Aliquots were removed at various times as indicated (in min) and quenched by the addition of an equal volume of loading buffer (98% deionized formamide, 10 mM EDTA, 1 mg/mL bromophenol blue, and 1 mg/mL xylene cyanol), followed by heating to 95 °C for 5 min. Cleavage products were resolved on 16% denaturing PAGE and visualized by autoradiography.

2.6.3 Buffer and sample preparation

For initial osmotic stressing experiments, samples were made in pure phosphate buffer with physiological K^+ concentrations (140 mM KCl, 5 mM Na_2HPO_4, 1 mM $MgCl_2$, pH 7.2). After an initial T_m experiment, the volume was reduced somewhat, the appropriate mass/volume of osmolyte was added, and the volume was brought back to 1 mL using pure water. This was repeated for each concentration of osmolyte (5 to 20%).

For the second round of more rigorous experiments, a stock solution of CNE buffer was prepared such that 0.8 mL of stock would provide, after dilution, 1.0 mL of a solution containing 10 mM sodium cacodylate, 300 mM NaCl, 0.1 mM EDTA, pH 7.2. 20-mL aliquots of this stock were removed, an appropriate mass of the osmolyte of interest (if any) was added, and the solution diluted to 25 mL. These buffers were refrigerated when not in use. Normally, 2 nmol of each strand was dried in a microtube, the buffer of interest (1 mL) was added and the sample was annealed by heating to 95 ºC and slowly cooling to room temperature. Samples for concentration dependence studies ranged from 0.5 to 15 nmol duplex, and were diluted in pure CNE buffer. Samples at high concentrations (150 and 40 µM) were achieved by diluting 15 or 5 nmol duplex in small volumes of buffer (200 or 250 µL, respectively). For these samples only, a 0.1 cm path length cell was used instead of a standard 1 cm path length cell.

2.6.4 UV spectroscopy

Six samples at a time were analyzed in a Cary 300 UV spectrophotometer. The samples were heated at a rate of 0.5 ºC/min while monitoring A_{260}. At

temperatures below 15 ºC, the sample chamber was flushed with N_2 to prevent condensation from building up on the cuvettes. At the end of the T_m experiment, the samples were reannealed in the UV instrument by cooling at a rate of 1 ºC/min. Further T_m experiments (up to five total) were run on the same samples. Generally the UV cells were inverted after each run, to ensure that any condensate on the top of the cells was mixed with the rest of the sample again. About 5–8 experiments were carried out per data point, using one or two independently prepared samples. Fewer experiments, however, were carried out for the highly concentrated, low volume samples used as part of the concentration series for the ΔH calculation, which tended to evaporate (and as such did not provide reliable information beyond the first repetition with the same sample) and required too much material to prepare multiple samples. T_m runs that were overly noisy were not used.

2.6.5 Thermodynamic parameters

Thermodynamic parameters were extracted from the UV melting data in two ways. A van't Hoff plot, ln(K) vs $1/T_m$, can be used to determine ΔH and ΔS, according to the equation $\Delta H = -R\,[d(\ln K)/d(1/T_m)]$.[309] Since the equilibrium constant K can be written in terms of the mole fraction of duplex, α, it is straightforward to calculate the value of K at the T_m where $\alpha = 0.5$. This calculation can be carried out within the Cary software provided with the UV spectrophotometer.

Alternatively, the concentration dependence of the T_m can be used to calculate ΔH. Starting with the well known equation $-RT[\ln(K)] = \Delta H^\circ + T\Delta S^\circ$, for a non-self-complementary bimolecular equilibrium, this equation can be expanded and rearranged to give the following: $1/T_m = [R/\Delta H^\circ]\ln(C_T) + [(\Delta S^\circ - R\ln(4))/\Delta H^\circ]$, where C_T represents the total strand concentration, not the duplex concentration. Thus, a plot of $1/T_m$ vs. $\ln(C_T)$ is linear with slope $R/\Delta H^\circ$.

2.6.6 Calculation of Δn_w

The changes in hydration upon duplex melting were calculated according to the method of Spink and Chaires:[325] $\Delta n_w = (-\Delta H/nR)[d(T_m^{-1})/d(\ln a_w)]$, where n is the number of base pairs in the duplex and R is the ideal gas constant,

1.986 cal/mol/K. We used the enthalpy determined from the concentration dependence studies for $-\Delta H$. The value of $d(T_m^{-1})/d(\ln a_w)$ is, of course, the slope of a plot of $1/T_m$ vs $\ln(a_w)$ at various osmolyte concentrations. The values of $\ln(a_w)$ were determined by vapor pressure osmometry[325] by Profs. Charles Spink (SUNY Cortland) and Jonathan Chaires (University of Mississippi Medical Center), and graciously provided by them.

2.6.7 Statistical analysis

Standard deviations of multiple measurements were calculated using the STDEVP function in Microsoft Excel, as follows: $\sigma = [\Sigma(x-x_{avg})^2/n]^{0.5}$. For the T_m values, this was then converted to relative standard deviation so it could also be applied to $1/T_m$.

To estimate the errors in the slopes of fittings (for calculation of ΔH and Δn_w), the method of Rozners and Moulder was used.[326] Two alternative plots were constructed, using the error bars at the terminal data points (*e.g.* $1/T_m$ plus standard deviation at 0% cosolute and $1/T_m$ minus standard deviation at 20% cosolute gave one alternative plot, while $1/T_m$ minus standard deviation at 0% cosolute and $1/T_m$ plus standard deviation at 20% cosolute gave the other.) The deviations of these slopes from the true slope were averaged as $[(dev_1^2 + dev_2^2)/2]^{0.5}$, and this number was considered the error in the slope (σ_{slope}).

The final errors in the values of Δn_w were calculated as follows: $\sigma\Delta n_w = \Delta n_w[(\sigma\Delta H/\Delta H)^2 + (\sigma_{slope}/slope)^2]^{0.5}$.

Chapter 3. Further explorations of the properties of 2'F-ANA

3.1 Introduction

In this chapter we explore various properties of 2'F-ANA oligonucleotides. In Section 3.2, we present an investigation of the remarkable hydrolytic stability of 2'F-ANA under acidic conditions. We then examine several possible applications for this stability. In Section 3.3, we continue our focus on hydrolytic stability, but this time under conditions of nuclease-catalyzed cleavage. We explore the stereochemistry of PS-2'F-ANA cleavage by snake venom phosphodiesterase (SVPDE), and report on the nuclease stability of three 2'F-ANA and DNA sequences by SVPDE and fetal bovine serum (FBS). Finally, in Section 3.4 we report the first use of 2'F-ANA in an exciplex probe system for nucleic acid diagnostics. In the post-genomic era, detection of single-nucleotide polymorphisms (SNP) is becoming more and more important for effective diagnosis and treatment. This exciplex probe system is a step toward better SNP detection.

3.2 Stability of 2'F-ANA to acid-catalyzed hydrolysis

3.2.1 Background to acid-catalyzed hydrolysis of nucleic acids

DNA oligonucleotides are vulnerable to depurination and cleavage under acidic conditions (proposed mechanism, Figure 3.1).[360-362] Depyrimidination can occur as well, but several orders of magnitude more slowly. The final step (β-elimination) can occur under basic conditions, but heat and salt are adequate according to Holmquist.[361]

RNA is much less vulnerable to depurination since the electronegative 2' oxygen renders the oxocarbonium ion intermediate less stable.[363,364] However, RNA can undergo 3'-2'-migration or cleavage under acidic conditions through attack of the 2'-hydroxyl group on the protonated phosphate group (Figure 3.2).

Because of the very high electronegativity of fluorine, the oxocarbonium ion intermediate is even less stable for 2'-fluorinated nucleosides, protecting them from depurination. 2'-Fluorinated nucleosides have therefore been proposed as

acid-stable nucleoside drugs.[208,241,242,330] One of these drugs is now approved for clinical use.[229] 2'-Fluorinated oligonucleotide phosphoramidates have also shown acid-resistance.[365]

Because of the past success of 2'-fluorinated nucleosides, we predicted that 2'F-ANA oligonucleotides would show resistance to acid-mediated depurination, and because of the absence of a 2'-hydroxyl group, they are not vulnerable to the phosphate attack observed for RNA. In this study, we show that 2'F-ANA oligonucleotides demonstrate exceptional acid stability as compared to DNA and RNA with either phosphodiester or phosphorothioate backbones.

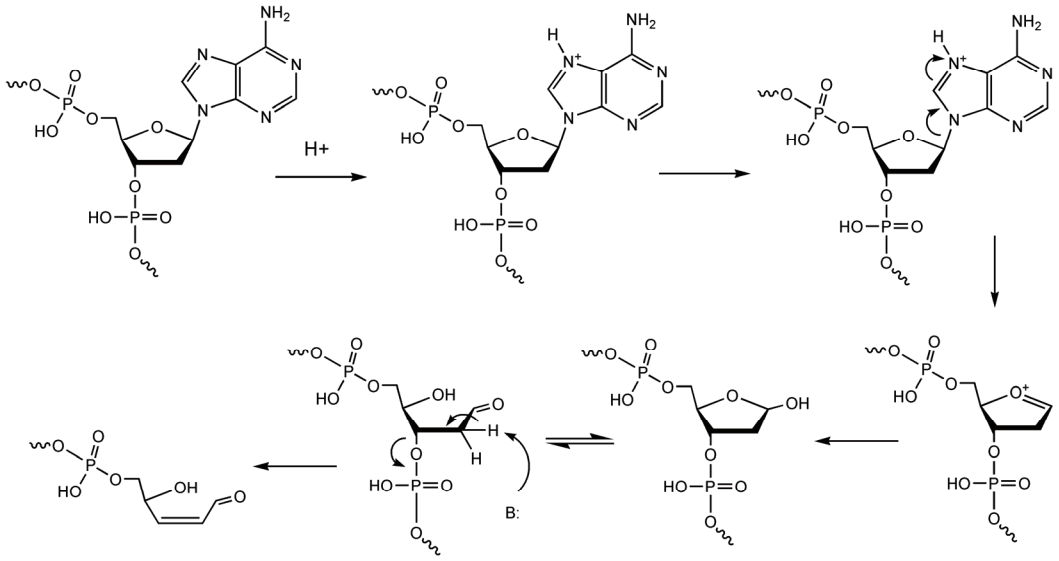

Figure 3.1. Mechanism of acid-catalyzed depurination and cleavage in DNA. Shown for adenine base, but can also occur with guanine. While N-1 is the most basic and is protonated first, a finite population of N-7 is likely also protonated to allow breakage of the glycosyl bond.[363] In the case of 2'F-ANA, the presence of fluorine at the 2' position destabilizes the oxycarbonium ion intermediate and disfavors depurination, largely preventing this mechanism of degradation.

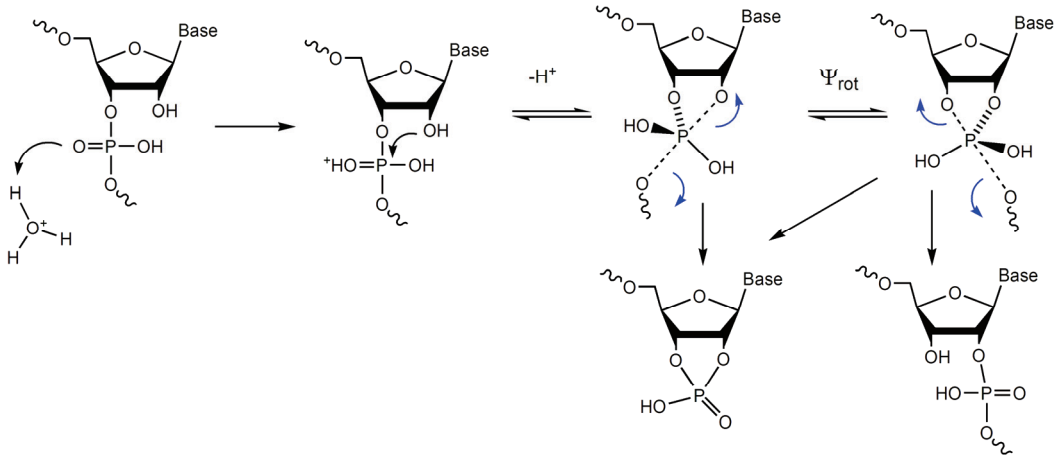

Figure 3.2. Mechanism of RNA cleavage and 3'-2'-migration under strongly acidic conditions (pH < 2).[366] The blue arrows indicate alternate pathways for the breaking of the pentavalent phosphate. During phosphate hydrolysis, groups can only enter and leave through apical positions (dashed lines). Under acidic conditions, pseudorotation (Ψ_{rot}) is favorable, allowing 3'-2' phosphate migration (rightmost structures) as well as cleavage. (The latter is the sole product observed under basic hydrolysis conditions, where pseudorotation is not favorable because the deprotonated non-bridging oxygens prefer to maintain equatorial positions.)

3.2.2 Results of acid stability studies on 2'F-ANA

Sequences of DNA, RNA and 2'F-ANA were prepared (Table 3.1) and exposed to an enzyme-free simulated gastric fluid[367] for varying amounts of time. Aliquots were removed, frozen in dry ice and immediately lyophilized to dryness. Results are shown in Figure 3.3.

The DNA strands were degraded very rapidly, with half lives on the order of minutes. RNA strands were longer-lasting, with half lives on the order of hours (PO linkages) or days (PS linkages). 2'F-ANA strands, however, showed minimal degradation up to 46 h.

Name	Description	Sequence (5' – 3')
Ac1	PO-RNA	PO(AGCUAGCU)
Ac2	PO-2'F-ANA	PO(*AGCTAGCT*)
Ac3	PO-DNA	PO(agctagct)
Ac4	PS-RNA	PS(AGCUAGCU)
Ac5	PS-2'F-ANA	PS(*AGCTAGCT*)
Ac6	PS-DNA	PS(agctagct)
Ac7	PO-RNA	PO(AGAUUGGAGAAGGCUUGUAUU)
Ac8	PO-2'F-ANA	PO(*AGATTGGAGAAGGCTTGTATT*)
Ac9	PO-2'F-RNA	PO(TCCTTCTC)
Ac10	PO-2'F-ANA	PO(*TCCTTCTC*)
Ac11	PO-DNA	PO(tccttctc)

Table 3.1. Strands prepared for the acid stability study. Legend: dna, RNA, *2'F-ANA*, 2'F-RNA. Abbreviations: PO, phosphodiester; PS, phosphorothioate. Note that although sequences **Ac1**–**Ac6** are self-complementary, no duplex formation was observed under the acidic conditions of SGF.

We confirmed the integrity of the PO-FANA 21-mer **Ac8** by neutralizing a portion of the reaction mixture at 48h using a phosphate buffer, desalting and analyzing by ESI-MS. More than 95% of the resulting peaks corresponded to full-length product with no evidence of depurination. As a further test of the integrity of the acid-treated **Ac8**, we neutralized and desalted it, annealed it to complementary RNA, and verified the T_m of the resulting duplex, which was unchanged with respect to untreated **Ac8**.

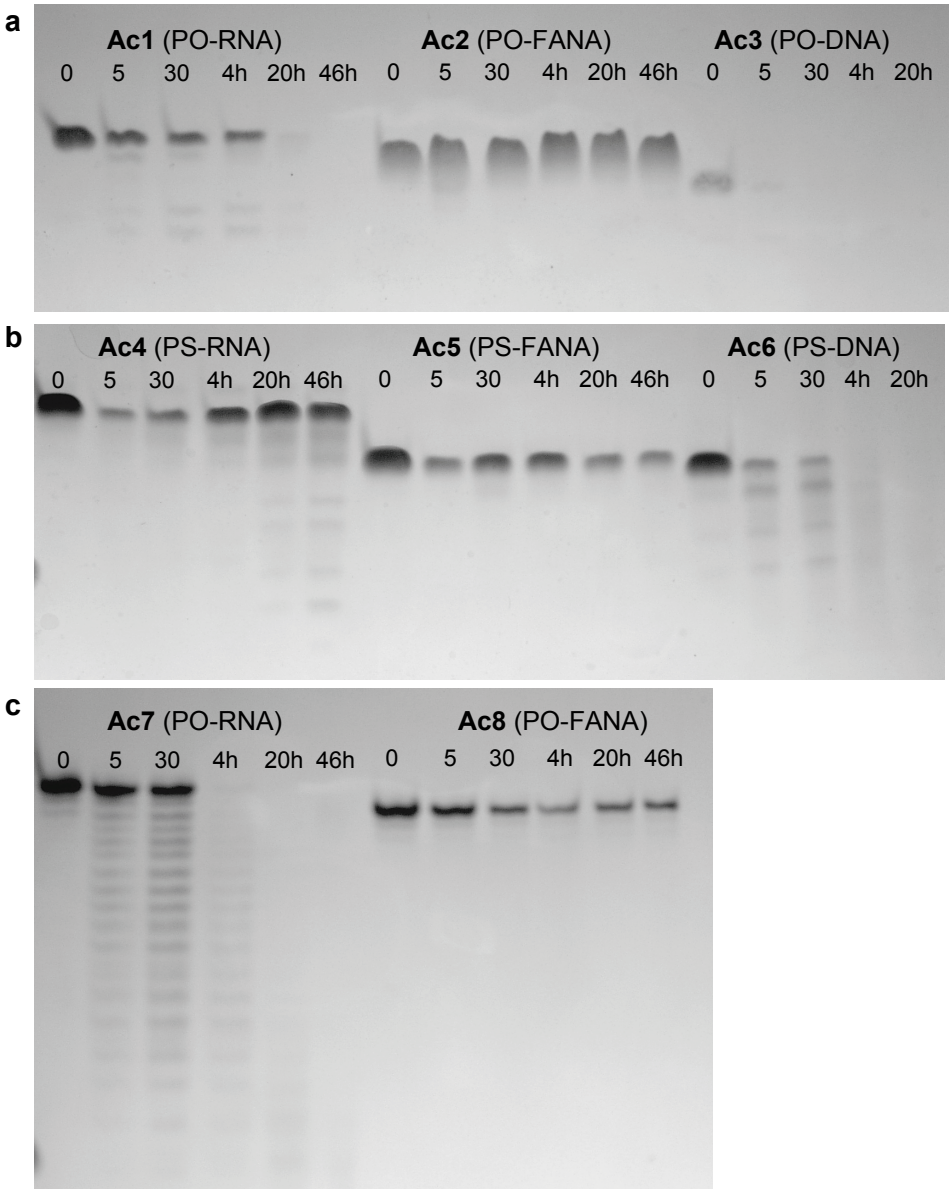

Figure 3.3. 24% denaturing PAGE comparing the acid stability of DNA, RNA and 2'F-ANA to simulated gastric fluid at 37 ºC. (a) PO sequences **Ac1**–**Ac3** ; (b) PS sequences **Ac4**–**Ac6**; (c) 21mer PO sequences **Ac7**–**Ac8**. Gels were developed using Stains-All dye. Timepoints are in minutes unless otherwise indicated.

A dramatic improvement in the acid stability of RNA was obtained upon phosphorothioation. This is consistent with the results of Lonnberg and coworkers, who explain the greater stability of PS-RNA to strong acid by noting that the stronger acidity of a $P(V)SH^+$ moiety would disfavor the monocationic cleavage mechanism adopted by PO-RNA at very low pH (Figure 3.2).[366,368,369]

The increased stability is particularly striking in light of the fact that replacing a *bridging* oxygen by sulfur leads to decreased acid stability.[370,371] As for DNA, thioation of the phosphodiester leads to slightly increased resistance to acid hydrolysis, but it is beyond the scope of this study to examine whether this is due to slower depurination or slower β-elimination.

We attempted to compare the stability of 2'F-ANA and its 2'-epimer, 2'F-RNA, to acid. However, only the pyrimidine monomers were available to us at the time, and pyrimidines are much more resistant to acid-catalyzed cleavage. After three months in acid at 55 ºC, 2'F-ANA or 2'F-RNA pyrimidine sequences (**Ac9**–**Ac10**) were at least 90% intact (Figure 3.4). No significant differences were observed between the two chemistries, although there seems to have been slightly more degradation for 2'F-ANA than 2'F-RNA at the 97 day timepoint. An isosequential DNA, **Ac11**, had a half-life of about three weeks under similar conditions.

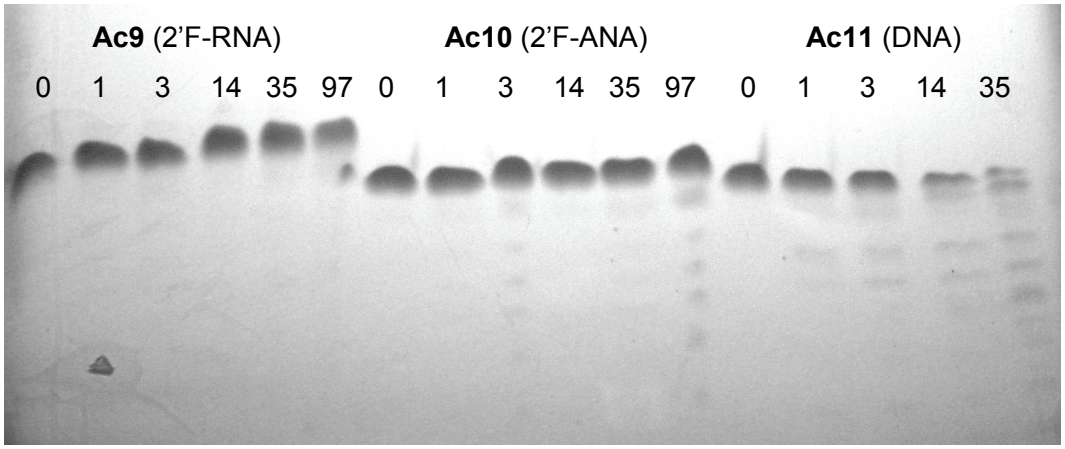

Figure 3.4. 24% denaturing PAGE comparing the acid stability of 2'F-RNA, 2'F-ANA and DNA sequences **Ac9**–**Ac11** to simulated gastric fluid at 55 ºC. Gels were developed using Stains-All dye. Timepoints are indicated in days.

3.2.3 Conclusions and applications of acid-stable 2'F-ANA

It has long been known that 2'-fluorinated nucleosides have excellent resistance to acid-catalyzed depurination.[208,241,242,330] As this study has now demonstrated, that property enables 2'F-ANA oligonucleotides to show excellent resistance to acid-catalyzed degradation.

The striking stability of 2'F-ANA oligonucleotides to acidic conditions suggests many possible applications; we now briefly discuss five of them.

Firstly, the oral delivery of oligonucleotides has until now been an extraordinary challenge and has been achieved with limited success.[372] While the acidic conditions in the stomach are only one of many challenges in the successful oral delivery of oligonucleotides, the use of 2'F-ANA oligonucleotides or 2'F-ANA–PS-RNA chimeras would overcome this challenge.

Secondly, many oligonucleotides are currently introduced into cells by lipid-mediated transfection. The oligonucleotides must pass through an increasingly acidic endosome to be released into the cell (the last compartment in the process of endocytosis, the lysosome, has a pH of 5 or lower.)[373,374] While these conditions are much milder than those encountered in the stomach, increased acid stability of oligonucleotides can only help ensure that more of the intact product is released from the lysosome into the cytoplasm.

Another potential application is in the area of 2'F-ANA-modified aptamers. Certain aptamers must operate under acidic conditions. For example, photoaptamers can be washed with acid after covalent linking to proteins. 2'F-ANA-modified aptamers (whether created by SELEX using 2'F-ANA triphosphates[300] or by modification of an existing aptamer[297]) would be more robust to these conditions with a corresponding increased sensitivity.

Oligonucleotide microarrays could benefit from 2'F-ANA modification not only because of the increased binding affinity of 2'F-ANA, but also because treatment with acid could be used to wash away all of the analyte (by disruption of Watson-Crick base pairing) without affecting the integrity of the 2'F-ANA probes of the array. This might prove especially useful to ensure that highly stable secondary structures are effectively eliminated. LNA-DNA chimeric probe oligonucleotides are currently used in microarrays for mRNA[375] or miRNA[376] expression. The use of LNA–2'F-ANA or LNA–2'F-RNA chimeric probe oligonucleotides would potentially allow these valuable diagnostic tools to be reused many more times, reducing the long-term cost. This is an important issue, since miRNA expression profiling is becoming increasingly important in clinical cancer diagnosis and treatment.[377]

Finally, another rapidly expanding field is that of nucleic acid-based nanotechnology and materials science. It is easy to envision applications where the additional acid stability of 2'F-ANA would be desirable.

For some of these applications, the 2'-epimer of 2'F-ANA (*i.e.* 2'F-RNA) would be equally appropriate, as we have noted above that it is also remarkably acid-resistant. However, more tools are always better; the DNA-like and RNA-like properties of 2'F-ANA and 2'F-RNA, respectively, may be more appropriate for different spheres of application. For example, most of the work currently being done in the field of nucleic acid based nanotechnology relies on DNA (probably because of its ease of synthesis). Thus 2'F-ANA may be more directly applicable to the systems being developed currently.

3.2.4 Experimental methods, acid stability of 2'F-ANA

All sequences were synthesized on an ABI 3400 DNA synthesizer. Standard conditions were used for synthesis and deprotection. Oligonucleotides were purified by preparative denaturing PAGE, followed by desalting on Nap-25 Sephadex columns.

Masses of oligonucleotides were verified by ESI-MS at the Biotechnology Research Institute (NRC) or Concordia University. Samples were prepared for these MS services by simply drying down 0.05 to 0.1 ODU of a well-desalted oligonucleotide.

Pepsin-free SGF was made by dissolving 0.20 g NaCl in 99 mL MilliQ water and autoclaving this solution, then adding 0.70 mL HCl (final pH ~1.2). For acid stability assays on sequences **Ac1**–**Ac8**, 0.7 ODU of each sequence was dissolved in 100 µL of SGF at 37 ºC. 10-µL aliquots were removed at various timepoints as indicated, frozen on dry ice, then immediately evaporated to dryness and stored in the freezer. The assay was then analyzed by 24% denaturing PAGE (7 M urea) which was developed using Stains-All dye. For acid-stability assays on pyrimidine-rich sequences **Ac9**–**Ac11**, 2 ODU of each sequence was dissolved in 100 µL of SGF at 55 ºC. A microtube with a tightly sealing screw-top was used for each reaction, and the solution was topped with mineral oil to avoid loss of

water and acid. The pH of the solution was verified at the end of the experiment and had not changed. 14-μL aliquots were removed at various timepoints and treated as above. The analytical gel was examined by UV shadowing since pyrimidine-only sequences do not stain well in Stains-All.

3.3 Stability of 2'F-ANA to enzymatic hydrolysis

3.3.1 Introduction to nuclease stability of 2'F-ANA

The improved nuclease stability of 2'F-ANA oligonucleotides has long been appreciated. For example, the first group to work on 2'F-ANA found a 4-8 fold increase in stability to nuclease P1, with respect to DNA.[267] Others have also observed increased stability of 2'F-ANA to snake venom phosphodiesterase (SVPDE, a highly active 3'-exonuclease) or serum. Noronha *et al*. subjected various homopyrimidine sequences to SVPDE hydrolysis and found the following order of stability: PS-DNA >> ANA > 2'F-ANA ≈ RNA > 2'F-RNA > DNA.[277] An interesting observation from this study is that arabinonucleic acids (2'-OH or 2'-F) are generally more stable to SVPDE than the corresponding ribonucleic acids (ANA > RNA and 2'F-ANA > 2'F-RNA). Furthermore, enzymatic stability seems to increase as the van der Waals radius of the 2'-substituent increases within each series, *i.e.* DNA ($2'H_{\beta}$) < 2′F-ANA ($2'F_{\beta}$) < ANA ($2'OH_{\beta}$); and DNA ($2'H_{\alpha}$) < 2′F-RNA ($2'F_{\alpha}$) < RNA ($2'OH_{\alpha}$).[277]

2'F-ANA can also confer nuclease resistance to duplexes and higher order structures. Dowler *et al*. showed that 2'F-ANA modification of one strand of an siRNA duplex provided significant additional serum stability to the whole duplex ($t_{1/2}$ ~5 h, vs. ~5 min for the unmodified duplex).[120] This could be further enhanced by incorporating 2'F-araN units into the 3'-overhang of the antisense strand as well.[120] 2'F-ANA-modification of a G-tetrad-containing thrombin-binding aptamer resulted in up to 48-fold greater serum stability compared to the unmodified DNA tetrad.[297]

While phosphodiester (PO)-2'F-ANA does provide some advantages in terms of nuclease stability, it cannot match the dramatic increase in stabilization provided by a phosphorothioate (PS) backbone.[378] However, when the two modifications

(PS and 2'F-ANA) are combined, the resulting PS-2'F-ANA oligonucleotide is highly resistant to most nucleases. Two recent studies have examined the persistence of PS-2'F-ANA AONs in cell culture, and explored the relationship with gene knockdown efficacy.[63,290] Kalota *et al*. observed that chimeric PS-2'F-ANA–DNA oligomers had greater persistence in cultured K562 cells (greater than 70% of the oligonucleotide was still recoverable from the cells after 96 h, while very little PS-DNA remained after this time.)[290] This suggests either that PS-2'F-ANA is more resistant to nucleases than PS-DNA, or that it is retained by cells to a greater extent. Correspondingly, this study found a lower effective dose and longer duration of action of PS-2'F-ANA oligomers with respect to PS-DNA.[290] Another study found that two PS-2'F-ANA sequences were more stable to serum nucleases than most other sequences (with some exceptions.)[63] Again, this paralleled excellent activity (luciferase knockdown in HeLa cells) over extended assay times.[63]

In PS-DNA, only the R_p stereoisomer is a substrate for SVPDE (in a study on model compounds, the R_p isomer was cleaved 13 000 times more quickly than the S_p).[379,380] In this study, we show that a similar phenomenon is observed for the diastereomers of 2'F-ANA. We also explore the relative rates of hydrolysis of PO-DNA, PO-2'F-ANA, PS-DNA and PS-2'F-ANA oligomers by SVPDE and serum.

3.3.2 Stereochemistry of PS-2'F-ANA degradation by SVPDE

Four dinucleotide monophosphorothioates were synthesized (Table 3.2). The purified dimers were incubated with SVPDE and aliquots were removed and analyzed by HPLC. Because an internal standard was not included, this data should be considered semi-quantitative.

For two of the dimers, **AT** and ^{f}**AT**, the phosphorothioate diastereomers proved very hard to resolve, even after trying several systems on both anion exchange and reverse-phase columns. However, the data from dimers ^{f}**A**^{f}**T** and **A**^{f}**T** are given in Table 3.2 and Figure 3.5. Furthermore, based on the shape of the curve from the sum of the two diastereomers of **AT** and ^{f}**AT**, the half lives of their diastereomers were also estimated and are given in Table 3.2.

It is clear from the results on $^{f}\mathbf{A}^{f}\mathbf{T}$ that SVPDE prefers one isomer of PS-2'F-ANA as it does for PS-DNA. The preference has been associated with the mechanism of cleavage of PS-DNA by SVPDE,[378] which thus does not appear to be affected by the switch to PS-2'F-ANA.

Another very interesting result from this study is that the 5'-nucleotide of the dimer has a significant effect on the rate of cleavage by SVPDE (in spite of the fact that SVPDE is a 3'-exonuclease). Thus, dA in the 5'-position led to much slower cleavage rates than did 2'F-araA (the faster-cleaved diastereomer of $\mathbf{A}^{f}\mathbf{T}$ is cleaved ~40 times more slowly than that of $^{f}\mathbf{A}^{f}\mathbf{T}$). This may be due to conformational issues; furthermore, it implies that $\mathbf{A}^{f}\mathbf{T}$ is a poorer substrate for cleavage, and/or that it is an inhibitor of the enzyme, preventing other substrates from being cleaved. We also sought to know whether this architecture was relevant to oligonucleotides, or only to dimers, and to PO backbones as well as PS. Therefore oligonucleotides were synthesized containing $\mathbf{A}^{f}\mathbf{T}$ structure at their 3'-ends, as part of a larger study of the nuclease stability of (PS and PO) 2'F-ANA and DNA, described in the next section.

Name	Sequence (5' – 3')	$t_{1/2}$ (d1)
AT	PS(at)	~40h
$\mathbf{A}^{f}\mathbf{T}$	PS(a***T***)	~250 h
$^{f}\mathbf{AT}$	PS(***A***t)	~2-8 h
$^{f}\mathbf{A}^{f}\mathbf{T}$	PS(***AT***)	~10 h

Table 3.2. Dinucleoside monophosphorothioates prepared for this study. Legend: dna, ***2'F-ANA***. Abbreviations: PS, phosphorothioate; $t_{1/2}$ (d1), the half life for SVPDE degradation of the shorter-lived diastereomer. The $t_{1/2}$ of the longer-lived diastereomer was too long to measure using our techniques.

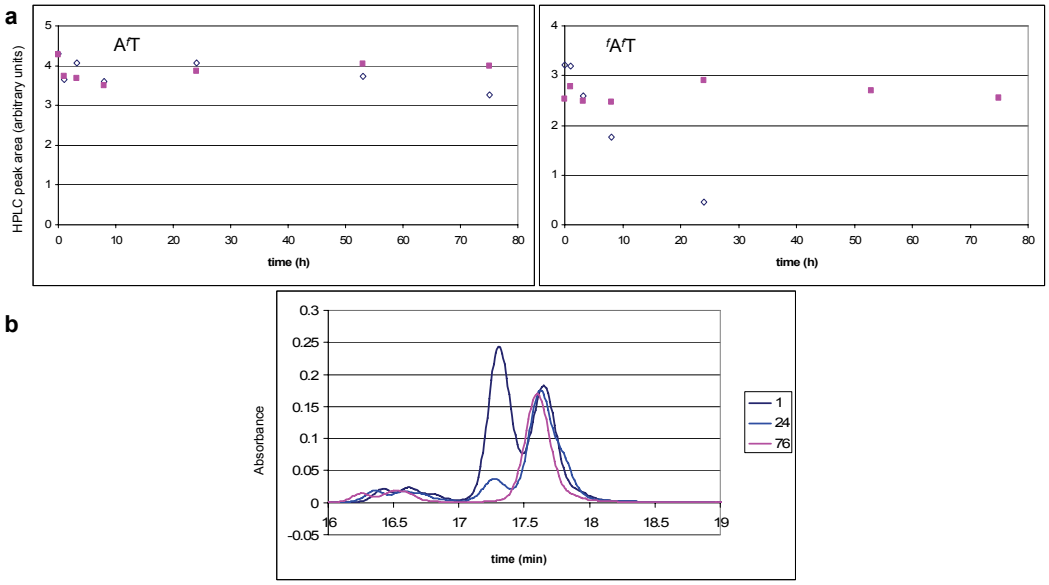

Figure 3.5. SVPDE selectively cleaves one diastereomer of PS-2'F-ANA. (a) Peak areas from HPLC analysis of SVPDE degradation of $\mathbf{A^fT}$ and $\mathbf{^fA^fT}$. The shorter-lived diastereomer is indicated with hollow diamonds and the longer-lived diastereomer with filled squares. (b) The PS-dimer diastereomer region of HPLC traces from SVPDE degradation of $\mathbf{^fA^fT}$ after 1h, 24h and 76h. The x axis of the 24h trace was shifted by nine seconds to make the superposition clearer. The small broad peak at 16.5 min is unidentified.

3.3.3 2'F-ANA oligonucleotide degradation by SVPDE and serum

To explore the enzymatic hydrolysis of 2'F-ANA and DNA oligonucleotides, we initially used the sequences **Ac2**, **Ac3**, **Ac5** and **Ac6** (Tables 3.1 and 3.3). Because these strands are self-complementary, we initially ran the assay at 15 ºC (7 ºC lower than the T_m of sequence **Ac6** (PS-DNA), the least stable duplex (see T_m values, Table 3.3). In this way, we hoped to study the nuclease stability of duplexes.

Name	Description	Sequence (5' – 3')	T_m (ºC)
Ac2	PO-2'F-ANA	PO(***AGCTAGCT***)	44.3
Ac3	PO-DNA	PO(agctagct)	26.5
Ac5	PS-2'F-ANA	PS(***AGCTAGCT***)	27.5
Ac6	PS-DNA	PS(agctagct)	22.4

Table 3.3. T_m values of **Ac2**, **Ac3**, **Ac5** and **Ac6** in SVPDE buffer. Legend: dna, ***2'F-ANA***. Abbreviations: PO, phosphodiester; PS, phosphorothioate.

Aliquots were removed and analyzed by PAGE. 2'F-ANA provided significant stabilization in the context of both PO and PS backbones. For the PO backbone, $t_{1/2\ (DNA)}$ was ~1 h, while the $t_{1/2\ (2'F\text{-}ANA)}$ was >24 h. For the PS backbone, since only one diastereomer could be cleaved, some of the full-length product was always visible. However, in the case of DNA, the other diastereomer had a half-life of about 8 h, while for 2'F-ANA no cleavage of either diastereomer was visible up to 5 d (Figure 3.6).

However, because these strands are self-complementary, even though they were done at 15 ºC is it possible that the cleavage we observe is through a small amount of the single stranded oligonucleotide present at equilibrium. More of the sample would be in its single-stranded form in the case of DNA than 2'F-ANA, because of the higher thermal stability of the latter. Therefore, it is not clear that these results are relevant to non-self-complementary single-stranded oligonucleotides. They are, however, of interest for applications of 2'F-ANA in duplex environments, including siRNA (see below and Chapter 5).

We therefore carried out a second assay at 50 ºC (6 ºC higher than the T_m of sequence **Ac3** (PO-2'F-ANA), the most stable duplex. In this case, very little difference was observed between 2'F-ANA and DNA (data not shown). We therefore wondered whether the stabilization observed above was primarily due to the greater thermal stability of 2'F-ANA.

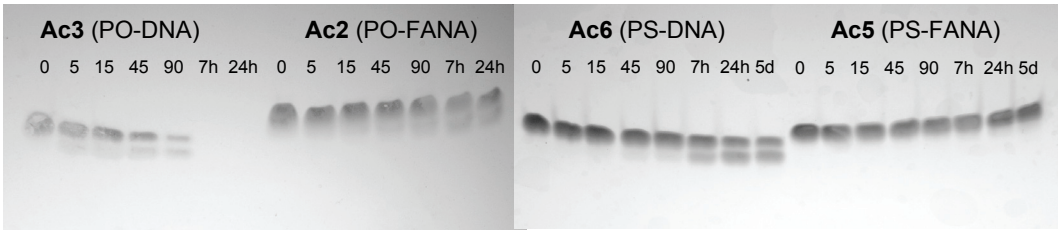

Figure 3.6. SVPDE assay on self-complementary sequences at 15 ^{o}C. 1 ODU of each sequence was dissolved in 60 µL buffer along with 2.5 units SVPDE. Aliquots were removed at various times (in minutes unless otherwise indicated), quenched with an equal volume of formamide, and stored at -20 ºC until PAGE analysis.

Therefore, to characterize the nuclease stabilization incurred by 2'F-ANA modification of a single strand, another series of assays was carried out, using non-self-complementary oligonucleotides **E1**–**E12** (Table 3.4). Strands **E1**–**E4** were of one sequence, and strands **E5**–**E8** were of a complementary sequence (this was to allow testing of two independent single-stranded sequences, but also left the door open for testing of duplexes). Strands **E9**–**E12** were of the first sequence, but were 2'F-ANA–DNA chimeric strands designed to test whether the extra stability of the $\mathbf{A^fT}$ dimer (see above) would be carried into oligonucleotides as well, therefore they contained dA–2'FaraT sequences at their 3'-end.

Name	Description	Sequence (5' – 3')
E1	PO-2'F-ANA	PO(***CGACCTGTGCAT***)
E2	PS-2'F-ANA	PS(***CGACCTGTGCAT***)
E3	PO-DNA	PO(cgacctgtgcat)
E4	PS-DNA	PS(cgacctgtgcat)
E5	PO-2'F-ANA	PO(***ATGCACAGGTCG***)
E6	PS-2'F-ANA	PS(***ATGCACAGGTCG***)
E7	PO-DNA	PO(atgcacaggtcg)
E8	PS-DNA	PS(atgcacaggtcg)
E9	PO-mix1	PO(***C***g***ACCTGTGC***a***T***)
E10	PS-mix1	PS(***C***g***ACCTGTGC***a***T***)
E11	PO-mix2	PO(***C***gacctgtgca***T***)
E12	PS-mix2	PS(***C***gacctgtgca***T***)

Table 3.4. Further strands prepared for the nuclease stability study. Legend: dna, ***2'F-ANA***. Abbreviations: PO, phosphodiester; PS, phosphorothioate.

Nuclease stability assays were carried out on single-stranded **E1**–**E12**. These reactions were carried out at 37 ºC, using PCR tubes topped with mineral oil to avoid error due to evaporation. The assays comparing 2'F-ANA and DNA with a single chemistry (*i.e.* strands **E1**–**E8**, not chimeric strands) are shown in Figure 3.7. Very little difference was observed between 2'F-ANA and DNA for these sequences. PO-2'F-ANA showed slightly more resistance to SVPDE (Figure 3.7a), but no significant differences were observed between PS-2'F-ANA and PS-DNA in this assay (Figure 3.7b). Furthermore, no differences were

observed between 2'F-ANA and DNA in serum with either linkage (PO or PS) (Figure 3.7c-d).

As observed in the introduction to this study (Section 3.3.1), other researchers have observed stabilization of non-self-complementary single strands upon 2'F-ANA modification. For example, Ferrari *et al* showed that an 18mer phosphorothioate AON showed decreasing serum stability in the order 2'F-ANA gapmer > 2'F-ANA altimer > DNA.[63] This order of stability corresponded to the potency and duration of action of the AONs.[63] Thus, there is some sequence dependence to the stabilization of 2'F-ANA-modified oligonucleotides.

Chimeric strands **E9**–**E12** were run concurrently with **E1**–**E8**, but some of the gels were damaged and the results are not shown here. However, no significant differences in cleavage rate were observed, consistent with the fact that DNA and 2'F-ANA were cleaved at a similar rate when in separate strands. Therefore the additional SVPDE stability observed for the dA-2'FaraT dinucleoside monophosphorothioate does not seem to be applicable to 3'-terminal dA-2'FaraT units in oligonucleotides.

However, one property that does carry over from the dinucleoside monophosphorothioates to oligonucleotides is the preference of SVPDE for one phosphorothioate diastereomer. As seen in Figure 3.7(b and d), for both DNA and 2'F-ANA and under conditions of both SVPDE and FBS, the amount of full-length strand never drops below about 50% of the original amount. At longer timepoints, ~25% of the n-1 species is visible, ~12% of the n-2, and so on. Therefore, when the full-length strand of either DNA or 2'F-ANA was cut, the SVPDE enzyme was only able to excise a nucleotide or two before, apparently, reaching a linkage that it was unable to cleave. This resulted in very long-lived, nearly full-length species, probably all containing S_p phosphorothioate linkages at the 3'-terminus, assuming that the same isomer is preferred for both DNA and 2'F-ANA. In the case of serum nucleases, endonuclease cleavage is likely the dominant mechanism for the eventual degradation of these stable species. In fact, this may be true of both nuclease systems we tested, since a small amount of endonuclease-type cleavage has been observed for SVPDE.[381]

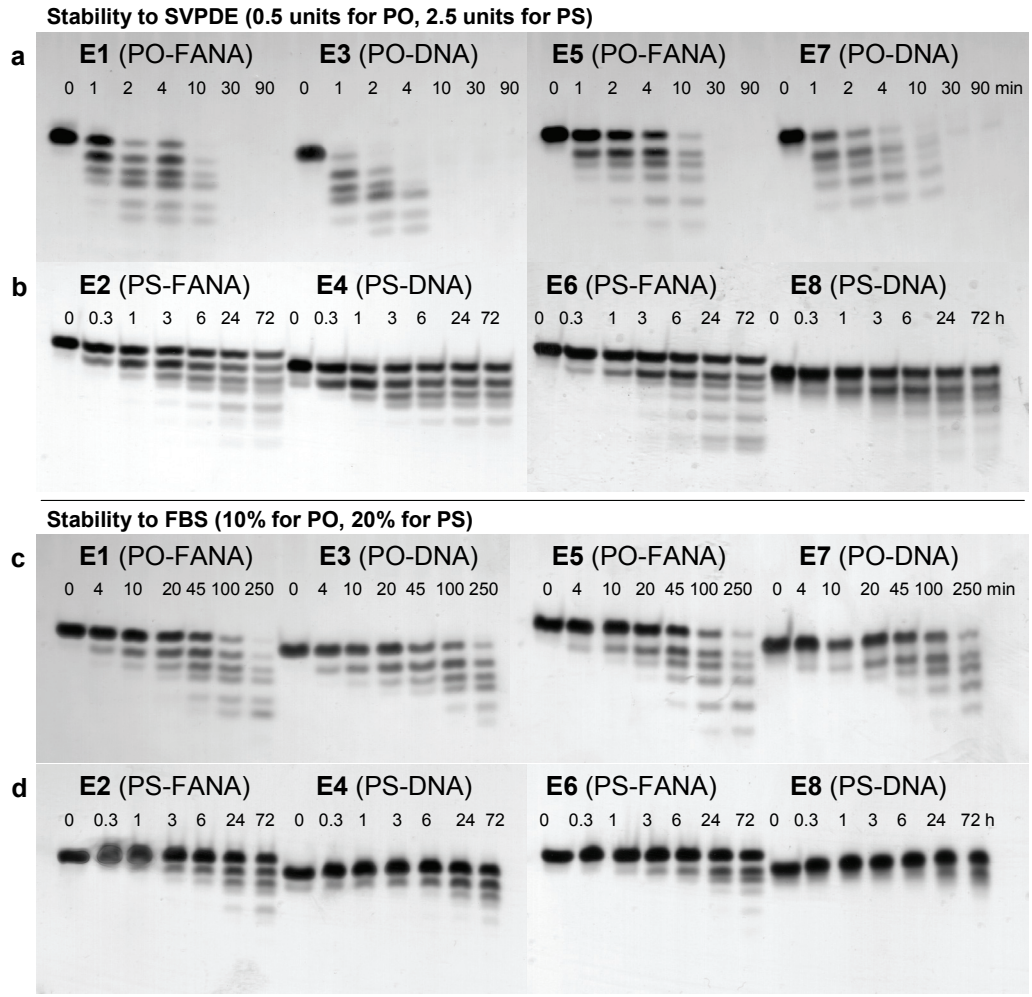

Figure 3.7. 24% Denaturing PAGE showing nuclease stability of 2'F-ANA and DNA sequences **E1**–**E8** (visualized by Stains-All). (a) 5 nmol of each PO sequence was incubated with 0.5 units SVPDE in buffer, aliquots were removed at the times indicated, in minutes. (b) 5 nmol of each PS sequence was incubated with 2.5 units SVPDE in buffer, aliquots were removed at the times indicated, in hours. (c) 5 nmol of each PO sequence was incubated in 10% FBS in DMEM, aliquots were removed at the times indicated, in minutes. (d) 5 nmol of each PS sequence was incubated in 20% FBS in DMEM, aliquots were removed at the times indicated, in hours.

3.3.4 Conclusions and future work, enzymatic stability of 2'F-ANA

One clear conclusion from this study is that one diastereomer of 2'F-ANA phosphorothioates is selectively cleaved by SVPDE and serum nucleases, parallel to observations of PS-DNA cleavage by these nucleases.

However, other research described in this section raises questions that should be followed up. One of these questions is how much of the SVPDE stabilization achieved by 2'F-ANA sequences **Ac2** and **Ac5** is related to their higher thermal stability vs DNA. To explore this question more fully, a nuclease stability assay could be carried out by labeling strands **E1**–**E4**, then annealing them with **E5**–**E8** before carrying out the assay. As well as comparing the stability of ds-2'F-ANA and dsDNA, it would also be possible to compare the stability, for example, of a DNA strand bound to 2'F-ANA and one bound to DNA.

An ongoing subject of interest, related to this, is the sequence-dependence of 2'F-ANA's nuclease protection. Even if some of the nuclease resistance of 2'F-ANA oligomers **Ac2** and **Ac5** is related to their thermal stability, many others have observed stabilization by 2'F-ANA for single-stranded oligonucleotides. It would be interesting to understand why the two sequences corresponding to oligomers **E1**–**E8** were not significantly protected from nuclease cleavage by 2'F-ANA.

Finally, it would also be interesting to repeat the assay on the dinucleoside monophosphorothioates, after finding conditions which allow separation of the diastereomers of all four dimers. Since the dramatic additional stability provided by dA-2'F-araT units is not applicable to the context of oligonucleotides, this project might be more academic than practical, but it is nonetheless an interesting finding, and worth exploring. Questions that could be investigated include whether dimers of other base sequences also show such a strong synergy between DNA and 2'F-ANA in resistance to SVPDE cleavage. It would also be interesting to know why this synergy exists. A simple starting point would be an inhibition assay using the isolated diastereomers, in the presence of labeled substrates, to explore whether either one of the $\mathbf{A}^{f}\mathbf{T}$ diastereomers is an inhibitor of SVPDE. If so, and if it is the non-cleavable isomer of $\mathbf{A}^{f}\mathbf{T}$ that inhibits SVPDE, the

structural/conformational reasons for the superiority of **A^{f}T** would be straightforward to investigate by NMR structural studies.

3.3.5 Experimental methods, enzymatic stability of 2'F-ANA

Oligonucleotide synthesis and PAGE were carried out as described in Section 3.2.4.

Dinucleoside monophosphorothioates were synthesized and purified by Julia Viladoms, a summer student in our lab. After solid phase synthesis and deprotection as for the oligonucleotides, these dimers were desalted using Sep-Pak solid-phase extraction cartridges.

Anion exchange HPLC (used to resolve the diastereomers of ^{f}**A^{f}T**) was carried out using a Waters Protein-Pak DEAE 5PW column. A 30 min gradient from pure water to 0.20 M $LiClO_4$ was used. For reverse phase HPLC (used to resolve the diastereomers of **A^{f}T),** a Waters Symmetry C18 5 μm 4.6×150 mm column was used with a gradient of 0-25% methanol in water, containing 100 mM triethylammonium acetate.

The low-temperature SVPDE assay on self-complementary sequences **Ac2**–**Ac6** was carried out at 15 ^oC. 1 ODU of each sequence was dissolved in 60 μL buffer along with 2.5 units SVPDE. 7-μL aliquots were removed at various times (in minutes unless otherwise indicated), quenched with an equal volume of formamide, and stored at -20 ºC until analysis by denaturing 24% PAGE.

All other SVPDE assays were carried out in PCR tubes. Typically, 5 nmol of oligonucleotide was dissolved in 20 μL of SVPDE buffer (100 mM Tris-HCl, 100 mM NaCl, 14 mM $MgCl_2$, pH 8.9) and warmed to 37 ºC. 2.5 μL was removed as a zero point. 17.5 μL of the same buffer containing 0.5 or 2.5 units of SVPDE (Phosphodiesterase I from *Crotalus adamanteus* venom, USB Corporation, Cleveland, Ohio) was warmed to 37 ºC, then added to start the reaction. 0.5 Units of SVPDE was used in the case of PO oligonucleotides, while 2.5 units of SVPDE was used for PS oligonucleotides. 1.5 Units of SVPDE was used for the high-temperature (50 ºC) assay on sequences **Ac2**–**Ac6**. Aliquots (5 μL) were removed at various timepoints as indicated, pipetted onto 5 μL formamide, heated to 95 ºC

for 1 minute and then stored at -20 ºC until analysis by denaturing 24% PAGE. Bands were visualized using Stains-All dye. For assays longer than four hours, the reactions were topped with mineral oil (10–20 μL).

FBS stability assays were also carried out in PCR tubes; 5 nmol of oligonucleotide was dissolved in 20 μL of Dulbecco's modified Eagle medium (DMEM) and warmed to 37 ºC. 2.5 μL was removed as a zero point. 17.5 μL of 20% FBS in DMEM was warmed to 37 ºC, then added to start the reaction. Treatment of aliquots, use of mineral oil and analysis were as for the SVPDE assays. Serum stability assays were repeated, for confirmation, using 5% FBS (final concentration) on the PO series **E1**, **E3**, **E5** and **E7**; for this assay the aliquots were simply frozen on dry ice, evaporated to dryness, and taken up in formamide for electrophoresis. This procedure gave comparable results (no differences observed between 2'F-ANA and DNA).

3.4. Application of 2'F-ANA in an exciplex system

3.4.1 Introduction to exciplex-based diagnostics

An exciplex is a complex that only exists when one of the partners is in the excited state.[382] When the partners are identical, the exciplex is termed an excimer (from "excited dimer").[383] The individual atoms, molecules or groups that make up an exciplex are called exci-partners.

When exciplexes relax, they often fluoresce. Furthermore, the Stokes shift ($\lambda_{emission} - \lambda_{excitation}$) of exciplexes is often very large, which helps ensure a large signal-to-noise ratio in measurements of exciplex fluorescence.

Most traditional techniques for DNA sequence detection are based on the change in the fluorescence of a labeled probe oligonucleotide upon hybridization of a complementary oligonucleotide, but these systems have a high background signal and give poor resolution between sequences that differ only by a single mismatch. Furthermore, they often depend primarily on a change in fluorescence intensity, without much change in wavelength.[384] An exciplex system, on the other hand, produces a large change in wavelength (because of the large Stokes

shift), leading to a visible color change.[384,385] Furthermore, an exciplex is structurally more demanding, since the exci-partners must be precisely aligned to produce an exciplex signal. (The pyrene excimer requires that the exci-partners approach each other to about 3.5 Å, thus this technique could have resolution on the order of a base pair. In contrast, FRET techniques usually operate over distances of 10-100 Å, corresponding to at least 3 bp.)[385]

Therefore, an exciplex system can be applied to one of the challenges of nucleic acid diagnostics: detection of single-nucleotide polymorphisms. Ideal for this task is a split-probe exciplex system, consisting of two short oligonucleotide probes, complementary to neighboring sites on a target oligonucleotide and each conjugated to an exci-partner (Figure 3.8).[385] A single mismatch, deletion or insertion within the target sequence complementary to either of the two probes is enough to reduce the exciplex signal tremendously.

Various groups have used the pyrene excimer in this kind of system (in Figure 3.8, A = B = pyrene).[384,386] However, an exciplex system in which the two groups can vary independently from one another would allow greater flexibility and perhaps a wider range of applications.

The groups 1-pyrenylmethylamine and *N′*-methyl-*N′*-naphthalen-1-yl-ethane-1,2-diamine (see Figure 3.9) can be appended to 5' and 3' terminal phosphate groups on the split-probe oligonucleotides, resulting in a functional exciplex system. However, the solvent system required for this functional split-probe exciplex system consists of 80% trifluoroethanol (TFE) with 20% aqueous buffer.[385] It is not clear why this peculiar solvent system is required, but there are several possibilities:

(1) The decreased polarity of the solvent system favors exciplex emission, consistent with the observation by many groups that exciplex emission is quenched in solvent systems more polar than acetonitrile (dielectric constant = 35). However, an intramolecular exciplex was recently found to fluoresce even in *N*-methylformamide (dielectric constant ~ 120).[387]

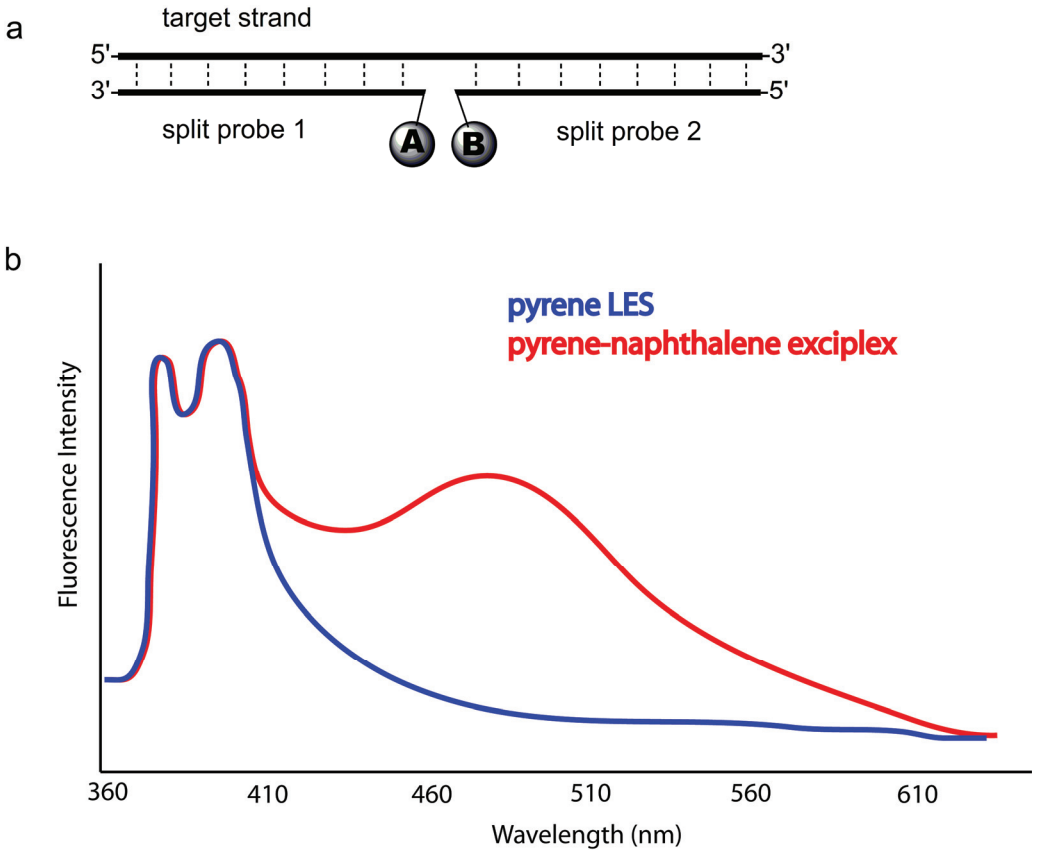

Figure 3.8. A split-probe exciplex system. (a) A schematic of a split-probe exciplex system, with the exci-partners represented as A and B, respectively.[385] (b) An idealized fluorescence emission spectrum, showing expected behaviour for a pyrene locally excited state (LES; A = pyrene, B not present) and a pyrene-naphthalene exciplex (A = pyrene, B = naphthalene). Excitation wavelength is 350 nm; note that the exciplex Stokes shift is thus greater than 100 nm.

(2) The nonpolar solvent system allows the exci-partners (pyrene and naphthalene) to interact with each other in the bulk solution, instead of being forced into the DNA grooves by hydrophobic interactions.[388]

(3) It is possible for DNA duplexes to undergo changes in helical structure when the humidity of the medium is changed. For example, methanol,[389] ethanol,[390-392] TFE,[393-395] and different cations[396] can induce this transition. TFE can cause B-form to A-form transitions, but has also causes B-form to Z-form transitions or changes between different B-type isoforms.[396] Hydrophobic TFE molecules disrupt the water structure in the minor groove to induce the B–A

transition.[391,393,394] Strikingly, the B–A transition is seen in solutions of 70-80 % TFE, which coincides with the required optimal percentage of TFE for exciplex emission, suggesting that A-form helical structure may favor exciplex formation.

Because of the possibility of fluorine-fluorine interactions, and because 2'F-ANA may be less hydrated than other oligonucleotides (see Section 2.3), we wished to investigate the effect of 2'F-ANA oligonucleotides on exciplex formation using the split-probe system previously described.[385] This work was done in collaboration with Stefanie Lang, Elena Bichenkova and Kenneth Douglas at the University of Manchester, UK. Synthesis of the 2'F-ANA target strand was carried out at McGill, and DNA probe synthesis and exciplex measurements were carried out by our collaborators.

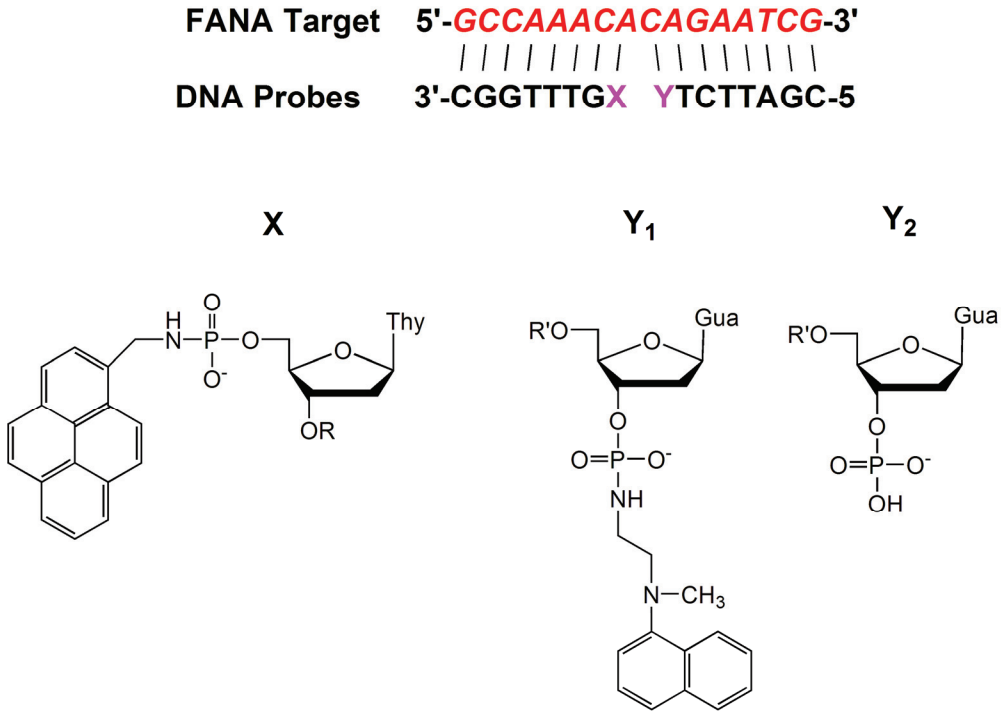

Figure 3.9. The split probe exciplex system containing a 2'F-ANA target strand. For the full exciplex system, Y = Y_1, and for the control system, Y = Y_2.

The sequence was the same as that of the previous exciplex system.[385] Probe strands are synthesized with a 3' or 5' phosphate (using phosphate-ON CPG solid

support, or a 5'-phosphorylating reagent after oligonucleotide synthesis, respectively). The phosphate is then conjugated to 1-pyrenylmethylamine or *N′*-methyl-*N′*-naphthalen-1-yl-ethane-1,2-diamine (Figure 3.9) as previously described.[385]

3.4.2 Results

A 2'F-ANA strand was used to replace the target strand of the exciplex system described above (Figure 3.9). DNA probe strands were used as for the previous system.

The first set of experiments tested the hybridization of the system. The 2'F-ANA system hybridized in all buffers, from 0 to 80% TFE. Similar results were obtained by three types of T_m experiments (monitoring A_{260}, monitoring the fluorescence of the pyrene locally excited state (LES) at 380 nm, and monitoring the exciplex emission at 480 nm). Futhermore, evidence for hybridization was visible in the UV absorption spectra, as the pyrene peaks were red-shifted and their extinction coefficients decreased. The T_m decreased with increasing concentrations of TFE up to 70% (for the full system, Y = Y_1) or 60% (for the control, Y = Y_2), then it increased again (Figure 3.10 and Table 3.5). The reasons for this nonlinear dependence of thermal stability on TFE concentration are not clear.

As expected, use of 2'F-ANA does stabilize the system somewhat relative to DNA. The all-DNA system had T_m values of 36 and 25 ºC in buffer and 80% TFE, respectively,[385] while the 2'F-ANA exciplex system had T_m values of 38 and 28 ºC under the corresponding conditions.

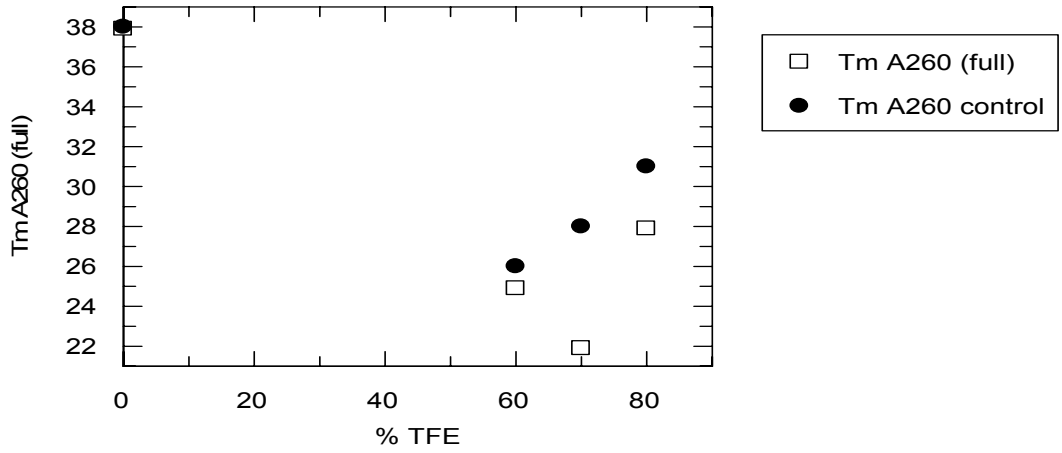

Figure 3.10. T_m of the full 2'F-ANA exciplex system (Y = Y_1, hollow squares) and the control system (Y = Y_2, black circles), in various mixtures of TFE and buffer. These T_m data were obtained by measuring A_{260} with increasing temperature. Data taken from Table 3.5.

	0% TFE	60% TFE	70% TFE	80% TFE
2'F-ANA full exciplex system (Y = Y_1)				
A_{260}	37.9 ± 0.7 ºC	24.9 ± 0.6 ºC	21.9 ± 0.7 ºC	27.9 ± 0.4 ºC
A_{350}	-	-	24.0 ± 0.6 ºC	29.0 ± 0.6 ºC
F λem $_{376}$	34.0 ± 0.5 ºC	29.0 ± 0.7ºC	22.0 ± 0.7 ºC	27.1 ± 0.6 ºC
F λem $_{480}$	-	-	22.0 ± 0.6 ºC	27.1 ± 0.5 ºC
2'F-ANA control system (Y = Y_2)				
A_{260}	38.0 ± 0.6 ºC	26.0 ± 0.6 ºC	28.0 ± 0.6 ºC	31.0 ± 0.3 ºC
A_{350}	-	-	29.1 ± 0.5 ºC	33.0 ± 0.7 ºC
F λem $_{376}$	36.0 ± 0.6ºC	25.0 ± 0.6 ºC	27.0 ± 0.6 ºC	30.0 ± 0.7 ºC
F λem $_{480}$	-	-	-	30.0 ± 0.7 ºC

Table 3.5. T_m values from UV and fluorescence, for the 2'F-ANA exciplex full system (Y = Y_1) and control system (Y = Y_2).

Exciplex emission was observed for the full system (Y = Y_1) at 70% and 80% TFE (in contrast, when a DNA target is used, the buffer must contain 80% TFE to observe exciplex emission). In both solvent systems, the exciplex emission (in terms of shape and intensity) was similar to that observed for the DNA target.

When the control probe (Y = Y_2) was used, only the pyrene exci-partner was present, and therefore no exciplex signal should have been observed. However, some background exciplex emission was observed for this control system in 80% TFE, probably because pyrene can interact to form exciplexes with nucleobases directly, especially guanine.[397] On the other hand, this background exciplex formation was not observed in 70% TFE, nor was it observed with a DNA target in 80% TFE.[385]

Fluorescence emission spectra are shown in Figure 3.11, and spectral data are summarized in Table 3.6. The ratio of fluorescence intensities at 480 and 380 nm (I_E/I_M) is used to evaluate the usefulness of the exciplex signal. For the full system, the I_E/I_M value is higher in 70% TFE than in 80% TFE, indicating better exciplex formation in the former solvent. Furthermore, because of the background exciplex fluorescence observed in 80% TFE, the control I_E/I_M is lower in 70% TFE than 80% TFE. These two phenomena make for a much lower (*i.e.* better) background-to-signal ratio ($I_E/I_{M\ control}$) / ($I_E/I_{M\ system}$) in 70% TFE.

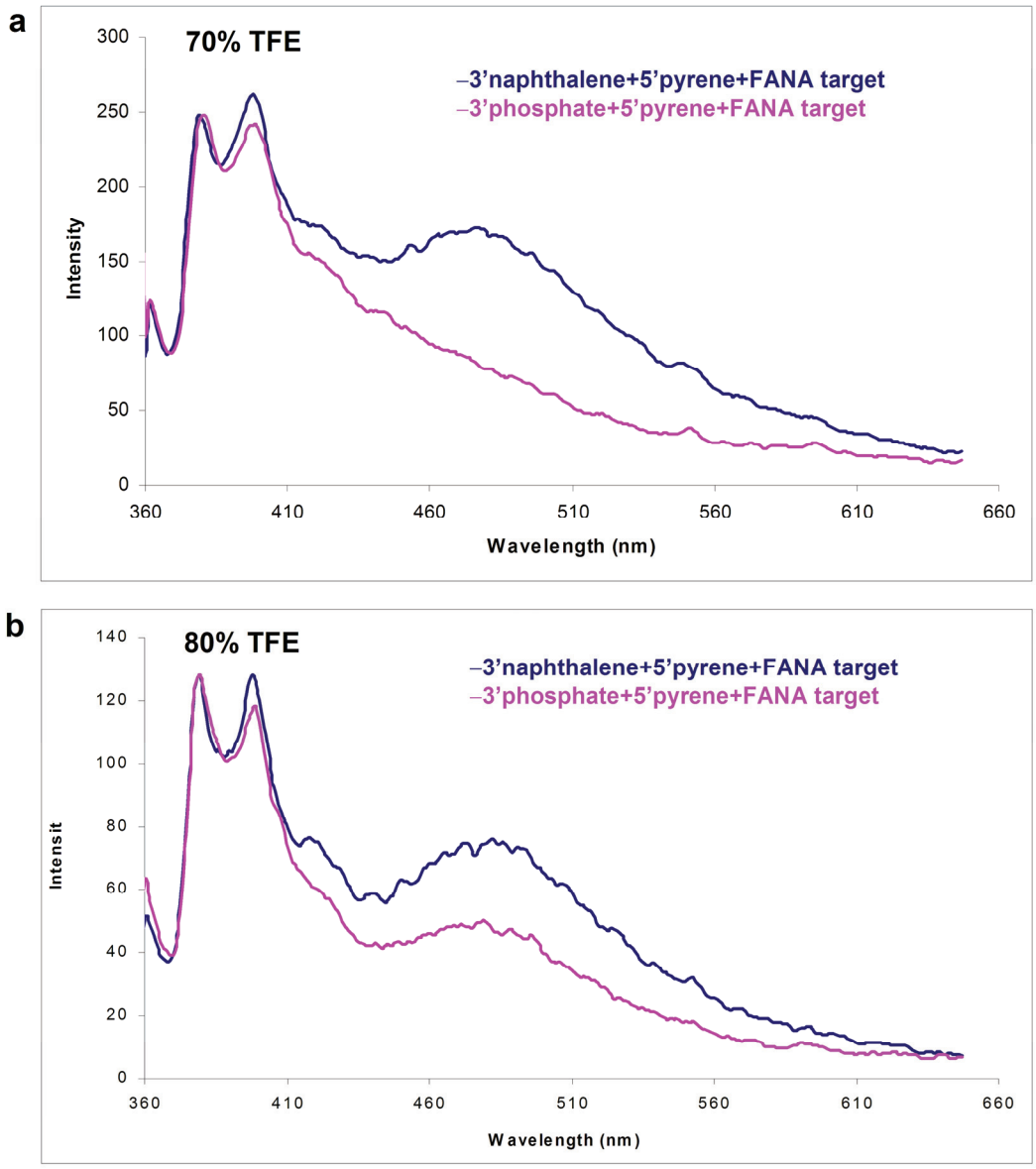

Figure 3.11. Fluorescence emission spectra, normalized to 380 nm, of 2'F-ANA exciplex and control systems in (a) 70% TFE or (b) 80% TFE. Both systems contained 0.01 M Tris-HCl, 0.1 M NaCl, pH 8.4. All spectra were obtained at 5 ºC, slitwidth 5 nm, λ_{exc} 350 nm.

%TFE	λ_{max} pyrene LES	λ_{max} exciplex full system (Y = Y_1)	I_E/I_M system	λ_{max} exciplex control (Y = Y_2)	I_E/I_M control	$(I_E/I_{M\ control})/(I_E/I_{M\ system})$
70	380	480	0.682	-	0.312	0.46
80	379	480	0.585	480	0.378	0.65

Table 3.6. Effect of TFE concentration on fluorescence emission of the FANA exciplex and control systems in 0.01 M Tris-HCl, 0.1 M NaCl buffer pH 8.4 at 5 ºC. I_E/I_M is the ratio of fluorescence intensities at 480 nm and 380 nm.

3.4.3 Conclusions and future work, exciplexes

Use of a 2'F-ANA target in the split probe exciplex system did not increase exciplex emission, but did allow some reduction in the TFE required for exciplex formation. Since 2'F-ANA duplexes do not preorganize a 2'F-ANA-DNA hybrid duplex to the A-form, but do change the hydration properties of a duplex (Chapter 2), this supports the idea (discussed above) that the hydration environment of the system may be an important factor in the effectiveness of the system, and may explain part of the need for TFE.

However, our UK colleagues (Elena Bichenkova, Kenneth Douglas *et al*.) have recently shown that LNA-modified probes increase the exciplex emission of this split probe system (unpublished data). LNA nucleotides are constrained in a C3'-*endo* (north) conformation and can even induce a conformational shift to the north in neighboring nucleotides.[398] This supports the idea (discussed above) that A-form helical structure is crucial for effective exciplex formation.

It is possible that an A-form fluorinated oligonucleotide such as 2'F-RNA will be able to combine these two advantages, offering higher exciplex emission at lower concentrations of TFE. Therefore, we recently sent to our UK colleagues both the target and probe structures, fully-modified with 2'F-RNA. We have also sent 2'F-ANA probe strands, since the work discussed above was done using only the target strand, and we would like to be able to study phenomena such as 2'F-ANA recognition of 2'F-ANA or RNA targets. These new exciplex studies are in progress and will be published in due course.

On the other hand, use of a 2'F-ANA target increased the background fluorescence (relative to DNA) at 80% TFE. It is not clear why this is the case. Comparison with 2'F-RNA may shed some light on whether this is related either to the hydrophobicity or to the structure of the oligonucleotide strand.

Chapter 4. Synthesis and conformational analysis of 2'-fluoro-4'-thioarabinouridine and related compounds

4.1 Introduction

The conformation of oligonucleotides is believed to depend strongly upon the conformation of the nucleotide monomers that make them up.[399] Thus, to understand and design oligonucleotide therapeutics successfully, it is essential to be able to understand and manipulate nucleoside conformations.

As part of our ongoing program to develop new nucleic acid chemistries, we chose to replace the 4' oxygen of 2'-deoxy-2'-fluoro-5-methylarabinouridine (FMAU) with a sulfur atom. On a chemical level, it was envisaged that this modification would modulate stereoelectronic and steric effects in the 2'-fluoroarabinofuranose moiety. We were especially interested to investigate the effect of the 4'-thio modification in conjunction with the presence of the 2'-fluorine, which led to favorable biological properties in the case of the 2'F-ANA oligonucleotides.[400,401] While 2'-deoxy-2'-fluoro-4'-thioarabinonucleosides have previously been synthesized,[402-405] this is the first time their conformation has been examined.

On the other hand, various groups have undertaken conformational studies of 2'-fluoroarabinonucleosides. Early computational work suggested that pyrimidine base of FMAU was locked into an *anti* orientation because of the presence of the top-face fluorine at 2', and that the nucleoside puckered in the south (C2'-*endo*).[406] An NMR study later showed that FMAU had about 65% "south character" (characterized only vaguely, no specific P value was calculated) over a wide range of temperatures.[407]

More recently, quantitative conformational studies have been done using the program PSEUROT,[408] which assumes a two-state conformational equilibrium. This has been a key tool in allowing conformational discussions to move beyond vague references to "north" and "south" conformers. We summarize the available quantitative solution-phase parameters in Table 4.1 and Figure 4.2 (structures of canonical and modified purine bases are shown in Figure 4.1). Parameters for

normal 2'-deoxyribo- and ribonucleosides (dN and rN) are included for comparison.

Nucleoside	$P_N(\phi_{max})$	$P_S(\phi_{max})$	% N	Ref
Normal nucleosides				
rN (pyrimidine)[a]	15 (43)	165 (43)	59	41
rN (purine)[a]	10 (42)	170 (42)	42	41
dN (pyrimidine)[a]	13 (41)	167 (41)	42	41
dN (purine)[a]	9 (42)	171 (42)	32	41
2'-Fluoroarabino nucleosides (canonical bases)				
2'F-araG	54 (41)	181 (41)	50	263
2'F-araG	66 (43)	173 (43)	57	409
2'F-araA	26 (40)	133 (40)	36	263
2'F-araA	-9 (40)	128 (40)	32	410
2'F-araA	70 (43)	168 (43)	58	409
2'F-araA	9 (36)	132 (37)	36	411
2'-Fluoroarabino nucleosides (modified bases)				
4a	-2 (41)	129 (41)	35	412
4b	10 (41)	130 (41)	34	412
4c	-4 (41)	131 (41)	36	412
4d	-2 (41)	131 (41)	37	412
4e	5 (41)	130 (41)	36	412
4f	-2 (37)	108 (42)	98	409
4g	-2 (38)	126 (42)	100	409

Table 4.1. 2'-deoxy-2'-fluoroarabinonucleosides for which quantitative solution-phase pseudorotational parameters are available. Purine structures are shown in Figure 4.1. [a]Results for the *anti* base orientation are given, since 2'-fluoroarabinonucleosides have a higher proportion of the *anti* orientation than their deoxynucleotide congeners.[297,406]

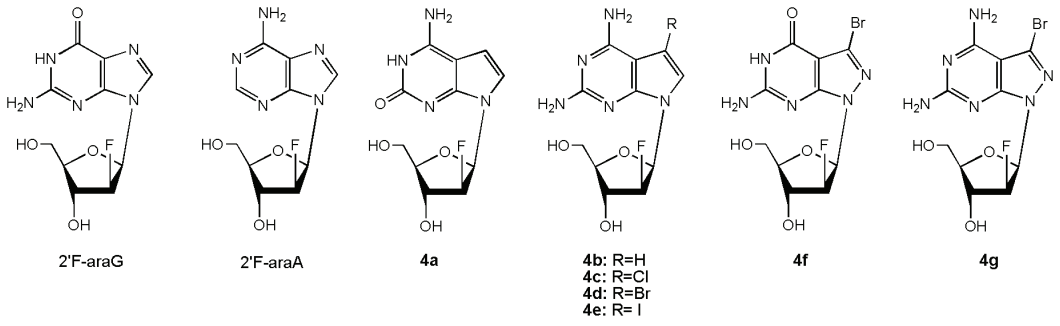

Figure 4.1. 2'-fluoroarabino purine nucleosides (with canonical and modified bases) for which quantitative solution-phase conformational parameters are available.

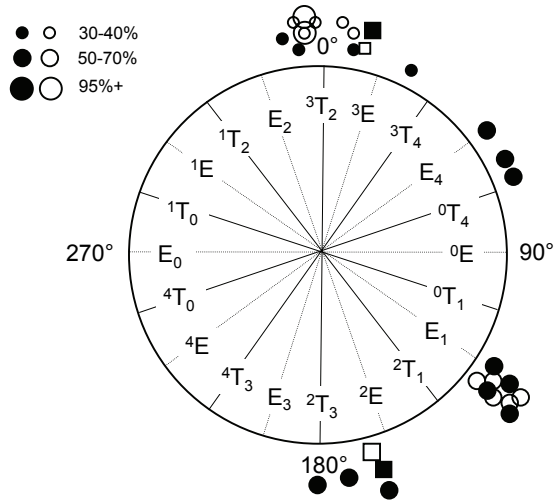

Figure 4.2. The conformational parameters from Table 4.1 shown on the pseudorotational wheel. Legend: filled squares, rN; empty squares, dN; filled circles, 2'F-araN with canonical bases; empty circles, 2'F-araN with modified bases. Values for dN and rN are averages for purine and pyrimidine values. Sizes of circles are approximately proportional to the mole fraction of each conformer shown.

It becomes clear from Table 4.1 and Figures 4.1–4.2 that there are differences within the literature on the solution-phase conformation of 2'-fluoroarabinonucleosides, specifically 2'F-araA and 2'F-araG. The 2'F-araN conformations, whether with canonical or modified bases, fall into four groupings, in the north, northeast, southeast and south. Five researchers have found a pair of conformations in the north and southeast for the 2'-fluoroarabinonucleosides, while two others have found a pair of conformations in the northeast and south. For 2'F-araA and 2'F-araG, both of these pairs of conformations have been independently found. One explanation may be that these nucleotides are in fact characterized by a three- or four-state equilibrium, but either of the two pairs is sufficient to reproduce the observed coupling constants. (The PSEUROT program can only resolve equilibria of one or two conformers). Denisov *et al.* have described an oligonucleotide (hairpin) for which the two-state model adopted by PSEUROT was not adequate to explain the observed NOEs, but a three-state model (explored through molecular modeling) was suitable.[329]

One property that emerges very clearly from the data is the presence of eastern conformations for 2'F-araN. (The eastern conformation was first observed for

2'F-araN in 1998, in the context of oligonucleotides, by Berger *et al.*[269]) All of the nucleosides studied have a predominant population of either the northeast or southeast conformer, with the sole exceptions of those with the unusual 3-bromopyrazolo[3,4-*d*]pyrimidine bases (**4f** and **4g**) and a couple of other more extreme base modifications not included in Table 4.1.[409,413] Thus, whichever description of the 2'-araN conformation is correct (north + southeast, northeast + south, or a four-state equilibrium), an eastern shift is observed when comparing 2'F-araN to dN: either the south becomes southeast, or the north becomes northeast, or two new eastern conformations are added to the equilibrium. Consistent with this shift to the east, strong NOE contacts have been observed between H1' and H4' of 2'F-araA.[119] These strong NOE contacts have also been observed in 2'-fluoroarabinooligonucleotides, as described in Chapter 2.

In this chapter we describe the synthesis and conformational analysis of the 4'-thio analogue of FMAU. For comparison, we also carried out the first quantitative conformational analysis of FMAU itself. The synthesis of the related compound 2'-deoxy-2'-fluoroarabinouridine (FAU), and of the phosphoramidite derivatives of both compounds, is also described.

4.2 Nucleoside synthesis

2,3,5-Tri-*O*-benzyl-1,4-anhydro-4-thio-arabinitol (**4.1**) was prepared from L-xylose following a procedure similar to that of Satoh *et al.*[414] The benzyl protecting groups were removed by Birch reduction using Li/liq. NH_3 to give the triol **4.2**.[415] Treatment of the triol **4.2** with equimolar ratios of 1,3-dichloro-1,1,3,3-tetraisopropyldisiloxane ($TIPSCl_2$)[416] in pyridine gave mainly the desired compound **4.3** which, when treated with diethylaminosulfur trifluoride (DAST), gave within 10 min the desired 2-fluoro derivative **4.4** in 80% yield. Moreover, the reaction proceeded with retention of configuration, presumably through an episulfonium ion intermediate.[403,417,418]

In order to install the pyrimidine base at C-1, we chose to functionalize C-1 as an acetate derivative through the Pummerer reaction, as reported by Naka *et al.*[416] The thioether **4.4** was thus subjected to ozonization at –78°C to give the sulfoxide **4.5** quantitatively. When compound **4.5** was treated with Ac_2O at 70°C, several

components were observed on TLC, suggesting that the silyl protecting group was being removed. We therefore decided to replace the 3,5-*O*-disiloxane bridge with benzoyl protecting groups. Thus, the thioether **4.4** was treated with Bu_4NF followed by BzCl in pyridine to give compound **4.7** in excellent yield. Ozonization of thioether **4.7** at –78°C afforded the sulfoxide **4.8** which, when treated with Ac_2O at 110°C, gave mainly the desired 1-*O*-acetyl derivative **4.9** as an anomeric mixture (α:β 1:2 to 1:14). Synthetic work up to this point was carried out by our collaborators N. Choubdar, K. Sadalapure and B.M. Pinto at Simon Fraser University, and compound **4.9** was sent to us for further synthesis.

The minor isomer, the 4-*O*-acetate **4.10,** was quite difficult to separate from **4.9**, which was itself an anomeric mixture. However, compound **4.10** was found to undergo spontaneous elimination of acetic acid to yield the exocyclic olefin **4.11** over a period of several weeks at room temperature (Scheme 4.1). By installing trifluoroacetate instead of acetate during the Pummerer reaction, the rate of this elimination can be increased so that it takes only a few hours, instead of a few weeks. This greatly facilitates the purification of the desired compound (N. Choubdar and B.M. Pinto, personal communication.)

N-Glycosylation of acetate derivative **4.9** was next accomplished by coupling to thymine in the presence of TMS-trifluoromethanesulfonate as the Lewis acid catalyst (Scheme 4.1), to give nucleoside **4.12a**. We propose that the α-face of the molecule is partially blocked by a benzoxonium ion resulting from attack of the benzoate ester on the thiacarbenium ion (Figure 4.3), as has been observed using other 3'-directing groups.[419-422] This mechanism would be more favored in nonpolar solvents where a localized cation is highly unstable (Table 4.2). Accordingly, our use of nonpolar solvents improves the β:α ratio significantly over that reported in the literature for similar Lewis acid-catalyzed glycosylations,[405] and gives a comparable yield of β product to that obtained *via* a fusion reaction of the corresponding glycosyl bromide with cytidine.[404]

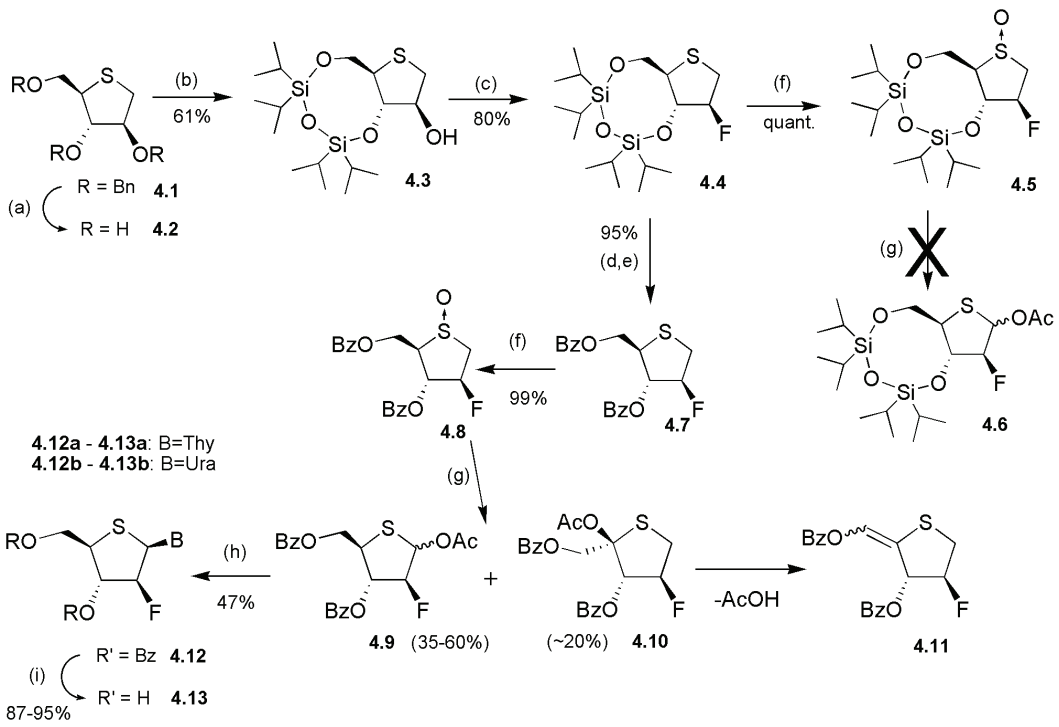

Scheme 4.1. Synthesis of 2'-fluoro-4'-thioarabinonucleosides. Reagents and conditions: (a) Li, liq. NH_3, -78ºC; (b) $TIPSCl_2$, pyridine, rt, 3h; (c) DAST, CH_2Cl_2, -15ºC, 15 min; (d) Bu_4NF, THF, rt, 30 min; (e) BzCl, pyridine, rt, 6h; (f) O_3, CH_2Cl_2, -78ºC, 30 min; (g) Ac_2O, 110ºC, 3h; (h) bis-silylated thymine or uracil, TMSOTf, CCl_4, reflux, 16h; (i) 2M NH_3 in MeOH, rt, 23 h.

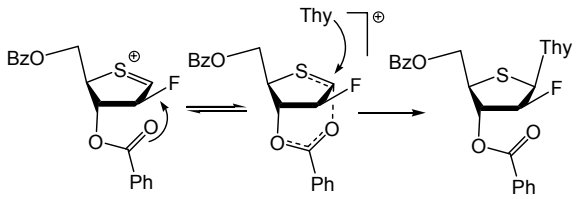

Figure 4.3. Proposed 3'-*O*-benzoate participation in the glycosylation reaction. Increased participation occurs in nonpolar solvents in which the thiacarbenium ion is less stable.

After removal of the α nucleoside by silica gel chromatography, the desired β nucleoside **4.12a** was obtained and debenzoylated using 2 M methanolic ammonia to give **4.13a** in 87% yield. Compounds **4.12b** and **4.13b**, the uracil analogues of **4.12a** and **4.13a**, were prepared analogously.

Solvent	Dielectric constant[423]	Product α:β ratio
CH_3CN	37.5	3:1
CH_2Cl_2	9.1	1.7:1
$CHCl_3$	4.8	0.9:1
CCl_4	2.2	0.7:1

Table 4.2. Anomeric ratio of nucleoside products for glycosylations with the β-acetate **4.9β** as starting material ($\alpha \leq 10\%$).

4.3 Conformational Analysis

The vicinal proton-proton and proton-fluorine coupling constants of the fully deprotected nucleoside **4.13a** were examined and compared with those of its 4'-oxygen congener **4.14** (Table 4.3). The Karplus equation predicts that a northern conformer of an arabino sugar will have large values of $^3J_{H2'-H3'}$ and $^3J_{H3'-H4'}$, while a southern conformer will have large values of $^3J_{H1'-F2'}$, since the nuclei are nearly antiperiplanar in all these cases.[316] Taken together, the changes in these ^3J values showed that a northern conformer was preponderant for the 4'-thionucleoside.

A large decrease of 7.5 Hz was observed in $^3J_{F2'-H3'}$ upon changing the ring heteroatom from oxygen to sulfur. One obvious explanation for the large $^3J_{F2'-H3'}$ in the 4'-oxo species would be a contribution from an eastern conformer, in which F-2' and H-3' are eclipsed. Indeed, this conformation has been shown to exist in 2'F-ANA (4'-oxo) *oligomers*.[269,424] This putative eastern conformation would be less significant for the 4'-thio species according to the reduced value of $^3J_{F2'-H3'}$.

	4'S-FMAU (**4.13a**)	FMAU (**4.14**)
H1'-H2'	6.0	4.0
H1'-F2'	7.9	16.9
H2'-H3'	7.1	2.9
F2'-H3'	12.1	19.6
H3'-H4'	7.0	5.0

Table 4.3. Vicinal ^{1}H-^{1}H and ^{1}H-^{19}F coupling constants (in Hz) for 4'S-FMAU (**4.13a**) and FMAU (**4.14**) nucleosides in D_2O.

While this qualitative examination of vicinal ^{1}H-^{1}H and ^{1}H-^{19}F coupling constants is helpful to a certain extent, the conclusions are approximate because of the rapid interconversion of nucleoside conformers at room temperature. We turned, therefore, to the use of the PSEUROT 6.3 program developed by Altona and co-workers,[408] which is able to account for a two-state equilibrium and provide the pseudorotational parameters for two interconverting conformers. Although some conformational work has previously been done on the nucleoside **4.14**,[406,407,425] detailed, empirically-derived data was not available, and we therefore undertook a PSEUROT study of both nucleosides **4.13a** and **4.14**.

Several sets of parameters are necessary for the PSEUROT calculations. Valence angles are not perfectly tetrahedral, and an equation is needed to relate the external torsion angles (therefore the vicinal coupling constants) to the internal torsion angles (therefore the pseudorotational parameters P and ϕ_{max}). These two sets of angles are related as follows:

$$\phi_j^{ext} = A_j \phi_j + B_j$$

for j = 0, ... , 4. The definitions of the internal torsion angles are shown in Figure 4.4. As these parameters were unknown for 2'-fluoroarabino or 2'-fluoro-4'-thioarabino configurations, we obtained them from DFT calculations[426] (Table 4.4).

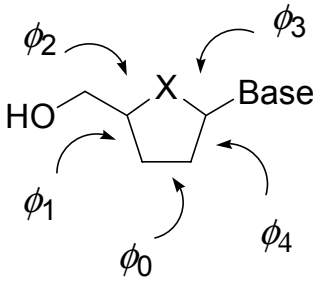

Figure 4.4. Definitions of internal torsion angles in a nucleoside.

	4'S-FMAU **(13a)**		FMAU **(14)**	
	$\mathbf{A}_j$	$\mathbf{B}_j^a$	$\mathbf{A}_j$	$\mathbf{B}_j^a$
$H_{1'}$-$H_{2'}$	1.098	2.24	1.041	1.14
$H_{1'}$-$F_{2'}$	1.081	123.24	1.029	122.28
$H_{2'}$-$H_{3'}$	1.072	119.96	1.150	122.27
$F_{2'}$-$H_{3'}$	1.076	0.54	1.177	1.77
$H_{3'}$-$H_{4'}$	1.043	-125.80	1.057	-127.20

Table 4.4. A_j and B_j parameters for **4.13a** and **4.14**. [a] In degrees.

A second set of parameters helps compensate for the non-equilateral nature of the rings. These parameters, α_j and ε_j, named after Ernesto Díez, are used to modify the classical pseudorotation equations.[427-429] Thus, in place of the standard pseudorotation equation,

$$\phi_j = \phi_{\max} \cos(P + 144°(j)),$$

the equation is extended to yield,

$$\phi_j = \alpha_j \phi_{\max} \cos(P + \varepsilon_j + 144°(j)).$$

Including the α_j and ε_j parameters in calculations on 4'-thionucleosides is particularly important because of their greater deviation from equilateral geometry.[430] These parameters were therefore obtained for both systems studied by least squares minimization using the DFT-calculated structures mentioned above and the program FOURDIEZ[431] (Table 4.5).

	4'S-FMAU **(4.13a)**		FMAU **(4.14)**	
	α_j	ε_j [a]	α_j	ε_j [a]
ϕ_1	1.030	-3.615	0.998	1.621
ϕ_2	0.955	-0.355	1.012	0.252
ϕ_3	0.952	0.435	1.016	-0.223
ϕ_4	1.032	3.478	0.995	-1.415
ϕ_0	1.035	-0.057	0.981	-0.229

Table 4.5. Diez parameters α_j and ε_j for **4.13a** and **4.14**. [a] In degrees.

A generalized Karplus equation has been developed for ^{1}H-^{19}F couplings, and proved to be useful for this work.[432,433] However, since the ^{1}H-^{19}F coupling constant is not as well characterized as the ^{1}H-^{1}H coupling constant, our initial PSEUROT calculations were carried out using only the three ^{1}H-^{1}H coupling values. To identify all possible solutions, 2400 consecutive calculations were carried out with different initial values of the five pseudorotational parameters, optimizing three of them at a time. The results were sorted by their rms error and the best several hundred solutions were examined carefully. Multiple possible solutions emerged (Table 4.6).

Nucleoside	P_I (ϕ_{maxI}) [a]	P_{II} (ϕ_{maxII}) [a]	Ratio
4.13a	-6 (44)	200 (44)	77:23
4.13a	-40 (51)	45 (51)	70:30
4.13a	-90 (48)	0 (48)	25:75
4.14	-20 to 20 (38)	124 (42-52)	30:70

Table 4.6. General regions corresponding to mathematically possible solutions of the initial PSEUROT calculations (based on ^{1}H-^{1}H coupling constants only.) [a] In degrees.

To differentiate between these possible solutions and to refine the structures, the ^{1}H-^{19}F coupling information was included. Each of the possible regions from the initial calculations was taken in turn as the starting point for the calculations. Inclusion of the fluorine couplings led to one set of pseudorotational parameters for the 4'-thionucleoside **4.13a** being easily identified (Table 4.7). For the 4'-oxo nucleoside **4.14**, the solution of best fit corresponded to a very unlikely arrangement, with the two conformers showing drastically different ϕ_{max} values and the second conformer too highly puckered for an oxacyclic nucleoside.[434] Therefore, the calculations were also carried out constraining the ϕ_{max} of both conformers to 36°, a likely value according to the computed structures. The phase angles and mole fractions obtained from these two sets of calculations were similar; both results are listed in Table 4.7.

Whichever of the two solutions best describes nucleoside **4.14**, it is clear that, as predicted by the qualitative examination of coupling constants, a northern pseudorotamer is preponderant for **4.13a**, while **4.14** is dominated by a conformer remarkably close to the southeast (see Figure 4.2).

The reasons for this dramatic conformational change are complex. The steric effects between the thymine base and the sugar ring would be reduced for a 4'-thionucleoside with its longer C-S bonds, thus favoring a north conformation in which the base is pseudoaxial (Figure 4.5c). O-C-C-X gauche effects are typically of greater magnitude than S-C-C-X gauche effects,[435] and accordingly, we would expect greater $\sigma_{C3'H3'} \rightarrow \sigma^*_{C4'O4'}$ and $\sigma_{C2'H2'} \rightarrow \sigma^*_{C1'O4'}$ interactions relative to the $\sigma_{C3'H3'} \rightarrow \sigma^*_{C4'S4'}$ and $\sigma_{C2'H2'} \rightarrow \sigma^*_{C1'S4'}$ overlap (Figure 4.5b). One predicts, therefore, that the gauche effects would also provide a strong driving force for the south (or east) conformation in the case of the oxygen congener. On the other hand, a greater anomeric effect in the case of the oxygen congener[435-437] would favor the north conformation. It follows that the observed conformational preferences are dominated by the steric and gauche effects.

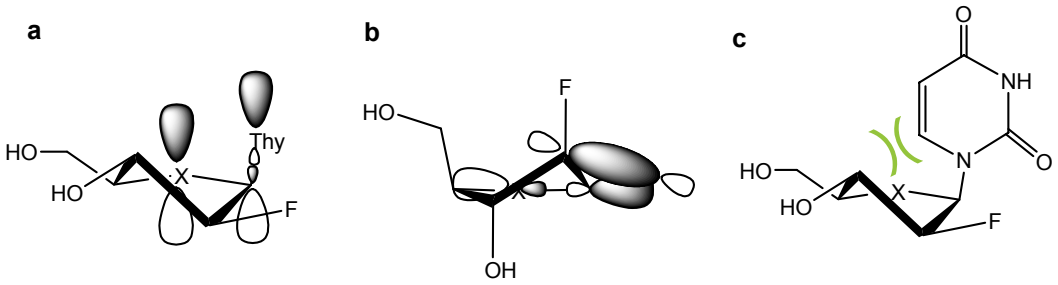

Figure 4.5. Stereoelectronic and steric rationalization of the conformational switch induced by replacing the ring heteroatom of FMAU with sulfur. (a) The anomeric effect, $n_{X4'} \rightarrow \sigma^*_{C1'\text{-}N1'}$, available in the northern conformer, should be reduced when X = S, therefore this effect must not be a major player in the conformational switch. (b) The $\sigma_{C2'H2'} \rightarrow \sigma^*_{C1'X4'}$ gauche effect, favoring the south, would be reduced when X = S, therefore this effect may be a major player in the conformational switch. An analogous effect exists for the $\sigma_{C3'H3'} \rightarrow \sigma^*_{C4'X4'}$ overlap. (c) Steric effects between the base and C3'/H3' would disfavor the north, and should be reduced when X = S because of the longer S–C bonds. Therefore steric effects may also play a significant role in the conformational switch.

It is of interest to note that whereas 4'S-FMAU (**4.13a**) adopts predominantly the north conformation, the 2'-deoxynucleoside, *i.e.*, 4'-thiothymidine (4'S-dT), adopts a south conformation in the solid state and a predominantly south conformation in solution.[430] However, in the latter case, evidence was presented for representation of the north conformation in the conformational ensemble.[430] The shift from a predominantly south conformation in 4'S-dT to the north conformation in **4.13a** may be caused by the greater F2' steric effect in the south conformation that outweighs the stabilization gained by the F2'-S4' and O3'-S4' gauche effects in 4'S-FMAU. A $\sigma_{C3'C4'} \rightarrow \sigma^*_{C2'F2'}$ orbital interaction is also possible for 4'S-FMAU (but not 4'S-dT) in the north.

Evidence for an accentuated steric effect in arabinofuranosyl nucleosides in the south conformation may be inferred by the significant population of the north conformation in 4'-thio-arabinoadenosine (4'S-araA);[438] we propose that this unfavorable interaction derives from syn-axial interactions between the CH_2OH moiety at C-4' and the substituent at C-2'. Note, in Table 4.1, that some base-modified 2'-fluoroarabinonucleosides are also dominated by northern conformations.

Nucleoside	P_I (ϕ_{maxI})[a]	P_{II} (ϕ_{maxII})[a]	Ratio	RMS error of the fit
4.13a	-4 (44)	199 (43)	77:23	0.000 Hz
4.14[b]	-6 (36)	126 (36)	31:69	0.595 Hz
4.14[c]	-35 (39)	116 (53)	37:63	0.000 Hz

Table 4.7. Final results from PSEUROT calculations (including ^{1}H-^{19}F coupling constants) for 4'S-FMAU (**4.13a)** and FMAU (**4.14)**. [a] In degrees. [b] With ϕ_{max} of both conformers constrained at 36º. [c] With no constraints on the minimization.

4.4 Phosphoramidite synthesis

The 5'-hydroxyl group of nucleosides **4.13** was protected using either 4-monomethoxytrityl (MMT) or 4,4'-dimethoxytrityl (DMT) chloride, but the latter required significantly shorter reaction times and was preferred (Scheme 4.2). Phosphitylation of the tritylated compounds **4.15** using bis(diisopropylamino)-β-cyanoethylphosphoramidite in the presence of diisopropylammonium tetrazolide, followed by precipitation from cold hexanes, gave the phosphoramidites **4.16** of suitable purity for solid phase oligonucleotide synthesis. The tritylation and phosphitylation reactions were in general much slower for these modified nucleosides than for standard deoxyribo- or ribonucleosides.

4.5 Conclusions

The 4'-modified nucleosides 2'-deoxy-2'-fluoro-5-methyl-4'-thioarabinouridine (4'S-FMAU) and 2'-deoxy-2'-fluoro-4'-thioarabinouridine (4'S-FAU) were synthesized. Use of nonpolar solvents during the glycosylation step improved the yield of β anomer, likely due to neighboring group participation from the 3'-benzoyl ester.

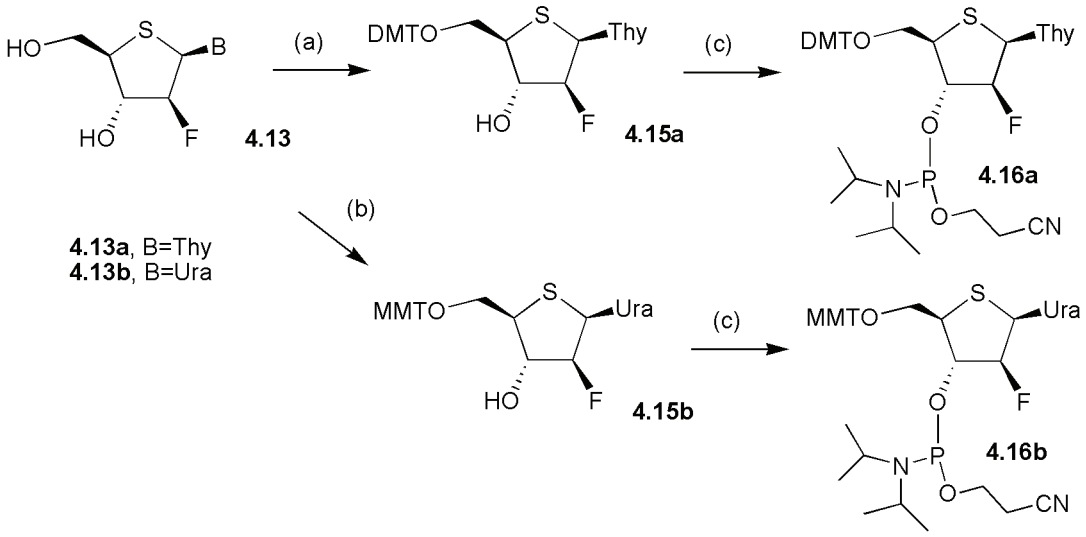

Scheme 4.2. Synthesis of 4'S-FANA phosphoramidites. Reagents and conditions: (a) DMTrCl, pyridine, rt, 44 h; (b) MMTrCl, pyridine, DMAP rt, 72 h, 73%; (c) $(N(^{i}Pr_2))_2P(OCH_2CH_2CN)$, Diisopropylammonium tetrazolide, CH_2Cl_2, rt, 46-68 h, 44-65%.

Conformational analysis of 4'S-FMAU showed that it adopted north (-6º) and south (199º) conformations with a 77% preference for the north. This is in sharp contrast to the southeast (~120º) conformer that dominates the conformational equilibrium of its 4'-oxygen congener (~65%). Arguments are presented to suggest that replacement of oxygen by the cognate sulfur atom at the 4' position leads to a decrease in the magnitudes of C5'-base steric effects and various gauche effects, and a corresponding shift to a north conformation.

The 3'-*O*-phosphoramidites of both nucleosides were synthesized and characterized. Oligonucleotide synthesis using these phosphoramidites is described in the next chapter.

4.6 Experimental methods

4.6.1 Synthetic protocols and characterization

Synthetic details for compounds **4.1**–**4.9** are given in the paper published on this work.[439] They are not included here since this work was carried out by N. Choubdar, K. Sadalapure and B.M. Pinto at Simon Fraser University.

(2*S*,3*S*,4*S*)-2-Acetoxy-3-benzoyloxy-2-benzoyloxymethyl-4-fluorotetrahydrothiophene (4.10): ^{1}H NMR (400.13 MHz, $CDCl_3$): δ 7.96, 7.85 (2 d, 4H, *meta* of OBz), 7.52, 7.37 (2 m, 6H, *ortho* and *para* of OBz), 6.19 (dd, 1H, $J_{H3\text{-}H2}$ = 4.3 Hz, $J_{H3\text{-}F}$ = 9.4 Hz, H-3), 5.29 (dddd, $J_{H2\text{-}F}$ = 50 Hz, $J_{H2\text{-}H1} \approx J_{H2\text{-}H1}$ = 4.4 Hz, H-2), 5.25, 4.66 (2 d, 2H, $J_{H5\text{-}H5'}$ = 12.0 Hz, H-5, H-5'), 3.37 (m, 2H, H-1, H-1'), 2.12 (s, 3H, CH_3). ^{13}C NMR (100 MHz, $CDCl_3$): δ 169.5, 165.4, 164.5 (3 C=O), 134-128.5 (aromatic), 94.0 (C-4), 93.8 (d, $J_{C2\text{-}F}$ = 190 Hz, C-2), 80.1 (d, $J_{C3\text{-}F}$ = 26.2 Hz, C-3), 64.2 (C-5), 34.4 (d, $J_{C1\text{-}F}$ = 22.3 Hz, C-1), 22.2 (CH_3). ESI-MS calcd. for $C_{21}H_{17}FO_6S$+Na: 441.08, found, 441.0. Stereochemistry was assigned and the structure confirmed by X-ray crystallography (data not shown.)

(3*S*,4*S*)-2-Benzoyloxy-1-benzoyloxymethylenyl-3-fluorotetrahydrothiophene (4.11): ^{1}H NMR (400.13 MHz, $CDCl_3$): δ 8.10 (dd, 2H, *meta* of one OBz), 8.04 (s, 1H H-5), 8.00 (dd, 2H, *meta* of other OBz), 7.58, 7.45 (2 m, 6H, *ortho* and *para* of OBz), 6.17 (dd, 1H, $J_{H3\text{-}H2}$ = 1.6 Hz, $J_{H3\text{-}F}$ = 8 Hz, H-3), 5.35 (ddd, $J_{H2\text{-}F}$ = 48 Hz, $J_{H2\text{-}H1}$ = 3.2 Hz, H-2), 3.62 (ddd, 1H, $J_{H1\text{-}F}$ = 36 Hz, $J_{H1\text{-}H1'}$ = 13 Hz, H-1), 3.45 (dd, 1H, $J_{H1'\text{-}F}$ = 18 Hz, H-1'). NOESY crosspeaks were observed between H-3 and H-5, suggesting the Z-alkene. ^{13}C NMR (100 MHz, $CDCl_3$): δ 165.0, 162.5 (2 OBz), 134.0, 133.8, 133.2 (2 *para* C and C-5), 130.3-128.6 (6 signals; *meta, ortho* and *ipso* C), 121.8 (C-4), 93.8 (d, $J_{C2\text{-}F}$ = 180 Hz, C-2), 77.8 (d, $J_{C3\text{-}F}$ = 31 Hz, C-3), 37.0 (d, $J_{C1\text{-}F}$ = 30 Hz, C-1). ^{19}F NMR (282.3 MHz , $CDCl_3$): δ -185.85 (dddd, J = 8, 18, 36, 48 Hz). ESI-MS Calcd for $C_{19}H_{15}FO_4S$+Na: 381.06; Found, 380.9.

1-(3,5-Di-*O*-benzoyl-2-deoxy-2-fluoro-4-thio-β-D-arabinofuranosyl)-thymine (4.12a). To anhydrous thymine (85 mg, 0.67 mmol) in a 25-mL round-bottomed flask was added acetonitrile (4 mL) followed by HMDS (200 μL, 153 mg, 0.95 mmol), with stirring. The mixture was heated to reflux, and became clear. After 4 h, the solvent was removed. A solution of 1-*O*-acetyl-2-deoxy-2-fluoro-3,5-di-*O*-benzoyl-4-thio-D-arabinofuranose (**4.9**, 64 mg, 0.15 mmol) in carbon tetrachloride (8 mL) was added followed by TMS-triflate (60 μL, 69 mg, 0.29 mmol). The flask that had contained the dry sugar was then rinsed with another 2-mL aliquot of carbon tetrachloride. The reaction was stirred at reflux for 16 h and monitored by TLC. It was then diluted with 15 mL CH_2Cl_2 and washed with 20 mL 5% aq. $NaHCO_3$. The aqueous layer was washed with 2 x 15 mL CH_2Cl_2. Combined organic layers were washed with 15 mL brine. The aqueous layer was washed with 10 mL CH_2Cl_2. Organic layers were dried on $MgSO_4$, concentrated, and purified on a silica gel column using chloroform as eluent. This system allowed partial separation of the two anomers. The β isomer, compound **4.12a**, eluted first (34 mg, 47%) and was concentrated to yield an amorphous solid:

^{1}H NMR (400 MHz, $CDCl_3$): δ 8.10, 8.04 (2d, 4H, *meta* of OBz), 7.70 (s, 1H, H-6), 7.60 (q, 2H, *para* of OBz), 7.47 (d, 4H, ortho H of 2 OBz), 6.80 (dd, 1H, $J_{H1'-F2'}$ = 25.2 Hz, $J_{H1'-H2'}$ = 3.8 Hz, H-1'), 5.86 (ddd, 1H, $J_{H3'-F2'}$ = 9.4 Hz, $J_{H3'-H2'}$ = 1.8 Hz, $J_{H3'-H4'} \approx$ 1 Hz, H-3'), 5.26 (ddd, 1H, $J_{H2'-F2'}$ = 49.2 Hz, H-2'), 4.69 (m, 2H, H-5', H-5"), 4.00 (dd, 1H, $J_{H4'-H5'} = J_{H4'-H5"}$ = 7.8 Hz, H-4'), 1.94 (s, 3H, CH_3 on C5). Two pairs of NOESY crosspeaks (H6-H3', H6-H5') demonstrate the presence of top-face thymine and therefore the β nucleoside.

The α anomer was also characterized: ^{1}H NMR (400 MHz, $CDCl_3$): δ 8.04, 7.91 (2d, 4H, *meta* of OBz), 7.62 (s, 1H, H-6), 7.59 (q, 2H, *para* of OBz), 7.42 (d, 4H, ortho H of 2 OBz), 6.38 (dd, 1H, $J_{H1'-F2'}$ = 16.0 Hz, $J_{H1'-H2'}$ = 3.1 Hz, H1'), 5.81 (ddd, 1H, $J_{H3'-F2'}$ = 12.0 Hz, $J_{H3'-H2'} = J_{H3'-H4'}$ = 4.0 Hz, H3'), 5.36 (ddd, 1H, $J_{H2'-F2'}$ = 47.8 Hz, H-2'), 4.53 (m, 2H, H-5', H-5"), 4.24 (ddd, 1H, $J_{H4'-H5'} = J_{H4'-H5"}$ = 6.8 Hz, H-4'), 1.86 (s, 3H, CH_3 on C5). NOESY crosspeaks (H6-H2', H6-H4') confirmed the α configuration.

3',5'-Di-*O*-benzoyl-2'-deoxy-2'-fluoro-4'-thio-β-D-arabinouridine (4.12b). To anhydrous uracil (33 mg, 0.29 mmol, 4 eq) in a 10-mL round-bottomed flask was added acetonitrile (2 mL) followed by HMDS (62 μL, 0.29 mmol, 4 eq.), with stirring. The mixture was heated to reflux, and became clear. After 4 h, the solvent was removed. A solution of 1-*O*-acetyl 3,5-di-*O*-benzoyl-2-deoxy-2-fluoro-D-arabinofuranose (30 mg, 0.072 mmol) in carbon tetrachloride (2 mL) was added followed by TMS-triflate (20 μL, 0.11 mmol, 1.5 eq). The flask which had contained the dry sugar was then rinsed with another aliquot (1.5 mL) of carbon tetrachloride, which was added. The reaction mixture was stirred at reflux for 20 h until TLC indicated no further change. The mixture was poured onto a short column of silica gel and eluted with 0.5% triethylamine in chloroform. The separation of the anomers was achieved by a subsequent longer column of neutralized silica using chloroform as eluent. The less-polar β isomer, compound **4.12b**, was isolated as an amorphous solid (15.8 mg, 47%): ^{1}H NMR (500 MHz, $CDCl_3$) δ 8.78 (br s, 1H, imide-NH) 8.1-7.4 (m, 10H, 2 Bz), 6.77 (dd, 1H, $J_{H1'-H2'}$ = 4.0 Hz, $J_{H1'-F2'}$ = 23 Hz, H1'), 5.88 (ddd, 1H, $J_{H2'-H3'}$ = 2.5 Hz, $J_{H3'-F2'}$ = 9.6 Hz, $J_{H3'-H4'}$ = 2.0 Hz, H3'), 5.76 (d, 1H, J_{H5-H6} = 8.2 Hz, H5), 5.27 (ddd, 1H, $J_{H1'-H2'}$ = 4.0 Hz, $J_{H2'-H3'}$ = 2.5 Hz, $J_{H2'-F2'}$ = 49.6 Hz, H2'), 4.67 (m, 2H, H5',5''), 3.99 (m, 1H, H4'). ^{13}C NMR (125 MHz, $CDCl_3$): δ 166.25, 164.90, 162.74, 150.94 (4 CO), 142.28 (d, $J_{C6-F2'}$ = 4.7 Hz, C6), 134.37, 133.75, 130.27, 130.04, 129.53, 128.96, 128.82, 128.48 (2 OBz), 102.94 (C5), 94.66 (d, $J_{C2'-F2'}$ = 189.9 Hz, C2'), 153.59 (d, $J_{C3'-F2'}$ = 27.4 Hz, C3'), 64.68 (d, $J_{C5'-F2'}$ = 5.3 Hz, C5'), 61.83 (d, $J_{C1'-F2'}$ = 16.8 Hz, C1'), 50.96 (C4'). Two pairs of NOESY crosspeaks (H6-H3', H6-H5') provide strong evidence for top-face uracil and therefore the β nucleoside. FAB-HRMS: calcd. for $C_{23}H_{19}N_2O_6SF+H^+$: 471.1026; found: 471.1027.

1-(2-Deoxy-2-fluoro-4-thio-β-D-arabinofuranosyl)-thymine (4.13a). To 331 mg (0.68 mmol) of compound **4.12a** in a round-bottomed flask equipped with a magnetic stir bar was added a 2M solution of ammonia in cold methanol (50 mL, 100 mmol). The reaction was capped with a rubber septum and allowed to stir for 23 h. It was then evaporated to dryness, adsorbed onto silica and loaded onto a short column of silica gel. Dichloromethane containing 0-3% methanol was used

to elute compound **4.13a** which was concentrated to yield an amorphous solid (164 mg, 87%):

^{1}H NMR (400 MHz, D_2O): δ 8.03 (s, 1H, H6), 6.09 (dd, 1H, $J_{H1'-H2'}$ = 6.0 Hz, $J_{H1'-F2'}$ = 7.9 Hz, H1'), 4.93 (ddd, 1H, $J_{H2'-F2'}$ = 50.3 Hz, $J_{H2'-H3'}$ = 7.1 Hz, H2'), 4.17 (ddd, 1H, $J_{H3'-H4'}$ = 7.0 Hz, $J_{H3'-F2'}$ = 12.1 Hz, H3'), 3.70 (m, 2H, H5', H5"), 3.17 (ddd, 1H, $J_{H4'-H5'} \approx J_{H4'-H5"}$ = 4.3 Hz, H4'), 1.68 (s, 3H, CH_3).

^{13}C NMR (125 MHz, methanol-d_4): δ 165.0, 151.8 (C2, C4), 138.9 (d, $J_{F2'-C6}$ = 1.6 Hz, C6), 109.8 (C5), 96.3 (d, $J_{F2'-C2'}$ = 194.5 Hz, C2'), 73.2 (d, $J_{F2'-C3'}$ = 22.9 Hz, C3'), 60.8 (d, $J_{F2'-C5'}$ = 2.3 Hz, C5'), 58.4 (d, $J_{F2-C1'}$ = 16.8 Hz, C1'), 51.1 (d, $J_{F2'-C4'}$ = 4.6 Hz, C4'), 11.4 (CH_3).

FAB-HRMS: Calcd for $C_{10}H_{13}N_2O_4SF+H^+$: 277.0658; Found: 277.0659.

2'-Deoxy-2'-fluoro-4'-thio-β-D-arabinouridine (4.13b). To compound **4.12b** (173 mg, 0.37 mmol) was added a 2M solution of ammonia in cold methanol (30 mL, 60 mmol). The reaction mixture was capped with a rubber septum and allowed to stir for 48 h. It was then evaporated to dryness, adsorbed onto silica and loaded onto a short column of neutralized silica gel. Dichloromethane containing 0-5% methanol was used to elute compound **4.13b** as a solid (92 mg, 95%). ^{1}H NMR (400 or 500 MHz, methanol-d_4): δ 8.30 (dd, 1H, $J_{H6-F2'}$ = 1.6 Hz, J_{H6-H5} = 8.4 Hz, H6), 6.41 (dd, 1H, $J_{H1'-H2'}$ = 5.6 Hz, $J_{H1'-F2'}$ = 11.6 Hz, H1'), 5.71 (d, 1H, J_{H6-H5} = 8.4 Hz, H5), 5.00 (ddd, 1H, $J_{H1'-H2'}$ = 5.6 Hz, $J_{H2'-F2'}$ = 51.0 Hz, $J_{H2'-H3'}$ = 5.7 Hz, H2'), 4.36 (ddd, 1H, $J_{H3'-H4'}$ = 5.8 Hz, $J_{H3'-F2'}$ = 11.6 Hz, $J_{H2'-H3'}$ = 5.7 Hz, H3'), 3.82 (m, 2H, H5', H5"), 3.33 (m, 1H, H4'). ^{13}C NMR (125 MHz, methanol-d_4): δ 164.75, 151.55 (C2, C4), 143.31 (d, $J_{F2'-C6}$ = 2.3 Hz, C6), 101.07 (C5), 96.27 (d, $J_{F2'-C2'}$ = 193.8 Hz, C2'), 73.55 (d, $J_{F2'-C3'}$ = 23.6 Hz, C3'), 61.34 (d, $J_{F2'-C5'}$ = 2.4 Hz, C5'), 58.93 (d, $J_{F2-C1'}$ = 16.8 Hz, C1'), 51.88 (d, $J_{F2'-C4'}$ = 3.8 Hz, C4'). Two pairs of NOESY crosspeaks (H6-H3', H6-H5') provided strong evidence for top-face uracil and therefore the β nucleoside. FAB-HRMS: calcd. for $C_9H_{11}N_2O_4SF+H^+$: 263.0502; found: 263.0501.

1-(2-Deoxy-2-fluoro-5-*O*-(4,4'-dimethoxytrityl)-4-thio-β-D-arabinofuranosyl)-thymine (4.15a). 2'-Deoxy-2'-fluoro-5-methyl-4'-thio-β-D-arabinouridine (**4.13a**, 105 mg, 0.40 mmol) was coevaporated three times with pyridine. Dry pyridine (10 mL) was added, followed by 95% dimethoxytrityl chloride (198 mg, 0.56 mmol). Half of the solvent was removed, heating the flask slightly on a rotary evaporator. The reaction was allowed to stir for 44 h when TLC indicated virtual completion of the reaction. It was then diluted with dichloromethane (50 mL) and washed with saturated aqueous $NaHCO_3$ (2 x 50 mL); the aqueous layers were then washed with dichloromethane (2 x 50 mL). The organic layers were combined and concentrated. The residue was purified by preparative TLC (eluent 3.5% methanol, 0.2% triethylamine in dichloromethane) to yield **4.15a** (260 mg, 106%). In spite of the impurities detected by the excess yield and by TLC, this product was a stable white foam and was phosphitylated directly. ^{1}H NMR (400 MHz, acetone-d_6): δ 10.20 (br s, 1H, imide H-3), 7.60 (dd, 1H, $J_{H6\text{-}F2'} = J_{H6\text{-}Me5}$ = 1.4 Hz, H6), 7.60-6.90 (m, 14H, trityl), 6.52 (dd, 1H, $J_{H1'\text{-}H2'}$ = 5.2 Hz, $J_{H1'\text{-}F2'}$ = 15.2 Hz, H1'), 5.21 (br s, 1H, OH), 5.03 (ddd, 1H, $J_{H1'\text{-}H2'}$ = 5.2 Hz, $J_{H2'\text{-}F2'}$ = 50.8 Hz, $J_{H2'\text{-}H3'}$ = 5.2 Hz, H2'), 4.49 (ddd, 1H, $J_{H2'\text{-}H3'}$ = 5.2 Hz, $J_{H3'\text{-}F2'}$ = 11.5 Hz, $J_{H3'\text{-}H4'}$ = 4.8 Hz, H3') 3.79 (s, 6H, 2 OCH_3), 3.62-3.43 (m, 3H, H4', H5', H5"), 1.74 (d, 3H, $J_{H6\text{-}Me5}$ = 1.4 Hz, CH_3-5).

1-(2-Deoxy-2-fluoro-5-*O*-(4-methoxytrityl)-4-thio-β-D-arabinofuranosyl)-uracil (4.15b). 2'-Deoxy-2'-fluoro-4'-thio-β-D-arabinouridine (**4.13b**, 105 mg, 0.40 mmol) was coevaporated three times with pyridine and left in a vacuum dessicator for 48h. Monomethoxytrityl chloride (154 mg, 0.50 mmol, 1.25 eq.) was added along with a magnetic stir bar and septum, and the flask was flushed with nitrogen. Pyridine (4 mL) was then added via syringe and the reaction was allowed to stir. TLC showed that it had progressed to about 50% completion after 5h and did not proceed further. Another aliquot of MMT-Cl (0.6 eq) was therefore added. After 72h the reaction had stopped again; a few crystals of DMAP were added and the volume reduced by about half. The following day a third aliquot of MMT-Cl (0.5 eq) was added. The reaction reached completion after 7 days. Methanol (1 mL) and a small amount of neutralized silica were then

added and the reaction mixture evaporated to dryness. The product was purified by preparative TLC (eluent 5% methanol, 0.1% triethylamine in dichloromethane) to yield compound **4.15b** as a white foam (154 mg, 74%). ^{1}H NMR (500 MHz, acetone-d_6): δ 10.3 (s, 1H, imide H-3), 7.90 (d, 1H, $J_{H6\text{-}H5}$ = 7.5 Hz, H6), 7.6-6.9 (m, 14H, MMT), 6.50 (dd, 1H, $J_{H1'\text{-}H2'}$ = 4.9 Hz, $J_{H1'\text{-}F2'}$ = 13.7 Hz, H1'), 5.51 (d, 1H, $J_{H6\text{-}H5}$ = 7.5 Hz, H5), 5.22 (br s, 1H, OH), 5.05 (ddd, 1H, $J_{H1'\text{-}H2'}$ = 4.9 Hz, $J_{H2'\text{-}F2'}$ = 51.0 Hz, $J_{H2'\text{-}H3'}$ = 5.0 Hz, H2'), 4.54 (m, 1H, H3') 3.79 (s, 3H, OMe), 3.57-3.52 (m, 3H, H4', H5', H5") ^{13}C NMR (125 MHz, acetone-d_6): δ 162.84, 159.19, 151.16, 144.70, 144.62, 142.47, 135.26, 130.76, 128.68, 128.10, 127.30, 113.36, 101.72 (C5), 96.35 (d, $J_{C2'\text{-}F2'}$ = 192.3 Hz, C2'), 87.07 (O$\underline{C}$Ar$_3$), 74.70 (d, $J_{C3'\text{-}F2'}$ = 23.7 Hz, C3'), 63.99 (d, $J_{C5'\text{-}F2'}$ = 2.3 Hz, C5'), 58.86 (d, $J_{C1'\text{-}F2'}$ = 16.0 Hz, C1'), 54.94 (OMe), 50.85 (d, $J_{C4'\text{-}F2'}$ = 3.8 Hz, C4'). FAB-HRMS: calcd. for $C_{29}H_{27}N_2O_5SF+K^+$: 573.1262; found: 573.1261.

1-(3-*O*-(*β*-Cyanoethyl-*N,N*-diisopropylphosphoramidic)-2-deoxy-2-fluoro-5-*O*-(4,4'-dimethoxytrityl)-4-thio-β-D-arabinofuranosyl)-thymine (4.16a). The crude compound **4.15a** (260 mg) was coevaporated with dichloromethane and dried overnight over P_2O_5. It was then dissolved in dichloromethane (2 mL) and anhydrous diisopropylammonium tetrazolide (161 mg, 0.94 mmol) was added. Finally, 2-cyanoethyl-*N,N,N',N'*-tetraisopropylphosphordiamidite (202 μL, 184 mg, 0.61 mmol) was added via syringe under a nitrogen atmosphere. The suspension was stirred for 68h. A column was packed using neutralized silica in hexanes, and the reaction mixture was poured directly onto it. After elution in hexanes containing 10-50% ethyl acetate and 1% triethylamine, the fractions containing product were concentrated, and the product precipitated from cold hexanes to yield **4.16a** as a white foam (151 mg, 44% over two steps). The mixture of two diastereomers at phosphorus led to complex ^{1}H and ^{13}C NMR spectra. ^{31}P NMR (81 MHz, acetone-d_6): δ 151.9 (d, $J_{F\text{-}P}$ = 6.2 Hz), 151.3 (d, $J_{F\text{-}P}$ = 3.4 Hz). FAB-HRMS: Calcd for $C_{40}H_{48}N_4O_7FPS+K^+$: 817.2602; Found: 817.2606.

2'-Deoxy-2'-fluoro-3'-*O*-(β-cyanoethyl-*N,N*-diisopropylphosphoramidic)-5'-*O*-(4-methoxytrityl)-4'-thio-β-D-arabinouridine (4.16b). Compound **4.15b** (155 mg, 0.29 mmol) was dried over P_2O_5 for several days, coevaporated with dry dichloromethane halfway through this period. It was then dissolved in dichloromethane (2 mL) and anhydrous diisopropylammonium tetrazolide (102 mg, 0.60 mmol, 2.0 eq) was added. Finally, 2-cyanoethyl-*N,N,N′,N′*-tetraisopropylphosphordiamidite (115 μL, 0.35 mmol) was added via syringe under a nitrogen atmosphere. The suspension was stirred for 46h. The reaction mixture was loaded onto a column of triethylamine-neutralized silica and was purified by flash chromatography (using hexanes-ethyl acetate-triethylamine as eluent) to yield **4.16b** as a foam (138 mg, 65%), collected as pure amidite diastereomers. Another fraction was isolated containing a mixture of starting material and product, and was phosphitylated again to yield a further 10 mg of product, for a total yield of 70%. For the faster-moving diastereomer: ^{31}P NMR (81 MHz, acetone-d_6): δ 152.2 (d, $J_{F\text{-}P}$ =6.5 Hz). ^{1}H NMR (500 MHz, acetone-d_6): δ 10.19 (br s, 1H, H3 (uracil N3-H)), 7.86 (dd, 1H, $J_{H6\text{-}H5}$ = 8.0 Hz, $J_{H6\text{-}F2'}$ = 1.7 Hz, H6), 7.54-6.91 (m, 14H, trityl), 6.51 (dd, 1H, $J_{H1'\text{-}H2'}$ = 5.0 Hz, $J_{H1'\text{-}F2'}$ = 14.5 Hz, H1'), 5.49 (d, 1H, $J_{H6\text{-}H5}$ = 8.0 Hz, H5), 5.14 (ddd, $J_{H1'\text{-}H2'}$ = 5.0 Hz, $J_{H2'\text{-}F2'}$ = 50.5 Hz, $J_{H2'\text{-}H3'}$ = 4.6 Hz, H2'), 4.70 (m, 1H, H3'), 3.81 (s, 3H, OMe of MMT), 3.80-3.51 (m, 7H; H4', H5', H5'', OCH_2 of cyanoethyl, 2 NC<u>H</u>$(CH_3)_2$), 2.66 (t, 2H, J = 6.2 Hz), 1.20, 1.191, 1.187, 1.17 (4s, 12H, 2 NCH(<u>C</u>H_3)<u>$_2$</u>). ^{13}C NMR (125.7 MHz, acetone-d_6): δ 162.53, 159.23, 151.04, 144.61, 144.53, 135.19 (C2, C4, 4 tertiary aromatic carbons of MMT), 142.19 (d, $J_{C6\text{-}F2'}$ = 2.9 Hz, C6), 130.80, 128.72, 128.71, 128.11, 127.35, (aromatic carbons of MMT), 118.77 (CN), 113.35 (aromatic carbon of MMT), 101.86 (C5), 95.56 (dd, $J_{C2'\text{-}F2'}$ = 193.8 Hz, $J_{C2'\text{-}P}$ = 3.6 Hz, C2'), 87.20 (O<u>C</u>Ar_3), 76.48 (dd, $J_{C3'\text{-}P}$ = 16.2 Hz, $J_{C3'\text{-}F2'}$ = 24.3 Hz, C3'), 63.99 (d, $J_{C5'\text{-}F2'}$ = 3.6 Hz, C5'), 59.18, 59.03, 58.90, 58.76 (4 signals due to iPr methyls), 54.94 (OMe), 50.53 (dd, $J_{C4'\text{-}F2'} \approx J_{C4'\text{-}P} \approx$ 3 Hz, C4'), 43.40 (d, $J_{C\text{-}P}$ = 12.6 Hz, O<u>C</u>H_2CH_2CN), 24.27, 24.21, 24.16, 24.10 (4 Me of ^{i}Pr). ESI-MS: calcd for $C_{38}H_{44}FN_4O_6PS$+Na, 757.3; found, 757.0. Slower-moving diastereomer: ^{31}P NMR (81 MHz, acetone-d_6): δ 151.4 (d, $J_{F\text{-}P}$ = 3.7 Hz). ^{1}H and

^{13}C NMR very similar to those for the first diastereomer. Signals corresponding to the ^{i}Pr and cyanoethyl groups were, predictably, those for which the largest differences were observed. ESI-MS: calcd for $C_{38}H_{44}FN_4O_6PS$+Na, 757.3; found, 757.1. NOESY spectra provided no useful information for identifying the stereochemistry of the two diastereomers.

4.6.2 Computational methods for conformational analysis

4.6.2.1 Parameterization of PSEUROT for 2'-fluoroarabino configurations

A_j and B_j parameters for these two systems were obtained using a method similar to that of Houseknecht *et al.*[440] All DFT calculations were carried out on a PC using the Gaussian03W program.[441] All optimizations were carried out in the gas phase.

For the FMAU nucleoside **4.14**, a series of 32 envelope structures was optimized at the B3LYP/6-31G** level. In each case, one of the torsion angles ϕ_0-ϕ_4 was constrained to zero to span the full range of P accessible to nucleosides. The starting value of the glycosidic torsion angle X (C2-N1-C1'-O4') was also constrained to various values covering the full range of conformational space.

For the 4'S-FMAU nucleoside **4.13a**, a series of 12 envelopes spanning pseudorotational space were minimized at the B3LYP/3-21G** level. Starting structures were set to a ϕ_{max} of 35°. The value of the glycosidic torsion angle X (C2-N1-C1'-S4') was initially set to 220° in all cases, since this value is in the middle of the *anti* range where the minimum conformation of thymidine nucleosides is expected, especially given the presence of the 2'-fluoro substituent. O5' was set *anti* to C3' and OH3' and OH5' were set *anti* to C4'. Optimizations were carried out constraining only one torsion angle ϕ_0-ϕ_4 to zero.

The internal and external torsion angles were graphed (Figures 4.6–4.7) with linear plots having slope of A_j and a y-intercept of B_j. The resulting A_j and B_j paramters are given in Table 4.4.

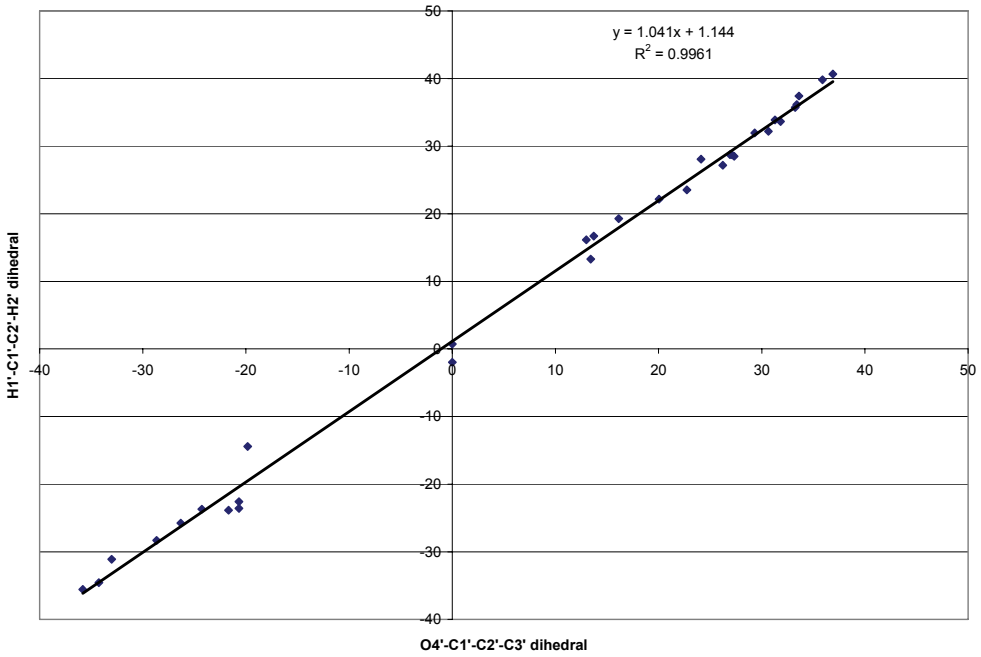

Figure 4.6a. A_j and B_j for H1'-H2' coupling in FMAU.

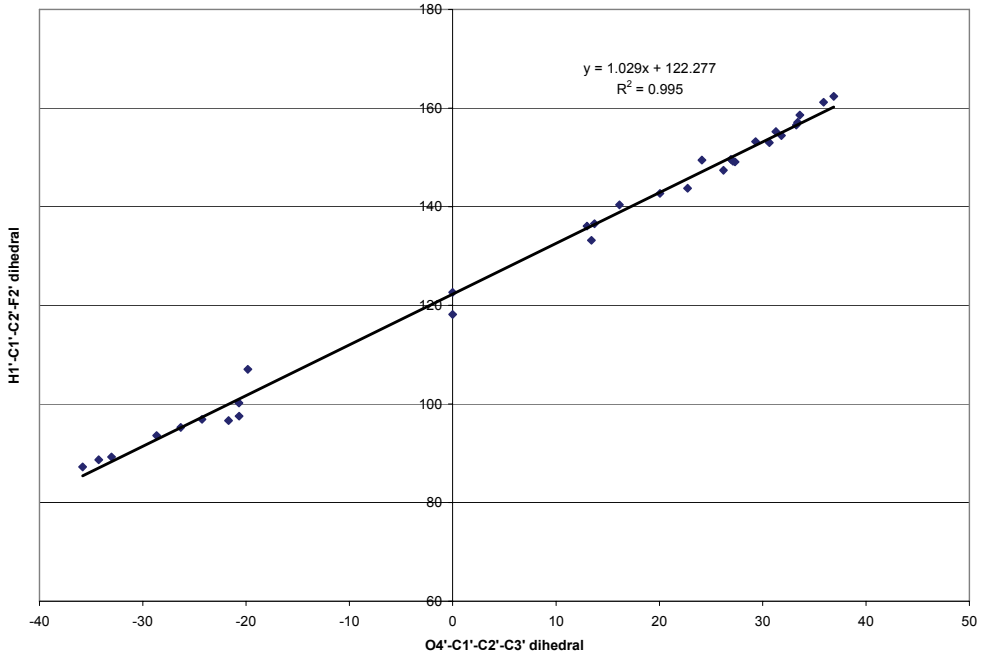

Figure 4.6b. A_j and B_j for H1'-F2' coupling in FMAU.

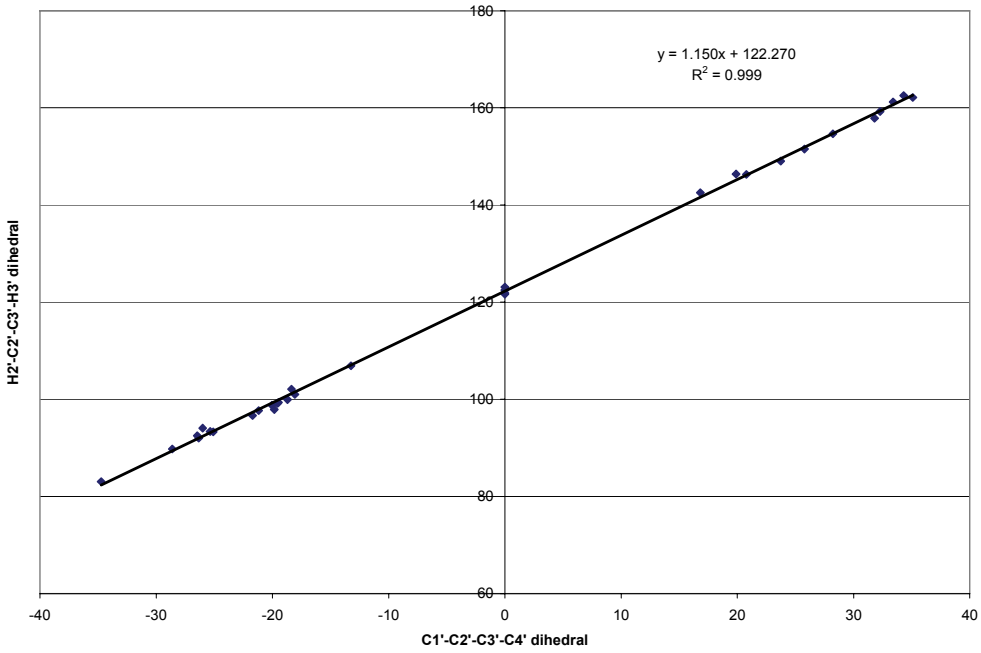

Figure 4.6c. A_j and B_j for H2'-H3' coupling in FMAU.

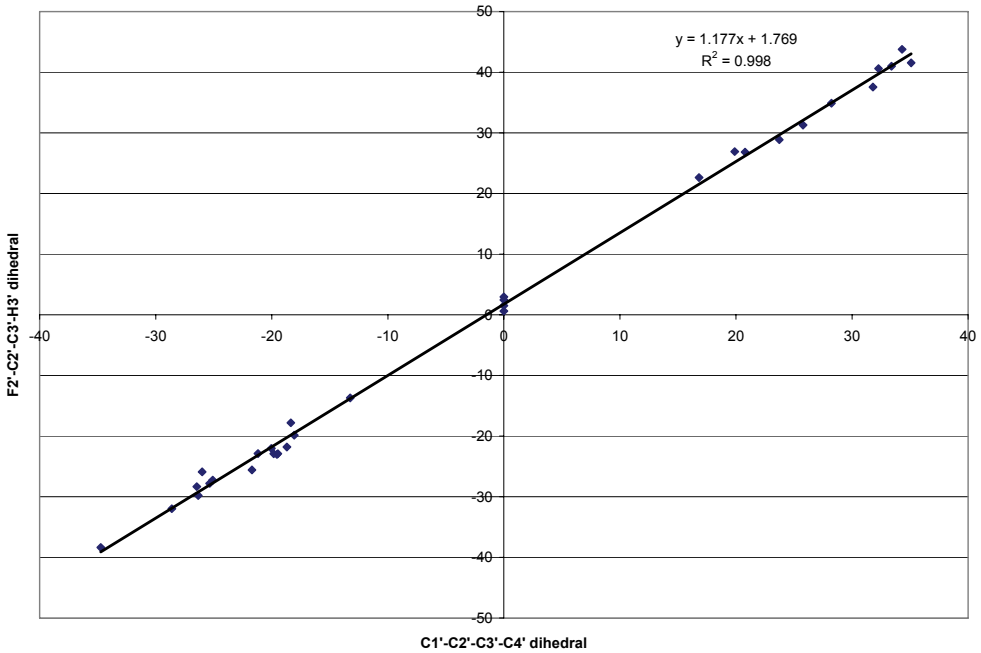

Figure 4.6d. A_j and B_j for F2'-H3' coupling in FMAU.

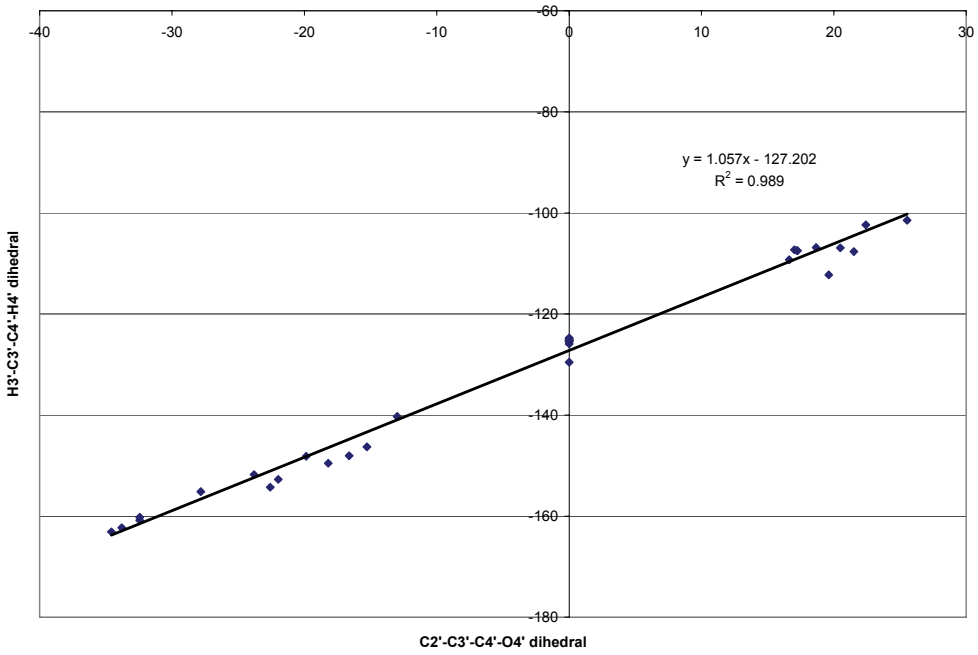

Figure 4.6e. A_j and B_j for H3'-H4' coupling in FMAU.

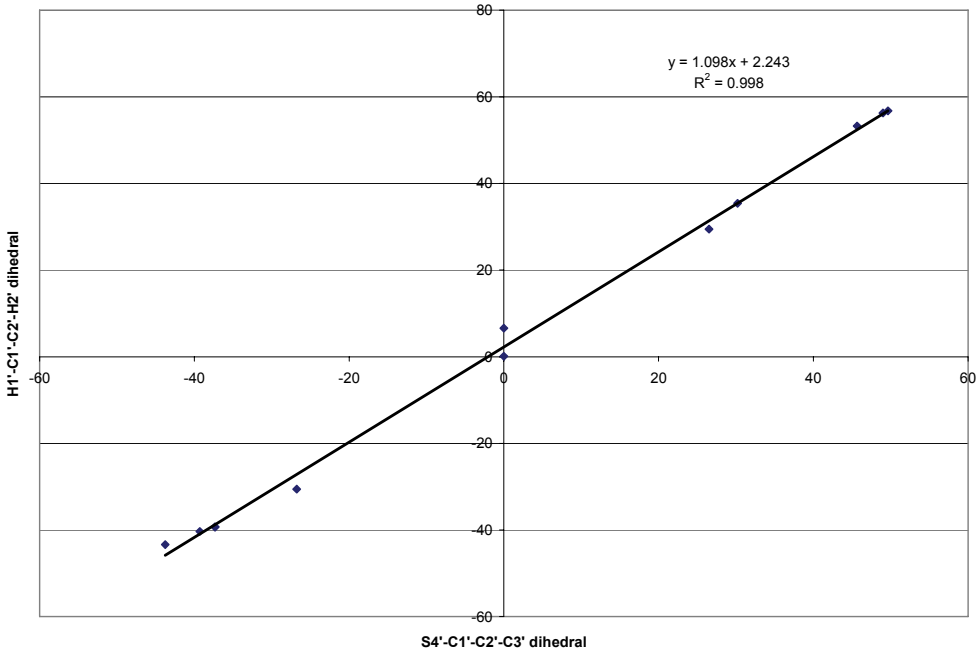

Figure 4.7a. A_j and B_j for H1'-H2' coupling in 4'S-FMAU.

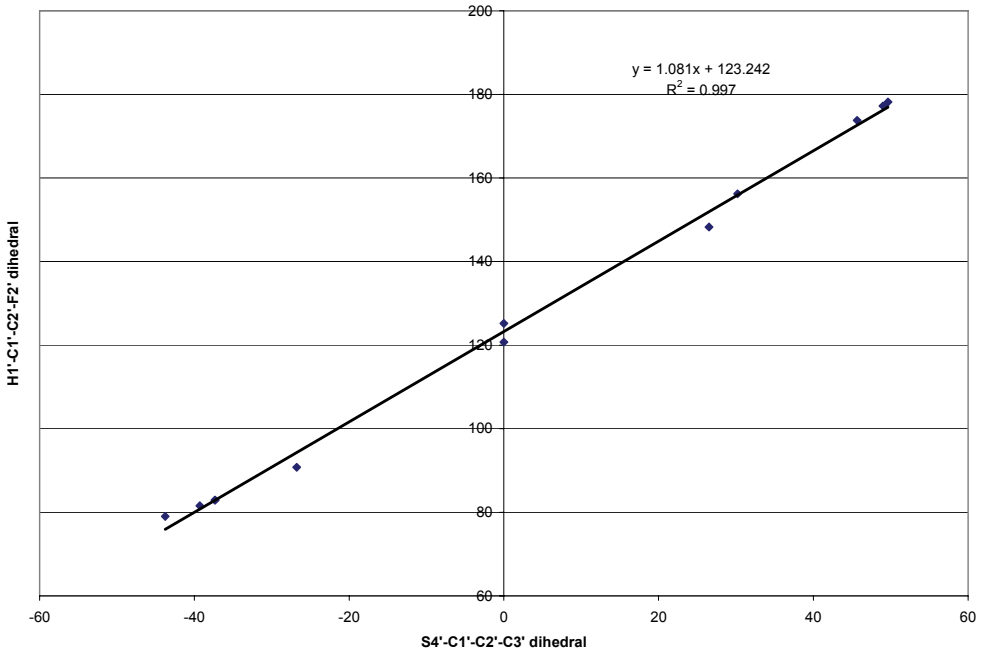

Figure 4.7b. A_j and B_j for H1'-F2' coupling in 4'S-FMAU.

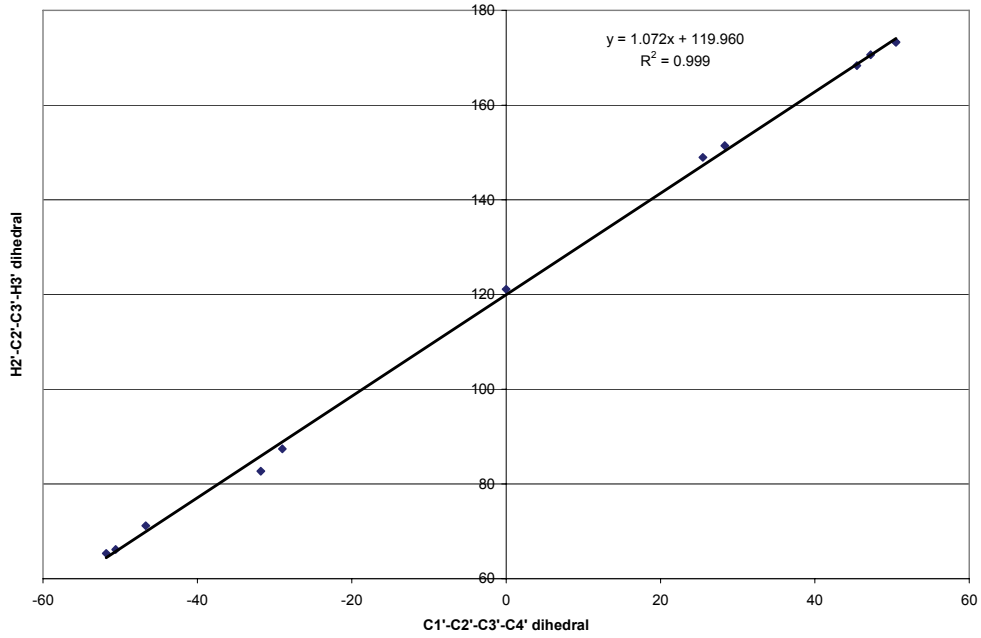

Figure 4.7c. A_j and B_j for H2'-H3' coupling in 4'S-FMAU.

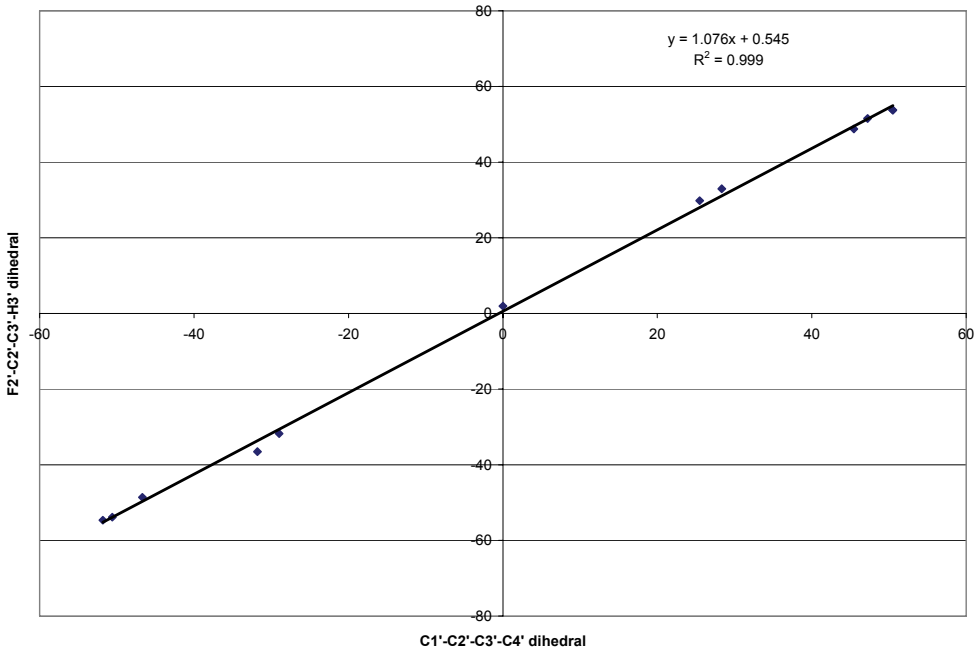

Figure 4.7d. A_j and B_j for F2'-H3' coupling in 4'S-FMAU.

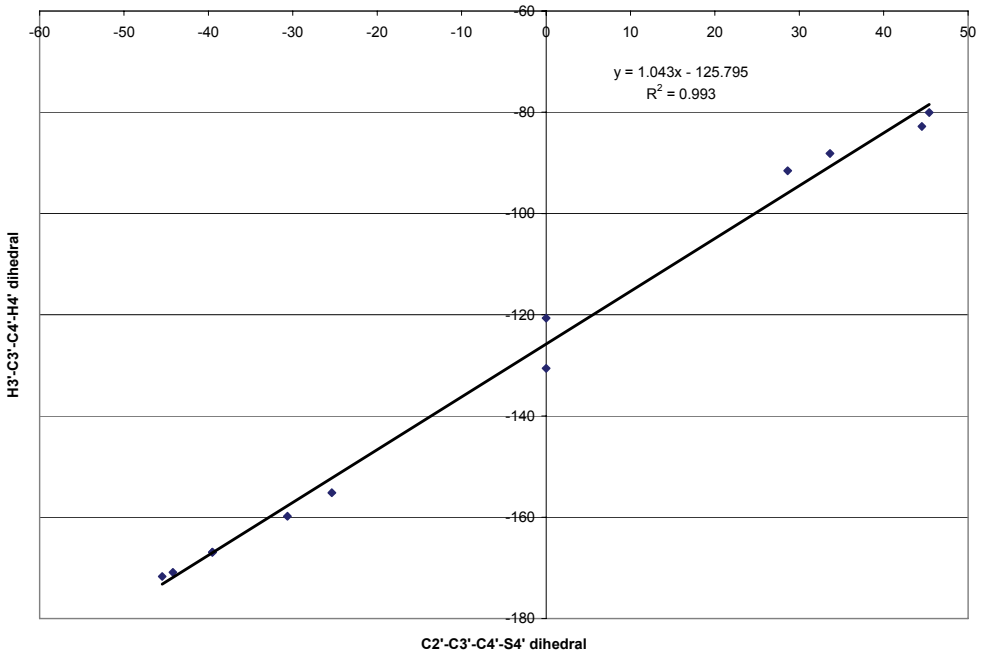

Figure 4.7e. A_j and B_j for H3'-H4' coupling in 4'S-FMAU.

4.6.2.2 PSEUROT calculations

Proton spectra were zero-filled to 128K and resolution-enhanced with Gaussian or sinebell functions. The vicinal coupling constants were then extracted directly. For the FANA species, the spectra were measured at various temperatures but only minute changes in the coupling constants were observed up to 40°C.

For the PSEUROT input files, all parameters were calculated as described above except the empirical group electronegativities, which were obtained from the literature.[442,443] The initial studies of 2400 different starting values were accomplished using PSEUROT's "MANY" function.

In all ^{19}F calculations, the ^{1}H-^{19}F coupling was given a weighting of 0.2, to compensate for the inherently larger value of its coupling constant and to give it slightly less weight since the parameterization of the corresponding generalized Karplus equation is less reliable. The FCC and HCC angles along the path of the coupling were chosen according to the method of Mikhailopulo *et al.*[444]

The initial calculations were executed both with and without the Diez extension of the pseudorotation equations. For both molecules, the results obtained were similar with and without the Diez parameters; however, the rms error tended to be slightly lower with the Diez parameters included for calculations on **4.13a**, and excluded for **4.14**. Therefore, for the final calculations, the Diez extension was used only for the 4'S-FMAU nucleoside **4.13a**.

The regions of pseudorotational space that gave low rms error (0.00 to 0.02 Hz for 4'S-FMAU, 0.00 to 0.50 Hz for FMAU) are shown in Table 4.6. The 4'-thio compound **4.13a** showed three distinct regions, all with very low rms error, but two of which included conformers in the western hemisphere that are highly unlikely according to DFT calculations and precedent. Its 4'-oxygen congener **4.14** showed one very broad region with higher rms error. The lowest rms error obtained within this general region was for a physically unlikely situation (ϕ_{maxII} = 52°, which is too large for a 4'-oxygen furanose) but other more feasible sets of parameters were found in the same region. The final answers (Table 4.7) were obtained from these possible regions by including the proton – fluorine couplings as described above.

Chapter 5. RNase H and siRNA studies using 2'-fluorinated oligonucleotides

5.1 Introduction

Gene silencing via the introduction of an antisense oligonucleotide (AON) or small interfering RNA (siRNA) into an organism is an attractive and elegant means of selectively blocking the expression of a deleterious gene.[56,445-447] The successful development of AON and siRNA as therapeutics will likely require modification of the oligonucleotide sugar-phosphate backbone to enhance delivery, stability, efficacy and specificity. In fact, progress toward routine use in the clinic, especially for AON therapy, has been slow, partly due to limitations in the currently available chemical modifications.[448]

5.1.1 Background: 2'F-ANA in antisense oligonucleotides

Particularly important for antisense therapeutics are modified AONs that trigger RNase H activity when bound to an mRNA, since this leads to the specific and permanent destruction of the mRNA target.[59,60] All known AONs with the ability to elicit RNase H activity[118,449,450] appear to share the same A-B type duplex conformation and minor groove width dimensions, which are believed to be key to maintaining RNase H activity.[451,452] In the case of 2'-deoxy-2'-fluoroarabinonucleic acids (2'F-ANA), RNase H cleavage efficiency can be significantly enhanced by incorporating flexible 2'-deoxyribonucleotides, aliphatic linkers, or seconucleosides within the sequence (Section 1.4.3.4).[284,288] This increased efficiency of cleavage appears to be related to the greater flexibility of the AON strand.[288]

5.1.2 Background: 2'F-ANA in siRNA

Much recent work has focused on the chemical modification of siRNA (discussed in detail in Section 1.3). A wide variety of RNA-like modifications can be introduced into siRNA duplexes without perturbing the overall A-form helical structure required for activity. It is not clear yet which chemical modifications will be the most advantageous.

We hypothesized that despite the generally DNA-like properties of 2'F-ANA, siRNA duplexes could be partially 2'F-ANA-modified without compromising

their recognition by RISC during the various steps of RNAi. Dowler *et al*. were the first to show that 2'F-ANA could be incorporated throughout the sense strand, including a fully-modified sense strand.[120] Modification of the antisense-strand 3'-overhang with 2'F-ANA brought a significant increase in potency.[120] Several of the 2'F-ANA-modified duplexes have been able to surpass the native siRNA in potency.[120]

Furthermore, siRNA duplexes with extensive 2'F-ANA modification were found to have a significantly longer serum half-life than unmodified siRNAs. For example, the serum half life of an siRNA was extended from 15 min to 5 h by replacing the sense strand with 2'F-ANA.[120] This is likely why the duration of action of siRNA was found to improve upon 2'F-ANA modification.[120]

While it is true that the siRNA duplexes containing entirely 2'F-ANA sense strands are capable of eliciting RNase H activity that would cleave the RNA antisense strands, this activity is not optimal for 2'F-ANA in the absence of DNA units or flexible linkers (Section 1.4.3.4)[284,288] and thus allows enough time for the antisense strand to be loaded into the RISC complex.

In summary, 2'F-ANA modified siRNA can have high efficacy, comparable to that of standard siRNAs, but with improved biostability provided by the 2'F-araN nucleotides, thus overcoming one of the therapeutic limitations of siRNA.

5.2 RNase H and siRNA activity of oligonucleotides containing 2'-fluoro-4'-thioarabinonucleosides

As part of our ongoing program to probe the substrate specificity of RNase H and the RISC complex, we chose to replace the 4' (ring) oxygen of 2'F-ANA with a sulfur atom to give 2'-deoxy-2'-fluoro-4'-thioarabinonucleic acids (4'S-FANA). 4'-Thiolation of RNA and DNA has been shown to enhance thermal stability and exo- and endonuclease resistance.[453-456] 4'-Thio-RNA is accepted by the RNAi machinery.[122-124] The 4'-thiolation of DNA[457] or 2'F-ANA (see Chapter 4) induces a conformational switch to the north (RNA-like), and we would thus expect that duplexes containing 4'S-FANA would adopt an A-form helix and also be accepted by the RNAi machinery.[107] Furthermore, evaluation of hybrids containing 4'S-FANA would help elucidate the structural factors that provide the

optimal AON/RNA substrate for RNase H. While 2'-deoxy-2'-fluoro-4'-thioarabinonucleosides have previously been synthesized[402,404,405,458] they have not, to the best of our knowledge, been incorporated into oligonucleotides.

5.2.1 Antisense oligonucleotide design

It has been shown that an 18-mer chimera containing six central 2'-deoxyribonucleotides[459-461] or 2'F-ANA[284,302] nucleotides surrounded by native RNA wings is a substrate for RNase H. The RNA wings serve to ensure tight binding, and the central section is adequate to elicit RNase H activity. In this way**,** new modifications can be tested for a true effect on RNase H activity without compromising the binding properties of the oligonucleotide. Oligonucleotides **As1**–**As5** (Table 5.1) were therefore synthesized by adopting this approach in the oligomer design, using standard solid-phase methodology. The three gapmers **As1**, **As2** and **As3** (containing six central dT, 4'S-FMAU, or FMAU residues, respectively) and two 18-mers **As4** and **As5** (DNA and RNA) were chosen to provide a wide range of duplex structure and thus varying degrees of RNase H hydrolysis. The RNA wings of the sequences chosen were of mixed base composition to minimize the formation of partial duplexes that could potentially occur when polyuridylates are hybridized to RNA. siRNA sequences were chosen for their continuity with previous studies on 2'F-ANA-modified siRNA.[120]

5.2.2 Oligonucleotide characterization

Synthesis of the modified nucleoside phosphoramidites **4.16** was described in Chapter 4. They behaved well during the solid-phase oligonucleotide synthesis, as described in detail in Section 5.4.

As a further characterization, we carried out a Snake Venom Phosphodiesterase / Alkaline Phosphatase (SVPDE/AP) digestion on strand **As2,** purified the resulting nucleosides by HPLC, and confirmed by ESI-MS that the isolated 4'S-FMAU was the authentic nucleoside. This provided further evidence that 4'S-FMAU is stable to oxidation under solid-phase coupling conditions.

Sequence		T_m (RNA target)	T_m (DNA target)
As1	5'-UGA CAU ttt ttt UCA CGU-3'	60.0	51.0
As2	5'-UGA CAU ***TTT TTT*** UCA CGU-3'	51.0	36.0
As3	5'-UGA CAU ***TTT TTT*** UCA CGU-3'	62.0	50.1
As4	5'-tga cat ttt ttt tca cgt-3'	42.1	55.5
As5	5'-UGA CAU UUU UUU UCA CGU-3'	59.1	40.2

Table 5.1. Antisense oligonucleotide sequences and thermal denaturation studies. Legend: RNA, dna, ***4'S-FANA***, ***2'F-ANA***. Complementary strands were as follows: RNA, 5'-ACG UGA AAA AAA AUG UCA-3', DNA, 5'-acg tga aaa aaa atg tca-3'.

5.2.3 Binding & CD studies

The "antisense" sequences **As1**–**As5** were hybridized to complementary ssRNA and ssDNA, and their thermal stability was examined by monitoring the change in hyperchromicity at 260 nm. All sequences and melting temperatures of the duplexes are shown in Table 5.1.

Sequences **As1**, **As3** and **As5** (DNA and 2'F-ANA gapmers, and an all RNA strand) had very similar affinity towards their common ssRNA target. In fact, this observation is precedented[284,305] and related to the purine-rich complementary RNA strand, 5'-ACG UGA AAA AAA AUG UCA-3', which predominantly dictates, in each case, adoption of the high-melting A-form helical conformation. In contrast, a drop in T_m of -1.4°C per insert with respect to **As5**•RNA is observed for sequence **As2** (4'S-FANA gapmer) and implies either that this modified AON cannot easily adopt the classical A-form geometry upon duplexation, or that there are unfavorable interactions within an A-form structure that weaken the association. Given that the nucleoside favors a northern conformation, and that the **As2**•RNA hybrid does display an A-like conformation (CD studies described below), the second option seems more likely. It is interesting to observe that 2'-fluoroarabino,[119] 4'-thio-RNA[456] and 4'-thio-DNA[457] modifications, taken alone, usually provide an increase in stability toward complementary strands. Thus it may be that the *combination* of the longer S4'–C1' bond (and the larger van der Waals radius of S *vs*. O) with the top-face fluorine is responsible for the

destabilization of the hybrid structure. This likely influences the *N*-glycosidic torsion angle in such a way as to cause destabilization. Indeed, this is manifest in the CD spectrum (discussed below), in which the long wavelength band (generally associated with nucleobase stacking) is quite weak for this duplex, and even more so when DNA is the target (Figure 5.1). Since both sulfur and fluorine are more hydrophobic than oxygen, another possible explanation for the lower thermal stability of the 4'S-FANA(**As2**)•RNA duplex relative to RNA(**As5**)•RNA is the more complete and favorable hydration of 4'-O and 2'-OH groups in the latter. Either modification (4'S or 2'F) taken alone may have enough hydrophilic character to avoid this destabilization.

For the ssDNA target, it is again worth comparing the binding behavior of the various gapmers. AONs containing DNA or 2'F-ANA gaps (**As1** and **As3**) had the highest affinity towards the ssDNA target. The 4'S-FANA gapmer **As2** provided the least stable AON•DNA duplex; however, its T_m was comparable to that of the RNA 18-mer **As5**. This is consistent with the well-known order of stability of oligonucleotide duplexes, where dPy:dPu > rPy:dPu[119,462] and the proposal that 2'F-ANA mimics the DNA structure (southeast pucker), whereas 4'S-FANA more closely resembles RNA (north pucker). The 4'S-FANA (**As2**) and RNA (**As5**) gapmers exhibit similar affinity towards the ssDNA target (ΔT_m = 4 ºC; Table 5.1). The same trend does not hold when the target is ssRNA; in this case, the RNA(**As5**)•RNA duplex is significantly more stable than the 4'S-FANA(**As2**)•RNA hybrid (ΔT_m = 8.1 ºC), suggesting that the 4'S-FANA modification prefers an alternative conformation that is available only when duplexed to the more flexible DNA target. In support of this notion, the CD spectrum of **As2**•DNA is neither A-form nor B-form, whereas that of **As2**•RNA is characteristic of A-form duplexes (discussed below).

Hybrids comprising any one of sequences **As1**–**As5** bound to either ssRNA or ssDNA targets were further evaluated for possible variations in duplex structure via CD spectroscopy, in the region from 320 – 200 nm (Figure 5.1). The spectra of all AON•RNA hybrids exhibit the characteristic A-form pattern, with the largest changes evident in the magnitude and positions of the positive Cotton effect at *ca*. 265 nm. The highest Cotton effect (molar ellipticity) observed

corresponds to that of the pure RNA•RNA duplex (**As5**•RNA). The Cotton effects of the 4'S-FANA gapmer (**As2**)•RNA duplex are blue-shifted, but the overall CD trace similarly indicates an A-form global geometry. The spectra of the AON•DNA hybrids, however, are much more varied in comparison. Most striking is the CD signature of the **As2**•DNA duplex, which bears no similarity to either A- or B-form reference spectra. Of note, for example, are the negative peak at 280 nm, the cross-over at 270 nm, and the positive peak at 257 nm, all of which are unique to the **As2**•DNA spectrum. The helical structure of this hybrid is apparently quite different from either A-form or B-form helices, thus supporting the notion that the increased S-C bond length, the smaller C-S-C bond angle or the more puckered ring causes a divergence from the classical helix structure, or might perturb the *N*-glycosidic orientation around the nucleotide sugars, thereby destacking the helix. The fact that greater structural distortions are observed with ssDNA instead of ssRNA targets (as measured by CD) suggests that the 4'S-FANA-modified strand only reveals its preferred conformation in a duplex when not overwhelmed by the A-form preference of RNA.

5.2.4 RNase H assays

The RNase H family of enzymes recognize and cleave the RNA strand of AON•RNA hybrids having a conformation that is intermediate between the pure A- or B-form conformations adopted by dsRNA and dsDNA, respectively. Sugar geometries that fall within the eastern (O4'-*endo*) range within the AON have been postulated to actively induce RNase H-assisted RNA strand cleavage.[328,333] Chemical changes of the sugar constituents or alterations in the sugar conformation (*e.g.*, orientation of the sugar to the base) or flexibility (*e.g.*, DNA versus the more rigid 2'F-ANA analogue) can all dramatically affect RNase H activation.[288]

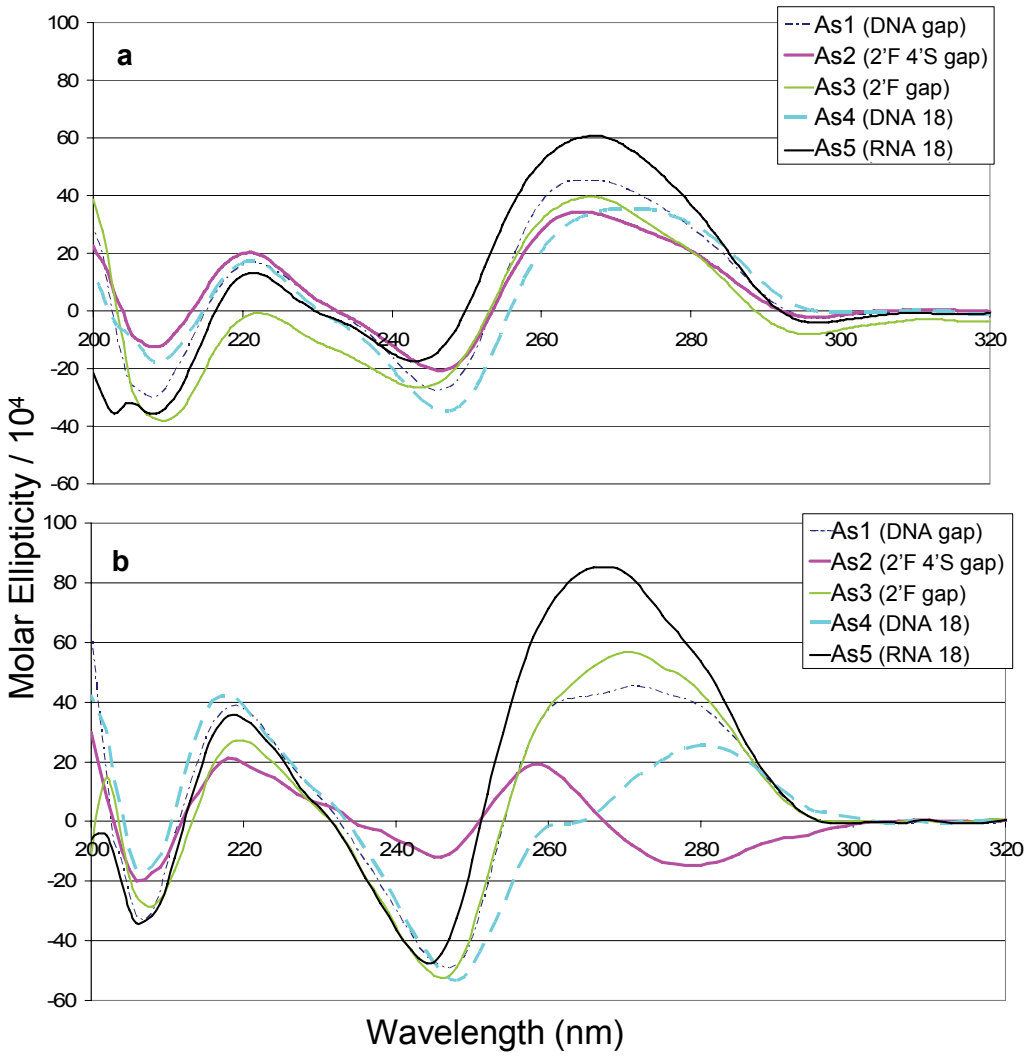

Figure 5.1. Circular dichroic spectra of gapmers and non-chimeric control strands, bound to RNA or DNA complementary ("target") strands. (a): **As1**–**As5**, ssRNA target; b: **As1**–**As5**, ssDNA target). Spectra were run at 20°C after annealing the duplexes under the same conditions described for the binding studies.

Oligomers **As1**–**As5** were assessed for their ability to elicit *E. coli* RNase HI and human RNase HII activity. As shown in Figure 5.2, the control DNA oligomer **As4** and DNA gap **As1** both promoted essentially complete degradation of the 5'-^{32}P-labeled RNA. As expected, the RNA duplex was not a substrate of RNase H. With the 2'F-ANA gap (**As3**) the enzyme activity was somewhat lower compared to DNA, although significant cleavage (>50%) occurred after 50 min

under these conditions, as previously observed.[284] Negligible or no cleavage was observed for the 4'S-FANA modified (**As2**)•RNA hybrid. The ability of the various gaps to elicit *E. coli* RNase HI activity followed the order: DNA > 2'F-ANA >> 4'S-FANA ≈ RNA (Figure 5.2a). The same trend was observed with the human enzyme (Figure 5.2b-d). The lack of RNase H activity supported by 4'S-FANA is fully consistent with the anticipated northern conformation (*C3'-endo*) of this modification.

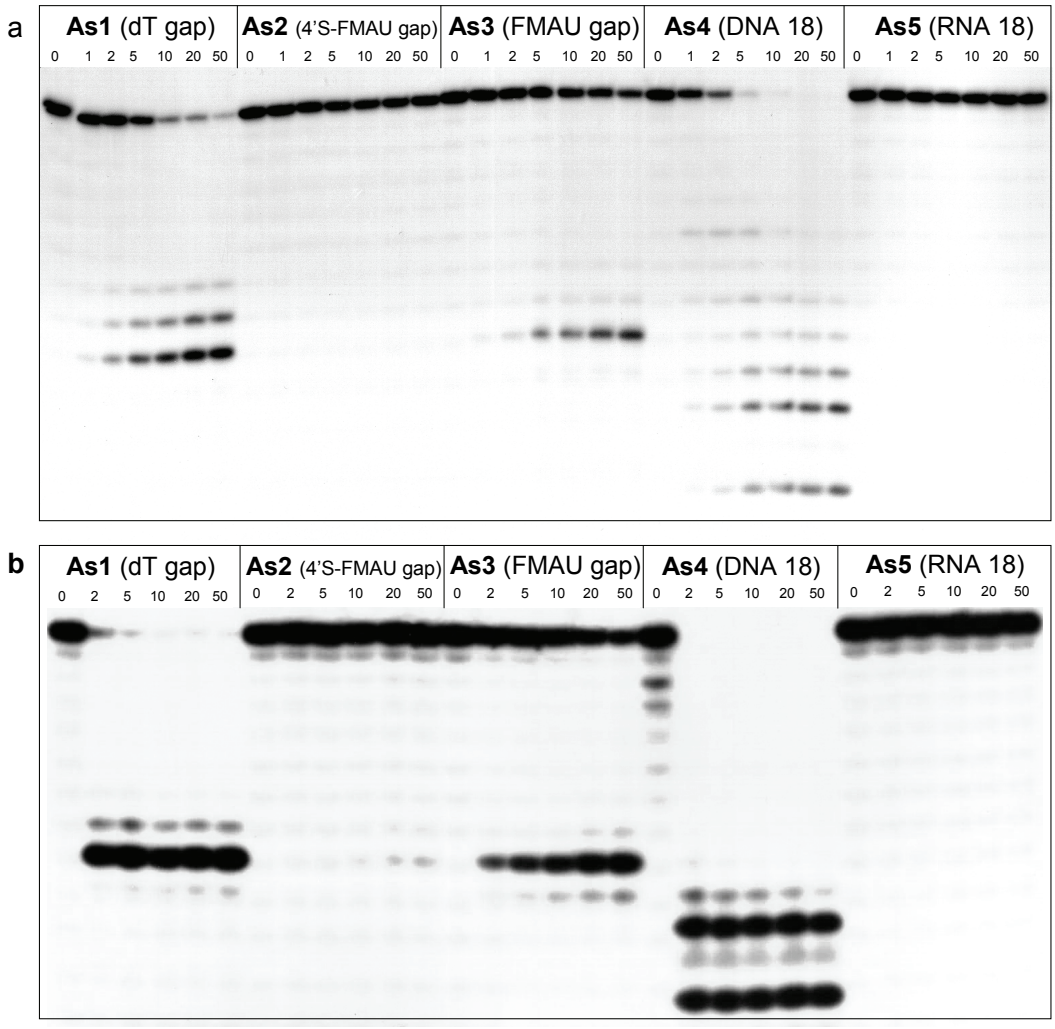

(Figure 5.2 continued next page…)

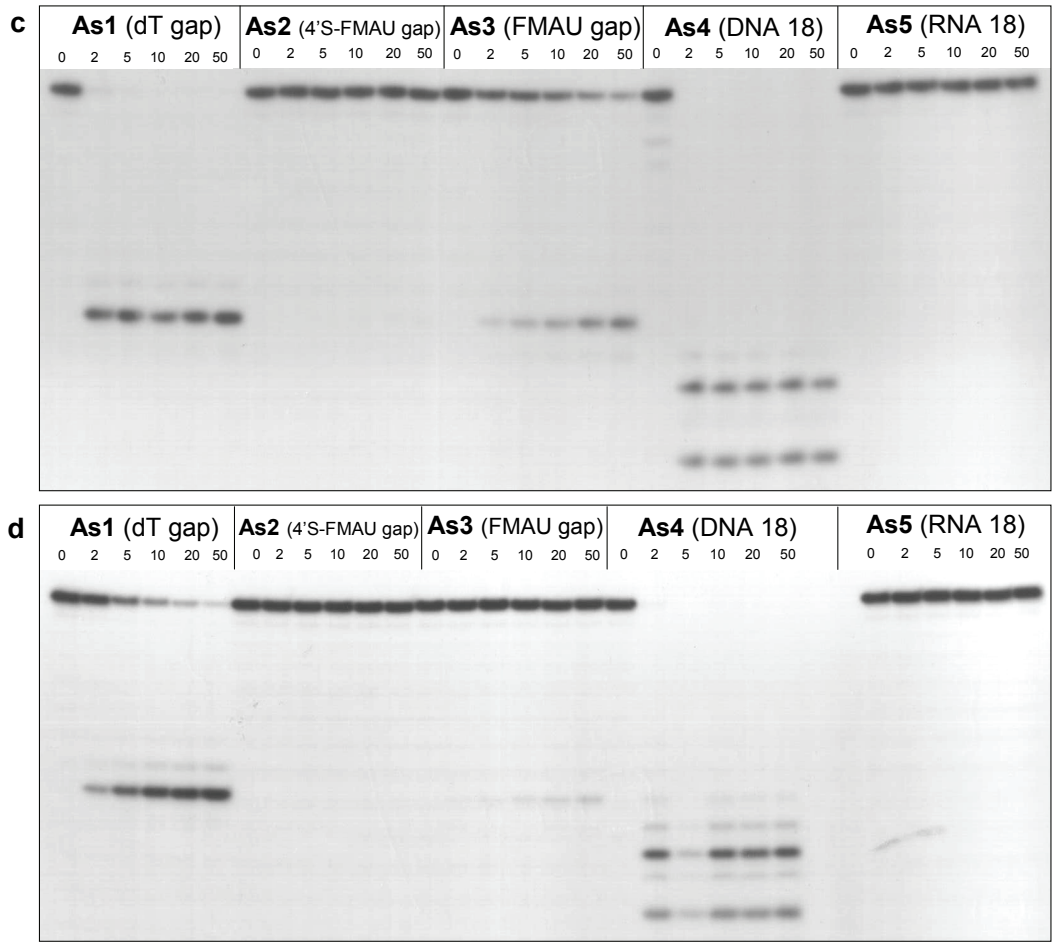

Figure 5.2. Ribonuclease H degradation of various hybrid duplexes. An 18-nt 5'-^{32}P-labeled target RNA (5'-ACG UGA AAA AAA AUG UCA-3') was preincubated with complementary 18-nt antisense oligomer **As1**–**As5**, and then added to reaction assays containing (a) *E. coli* RNase HI, (b) human RNase HII, 110 nM, long gel exposure time, (c) human RNase HII, 110 nM, shorter gel exposure time, or (d) human RNase HII, 37 nM. Aliquots were removed as listed on diagrams (in minutes). Base sequences of antisense oligomers are given in Table 5.1. See Section 5.4 for detailed assay conditions.

5.2.5 RNA interference

2'-Fluoro-4'-thioarabinouridine (4'S-FAU) was introduced at various positions into both strands of an siRNA sequence[120] targeting positions 1818-1836 of the firefly luciferase gene, RefSeq accession number M15077 (Table 5.2). siRNAs containing FMAU at the same positions were used as controls, along with native RNA. The resulting modified duplexes were transfected into HeLa X1/5 cells stably expressing firefly luciferase. (All transfections in this chapter were carried out by Francis Robert of the Pelletier research group, McGill Department of Biochemistry. Detailed protocols are in Section 5.4). Results are summarized in Tables 5.2 and 5.3, and Figures 5.3–5.5.

Duplex		T_m (°C)	IC_{50} (nM)
Ctl	5'-GCUUGAAGUCUUUAAUUAAtt-3' 3'-ggCGAACUUCAGAAAUUAAUU-5'	62.3	0.16
Ctl-p	5'-GCUUGAAGUCUUUAAUUAAtt-3' 3'-ggCGAACUUCAGAAAUUAAUUp-5'	n.d.	0.04
T1	5'-GCUUGAAGUCUUUAA*UU*AAtt-3' 3'-ggCGAACUUCAGAAAUUAAUU-5'	60.2	0.10
F1	5'-GCUUGAAGUCUUUAA*TT*AAtt-3' 3'-ggCGAACUUCAGAAAUUAAUU-5'	63.0	0.20
T2	5'-GCUUGAAGUCUUUAAUUAAtt-3' 3'-ggCGAACU*U*CAGAAAUUAAUU-5'	57.2	0.17
F2	5'-GCUUGAAGUCUUUAAUUAAtt-3' 3'-ggCGAACU*T*CAGAAAUUAAUU-5'	60.0	0.31
T3	5'-GCUUGAAGUCUUUAAUUAAtt-3' 3'-ggCGAACUUCAGAAAUUAA*UU*-5'	62.0	3.6
T3p	5'-GCUUGAAGUCUUUAAUUAAtt-3' 3'-ggCGAACUUCAGAAAUUAA*UU*p-5'	n.d.	0.16
F3	5'-GCUUGAAGUCUUUAAUUAAtt-3' 3'-ggCGAACUUCAGAAAUUAA*TT*-5'	62.1	1.0
F3p	5'-GCUUGAAGUCUUUAAUUAAtt-3' 3'-ggCGAACUUCAGAAAUUAA*TT*p-5'	n.d.	0.04

Table 5.2. siRNA sequences and thermal denaturation studies. Legend: RNA, dna, *4'S-FANA*, *2'F-ANA*. Sense strands are listed on top and antisense strands below. Duplexes with names ending in "p" were 5'-phosphorylated on the antisense strand (see text for details).

Duplex		T_m (°C)	IC_{50} (nM)
Ctl	5'-GCUUGAAGUCUUUAAUUAAtt-3' 3'-ggCGAACUUCAGAAAUUAAUU-5'	62.1	0.16
Ctl-gg	5'-GCUUGAAGUCUUUAAUUAAgg-3' 3'-ggCGAACUUCAGAAAUUAAUU-5'	61.7	0.87
Ctl-f	5'-*GCTTGAAGTCTTTAATTAAGG*-3' 3'-ggCGAACUUCAGAAAUUAAUU-5'	66.0	7.8
Ctl-fr	5'-*GCTTGAAGTCTTTA*ATTAA*TT*-3' 3'-ggCGAACUUCAGAAAUUAAUU-5'	63.0	2.4
Ctl-fm	5'-*GCTTGAAGTCTTTA*T*T*AA-3' 3'-ggCGAACUUCAGAAAUUAAUU-5'	62.1	>20
T2-f	5'-*GCTTGAAGTCTTTAATTAAGG*-3' 3'-ggCGAACU*U*CAGAAAUUAAUU-5'	61.0	17
T2-fr	5'-*GCTTGAAGTCTTTA*ATTAA*TT*-3' 3'-ggCGAACU*U*CAGAAAUUAAUU-5'	56.6	0.60
T2-fm	5'-*GCTTGAAGTCTTTA*T*T*AA-3' 3'-ggCGAACU*U*CAGAAAUUAAUU-5'	54.1	>20
F2-f	5'-*GCTTGAAGTCTTTAATTAAGG*-3' 3'-ggCGAACU*T*CAGAAAUUAAUU-5'	65.6	10.8
F2-fr	5'-*GCTTGAAGTCTTTA*ATTAA*TT*-3' 3'-ggCGAACU*T*CAGAAAUUAAUU-5'	61.6	0.87
F2-fm	5'-*GCTTGAAGTCTTTA*T*T*AA-3' 3'-ggCGAACU*T*CAGAAAUUAAUU-5'	61.1	>20

Table 5.3. Effect of significantly-modified sense strands with FAU point modifications in the antisense strand. Legend: RNA, dna, *4'S-FANA*, *2'F-ANA*. 2'F-ANA mismatches are indicated with grey text. Duplexes with names ending in "f" contained fully-2'F-ANA sense strands, "fr" indicated a 2'F-ANA sense strand containing 5 RNA inserts near the sense 3'-end, and "fm" indicated a 2'F-ANA sense strand with two internal mismatches near the sense 3'-end (see text for details).

The 4'S-FANA modification is generally well-tolerated by the RNAi machinery, with some dependence on position. The potencies of the 4'-S-FANA and 2'F-ANA modified strands are comparable.

When the terminal pair of nucleotides of the antisense strand is modified by either one of the nucleotides under investigation in this study, the activity is significantly reduced. We hypothesized that this was related to the inability of the strand to be 5'-phosphorylated *in vivo*, an essential step for incorporation into RISC. Indeed, chemical or enzymatic 5'-phosphorylation prior to transfection dramatically increased the activity of terminally-modified strands (Figure 5.4). Even the control strand showed an improvement in potency upon 5'-phosphorylation. This is understandable, given the fact that although the RISC

complex can phosphorylate exogenous siRNAs, the natural process involves fragments cleaved by Dicer and possessing a 5'-phosphate.[463]

It is significant that this 5'-terminal pair of nucleotides can be modified, if phosphorylated, with no significant loss in activity for the 2'S-FANA or 4'S-FANA. These positions have recently been shown to play a key role in reducing miRNA-type off target effects when modified with 2'-*O*-methylribonucleotides.[184] Given that the very small structural perturbation of a 2'-*O*-methyl group is effective in reducing off-target effects, we are optimistic that the larger conformational changes introduced by 4'S-FANA moieties may cause an even greater decrease in undesired miRNA-type silencing.

The 4'S-FANA antisense modifications were tested in combination with various heavily-modified sense strands. We previously reported that an all-2'F-ANA sense strand was tolerated by the RNAi machinery. We therefore included such a duplex in our assays (duplexes **Ctl-f**, **T2-f** and **F2-f**). To improve upon the activity of this strand, however, we made two other modifications. Functional siRNAs exhibit strand bias; at the 5'-end of the duplex (defined by the antisense strand), the duplex binding affinity should be reduced.[464,465] Hohjoh[466] showed that it is possible to introduce this strand bias and thus improve siRNA activity by introducing 1-4 internal mismatches near the 3'-end of the sense strand. Thus we attempted a similar design and made a fully-modified 2'F-ANA sense strand containing two appropriately-placed mismatches (duplexes **Ctl-fm**, **T2-fm** and **F2-fm**). Finally, in an attempt to both lower affinity and maintain a more authentic A-form helical structure, a sense strand was made containing 5 RNA inserts at its 3'-end (duplexes **Ctl-fr**, **T2-fr** and **F2-fr**). The 2-nucleotide 3'-overhang was left as 2'F-ANA to help provide 3'-exonuclease resistance. Results are given in Figure 5.5.

In all cases, the "fr" type sense strand was the best heavily-modified sense strand, reaching levels of potency close to that of the control. It is interesting to note the synergy between 4'S-FANA and 2'F-ANA in the **T2-fr** duplex, which gave particularly good results. Neither antisense strand modification was helpful in the case of the "f" type sense strand. The "fm" type sense strand showed very poor activity. Apparently the deviation in structure from an RNA duplex is great

enough in this case that it is not well-recognized by RISC. This significant difference in potency is in spite of the fact that the binding affinities of the "fm" and "fr" strands are similar (Table 5.3); thus in this case the duplex distortion is more important than the required strand bias discussed above.

The need for strand bias may explain why the 4'S-FANA-modified duplex **T1** is more potent than the control, since the duplex has lower affinity at the antisense 5'-end (Table 5.2). However, it remains to be seen if this strand bias will be generally applicable or will be overwhelmed by the helical distortions associated with 4'S-FANA inserts. For example, the 4'S-FANA-modified duplex **T3p** shows slightly reduced activity, even though the modification is appropriately placed at the antisense 5'-end of the duplex. Thus we believe that the slightly reduced activity of **T3p** with respect to **Ctl-p** can be attributed to the helical distortion observed and discussed above: although the nucleoside puckers in the north, the helix seems to be prevented from adopting a perfectly A-form duplex by other factors. When given a flexible target strand, as discussed above for the **II**:DNA duplex, 4'S-FANA seems to induce a duplex that is neither A-form nor B-form. Deviations of helical structure from the A-form (whether through unsuitable chemical modifications or antisense-strand bulges or mismatches) are known to divert RNAs from the siRNA pathway.[66,107] 2'F-ANA, on the other hand, prefers to adopt a southeast conformation (see Chapters 2 and 4) but its CD spectra discussed above correspond much more closely to an A-form helix; thus, it is more able to allow the RNA to dictate the helical conformation.

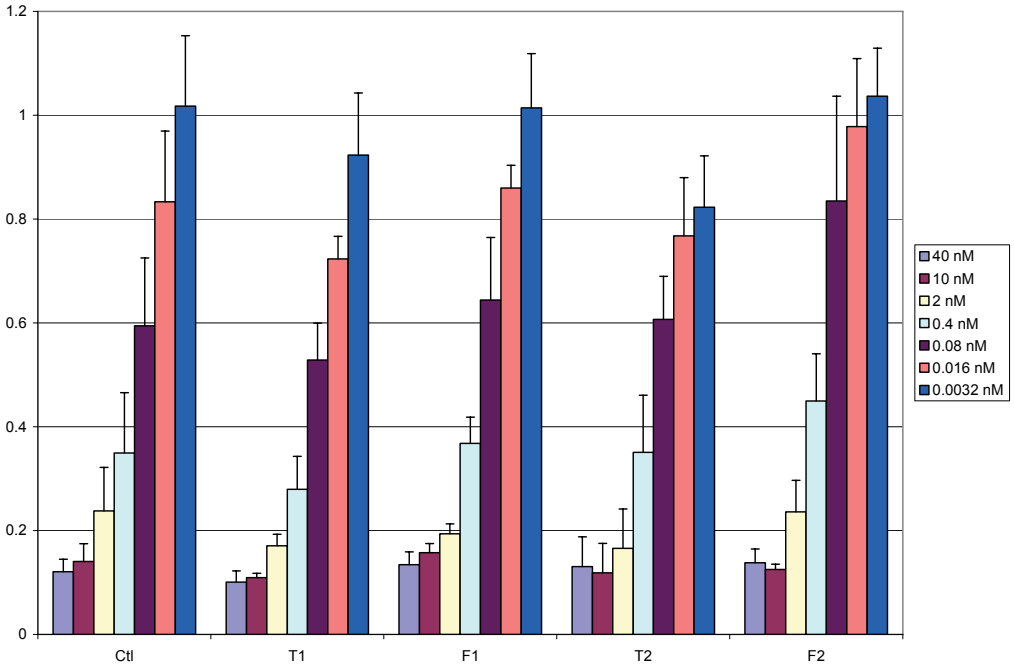

Figure 5.3. Activity of 4'S-FANA-modified siRNA (sequences given in Table 5.2).

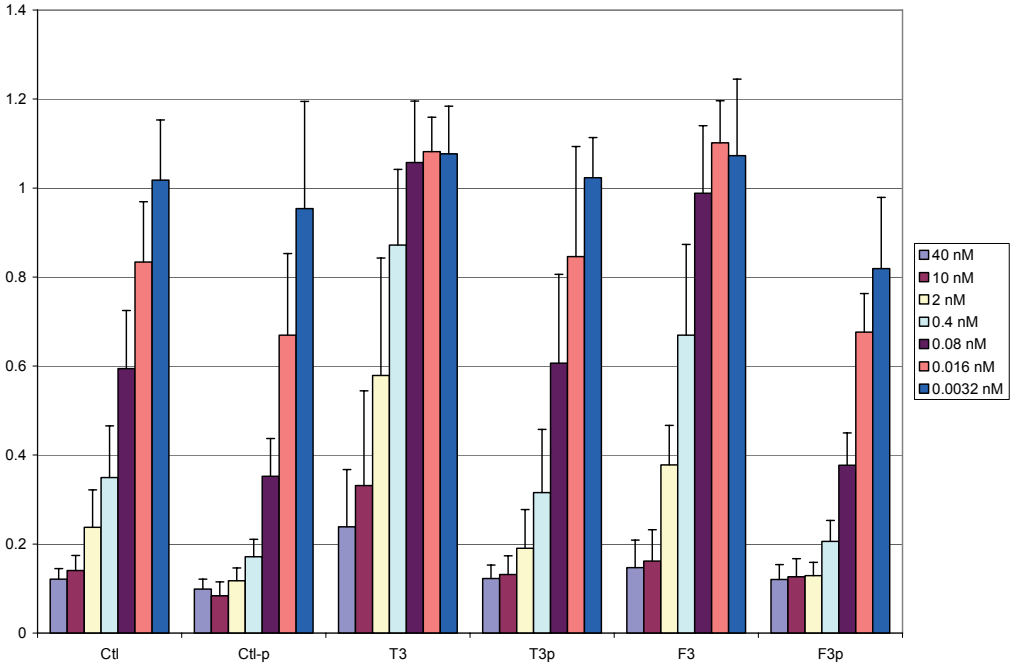

Figure 5.4. Effect of phosphorylation on siRNAs modified at the 5'-terminal of the antisense strand (sequences given in Table 5.2).

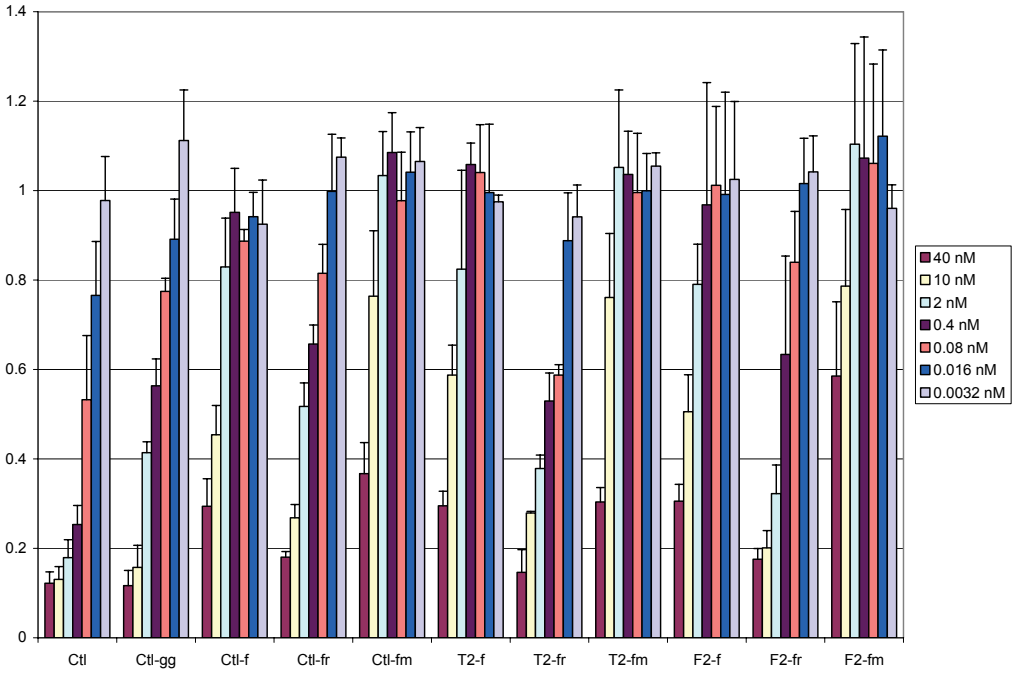

Figure 5.5. Activity of 4'S-FANA in combination with various heavily-modified sense strands (sequences given in Table 5.3).

5.2.6 Conclusions, Section 5.2

Modified duplexes containing 4'S-FANA units were thermodynamically less stable than unmodified duplexes and, as expected, they were unable to elicit *E. coli* or human RNase H activity. Since 4'S-FANA nucleosides are RNA-like (north) in conformation, these results lend further credence to the hypothesis that RNase H enzymes recognize duplexes in which the nucleoside building blocks of the antisense strand can adopt an eastern conformation.[333] They also highlight important structural differences that give rise to proficient enzymatic activity and further clarify the role of substrate conformation on the discriminatory properties of RNase H.

While 4'S-FMAU adopts a north conformation, CD spectra and thermal denaturation studies of oligomers containing this modification indicate that it perturbs the RNA structure. We believe that the main sources of this perturbation are steric hindrance and lower hydration compared to the native RNA. The

combination of the 2' "up" fluorine and the 4' sulfur substitution lead to destabilizing interactions not observed for either modification alone.

siRNAs containing 4'S-FANA units were able to enter the RNAi pathway. One or two inserts internally in either strand gave duplexes of potency comparable to that of the control. The 5'-end of the antisense strand can be modified as long as it is 5'-phosphorylated prior to the siRNA assay. The 4'S-FANA modification was also able to work with good efficiency in a duplex with a 75%-modified 2'F-ANA—RNA sense strand, demonstrating that the southern/eastern 2'F-ANA (with its preference for southern and eastern conformations) can achieve synergy with its northern cousin, 4'S-FANA, in RNAi gene silencing.

5.3 siRNA duplexes containing combinations of 2'F-ANA and 2'F-RNA

In the previous section, we noted a synergy between 4'S-FANA in the antisense strand, and 2'F-ANA in the sense strand. We wondered if synergy of this type would exist for antisense strands more heavily modified with RNA-like modifications. We also wondered if synergy of this type would also exist for combinations of 2'F-ANA with other more readily accessible RNA-like (northern) modifications. Since we had only one 4'S-FANA nucleobase available, and the synthesis of 4'S-FANA nucleosides required several steps, we turned to 2'F-RNA, a commercially available RNA-like modification. (Details on the previous use of 2'F-RNA in siRNA are given in Section 1.3.2.1).

5.3.1 Oligonucleotide design

We therefore made a series of duplexes containing fully-modified 2'F-ANA and 2'F-RNA strands (Table 5.4). A series of chimeric strands containing both 2'-fluoro epimers were also designed. Since the 2'F-RNA pyrimidine phosphoramidites are much less expensive than 2'F-RNA purine monomers,[467] one chimera consisted of 2'F-RNA pyrimidines and 2'F-ANA purines. Another pair of strands was a "1-1 altimer" structure, with alternating 2'F-ANA and 2'F-RNA residues. For all of these 2'F-ANA/2'F-RNA chimeric strands, the

3'-overhang was always made of 2'F-ANA, since this may lead to increased potency.[120] 2'F-ANA is also more resistant to 3'-exonucleases than is 2'F-RNA.[277]

5.3.2 RNA interference

The RNAi activity of all duplexes was tested under the same conditions described in Section 5.2.5; see detailed protocols in Section 5.4. Results are shown in Figure 5.6.

Two of the duplexes (**jg-4** and **jg-5**) were fully modified with a single chemistry: **jg-4** was entirely 2'F-RNA, and **jg-5** was entirely 2'F-ANA. Both duplexes were functional, and **jg-4** was more active than the control. We were surprised to find that complete 2'F-ANA modification (**jg-5**) was tolerated, since 2'F-ANA is not an ideal RNA mimic (see CD studies, Section 5.3.4).

Four of the duplexes (**jg-6**, **jg-8**, **jg-10** and **jg-12**) contained a modified sense strand paired with an RNA antisense strand. The best of these four duplexes is **jg-6**, containing a purine/pyrimidine chimeric sense strand. The second-best duplex is duplex **jg-8**, containing the 1-1 altimer configuration in the sense strand. Thus, combining the two 2'-F epimers in the sense strand yields better results than using either chemistry alone, and strikingly, with better results relative to the natural RNA (**jg-1**).

Comparison of the RNAi activity of duplexes **jg-6**–**jg-13** allows us to evaluate the appropriateness of each type of modified strand architecture (2'F-ANA, 2'F-RNA, purine/pyrimidine and 1-1 altimer) in the sense or antisense strands. Sense/antisense preferences are observed for all four types of modified strands. Duplexes **jg-6**, **jg-8** and **jg-12** are more active than **jg-7**, **jg-9** and **jg-13**, respectively, revealing that both chimeric constructs and the 2'F-ANA strand are better-tolerated in the sense strand than the antisense strand. The difference is particularly striking between duplexes **jg-8** and **jg-9** containing one 1-1 altimer strand; **jg-8** (1-1 altimer in the sense strand) was one of the most active duplexes tested, while **jg-9** (1-1 altimer in the antisense strand) was totally inactive.

Name	Description	Sequence	T_m
jg-1	Control	5'-GCUUGAAGUCUUUAAUUAAtt-3' 3'-ggCGAACUUCAGAAAUUAAUU-5'	61.8
jg-2	pur/pyr	5'-*G*CTT*GAAG*TCTTT*AA*TT*AATT*-3' 3'-*GG*C*GAA*CTTC*AGAAA*TT*AA*TT*p-5'	65.6
jg-3	1-1 altimer	5'-*G*C*T*T*G*A*A*G*T*C*T*T*T*A*A*T*T*A*A*T*T*-3' 3'-*GG*C*G*A*A*C*T*T*C*A*G*A*A*A*T*T*A*A*T*T*p-5'	36.8
jg-4	2'F-RNA	5'-GCTTGAAGTCTTTAATTAATT-3' 3'-GGCGAACTTCAGAAATTAATTp-5'	>90
jg-5	2'F-ANA	5'-*GCTTGAAGTCTTTAATTAATT*-3' 3'-*GGCGAACTTCAGAAATTAATT*p-5'	72.8
jg-6	pur/pyr RNA	5'-*G*CTT*GAAG*TCTTT*AA*TT*AATT*-3' 3'-ggCGAACUUCAGAAAUUAAUU-5'	62.5
jg-7	RNA pur/pyr	5'-GCUUGAAGUCUUUAAUUAAtt-3' 3'-*GG*C*GAA*CTTC*AGAAA*TT*AA*TT*p-5'	56.7
jg-8	1-1 altimer RNA	5'-*G*C*T*T*G*A*A*G*T*C*T*T*T*A*A*T*T*A*A*T*T*-3' 3'-ggCGAACUUCAGAAAUUAAUU-5'	48.2
jg-9	RNA 1-1 altimer	5'-GCUUGAAGUCUUUAAUUAAtt-3' 3'-*GG*C*G*A*A*C*T*T*C*A*G*A*A*A*T*T*A*A*T*T*p-5'	45.8
jg-10	2'F-RNA RNA	5'-GCTTGAAGTCTTTAATTAATT-3' 3'-ggCGAACUUCAGAAAUUAAUU-5'	76.5
jg-11	RNA 2'F-RNA	5'-GCUUGAAGUCUUUAAUUAAtt-3' 3'-GGCGAACTTCAGAAATTAATTp-5'	76.2
jg-12	2'F-ANA RNA	5'-*GCTTGAAGTCTTTAATTAATT*-3' 3'-ggCGAACUUCAGAAAUUAAUU-5'	64.7
jg-13	RNA 2'F-ANA	5'-GCUUGAAGUCUUUAAUUAAtt-3' 3'-*GGCGAACTTCAGAAATTAATT*p-5'	62.8
jg-14	2'F-ANA 2'F-RNA	5'-*GCTTGAAGTCTTTAATTAATT*-3' 3'-GGCGAACTTCAGAAATTAATTp-5'	80.1
jg-15	2'F-RNA 2'F-ANA	5'-GCTTGAAGTCTTTAATTAATT-3' 3'-*GGCGAACTTCAGAAATTAATT*p-5'	77.5

Table 5.4. siRNA strands containing mixtures of 2'F-ANA and 2'F-RNA. Legend: RNA, dna, *2'F-ANA*, 2'F-RNA.

It is true that the sense strand is usually more tolerant to chemical modifications, and the preference for these three chemistries in the sense strand is not surprising. What is somewhat surprising is that **jg-11** is more active than **jg-10**, thus *2'F-RNA is better-tolerated in the antisense than the sense strand*. We believe this is the first time a fully-modified or heavily-modified strand has been observed to be better tolerated in the antisense than the sense position.

Since 2'F-ANA and 2'F-RNA have complementary preferences for the sense and antisense strands, respectively, a duplex containing a 2'F-ANA sense strand and a 2'F-RNA antisense strand should be active as well. Indeed, synergy is observed in the case of duplex **jg-14**, which is more active than either of the duplexes **jg-11** or **jg-12** from which it is derived. On the other hand, reversing the sense/antisense combination gave **jg-15**, one of the least potent siRNAs tested in this study.

5.3.3 Binding affinity

The thermal stabilities of the duplexes were tested by heating the annealed duplexes, in physiological buffer, and measuring the change in A_{260}. Binding affinities of the modified duplexes vary widely. As expected, there is no correlation between RNAi activity and binding affinity. For example, two of the most active duplexes we tested were **jg-4** and **jg-8**, with T_m values of >90 ºC and 48.2 ºC, respectively. The most potent duplex, the fully fluorinated heteroduplex **jg-14**, had a T_m about 20 ºC higher than that that of native RNA (80.1 ºC vs 61.8 ºC).

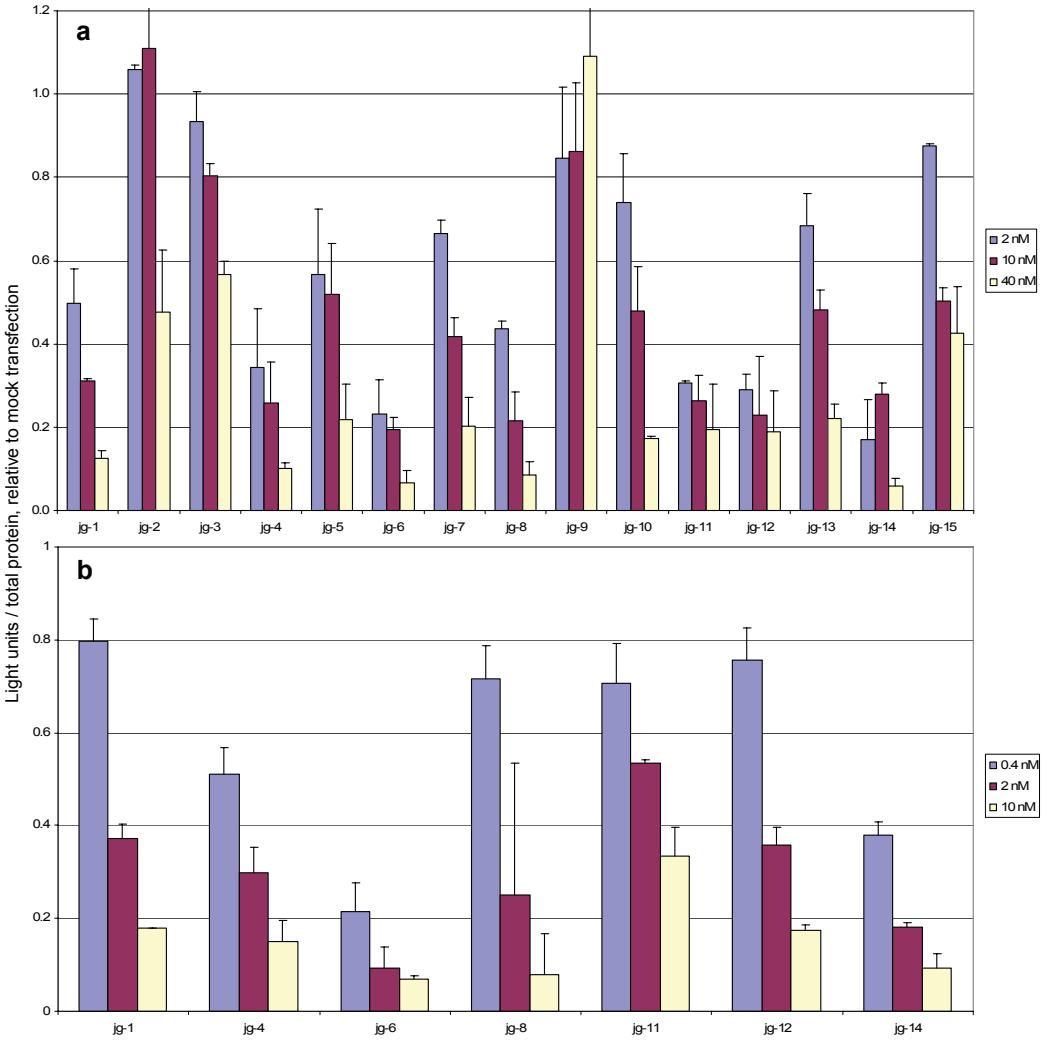

Figure 5.6. siRNA activity of 2'-fluorinated duplexes **jg-1**–**jg-15**. (a) Initial results (average of two transfections); (b) Confirmed activity of the most potent duplexes from part a, at lower concentrations (average of two transfections).

5.3.4 CD studies

The CD spectra of the modified duplexes were examined, to explore possible connections between helical structure and siRNA activity (Figure 5.7). The changes in the Cotton effects at 210–220 nm are noteworthy. Beginning with duplexes **jg-2**–**jg-5**, which have the same chemistry in both strands, it is noteworthy that for 2'F-RNA duplex **jg-4**, this band is of maximum intensity at 227 nm, which is slightly redshifted with respect to the control duplex **jg-1**

(224 nm). On the other hand, for the three duplexes containing 2'F-ANA, including the two chimeric architectures **jg-2** and **jg-3** and the all-2'F-ANA duplex **jg-5**, this band is blueshifted and reaches maximum intensity at about 220 nm. Furthermore, duplexes **jg-1** and **jg-4** feature a more strongly negative band at 210 nm. This is consistent with the degree of A-form helicity of the duplexes.[462] 2'F-RNA duplex **jg-4** also has the highest intensity for its 270 nm band, followed by native RNA duplex **jg-1**, then the 2'F-ANA-containing strands. Fully-2'F-ANA duplex **jg-5** is quite B-form in character, as evidenced by the fact that its 270 nm band is of the lowest intensity and contains a shoulder above 280 nm, and its 245 nm negative band is significantly more negative than the other duplexes.[462]

For duplexes **jg-6**–**jg-13**, a modified sense strand corresponded to higher molar ellipticity at 220 nm than was observed for the native and antisense-modified duplexes. Thus, the intensity of the 220 nm band for the various sense antisense pairs **jg-6**/**jg-7**, **jg-8**/**jg-9**, **jg-10**/**jg-11** and **jg-12**/**jg-13** was always higher for the first member of each pair. (Because sense modification led to higher potency for 3 of the 4 modified strand architectures, this higher intensity also corresponded with higher potency, with the exception of duplexes **jg-10** and **jg-11**, for which the 2'F-RNA-modified strand was better-accepted in the antisense than the sense). It is also interesting that modifying the sense strand, but not the antisense strand, with 2'F-RNA, led to a notable increase in the intensity of the Cotton effects at 270 nm.

It is not clear why modification of the sense strand seems to have a larger effect on duplex structure than antisense strand modification, for this sequence. Purine-rich strands tend to dictate duplex conformation more strongly than pyrimidine-rich strands,[462] but this sequence features a relatively equal distribution of purines in the base-paired region (9 in the sense strand, 10 in the antisense).

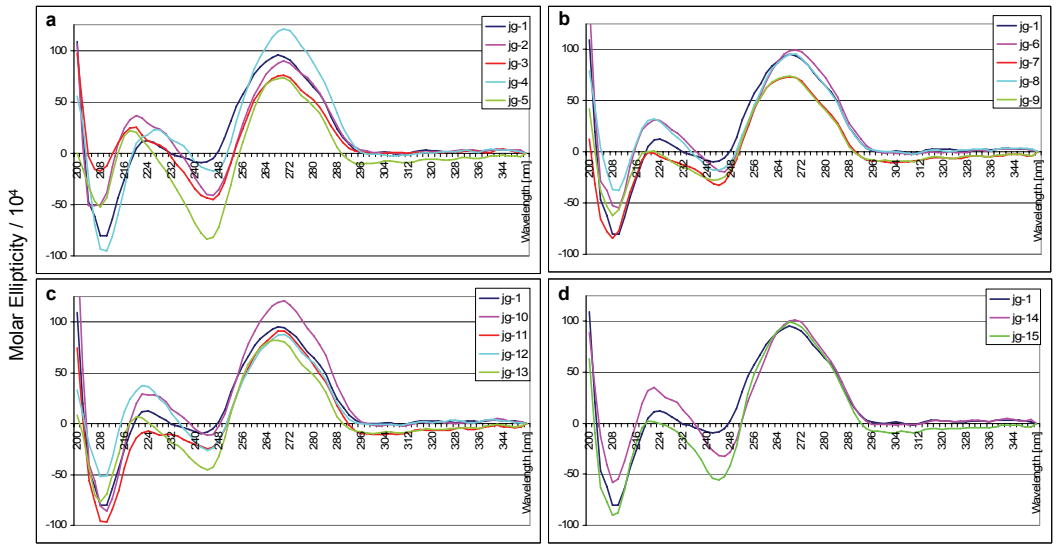

Figure 5.7. CD spectra of **jg-1**–**jg-15**. (a) **jg-1**–**jg-5**, in which both strands have the same chemistry; (b) **jg-6**–**jg-9**, in which one of the two strands is a fully-modified chimeric strand; (c) **jg-10**–**jg-13**, in which one of the two strands is a fully-modified strand of a single chemistry; and (d) fully modified heteroduplexes **jg-14**–**jg-15**. The control duplex **jg-1** is included in all spectra for comparison.

For duplexes **jg-14** and **jg-15**, in which both strands were modified, the more potent duplex **jg-14** featured higher intensity for its 220 nm band, and indeed, in the whole range from 205–250 nm. It is not clear why such a large difference is observed between these two duplexes at lower wavelengths. Duplex **jg-15** should have more A-form character since it has more strongly negative peaks at 210 nm,[462] but the higher T_m of **jg-14** implies that it has more A-form character than **jg-15**.[462] Therefore, the structure is too complicated to be explained by these simple rationalizations.

5.3.5 Sequence dependence: a second siRNA sequence

To investigate whether the potency and synergy obtained for 2'F-ANA–2'F-RNA combinations was applicable to other siRNA sequences, we tested another duplex against the same gene and cell line, this time targeting positions 515-533.[18,122] A series of fully or heavily 2'-fluorinated duplexes was designed, with the following principles in mind:

1) The preference of 2'F-ANA and 2'F-ANA–2'F-RNA chimeras for the sense strand, and of 2'F-RNA for the antisense strand;
2) The low binding affinity of 1-1 altimers of 2'F-ANA and 2'F-RNA (duplexes **jg-8** and **jg-9** had T_m values 23–26 ºC lower than the control sequence, see Table 5.4);
3) We wished to compare the activity of a fully-modified 2'F-ANA sense strand with that of the "fr-type" 2'F-ANA sense strand described in Section 5.2.5, which includes five RNA inserts near its 3'-end, when paired with a 2'F-RNA antisense strand.

Following a purine/pyrimidine pattern of modification did not seem advisable for the sense strand of this sequence, since it would have resulted in a sense strand with inappropriate strand bias: 5'-CGTACGCGGAATACTTCGATT would have significantly lower binding affinity at its 5'-end, because of the 1-1 altimer structure (see point 2 above). On the other hand, this type of chimeric strand seemed to be particularly promising for ensuring correct strand loading if designed in the reverse order, *e.g.* 5'-CGTACGCGGAATACTTCGATT (the last two nucleotides are in the overhang and are not included in the 1-1 altimer pattern).

The resulting duplexes are presented in Table 5.5. Each of two antisense strands (either RNA or 2'F-RNA) was paired with each of six modified sense strands (2'F-ANA or a 2'F-ANA–2'F-RNA chimera). The potency of these strands to induce RNAi was evaluated and the results are given in Figure 5.8.

Name	Description	Sequence
kl-ctl	Control	5'-CGUACGCGGAAUACUUCGAtt-3' 3'-ttGCAUGCGCCUUAUGAAGCU-5'
kl-1	2'F-RNA RNA	5'-CGUACGCGGAAUACUUCGAUU-3' 3'-ttGCAUGCGCCUUAUGAAGCU-5'
kl-2	2'F-ANA RNA	5'-*CGTACGCGGAATACTTCGATT*-3' 3'-ttGCAUGCGCCUUAUGAAGCU-5'
kl-3	"fr" type RNA	5'-*CGTACGCGGAATAC*UUCGA*TT*-3' 3'-ttGCAUGCGCCUUAUGAAGCU-5'
kl-4	3-3 altimer RNA	5'-*CGT*ACG*CGG*AAU*ACT*UCG*ATT*-3' 3'-ttGCAUGCGCCUUAUGAAGCU-5'
kl-5	3-3/1-1 alt RNA	5'-*CGT*ACG*CGG*AAU*AC*T*U*C*G*ATT*-3' 3'-ttGCAUGCGCCUUAUGAAGCU-5'
kl-6	1-1 altimer RNA	5'-*C*G*T*A*C*G*C*G*G*A*A*U*A*C*T*U*C*G*ATT*-3' 3'-ttGCAUGCGCCUUAUGAAGCU-5'
kl-7	2'F-RNA 2'F-RNA	5'-*G*C*T*T*G*A*A*G*T*C*T*T*T*A*A*T*T*A*A*T*T*-3' 3'-UUGCAUGCGCCUUAUGAAGCUp-5'
kl-8	2'F-ANA 2'F-RNA	5'-*CGTACGCGGAATACTTCGATT*-3' 3'-UUGCAUGCGCCUUAUGAAGCUp-5'
kl-9	"fr" type 2'F-RNA	5'-*CGTACGCGGAATAC*UUCGA*TT*-3' 3'-UUGCAUGCGCCUUAUGAAGCUp-5'
kl-10	3-3 altimer 2'F-RNA	5'-*CGT*ACG*CGG*AAU*ACT*UCG*ATT*-3' 3'-UUGCAUGCGCCUUAUGAAGCUp-5'
kl-11	3-3/1-1 alt 2'F-RNA	5'-*CGT*ACG*CGG*AAU*AC*T*U*C*G*ATT*-3' 3'-UUGCAUGCGCCUUAUGAAGCUp-5'
kl-12	1-1 altimer 2'F-RNA	5'-*C*G*T*A*C*G*C*G*G*A*A*U*A*C*T*U*C*G*ATT*-3' 3'-UUGCAUGCGCCUUAUGAAGCUp-5'

Table 5.5. Modification of a second siRNA sequence with combinations of 2'F-ANA and 2'F-RNA. Legend: RNA, dna, *2'F-ANA*, 2'F-RNA.

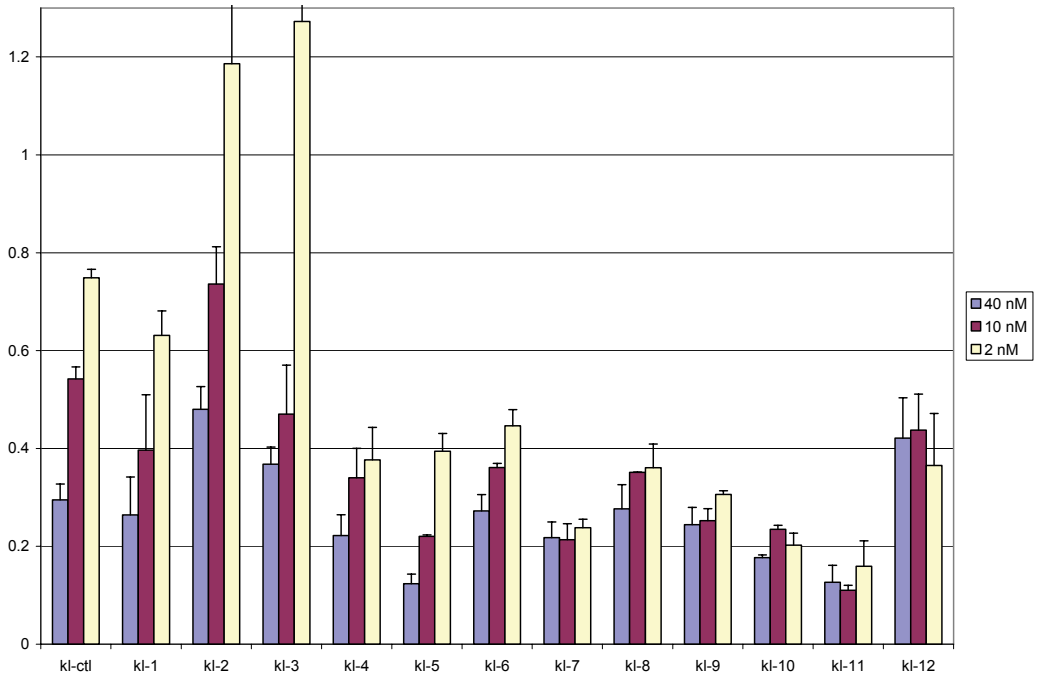

Figure 5.8. siRNA activity of 2'-fluorinated duplexes **kl-1**–**kl-12**.

Several results are clear from this set of duplexes. Perhaps the most striking is that nearly all of the duplexes are able to beat the control siRNA. Four fully-modified duplexes (**kl-7**, **kl-9**, **kl-10**, **kl-11**) and five other heavily-modified duplexes (**kl-4**, **kl-5**, **kl-6**, **kl-8**, **kl-12**) have greater potency than the control for this second sequence.

Furthermore, synergy between 2'F-RNA and 2'F-ANA is again visible. These duplexes can be thought of as belonging to two sub-series, the first with an RNA antisense strand (**kl-1**–**kl-6**) and the second with a 2'F-RNA antisense strand (**kl-7**–**kl-12**). Comparing the corresponding members of each series (**kl-1** to **kl-7**, **kl-2** to **kl-8**, etc), it is clear that all of the modified sense strands show better potency when paired to a 2'F-RNA antisense strand than an RNA antisense strand.

Taking each sub-series separately, and ranking the duplexes in order of potency, a pattern can be observed: the sense strands follow the same order, with either antisense strand. Thus, the "worst" sense strand is all 2'F-ANA (**kl-2** and **kl-8**), followed by the "fr-type" sense strand containing five RNA inserts (**kl-3** and

kl-9). We observe, however, that both **kl-8** and **kl-9** are nonetheless more potent than the control.

Use of the chimeric 2'F-ANA–2'F-RNA sense strands led to better potency, again irrespective of the antisense strand used. The best sense strand was the 3-3/1-1 altimer strand (**kl-5** and **kl-11**), suggesting that rational design for controlling thermodynamic bias does indeed improve potency. Duplex **kl-11** was unsurpassed in both potency and efficacy. It is not possible even to estimate an IC50 value for this duplex, since at 2 nM, the lowest concentration used for these transfections, the silencing is still at its maximal level.

Finally, it is worth noting that both duplexes **kl-7** and **kl-11** seem to be silencing at their maximum efficacy, since the dose response is essentially flat. The chimeric sense strand of **kl-11** thus allows higher efficacy silencing (relative luciferase level of 0.12–0.15 instead of 0.21–0.24).

5.3.6 Discussion

It is very significant that several combinations of 2'-fluorinated nucleotides lead to a duplex that is more potent than the natural siRNA. Only a handful of functional fully-modified siRNA duplexes are known in the literature, and fewer still are more potent than natural siRNA. For example, a fully-modified siRNA with significantly increased potency in an HBV mouse model consisted of a sense strand made of 2'F-RNA pyrimidines, DNA purines, and 5' and 3' inverted abasic end caps. The antisense strand was made of 2'F-RNA pyrimidines, 2'-*O*-Me purines, and a single phosphorothioate linkage at the 3'-terminus.[143] This fully modified duplex had a half-life in serum of 2-3 days, as compared with 3-5 min for the unmodified duplex.[143] This improved stability translated into higher efficacy *in vivo*. Higher potency was later obtained by including 1-3 RNA inserts at the 5'-end of the antisense strand, and this heavily-modified siRNA still had a serum half-life nearly 30 times longer than that of unmodified siRNA.[142] A duplex containing DNA overhangs, a PS-RNA antisense strand and a fully 2'-O-Me-modified sense strand was almost intact after 48 h in serum, with very little loss of potency relative to unmodified RNA.[103]

However, the most dramatic potency increase was observed for a fully modified siRNA made of a combination of 2'-*O*-Me and 2'F-RNA modified nucleotides, which was 500 times more potent than unmodified RNA.[159] This siRNA was found, unsurprisingly, to have greatly increased stability in serum.[159] While such a high degree of improvement was not observed for other sequences, this architecture was consistently of equal or greater potency and efficacy than unmodified RNA.[163]

One final example of a known fully-modified duplex is an siRNA made entirely of 2'F-RNA. In our hands, entire use of 2'F-RNA (**jg-4** and **kl-7**) gave improved potency over unmodified RNA (**jg-1** and **kl-ctl**). Another group has also reported that this architecture is functional and shows excellent nuclease resistance.[116] However, the fluorinated siRNA sequence used in their studies was less potent than the native RNA.[116] Therefore, as is often observed for chemically modified siRNA, it is not clear whether complete 2'F-RNA modification will be widely applicable or not.

The fact that 2'F-RNA modification is not universally found to be more potent should give us pause: we have found that *both* complete 2'F-RNA modification and our chimeric constructs work well for two sequences. We are therefore reminded that our constructs, too, may fall short for other targets or cell lines; further testing is essential. Nevertheless, the increase in potency and/or efficacy associated with our 2'F-RNA–2'F-ANA constructs is significantly greater than that of 2'F-RNA, for both sequences tested so far, thus our constructs may provide a more widely applicable pattern of modification.

5.3.7 Conclusions and future work, Section 5.3

2'F-ANA and 2'F-RNA can be combined in various ways in siRNA duplexes. Two types of combinations of these two modifications lead to increased potency: combining both chemistries in the sense strand, and combining an 2'F-RNA strand with a 2'F-ANA or chimeric sense strand. Examples of both of these types of synergistic combinations led to increased potency for two siRNA sequences.

Next, we plan to design duplexes against the EGFP gene. This will allow us to use fluorescence-assisted cell sorting (FACS) to examine whether the increased potency of these duplexes is related to their cellular uptake. We also plan to use a RISC-loading assay to explore the source of their increased potency. Finally, we plan to pursue clinically relevant genes using these architectures.

5.4 Experimental methods

Oligonucleotide synthesis. Standard conditions for solid-phase oligonucleotide synthesis were used for the synthesis of all oligonucleotides, at a 0.8 to 1.0 mmol scale. 4,5-Dicyanoimidazole (0.50 M in acetonitrile) or 5-ethylthiotetrazole (0.25 M in acetonitrile) were used as activators, and 0.10 M iodine in 1:2:10 pyridine:water:THF was used as oxidant (wait time during the oxidation step was 24 seconds). Phosphoramidites were prepared as 0.15 M solutions (RNA amidites) or 0.08–0.10 M solutions (DNA, 2'-fluoro and 4'-thio amidites). Coupling times were extended to 10–30 min for modified nucleotides. The oligonucleotides were treated with 3:1 ammonium hydroxide:ethanol for 16 h at 55 ºC to cleave them from the solid support and deprotect the phosphates and bases. Sequences containing ribonucleotides were concentrated and desilylated with Et_3N•3HF (100 µL) for 48 h at room temperature, or with a 3:4:6 ratio of *N*-methylpyrollidinone/triethylamine/ Et_3N•3HF (300 µL total) for 2 h at 65 ºC. Sequence purification was accomplished by anion exchange HPLC using 0–0.2 M $LiClO_4$ solution as eluent, or by preparative denaturing PAGE. Desalting was effected on Sephadex G-25 columns. Sequence purity was verified using denaturing PAGE.

5'-Phosphorylation of oligonucleotides was generally accomplished on the CPG solid support, by treating the newly-synthesized oligonucleotide with bis(2-cyanoethyl)-diisopropylaminophosphoramidite and 5-ethylthiotetrazole, followed by normal deprotection conditions. However, the antisense strand of duplex **T3p** was phosphorylated using enzymatic methods (treatment with T4 polynucleotide kinase and ATP under conditions recommended by the enzyme supplier). In all cases, ESI-MS was used to confirm the success of the phosphorylation reaction.

All 4'S-FANA-modified oligonucleotides were examined by MALDI-MS and were of the correct mass (Table 5.6). All other strands were verified by MALDI-MS or ESI-MS and were also correct (data not shown).

Name	Sequence	Calcd mass ($M-H^-$)	Found
As2	5'-UGACAU*TTTTTT*UCACGU-3'	5784.8	5785.2
T1-sense	5'-GCUUGAAGUCUUUAA*UU*AAtt-3'	6652.1	6652.7
T2-antisense	5'-UUAAUUAAAGAC*U*UCAAGCgg-3'	6690.1	6691.5
T3-antisense	5'-*UU*AAUUAAAGACUUCAAGCgg-3'	6708.2	6707.1

Table 5.6. MALDI-MS characterization of 4'S-FANA-modified strands.

SVPDE/AP digestions. Phosphodiesterase I from *Crotalus adamanteus* venom (SVPDE) was purchased from USB Corporation (Cleveland, OH). Calf intestine Alkaline Phosphatase (AP) was purchased from Amersham Biosciences (Piscataway, NJ). Enzymatic digestion assays combined 1-4 units of SVPDE and 16 units AP in 50 μL of reaction buffer (100 mM Tris-HCl, pH 8.9, 100 mM NaCl, 14 mM $MgCl_2$) along with 0.3 A_{260} units of the oligonucleotide to be digested. The assay was incubated at 37 ºC for 2-18 h, then diluted with 250 uL of water and an aliquot was injected onto a Waters Symmetry C18 5 μm 4.6×150 mm HPLC column. A gradient from 0-20% methanol in 20 mM NaH_2PO_4 buffer (pH 5.5), with a linear increase over 25 minutes, was used to elute the nucleosides. Fractions were desalted on Sep-Pak reverse phase columns, then analyzed by ESI-MS.

Thermal denaturation and CD studies. Equimolar amounts of complementary sequences were combined, dried and rediluted in pH 7.2 buffer containing 140 mM KCl, 1 mM $MgCl_2$ and 5 mM $NaHPO_4$ (1 mL). After heating to 90 °C, the samples were slowly cooled to room temperature and refrigerated overnight. They were then transferred into cold cuvettes in a Varian Cary 300 UV spectrophotometer. The change in absorbance at 260 nm was then monitored upon heating from 15 °C to 90 °C. Melting temperatures were determined as the maxima of the first derivatives (for Section 5.2) or using the baseline method, as implemented in the Cary software (for Section 5.3).

CD spectra were obtained on a Jasco J-720 or J-810 spectropolarimeter at 20 °C using samples annealed in the same buffer and under the same conditions as for the thermal denaturation studies. Spectra were baseline-corrected with respect to a blank containing the buffer but no duplex. Smoothing and adjustment for duplex concentration were effected using the Spectra-Manager program (Jasco).

RNase H assays. The RNase H assays described in this chapter (Figure 5.2) were carried out by Alex Wahba of our lab. The activity of *E. coli* RNase HI (USB Corporation, Cleveland, OH) was tested with antisense oligonucleotides under conditions recommended by the manufacturer (50 mM Tris-HCl, pH 7.5, 50 mM KCl, 25 mM $MgCl_2$, 0.25 mM EDTA, 0.25 mM DTT). The antisense and 5'-^{32}P labeled sense strands were combined in a 2:1 ratio and annealed by heating to 90 °C followed by slow cooling to room temperature. 2.5 Units (17 μg) of enzyme were incubated at 37 °C in the described buffer for 10 minutes, and 100 μL final volume reactions were initiated by addition of duplexed antisense/sense substrate to a concentration of 50 nM. Aliquots were removed at various times as indicated in Figure 5.2 and quenched by the addition of an equal volume of loading buffer (98% deionized formamide, 10 mM EDTA, 1 mg/mL bromophenol blue, and 1 mg/mL xylene cyanol), followed by heating to 95 °C for 5 min. Cleavage products were resolved on 16% denaturing PAGE and visualized by autoradiography.

Human RNase HII was expressed and purified using a slight modification of the published procedure.[468] The assays were performed analogously to that described above, using a 3:1 antisense:sense strand ratio, a buffer containing 60 mM Tris-HCl, pH 7.8, 60 mM KCl, 2.5 mM $MgCl_2$ and 2mM DTT, and enzyme concentrations of 37 and 110 nM. A gel from the assay at lower enzyme concentration is given in the Supporting Information.

siRNA assays. siRNA assays were carried out by Francis Robert of the Pelletier lab, Department of Biochemistry, McGill University. HelaX1/5 cells that stably express firefly luciferase were grown as previously described.[120] The day prior to transfection, 0.5 x 10^5 cells were plated in each well of a 24-well plate. The next day, the cells were incubated with increasing amounts of siRNAs premixed with Lipofectamine-Plus reagent (Invitrogen) using 1 μL of

lipofectamine and 4 μL of the Plus reagent per 20 pmol of siRNA (for the highest concentration tested). For the siRNA titrations, each siRNA was diluted into dilution buffer (30 mM HEPES-KOH, pH 7.4, 100 mM KOAc, 2 mM $MgOAc_2$) and the amount of Lipofectamine-Plus reagent used relative to the siRNAs remained constant. 24 hours after transfection, the cells were lysed in hypotonic lysis buffer (15 mM K_3PO_4, 1 mM EDTA, 1% Triton, 2 mM NaF, 1 mg/ml BSA, 1 mM DTT, 100 mM NaCl, 4 μg/mL aprotinin, 2 μg/mL leupeptin and 2 μg/mL pepstatin) and the firefly light units were determined using a Fluostar Optima 96-well plate bioluminescence reader (BMG Labtech) using firefly substrate as described.[469] The luciferase counts were normalized to the protein concentration of the cell lysate as determined by the DC protein assay (BioRad). Error bars represent the standard deviation of at least four transfections. Cotransfecting the siRNAs and the plasmid pCI-hRL-con expressing the *Renilla* luciferase mRNA[470] in the same cell line showed no difference in expression of this reporter, demonstrating the specificity of the RNAi effects (data not shown).

Chapter 6. First synthesis and biophysical characterization of oligonucleotides containing a 4'-selenonucleotide

6.1 Introduction

6.1.1 Biological effects of 4'-chalcogen substitution of nucleic acid derivatives

The replacement of the sugar ring (4'-) oxygen of nucleosides and nucleic acids by sulfur has been the subject of numerous studies. In the case of DNA and 2'F-ANA, sulfur substitution causes a conformational switch to northern, RNA-like, conformations that leads to interesting biological properties.[121,457] 4'-S-DNA can be amplified by PCR and can direct transcription in mammalian cells.[471] The conformational shift observed for 4'-S-FANA has made it useful for siRNA gene silencing (Section 5.2.5). 4'-S-RNA has also been applied to modification of aptamers and siRNA.[123,124,454,456] It is of interest, therefore, to examine the biological properties of the corresponding selenium congeners.

6.1.2 Use of selenium modification for MAD phasing in X-ray crystallography

Besides our interest in the biological properties of 4'-seleno nucleic acids, we note that selenium derivatization is becoming an increasingly important tool for multiwavelength anomalous dispersion (MAD) phasing, in X-ray crystallography of proteins and nucleic acids. Among the most notable selenium nucleic acid derivatives developed in recent years are the phosphoroselenoates,[472-476] 5'-seleno[477,478] and 2'-selenomethyl[479-486] modifications, and substitution at O4 of thymidine.[487] These selenium-modified nucleic acids have been used to study the crystal structure of ribozymes[488] and the hexose nucleic acid "homo-DNA"[489] as well as normal nucleic acids.[473]

It is important to develop access to new sites of heavy-atom modification for crystallography. Base modification, for example with halogens at pyrimidine position 5, can disrupt base stacking[480] and leads to photoactive species.[490] Modification of the 2'-OH may disrupt a structurally important hydrogen bond. A 4'-selenium-modified nucleotide is an attractive option. In principle, this modification could be made at any nucleotide, and because it is an internal position, there is no danger of H-bond disruption. However, selenium

modification of the 4'-position of RNA has been one of the most challenging substitutions.

6.1.3 Conformational effects of 4'-selenium substitution in nucleosides

Three groups have independently reported, very recently, the synthesis of 4'-selenonucleosides containing adenine, cytosine, thymine and uracil bases.[491-493] All three studies showed that 4'-selenoribonucleosides adopt southern, DNA-like, conformations. This fact is surprising because of the presence of an α-face 2'-OH group. It would be even more surprising if this conformational preference were manifested in the context of oligonucleotides. For example, in the case of 4'-thio-DNA, a DNA-like conformation is observed for nucleosides,[430] but an RNA-like conformation is displayed by oligonucleotides.[457] For 4'-SeRNA, a larger ring atom, together with the fact that the α-face 2'-OH group is incompatible with a B-form helix,[43] should similarly favor an RNA-like conformation. To explore this hypothesis, we have undertaken a study of the synthesis and biophysical properties of oligonucleotides containing 5-methyl-4'-selenouridine (abbreviated here for convenience as 4'-Se-rT), and report herein the first synthesis of this class of compounds.

6.2 Results and discussion

6.2.1 Phosphoramidite synthesis

The phosphoramidite derivative of 4'-Se-rT was synthesized using standard procedures, beginning from 4'-Se-rT, which was obtained from B.M. Pinto (Scheme 6.1).[491] Thus, the 5'-OH was selectively monomethoxytrityl-protected, then the 2'-OH was protected as a silyl ether using TBDMS-Cl and imidazole in DMF,[494] and the 3'-silylated byproduct was removed by chromatography. Regiochemistry of the silylation reaction was confirmed by COSY NMR, which showed a clear coupling between OH-3' and H3'. Finally, the 3'-phosphoramidite was synthesized by treatment with diisopropylamino-(2-cyanoethyl)-phosphoramidic chloride and diisopropylethylamine (DIPEA) in THF.

We observed that the 3'-*O*-phosphitylation reaction is slowed down by the presence of selenium at the 4' position. For example, significant progress of the phosphitylation reaction is indicated in THF by a precipitate of

diisopropylethylammonium chloride, and in the case of 4'-Se-rT monomer **3**, it took more than an hour to appear instead of 2-10 minutes as it does for unmodified nucleosides.

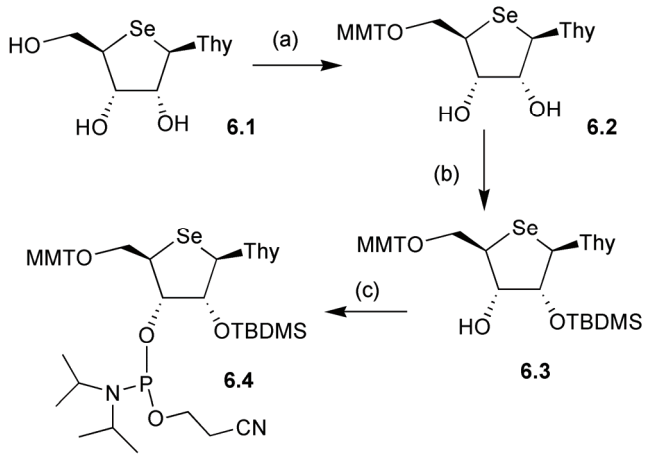

Scheme 6.1. Synthesis of the 4'-selenonucleoside phosphoramidite. Reagents and conditions: (a) MMT-Cl, DMAP, pyridine, quant.; (b) TBDMS-Cl, imidazole, DMF, 39% (c) ($^{i}Pr_2$)NP(OCH_2CH_2CN)Cl (1.8 equiv.), DIPEA (4 equiv.), 12 h, 94%; or ($^{i}Pr_2$)NP(OCH_2CH_2CN)Cl (1.0 equiv.), DIPEA (1.16 equiv.), 2-24 h, followed directly by solid phase coupling.

6.2.2 Solid-phase oligonucleotide synthesis

Either this isolated phosphoramidite or an *in situ* phosphitylation and coupling procedure could be used for solid-phase oligonucleotide synthesis, with comparable results. For the latter procedure, 5'-MMT-2'-TBDMS-4'-Se-rT (30 μmol) was combined with 1 equiv. diisopropylamino-(2-cyanoethyl)-phosphoramidic chloride and 1.16 equiv. DIPEA in acetonitrile, and this reaction mixture was stirred for 2-12 h, then injected onto a solid-phase synthesis column containing a 5'-deprotected growing oligonucleotide, in the presence of 5-ethylthiotetrazole or 4,5-dicyanoimidazole activator. After 2-4 h, the column was returned to the DNA synthesizer for oxidation and addition of subsequent nucleotides. This procedure avoids the waste associated with priming the lines of the synthesizer, as well as any loss during synthesis and purification of the phosphoramidite. Oligonucleotides were deprotected using methylamine (5 h, rt) or 3:1 NH_4OH:EtOH (48 h, rt) followed by tetrabutylammonium fluoride (1 M in THF, 24 h, rt), and were purified by HPLC, as described in detail in Section 6.4.

Coupling yields using either method were in the range of 10-40%, and the major byproduct in most of our syntheses was an oligonucleotide truncated immediately before the 4'-Se-rT insert (isolated in yields equal to or greater than those of the full-length product). The other major byproduct was of mass 260 a.m.u. greater than that of the truncated product, suggesting that the 4'-Se-rT product does break down after incorporation, at a later stage of the synthesis cycle.

Micura and coworkers observed a reversible oxidation of 2'-SeMe-modified nucleotides during solid-phase synthesis.[483-485] To avoid degradation of the selenoxide products, they included a reduction step (treatment with dithiothreitol in ethanol/water) after each iodine oxidation step. However, Huang's group did not observe such an oxidation.[482] We obtained similar results with or without a DTT reduction step of this type. A second potential source of breakdown products is the detritylation step, as observed by Carrasco *et al*. in the context of 2'-SeMe oligonucleotides.[482] Thus we kept TCA treatment steps to 100 s during the synthesis. Finally, it is conceivable that the breakdown could occur under the basic deprotection conditions, but no differences were observed between the conditions we tried.

Three self-complementary sequences were modified with 4'-Se-rT as well as dT, rT and LNA-T controls (Table 6.1). We chose to modify one RNA 15mer (**A**), one B-form DNA sequence (the Dickerson-Drew dodecamer, **B**) and one 10mer DNA sequence which often crystallizes in the A-form when modified with an RNA insert (**C**).[495] In addition to these three sequences, a non self-complementary DNA 10-mer (**D**) was also modified with a central 4'-Se-rT and the corresponding controls. Finally, single strand, duplex and hairpin controls were used for the biophysical characterization (Section 6.2.3) and their sequences are also given in Table 6.1.

Name	Sequence (5'→3')	Mass (calcd)	Mass (obs)
A1	GGA CUG AtC AGU CCA	4772.9	4773
A2	GGA CUG ATC AGU CCA	4788.9	4789
A3	GGA CUG AXC AGU CCA	4852.0	4852
A4	GGA CUG ALC AGU CCA	4800.9	4801
B1	cgc gaa ttc gcg	3646.3	3647
B2	cgc gaa Ttc gcg	3662.3	3662
B3	cgc gaa Xtc gcg	3725.3	3725
B4	cgc gaa Ltc gcg	3674.3	3675
C1	gcg tata cgc	3028.0	3028
C2	gcg taTa cgc	3044.0	3044
C3	gcg taXa cgc	3107.0	3107
C4	gcg taLa cgc	3056.0	3056
D1	cca tta tagc	2986.9	2987
D2	cca tTa tagc	3002.9	3003
D3	cca tXa tagc	3065.9	3066
D4	cca tLa tagc	3014.9	n.d.[a]
SS1	GCA GUA UGC AGC UCA	4774.8	4776
SS2	GAG CUG CAU ACU GCA	4774.8	4776
HP	GGA UCU UCG GAU CCA	4751.8	4753

Table 6.1. Sequences and MS data for 4'-Se-rT-modified and control oligonucleotides. Legend: RNA, dna; 4'-Se-rT = X; LNA-T = L. [a]not determined.

6.2.3 Biophysical studies

Thermal denaturation studies of the four sequences revealed that the thermal affinity behavior of 4'Se-RNA insert is usually between that of RNA and LNA (Tables 6.2–6.3). For A-form and hybrid duplexes (**A** and **D**:RNA), the progression in T_m was always dT < rT < 4'-Se-rT < LNA-T. As such, 4'-Se-rT inserts led to significant stabilization in these contexts.

In a B-form helix (**D**:DNA), both 4'-Se-rT and rT inserts led to slight destabilization (ΔT_m = –1.9 ºC), consistent with the hypothesis that 4'-Se-rT adopts an RNA-like conformation (Table 6.3). In contrast, LNA, whose high preorganization apparently outweighs the conformational differences, led to a moderate increase.

For sequences **B1–B3** and **C1–C3**, the low hyperchromicity of melting (%H, Table 6.2) implies that a hairpin structure is the main species present under the

conditions of our T_m experiments. Thus, the fact that sequence **B** is stabilized by RNA and 4'Se-RNA, while sequence **C** is destabilized, likely reflects the effect of these modifications on the loop structure. Much higher %H values for **B4** and **C4** suggest that an LNA insert, on the other hand, stabilizes the duplex structure of these sequences because of its very high binding affinity. We note that in both loops, 4'-Se-RNA behaves more like RNA than either DNA or LNA.

Name	Sequence (5'→3')	T_m [a]	ΔT_m [b]	%H
A1	GGACUGAtCAGUCCA	65.8	-	27.4
A2	GGACUGATCAGUCCA	68.4	+2.6	26.6
A3	GGACUGAXCAGUCCA	76.3	+10.5	15.7
A4	GGACUGALCAGUCCA	85.7	+19.9	26.3
B1	cgcgaattcgcg	53.2	-	8.0
B2	cgcgaaTtcgcg	67.6	+14.4	3.7
B3	cgcgaaXtcgcg	70.8	+17.6	4.9
B4	cgcgaaLtcgcg	63.0	+9.8	15.2
C1	gcgtatacgc	68.9	-	2.0[c]
C2	gcgtaTacgc	64.0	–4.9	4.5
C3	gcgtaXacgc	62.6	–6.3	5.3
C4	gcgtaLacgc	51.5	–17.4	16.5

Table 6.2. Sequences and T_m values of self-complementary 4'-Se-rT-modified and control oligonucleotides. Legend: RNA, dna; 4'-Se-rT = X; LNA-T = L. [a]in ºC. [b]Change in T_m relative to **A1**, **B1** and **C1**, respectively. [c]A lower temperature transition was also observed for this sample only; this value represents only the hyperchromicity of the higher temperature transition.

Name	Sequence (5'→3')	RNA Target [a]			DNA Target [b]		
		T_m [c]	ΔT_m [d]	%H	T_m [c]	ΔT_m [d]	%H
D1	ccattatagc	30.8	-	19.1	33.4	-	19.4
D2	ccatTatagc	31.2	+0.4	18.4	31.6	–1.9	15.2
D3	ccatXatagc	32.7	+1.9	14.5	31.6	–1.9	12.9
D4	ccatLatagc	38.8	+8.0	22.9	37.4	+4.0	19.7

Table 6.3. Sequences and T_m values of non-self-complementary 4'-Se-rT-modified and control oligonucleotides. Legend: as for Table 6.2. [a]Target strand: 5'-GCUAUAAUGG. [b]Target strand: 5'-gctataatgg. [c]in ºC. [d]Change in T_m relative to **D1**.

For sequence **A**, we have confirmed using native and denaturing PAGE (carried out by Alex Wahba of our laboratory) that RNA and 4'-Se-RNA stabilize the duplex structure (Figure 6.1). For both gels, single strand, duplex and hairpin controls were included, to enable the identification of the bands observed.

Under native conditions, sequences **A1**–**A3** existed entirely as duplex structures. The control sequences all appeared at the expected mobilities, with a small amount of single strand also visible for the duplex control. However, this gel does not conclusively prove that the samples are duplexes under the conditions of our biophysical experiments, since the conditions in the gel are different (including higher concentrations, which would tend to favor the bimolecular duplex structure.)

Under denaturing conditions (containing 7M urea to disrupt hydrogen bonding; the samples were also dissolved in formamide and heated to 95 ºC immediately before loading), the results were more conclusive about the relative stability of the bimolecular duplexes of **A1**–**A3**. The secondary structures formed by these species are clearly very stable, since they are visible even under denaturing conditions: the single-stranded, duplex and hairpin controls still follow the expected order, showing bands of distinct mobilities in spite of the fact that all of the strands were 15-mers. Consistent with the presence of stable secondary structures, multiple bands were observed for **A1**–**A3**, suggesting various inter- and intramolecular species. Since **A1**–**A2** had previously been purified by PAGE (cutting a single band), and **A3** by HPLC, we attribute these multiple bands to the presence of secondary structures in the gel. Further evidence for strand purity was obtained from the fact that the native gel did not show multiple bands for **A1**–**A3**. Faint bands of very high mobility observed for **A3** under denaturing conditions may perhaps, however, be attributed to truncated sequences. The most important observation from this denaturing gel, however, is that the bimolecular duplex structure is stabilized by the presence of rT or 4'-Se-rT, relative to dT. Thus, the observed changes in T_m reflect binding affinity in a double helical environment. Furthermore, 4'-Se-rT does not appear to cause distortion or strand bending that would favor a hairpin structure.

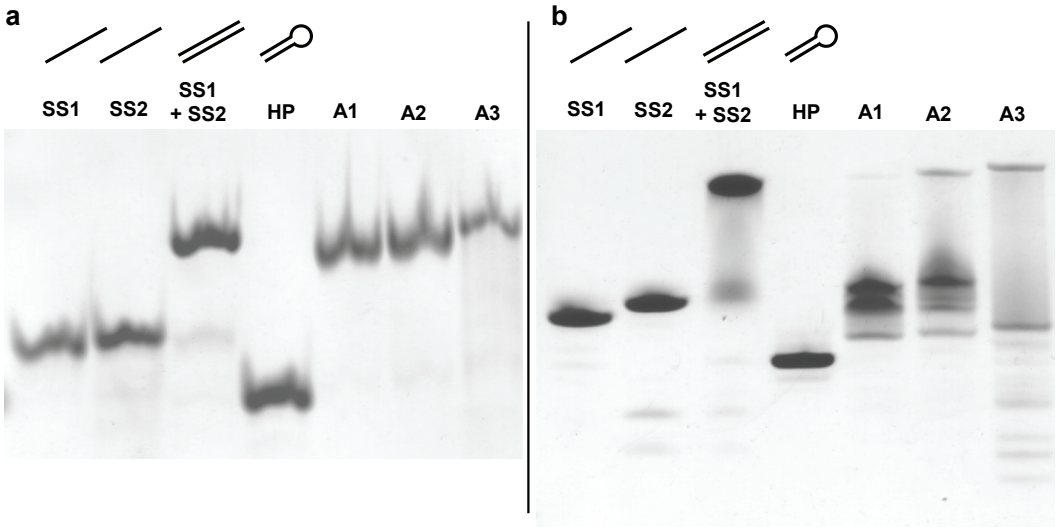

Figure 6.1. (a) 26% Native PAGE and (b) 24% denaturing PAGE demonstrating that RNA and 4'-Se-RNA stabilize the duplex structure of sequence **A**. Sequences of control strands (Table 6.1) were designed to form a single strand, or a duplex or hairpin with 3'-overhanging A units, as would be the case for sequence **A**. These control sequences follow the expected order of mobility.

Two pieces of evidence suggest that despite its increased binding affinity, 4'-Se-RNA leads to a decrease in base stacking. The first is the lower hyperchromicity of melting observed for **A3** (Table 6.2), indicating that the bases are not as well-stacked for this species. The second is the CD spectrum of sequence **A3**, which follows much the same pattern as those of **A1** and **A2**, but with lower intensity for the 265 nm band, which is often associated with base stacking (Figure 6.2). The same order of CD band intensities is observed for sequence **D**, with both RNA and DNA target strands (Figure 6.3). The differences are smaller than for sequence **A**, however, perhaps because the greater flexibility of DNA allows it to adapt to the 4'-Se-rT structure with less reduction in base stacking, and also because sequence **D** contains only one insert per duplex instead of two.

The CD spectra of sequences **B1**–**B3** and **C1**–**C3** were very similar, and somewhat larger changes were observed in the case of the LNA-modified sequences **B4** and **C4** (Figure 6.2). For sequence **C**, there were also significant differences observed for sequence **C1** in the region from 210–230 nm. Thus, once again, the conformational effect of 4'-Se-RNA is most similar to that of RNA.

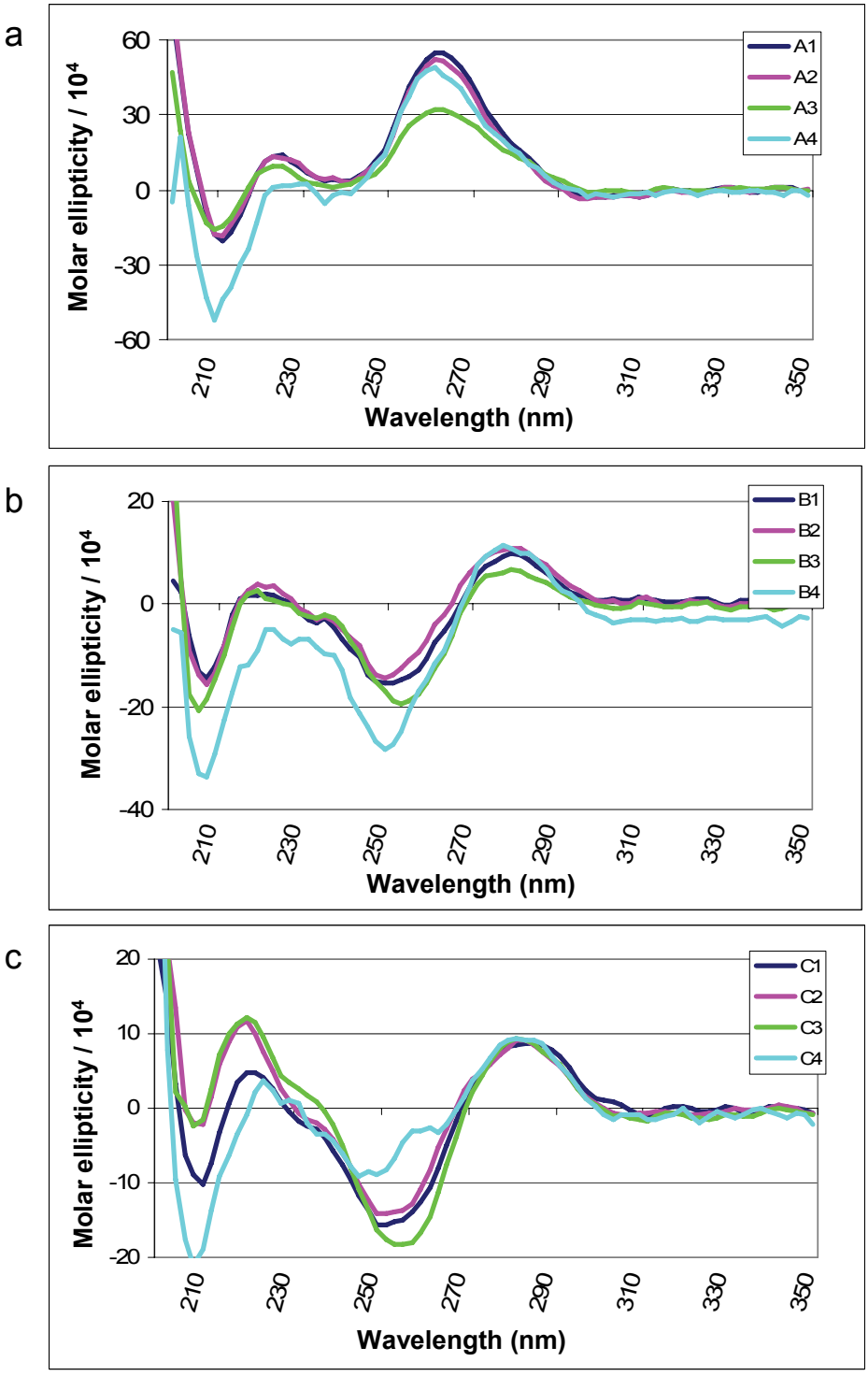

Figure 6.2. CD spectra of (a) sequences **A1**–**A4**, (b) sequences **B1**–**B4**, (c) sequences **C1**–**C4**.

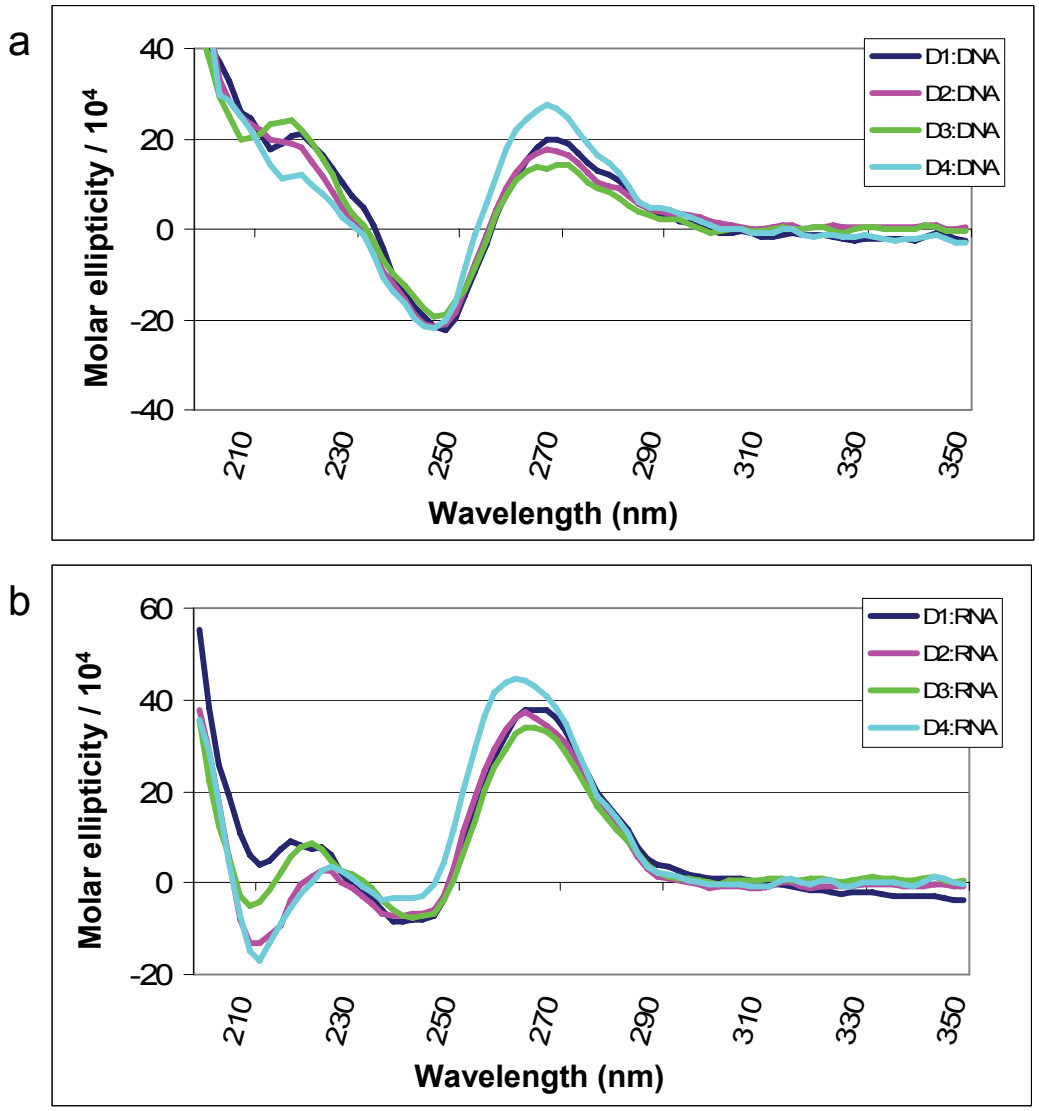

Figure 6.3. CD spectra of sequences **D1**–**D4** with (a) DNA target strand or (b) RNA target strand.

6.3 Conclusions

The first oligonucleotides containing a 4'-selenoribonucleotide have been synthesized and characterized. In contrast to the DNA-like conformation observed for 4'-Se-rT nucleosides, a 4'-Se-rT insert in an oligonucleotide behaved more like RNA than DNA, both in terms of its thermal binding affinity and its effect on hairpin loop structure. 4'-Se-rT modification of A-RNA and hybrid duplexes led to increased binding affinity. Paradoxically, it also caused base destacking.

Studies on the use of 4'-Se-RNA modifications in the phasing of X-ray crystallographic data, which will also allow confirmation of the RNA-like structure of 4'-Se-RNA, are underway.

6.4 Experimental methods

6.4.1 Solution-phase synthesis and characterization

5-Methyl-5'-*O*-monomethoxytrityl-4'-selenouridine (6.2). Compound **6.1** (215 mg, 0.67 mmol, which was made by B.M. Pinto and colleagues[491]) and 4-(dimethylamino)pyridine (DMAP, 82 mg, 0.67 mmol) were placed in a round-bottomed flask and coevaporated with dry pyridine (2 × 5 mL). Another aliquot of pyridine (10 mL) was then added, followed by monomethoxytrityl chloride (309 mg, 1.0 mmol, 1.5 equiv.) About half the solvent was removed on a rotary evaporator with gentle warming, then the reaction was stirred at room temperature for 24 h. At this point more monomethoxytrityl chloride (0.2 equiv) was added and the reaction was allowed to stir overnight, at which point TLC indicated that the reaction had reached completion. Methanol (1 mL) was added and most of the solvent was removed under vacuum. The viscous residue was dissolved in CH_2Cl_2 (50 mL) and extracted with 5% aq. $NaHCO_3$ (2 × 50 mL). The organic layer was dried on $MgSO_4$ and concentrated to yield a yellowish foam. This foam was purified on a column of silica that had been neutralized by pre-treatment with 1% triethylamine in CH_2Cl_2, using mixtures of CH_2Cl_2 and methanol, to give **6.2** as a white foam in quantitative yield. ^{1}H NMR (400.12 MHz, acetone-d6), δ 7.55-6.91 (m, 15H, aromatics of MMTr and H-6), 6.31 (d, 1H, $J_{1'-2'}$ = 6.8 Hz, H-1'), 4.33 (m, 2H, overlapping signals of H-2' and H-3'), 3.80 (s, 3H, OMe), 3.71 (ddd, 1H, $J_{3'-4'}$ = 2.7 Hz, $J_{4'-5'}$ = $J_{4'-5''}$ = 6.8 Hz, H4'), 3.57 (m, 1H, H5'), 3.50 (m, 1H, H5''), 1.73 (s, 3H, Me-5). ESI-HRMS calcd for $C_{30}H_{30}N_2O_6Se+Na^+$, 617.1161, found, 617.1155.

2'-*O*-*tert*-Butyldimethylsilyl-5-methyl-5'-*O*-monomethoxytrityl-4'-selenouridine (6.3). In a 5-mL round-bottomed flask, compound **6.2** (397 mg, 0.67 mmol) was kept under vacuum for several days, then dissolved in DMF (3.5 mL). Imidazole (118 mg, 1.7 mmol, 2.6 equiv.) and TBDMS-Cl (131 mg, 0.87 mmol, 1.3 equiv.) were added together with stirring, then the flask was capped

with a septum and flushed with nitrogen. TLC indicated that the reaction was complete after 25 h, and so it was poured into CH_2Cl_2 (100 mL) and extracted with 5% aq. $NaHCO_3$ (100 mL). The organic layer was dried on $MgSO_4$ and concentrated, and the residue was purified on a column of neutralized silica using mixtures of CH_2Cl_2 and diethyl ether. The desired 2'-silyl isomer eluted first and was evaporated to a white foam (150 mg, 32%). ^{1}H NMR (400.12 MHz, acetone-d6), δ 10.02 (s, 1H, N-H), 7.66 (q, 1H, $J_{Me\text{-}6}$ = 0.8 Hz, H-6), 7.5-6.9 (m, 14H, aromatics of MMTr), 6.32 (d, 1H, $J_{1'\text{-}2'}$ = 6.4 Hz, H-1'), 4.40 (dd, 1H, $J_{2'\text{-}3'}$ = 3.2 Hz, H-2'), 4.28 (ddd, 1H, $J_{3'\text{-}4'}$ ≈3 Hz , $J_{3'\text{-}OH}$ = 4.0 Hz, H-3'), 4.12 (d, 1H, OH-3'), 3.81 (s, 3H, OMe), 3.75 (m, 1H, H-4'), 3.59 (m, 1H, H-5'), 3.52 (m, 1H, H-5''), 1.72 (d, 3H, Me-5). Assignments were confirmed by a COSY experiment, and the 2'-position of the silyl group was confirmed since the hydroxyl proton couples to H3'. ESI-HRMS calcd for $C_{36}H_{44}N_2O_6SiSe+Na^+$, 731.2026, found, 731.2017. Another 34 mg (7%) of **6.3** was obtained by treating the undesired 3'-silyl product with pyridine/water (9:1) and repurifying after the 2'/3' isomeric mixture had reached equilibrium.

2'-*O*-*tert*-Butyldimethylsilyl-3-(*N,N*-diisopropyl-*O*-(2-cyanoethyl)-phosphoramidic)-5-methyl-5'-*O*-monomethoxytrityl-4'-selenouridine (6.4). Compound **6.3** (166 mg, 0.235 mmol) was azeotroped with several 2-3-mL portions of dry pyridine in a 10-mL round-bottomed flask. Dry THF (2 mL) and diisopropylethylamine (DIPEA, 120 µL, 0.70 mmol, 3 equiv.) were added with stirring, followed by diisopropylamino-(2-cyanoethyl)-phosphoramidic chloride (68 µL, 0.30 mmol, 1.3 equiv.) After 30 minutes, TLC indicated progress of the reaction, but no precipitate had formed. However, after 9 h, a precipitate of diisopropylethylammonium chloride had formed. A further 1 equiv. DIPEA and 0.5 equiv. phosphoramidic chloride were added after 11 h, and after 2 h further reaction the mixture was diluted with $CHCl_3$ (5 mL) and purified on a column of neutralized silica using chloroform as eluent. Evaporation from several portions of diethyl ether gave compound **6.4** as a semi-stable white foam (200 mg, 94%). TLC using 15% acetone in $CHCl_3$ allowed resolution of both phosphoramidite diastereomers (Rf 0.52 and 0.45, respectively; starting material Rf 0.39.) ^{31}P

NMR (81.0 MHz, acetone-d6), δ 151.3, 150.4; a small amount of the H-phosphonate resulting from hydrolysis of the phosphoramidic chloride was also visible at 14.7 ppm. ESI-HRMS calcd for $C_{45}H_{61}N_4O_5SiPSe+Na^+$, 931.3105, found, 931.3088.

6.4.2 *In situ* phosphitylation and solid phase coupling

To a nitrogen-filled vial containing anhydrous acetonitrile (2 mL) were added DIPEA (30.4 μL, 175 μmol) and diisopropylamino-(2-cyanoethyl)-phosphoramidic chloride (33.0 μL, 148 μmol). An aliquot of this solution was removed and tested on a readily available nucleoside, to verify its reactivity. Meanwhile, compound **6.3** was dissolved in benzene, and the solution was frozen and sublimed to dryness, to yield a dry, white powder. To a portion of this powder (21.0 mg, 29.7 μmol) was added 0.40 mL of the reaction solution (thus 1.0 equiv. (^{i}Pr$_2$)NP(OCH$_2$CH$_2$CN)Cl and 1.16 equiv. DIPEA). The resulting solution was allowed to react for 2–12 h.

Meanwhile, the portion of the oligonucleotide 3' to the SeRNA insert was prepared on solid phase, using standard conditions. After the final detritylation, the column was brought into a glove bag, and was fitted with two 1-mL syringes, one on each end of the column. In the first syringe was the phosphoramidite reaction solution, and in the other was 300 μL of ethylthiotetrazole activator solution (0.25 M ETT in acetonitrile, 75 μmol, 2.5 equiv.) These syringes were gently flushed back and forth to ensure that all of the reagents were able to contact the CPG solid support.

After 4 h, the column was returned to the DNA synthesizer for oxidation and subsequent strand synthesis. A copy of the synthesis cycle, as used on our ABI 3400 DNA synthesizer, is provided in the supporting information. This cycle was used with a 220 s detritylation step (3% trichloroacetic acid in CH_2Cl_2) for the 4'-selenonucleotide only, after which the detritylation was shortened to 110 s for the remainder of the oligonucleotide. (Use of the MMT protecting group on the 4'-Se-rT phosphoramidite itself provides two advantages: greater stability during solution-phase synthesis and silica gel purifications, and greater stability to the 5-ethylthiotetrazole (ETT) activator used in the extended coupling step used for

the SeRNA insert. The latter advantage allowed us to extend the 4'-Se-RNA coupling time without fear of multiple 4'-SeRNA incorporations due to premature detritylation during this extended coupling step.[496]) The coupling was followed by a capping step, then oxidation (0.02 M iodine in 1:2:10 pyridine:water:THF; 12 s delivery followed by 56 s wait time). The column was then washed with acetonitrile and treated with a DTT solution in the manner of Micura and coworkers (100 mM DTT in 2:3 EtOH:H_2O, 2 min wait time). Another acetonitrile wash and a second capping step finished the cycle.

After completion of the synthesis, the solid support was treated with DTT (150 mM in ethanol/water) for ~1h. Cleavage from the solid support and deprotection of the nucleobases was then effected by adding ~40% methylamine (1.2 mL in 1:1 ethanol/water) and leaving at room temperature for 6 h. The solution was then decanted from the solid support and evaporated to dryness. The silyl groups were removed by reaction with 1 M TBAF in THF (1 mL) for 24 h, then water was added, most of the THF was removed in a SpeedVac, and the mixture was desalted on Sephadex. Sequences were dried down and purified by RP-HPLC using 100 mM triethylammonium acetate buffer (pH 7.0).

Sequences not containing selenium were synthesized using standard conditions and purified by 24% PAGE. Sequences **SS1**, **SS2**, **HP** and sequences containing LNA inserts were purchased from the University Core DNA Services, University of Calgary, and were purified by PAGE.

6.4.3 Biophysical methods

0.20 ODU of each sequence was dried down and resuspended in 1 mL of a physiological buffer (140 mM KCl, 1 mM MgCl2 and 5 mM HaHPO4, pH 7.2). After heating to 95 ºC, the samples were slowly cooled to room temperature. Thermal denaturation experiments were carried out by monitoring the change in A_{260} using a Cary 300 UV spectrophotometer. Melting temperatures were determined by the baseline method.

CD spectra were obtained using a Jasco J-810 spectropolarimeter at 10 ºC using the same samples, after reannealing. Three spectra were obtained and averaged, then baseline-corrected with respect to a blank containing the buffer only.

Smoothing and conversion to molar ellipticity were effected using the Jasco software.

6.4.4 Analytical PAGE

Analytical gels were carried out by Alex Wahba, of our laboratory. Gels were run in TBE buffer using previously described conditions.[497] Approximately 0.2 ODU of each sample were dissolved in annealing buffer containing 10 mM sodium phosphate (pH 7.0) and 50 mM NaCl. Samples were then heated at 95 °C, allowed to cool to room temperature over 2 h, and stored at 4°C overnight.

For denaturing gels, 10 µl of each sample was added to an equal volume of loading buffer (98:2 formamide:10X TBE) and heated for 5 minutes at 95 °C, then immediately loaded on a 24 % polyacrylamide gel containing 7.5 M urea. Denaturing gels were run at 500V for 2.5 hours. Native gel samples were loaded in 25% glycerol on a 26 % polyacrylamide gel run at 100 V for 24 hours at 4 °C. Bands were visualized by UV shadowing and Stains-All (Sigma-Aldrich).

7. Contributions to knowledge

7.1 Summary of contributions to knowledge

7.1.1 Structure and hydration of 2'F-ANA and ANA

NMR/MD and osmotic stressing were used to compare the structure and hydration of 10-bp 2'F-ANA•RNA, ANA•RNA and DNA•RNA duplexes. The 2'F-ANA and ANA strands both featured sugars that pucker in the east (O4'-*endo*) conformation, as previously observed for hairpin structures containing hybrid stems. Osmotic stressing suggested that the 2'F-ANA•RNA duplex liberated fewer molecules of water upon melting than did ANA•RNA, which may give the former an entropic advantage that contributes to its far greater thermal stability.

7.1.2 Hydrolytic stability of 2'F-ANA

The stability of 2'F-ANA to acid-mediated hydrolysis was compared to that of DNA and RNA. Several phosphodiester (PO) or phosphorothioate (PS) 2'F-ANA sequences were incubated at pH ~1.2, and virtually no cleavage was observed after 2 days. In contrast, rapid degradation was observed for DNA ($t_{1/2}$ = minutes) and RNA ($t_{1/2}$ = hours (PO) or days (PS)).

The nuclease-catalyzed hydrolysis of 2'F-ANA was also explored in detail. One diastereomer of the PS-2'F-ANA linkage was much more vulnerable to enzymatic cleavage than the other, which is parallel to the properties observed for PS-DNA. We also show that the nuclease stability induced by 2'F-ANA depends on the oligonucleotide sequence.

7.1.3 Novel application of 2'F-ANA to an exciplex diagnostic system

In the post-genomic era, nucleic acid biosensors will become increasingly important as medical diagnostic tools. We have carried out the first application of 2'F-ANA to an exciplex-based nucleic acid biosensor system. Use of 2'F-ANA allows a lower trifluoroethanol content than is required for DNA-based exciplex systems.

7.1.4 Development of a 4'-thio analogue of 2'F-ANA

An improved synthesis of 2'-deoxy-2'-fluoro-5-methyl-4'-thioarabinouridine (4'S-FMAU) is described. Participation of the 3'-*O*-benzoyl protecting group in the thiosugar precursor influenced the stereochemistry of the *N*-glycosylation

reaction in nonpolar solvents, permitting a higher β:α ratio than previously observed for similar Lewis acid-catalyzed glycosylations. The nucleoside adopted a predominantly northern conformation, in contrast to 2'-deoxy-2'-fluoro-5-methylarabinouridine (FMAU), which adopts a dominantly southeast conformation.

The synthesis of oligonucleotides containing 2'-deoxy-2'-fluoro-4'-thioarabinonucleotides is then described. 18-mer antisense oligonucleotides (AON) containing 4'S-FMAU, unlike those containing FMAU, were unable to elicit *E. coli* or human RNase H activity, thus corroborating the hypothesis that RNase H prefers duplexes containing oligonucleotides that can adopt eastern (O4'-*endo*) conformations in the antisense strand. The duplex structure and stability of these oligonucleotides was also investigated via circular dichroism (CD) and UV binding studies. Replacement of the 4'-oxygen by a sulfur atom resulted in a marked decrease in melting temperature of AON•RNA as well as AON•DNA duplexes. 2'-Deoxy-2'-fluoro-4'-thioarabinouridine (4'S-FAU) was incorporated into siRNA and the resulting siRNA molecules were able to trigger RNA interference with good efficiency. Positional effects were explored, and synergy with 2'F-ANA was demonstrated.

7.1.5 Combination of 2'F-ANA and 2'F-RNA in siRNA

The synergy observed between 2'F-ANA and 4'S-FANA inspired us to combine other northern nucleosides with 2'F-ANA. We made the exciting discovery that combination of 2'F-RNA and 2'F-ANA leads to fully modified siRNA duplexes that are more potent than the control siRNAs. The most potent design contains a chimeric 2'F-ANA–2'F-RNA sense strands paired with a 2'F-RNA antisense strand. This is one of only a few known chemistries allowing fully modified siRNAs with increased potency. Several related patterns of chemical modification were used to modify two siRNA sequences targeting firefly luciferase.

7.1.6 Development of a 4'-seleno analogue of RNA

Continuing in the theme of 4'-chalcogen-modified nucleic acids, Chapter 6 describes the first examples of oligonucleotides containing a 4'-selenoribonucleotide. The conformational behavior of 4'-selenoribonucleotides appears to be quite different in the context of oligonucleotides than as free

nucleotides. This project makes a valuable contribution to the field of modified nucleic acids and their conformational behavior, and could also have useful applications in MAD phasing for X-ray crystallography.

7.2 Papers, patents and conference presentations

7.2.1 Papers published

Jonathan K. Watts, Blair D. Johnston, Kumarasamy Jayakanthan, Alexander S. Wahba, B. Mario Pinto and Masad J. Damha; "Synthesis and biophysical characterization of oligonucleotides containing a 4'-selenonucleotide," *Journal of the American Chemical Society*, in press, DOI: 10.1021/ja802205u.

Jonathan K. Watts, Glen F. Deleavey and Masad J. Damha; "Chemically modified siRNA: Tools and applications," *Drug Discovery Today*, in press.

Jonathan K. Watts and Masad J. Damha; "2'F-Arabinonucleic acids (2'F-ANA): History, properties and new frontiers," *Canadian Journal of Chemistry*, **86**: 641-656, 2008.

Jonathan K. Watts, Niloufar Choubdar, Kashinath Sadalapure, Francis Robert, Alexander S. Wahba, Jerry Pelletier, B. Mario Pinto and Masad J. Damha; "2'-Fluoro-4'-thioarabino-modified oligonucleotides: Conformational switches linked to siRNA activity," *Nucleic Acids Research*, **35**: 1441-1451, 2007.

Melissa L. Trapp, Jonathan K. Watts, Noham Weinberg, and B. Mario Pinto; "Component analysis of the X-C-Y anomeric effect (X = O, S; Y = F, OMe, NHMe) by DFT molecular orbital calculations and natural bond orbital analysis," *Canadian Journal of Chemistry*, **84**: 692-701, 2006.

Jonathan K. Watts, Kashinath Sadalapure, Niloufar Choubdar, B. Mario Pinto and Masad J. Damha; "Synthesis and conformational analysis of 2'-fluoro-5-methyl-

4'-thioarabinouridine (4'S-FMAU),” *Journal of Organic Chemistry*, **71**: 921-925, 2006.

7.2.2 Manuscripts in preparation

Nerea Martin-Pintado, Jonathan K. Watts, Jeremy Schwartzentruber, Carlos Gonzalez and Masad J. Damha; “Structure, dynamics and hydration of 2'F-ANA•RNA and ANA•RNA hybrid duplexes by NMR/MD and osmotic stressing.”

Jonathan K. Watts, Adam Katolik, Julia Viladoms and Masad J. Damha; “Stability of 2'F-ANA to acidic and enzymatic hydrolysis.”

Stefanie Lang, Jonathan K. Watts, Elena Bichenkova, Masad Damha and Kenneth Douglas, “Application of 2'F-ANA and 2'F-RNA in a split-probe exciplex system.”

Alexander S. Wahba, Jonathan K. Watts and Masad J. Damha; “One pot phosphitylation and solid phase coupling protocols for introduction of special moieties into oligonucleotides.”

Jonathan K. Watts, Francis Robert, Glen F. Deleavey, Jerry Pelletier and Masad J. Damha, “Synergy between 2'F-ANA and 2'F-RNA in fully modified siRNA duplexes with very high potency.”

7.2.3 Patents

M.J. Damha, J.K. Watts and B.M Pinto, "Thioarabinonucleotide-Containing Oligonucleotides, Compounds and Methods for Their Preparation and Uses Thereof," International Patent Application PCT/CA2006/002035, filed December 14, 2006 (Priority date US 60/750,838, December 16, 2005).

M.J. Damha and J.K. Watts, "Oligonucleotide duplexes and uses thereof," US Provisional Patent 61/059,186, filed June 5, 2008.

7.2.4 Conference presentations

The presenting author is underlined

"RNA targeting with 2'-fluoro-2'-deoxyarabinonucleic acids (2'F-ANA)," M.J. Damha, J.K. Watts, N. Bayó, J. Lackey, G. Deleavey, N. Wazen, M. El-Sabahy, and J.C. Leroux, presented (oral) at the 235th American Chemical Society National Meeting (New Orleans, LA, April 2008).

"Modified siRNAs containing 2'-fluorinated nucleotides," J. Watts, F. Robert, A. Kalota, J. Pelletier, J.M. García Fernández, J. Defaye, A.M. Gewirtz and M.J. Damha, presented (oral) at the 234th American Chemical Society National Meeting (Boston, MA, August 2007).

"Impact of 2'-F vs 2'-OH on the stability of arabinonucleic acid/RNA hybrids. Why such a large difference?" J. Watts and M.J. Damha, presented (oral and poster) at the Gordon Research Conference on Nucleosides, Nucleotides and Oligonucleotides (Newport, RI, July 2007).

"Synthesis and conformational analysis of 2'-fluoro-5-methyl-4'-thioarabinouridine (4'S-FMAU), and biophysical properties of the corresponding oligonucleotides," J. Watts, K. Sadalapure, N. Choubdar, M.J. Damha, B.M. Pinto, presented (poster) at the 89th Canadian Chemistry Conference (Halifax, NS,

May 2006), and at the XXIII[rd] International Carbohydrate Symposium (Whistler, BC, July 2006).

"Analyse des composants de l'effet anomère X-C-Y (X=O, S; Y=F, OMe, NHMe) par calculs DFT des orbitales moléculaires et analyses des orbitales naturelles de liaisons (« NBO »)," J. Watts, M.L. Trapp, N. Weinberg and B.M. Pinto, presented (oral) at the 74[th] conference of the Association Francophone pour le Savoir (Montreal, QC, May 2006).

"Component analysis of the X-C-Y anomeric effect (X=O, S; Y=F, OMe, NHMe) by DFT molecular orbital calculations and NBO analysis," J. Watts, M.L. Trapp, N. Weinberg and B.M. Pinto, presented (oral) at the 231[st] American Chemical Society National Meeting (Atlanta, GA, March 2006), at the 89[th] Canadian Chemistry Conference (Halifax, NS, May 2006), and at the XXIII[rd] International Carbohydrate Symposium (Whistler, BC, July 2006).

"Arabinose-modified siRNAs ('siANA and siFANA')," M.J. Damha, J. Watts, N. Ferrari, T. Dowler, D. Bergeron, A.-L. Tedeschi, L. Paquet, P. Renzi, presented (oral) at the 231[st] American Chemical Society National Meeting (Atlanta, GA, March 2006).

"Synthesis and conformational analysis of 2'-fluoro-5-methyl-4'-thioarabinouridine (4'S-FMAU)," J. Watts, K. Sadalapure, N. Choubdar, M.J. Damha, B.M. Pinto, presented (oral) at the 231[st] American Chemical Society National Meeting (Atlanta, GA, March 2006).

"Conformational analysis of 2'-fluoroarabino- and 2'-fluoro-4'-thioarabinonucleosides," J. Watts, K. Sadalapure, N. Choubdar, B.M. Pinto and M.J. Damha, presented (oral) at the 87[th] Canadian Chemistry Conference (London, ON, May 2004).

References and Endnotes

1 Couzin, J. *Science* **2002**, *298*, 2296-2297.

2 Kruger, K.; Grabowski, P. J.; Zaug, A. J.; Sands, J.; Gottschling, D. E.; Cech, T. R. *Cell* **1982**, *31*, 147-157.

3 Zaug, A. J.; Grabowski, P. J.; Cech, T. R. *Nature* **1983**, *301*, 578-583.

4 Zaug, A. J.; Been, M. D.; Cech, T. R. *Nature* **1986**, *324*, 429-433.

5 Guerrier-Takada, C.; Gardiner, K.; Marsh, T.; Pace, N.; Altman, S. *Cell* **1983**, *35*, 849-857.

6 Guerrier-Takada, C.; Altman, S. *Science* **1984**, *223*, 285-286.

7 Symons, R. H. *Annu. Rev. Biochem.* **1992**, *61*, 641-671.

8 Li, Y.; Breaker, R. R. *Curr. Opin. Struct. Biol.* **1999**, *9*, 315-323.

9 Cech, T. R. *Science* **2000**, *289*, 878-879.

10 Ban, N.; Nissen, P.; Hansen, J.; Moore, P. B.; Steitz, T. A. *Science* **2000**, *289*, 905-920.

11 Johnston, W. K.; Unrau, P. J.; Lawrence, M. S.; Glasner, M. E.; Bartel, D. P. *Science* **2001**, *292*, 1319-1325.

12 Mandal, M.; Breaker, R. R. *Nat. Rev. Mol. Cell Biol.* **2004**, *5*, 451-463.

13 Modrek, B.; Lee, C. *Nat. Genet.* **2002**, *30*, 13-19.

14 Schmucker, D.; Clemens, J. C.; Shu, H.; Worby, C. A.; Xiao, J.; Muda, M.; Dixon, J. E.; Zipursky, S. L. *Cell* **2000**, *101*, 671-684.

15 Fire, A.; Xu, S.; Montgomery, M. K.; Kostas, S. A.; Driver, S. E.; Mello, C. C. *Nature* **1998**, *391*, 806-811.

16 Zamore, P. D.; Tuschl, T.; Sharp, P. A.; Bartel, D. P. *Cell* **2000**, *101*, 25-33.

17 Elbashir, S. M.; Lendeckel, W.; Tuschl, T. *Genes Dev.* **2001**, *15*, 188-200.

18 Elbashir, S. M.; Harborth, J.; Lendeckel, W.; Yalcin, A.; Weber, K.; Tuschl, T. *Nature* **2001**, *411*, 494-498.

19 Lee, R. C.; Feinbaum, R. L.; Ambros, V. *Cell* **1993**, *75*, 843-854.

20 Wightman, B.; Ha, I.; Ruvkun, G. *Cell* **1993**, *75*, 855-862.

21 Lewis, B. P.; Burge, C. B.; Bartel, D. P. *Cell* **2005**, *120*, 15-20.

22 Lim, L. P.; Lau, N. C.; Garrett-Engele, P.; Grimson, A.; Schelter, J. M.; Castle, J.; Bartel, D. P.; Linsley, P. S.; Johnson, J. M. *Nature* **2005**, *433*, 769-773.

23 Rana, T. M. *Nat. Rev. Mol. Cell Biol.* **2007**, *8*, 23-36.

24 Bartel, D. P. *Cell* **2004**, *116*, 281-297.

25 Wu, L. G.; Fan, J. H.; Belasco, J. G. *Proc. Natl. Acad. Sci. U. S. A.* **2006**, *103*, 4034-4039.

26 Girard, A.; Sachidanandam, R.; Hannon, G. J.; Carmell, M. A. *Nature* **2006**, *442*, 199-202.

27 Aravin, A.; Gaidatzis, D.; Pfeffer, S.; Lagos-Quintana, M.; Landgraf, P.; Iovino, N.; Morris, P.; Brownstein, M. J.; Kuramochi-Miyagawa, S.; Nakano, T.; Chien, M. C.; Russo, J. J.; Ju, J. Y.; Sheridan, R.; Sander, C.; Zavolan, M.; Tuschl, T. *Nature* **2006**, *442*, 203-207.

28 Lau, N. C.; Seto, A. G.; Kim, J.; Kuramochi-Miyagawa, S.; Nakano, T.; Bartel, D. P.; Kingston, R. E. *Science* **2006**, *313*, 363-367.

29 Janowski, B. A.; Younger, S. T.; Hardy, D. B.; Ram, R.; Huffman, K. E.; Corey, D. R. *Nat. Chem. Biol.* **2007**, *3*, 166-173.

30 Janowski, B. A.; Huffman, K. E.; Schwartz, J. C.; Ram, R.; Nordsell, R.; Shames, D. S.; Minna, J. D.; Corey, D. R. *Nat. Struct. Mol. Biol.* **2006**, *13*, 787-792.

31 Janowski, B. A.; Huffman, K. E.; Schwartz, J. C.; Ram, R.; Hardy, D.; Shames, D. S.; Minna, J. D.; Corey, D. R. *Nat. Chem. Biol.* **2005**, *1*, 216-222.

32 Morris, K. V.; Chan, S. W. L.; Jacobsen, S. E.; Looney, D. J. *Science* **2004**, *305*, 1289-1292.

33 Li, L.-C.; Okino, S. T.; Zhao, H.; Pookot, D.; Place, R. F.; Urakami, S.; Enokida, H.; Dahiya, R. *Proc. Natl. Acad. Sci. USA* **2006**, *103*, 17337-17342.

34 Han, J.; Kim, D.; Morris, K. V. *Proc. Natl. Acad. Sci. USA* **2007**, *104*, 12422-12427.

35 Kapranov, P.; Cheng, J.; Dike, S.; Nix, D. A.; Duttagupta, R.; Willingham, A. T.; Stadler, P. F.; Hertel, J.; Hackermuller, J.; Hofacker, I. L.; Bell, I.; Cheung, E.; Drenkow, J.; Dumais, E.; Patel, S.; Helt, G.; Ganesh, M.; Ghosh, S.; Piccolboni, A.; Sementchenko, V.; Tammana, H.; Gingeras, T. R. *Science* **2007**, *316*, 1484-1488.

36 RIKEN Genome Exploration Research Group and Genome Science Group (Genome Network Project Core Group) and the FANTOM Consortium; Katayama, S.; Tomaru, Y.; Kasukawa, T.; Waki, K.; Nakanishi, M.; Nakamura, M.; Nishida, H.; Yap, C. C.; Suzuki, M.; Kawai, J.; Suzuki, H.; Carninci, P.; Hayashizaki, Y.; Wells, C.; Frith, M.; Ravasi, T.; Pang, K. C.; Hallinan, J.; Mattick, J.; Hume, D. A.; Lipovich, L.; Batalov, S.; Engstrom,

P. G.; Mizuno, Y.; Faghihi, M. A.; Sandelin, A.; Chalk, A. M.; Mottagui-Tabar, S.; Liang, Z.; Lenhard, B.; Wahlestedt, C. *Science* **2005**, *309*, 1564-1566.

37 The ENCODE Project Consortium *Nature* **2007**, *447*, 799-816.

38 Pheasant, M.; Mattick, J. S. *Genome Res.* **2007**, *17*, 1245-1253.

39 Mattick, J. S.,"The Human Genome: RNA Machine," *The Scientist*, *21*, 10, October **2007**, p. 61.

40 Altona, C.; Sundaralingam, M. *J. Am. Chem. Soc.* **1972**, *94*, 8205-8212.

41 Davies, D. B. *Prog. Nucl. Magn. Reson. Spectrosc.* **1978**, *12*, 135-225.

42 *Nucleic Acids in Chemistry and Biology, 3rd edition*; Blackburn, G. M.; Gait, M. J.; Loakes, D.; Williams, D. M., Eds.; RSC Publishing: Cambridge, 2006.

43 Tomita, K.-I.; Rich, A. *Nature* **1964**, *201*, 1160-1163.

44 Hall, K.; Cruz, P.; Tinoco Jr, I.; Jovin, T. M.; van de Sande, J. H. *Nature* **1984**, *311*, 584-586.

45 Levy, Y.; Onuchic, J. N. *Annu. Rev. Biophys. Biomol. Struct.* **2006**, *35*, 389-415.

46 Dickerson, R. E.; Drew, H. R.; Conner, B. N.; Wing, R. M.; Fratini, A. V.; Kopka, M. L. *Science* **1982**, *216*, 475-485.

47 Schneider, B.; Patel, K.; Berman, H. M. *Biophys. J.* **1998**, *75*, 2422-2434.

48 Egli, M.; Portmann, S.; Usman, N. *Biochemistry* **1996**, *35*, 8489-8494.

49 Mrevlishvili, G. M.; Carvalho, A. P. S. M. C.; da Silva, M. A. V. R.; Mdzinarashvili, T. D.; Razmadze, G. Z.; Tarielashvili, T. Z. *J Therm Anal Calorim* **2001**, *66*, 133-144.

50 Privalov, P. L.; Dragan, A. I.; Crane-Robinson, C.; Breslauer, K. J.; Remeta, D. P.; Minetti, C. A. S. A. *J. Mol. Biol.* **2007**, *365*, 1-9.

51 Sidorova, N. Y.; Rau, D. C. *Proc. Natl. Acad. Sci. USA* **1996**, *93*, 12272-12277.

52 Sidorova, N. Y.; Muradymov, S.; Rau, D. C. *J. Biol. Chem.* **2006**, *281*, 35656-35666.

53 Stephenson, M. L.; Zamecnik, P. C. *Proc. Natl. Acad. Sci. U. S. A.* **1978**, *75*, 285-288.

54 Zamecnik, P. C.; Stephenson, M. L. *Proc. Natl. Acad. Sci. USA* **1978**, *75*, 280-284.

55 Alvarado-Urbina, G.; Sathe, G. M.; Liu, W. C.; Gillen, M. F.; Duck, P. D.; Bender, R.; Ogilvie, K. K. *Science* **1981**, *214*, 270-274.

56 Uhlmann, E.; Peyman, A. *Chem. Rev.* **1990**, *90*, 543-84.

57 Crooke, S. T. *Annu. Rev. Med.* **2004**, *55*, 61-95.

58 Kurreck, J. *Eur. J. Biochem.* **2003**, *270*, 1628-1644.

59 Haeuptle, M. T.; Frank, R.; Dobberstein, B. *Nucl. Acids Res.* **1986**, *14*, 1427-1448.

60 Minshull, J.; Hunt, T. *Nucl. Acids Res.* **1986**, *14*, 6433-6451.

61 Gruenweller, A.; Wyszko, E.; Bieber, B.; Jahnel, R.; Erdmann, V. A.; Kurreck, J. *Nucl. Acids Res.* **2003**, *31*, 3185-3193.

62 Vickers, T. A.; Koo, S.; Bennett, C. F.; Crooke, S. T.; Dean, N. M.; Baker, B. F. *J. Biol. Chem.* **2003**, *278*, 7108-7118.

63 Ferrari, N.; Bergeron, D.; Tedeschi, A.-L.; Mangos, M. M.; Paquet, L.; Renzi, P. M.; Damha, M. J. *Ann. N. Y. Acad. Sci.* **2006**, *1082*, 91-102.

64 Scherer, L. J.; Rossi, J. J. *Nat. Biotech.* **2003**, *21*, 1457-1465.

65 Hemmings-Mieszczak, M.; Dorn, G.; Natt, F. J.; Hall, J.; Wishart, W. L. *Nucl. Acids Res.* **2003**, *31*, 2117-2126.

66 Tomari, Y.; Zamore, P. D. *Genes Dev.* **2005**, *19*, 517-529.

67 Grünweller, A.; Hartmann, R. K. *Curr. Med. Chem.* **2005**, *12*, 3143-3161.

68 Meister, G.; Landthaler, M.; Peters, L.; Chen, P. Y.; Urlaub, H.; Luhrmann, R.; Tuschl, T. *Curr. Biol.* **2005**, *15*, 2149-2155.

69 Meister, G.; Tuschl, T. *Nature* **2004**, *431*, 343-349.

70 Meister, G.; Landthaler, M.; Patkaniowska, A.; Dorsett, Y.; Teng, G.; Tuschl, T. *Mol. Cell* **2007**, *131*, 50-62.

71 Hamada, M.; Ohtsuka, T.; Kawaida, R.; Koizumi, M.; Morita, K.; Furukawa, H.; Imanishi, T.; Miyagishi, M.; Taira, K. *Antisense Nucleic Acid Drug Dev.* **2002**, *12*, 301-309.

72 Parrish, S.; Fleenor, J.; Xu, S.; Mello, C.; Fire, A. *Mol. Cell* **2000**, *6*, 1077-1087.

73 Lingel, A.; Simon, B.; Izaurralde, E.; Sattler, M. *Nat. Struct. Mol. Biol.* **2004**, *11*, 576-577.

74 Ma, J.-B.; Ye, K.; Patel, D. J. *Nature* **2004**, *429*, 318-322.

75 Song, J.-J.; Liu, J.; Tolia Niraj, H.; Schneiderman, J.; Smith Stephanie, K.; Martienssen Robert, A.; Hannon Gregory, J.; Joshua-Tor, L. *Nat. Struct. Biol.* **2003**, *10*, 1026-32.

76 Yan, K. S.; Yan, S.; Farooq, A.; Han, A.; Zeng, L.; Zhou, M.-M. *Nature* **2003**, *426*, 469-474.

77 Lingel, A.; Simon, B.; Izaurralde, E.; Sattler, M. *Nature* **2003**, *426*, 465-469.

78 Song, J.-J.; Smith, S. K.; Hannon, G. J.; Joshua-Tor, L. *Science* **2004**, *305*, 1434-1437.

79 Parker, J. S.; Roe, S. M.; Barford, D. *EMBO J.* **2004**, *23*, 4727-4737.

80 Liu, J.; Carmell, M. A.; Rivas, F. V.; Marsden, C. G.; Thomson, J. M.; Song, J.-J.; Hammond, S. M.; Joshua-Tor, L.; Hannon, G. J. *Science* **2004**, *305*, 1437-1441.

81 Meister, G.; Landthaler, M.; Patkaniowska, A.; Dorsett, Y.; Teng, G.; Tuschl, T. *Mol. Cell* **2004**, *15*, 185-197.

82 Rivas, F. V.; Tolia, N. H.; Song, J.-J.; Aragon, J. P.; Liu, J.; Hannon, G. J.; Joshua-Tor, L. *Nat. Struct. Mol. Biol.* **2005**, *12*, 340-349.

83 Parker, J. S.; Roe, S. M.; Barford, D. *Nature* **2005**, *434*, 663-666.

84 Ma, J.-B.; Yuan, Y.-R.; Meister, G.; Pei, Y.; Tuschl, T.; Patel, D. J. *Nature* **2005**, *434*, 666-670.

85 Till, S.; Lejeune, E.; Thermann, R.; Bortfeld, M.; Hothorn, M.; Enderle, D.; Heinrich, C.; Hentze, M. W.; Ladurner, A. G. *Nat. Struct. Mol. Biol.* **2007**, *14*, 897-903.

86 Pham, J. W.; Pellino, J. L.; Lee, Y. S.; Carthew, R. W.; Sontheimer, E. J. *Cell* **2004**, *117*, 83-94.

87 Tahbaz, N.; Kolb, F. A.; Zhang, H.; Jaronczyk, K.; Filipowicz, W.; Hobman, T. C. *EMBO Reports* **2004**, *5*, 189-194.

88 James, W.; Al-Shamkhani, A. *Curr. Opin. Biotechnol.* **1995**, *6*, 44-49.

89 Rossi, J. J. *Chem. Biol.* **1999**, *6*, R33-R37.

90 Rossi, J. J. *Trends Genet.* **1998**, *14*, 295-298.

91 Cech, T. R. *Curr. Opin. Struct. Biol.* **1992**, *2*, 605-609.

92 Krutzfeldt, J.; Rajewsky, N.; Braich, R.; Rajeev, K. G.; Tuschl, T.; Manoharan, M.; Stoffel, M. *Nature* **2005**, *438*.

93 Davis, S.; Lollo, B.; Freier, S.; Esau, C. *Nucl. Acids Res.* **2006**, *34*, 2294-2304.

94 Esau, C.; Davis, S.; Murray, S. F.; Yu, X. X.; Pandey, S. K.; Pear, M.; Watts, L.; Booten, S. L.; Graham, M.; McKay, R.; Subramaniam, A.; Propp, S.; Lollo, B. A.; Freier, S.; Bennett, C. F.; Bhanot, S.; Monia, B. P. *Cell Metabolism* **2006**, *3*, 87-98.

95 Mercatante, D. R.; Kole, R. *Biochimica et Biophysica Acta (BBA) - Molecular Basis of Disease* **2002**, *1587*, 126-132.

96 Kole, R.; Vacek, M.; Williams, T. *Oligonucleotides* **2004**, *14*, 65-74.

97 Taylor, J. K.; Zhang, Q. Q.; Wyatt, J. R.; Dean, N. M. *Nat. Biotech.* **1999**, *17*, 1097-1100.

98 van Deutekom, J. C. T.; Bremmer-Bout, M.; Janson, A. A. M.; Ginjaar, I. B.; Baas, F.; den Dunnen, J. T.; van Ommen, G.-J. B. *Hum. Mol. Genet.* **2001**, *10*, 1547-1554.

99 Boese, Q.; Leake, D.; Reynolds, A.; Read, S.; Scaringe, S. A.; Marshall, W. S.; Khvorova, A. *Methods Enzymol.* **2005**, *392*, 73-96.

100 Huesken, D.; Lange, J.; Mickanin, C.; Weiler, J.; Asselbergs, F.; Warner, J.; Meloon, B.; Engel, S.; Rosenberg, A.; Cohen, D.; Labow, M.; Reinhardt, M.; Natt, F.; Hall, J. *Nat. Biotech.* **2005**, *23*, 995-1001.

101 Yuan, B.; Latek, R.; Hossbach, M.; Tuschl, T.; Lewitter, F. *Nucl. Acids Res.* **2004**, *32*, W130-134.

102 Manoharan, M.; Rajeev, K. G. In *Antisense Drug Technology: Principles, Strategies, and Applications, Second Edition*; Crooke, S. T., Ed.; CRC Press: Boca Raton, FL, 2007, pp. 437-464.

103 Choung, S.; Kim, Y. J.; Kim, S.; Park, H. O.; Choi, Y. C. *Biochem. Biophys. Res. Commun.* **2006**, *342*, 919-927.

104 Soutschek, J.; Akinc, A.; Bramlage, B.; Charisse, K.; Constien, R.; Donoghue, M.; Elbashir, S.; Geick, A.; Hadwiger, P.; Harborth, J.; John, M.; Kesavan, V.; Lavine, G.; Pandey, R. K.; Racie, T.; Rajeev, K. G.; Rohl, I.; Toudjarska, I.; Wang, G.; Wuschko, S.; Bumcrot, D.; Koteliansky, V.; Limmer, S.; Manoharan, M.; Vornlocher, H.-P. *Nature* **2004**, *432*, 173-178.

105 Kraynack, B. A.; Baker, B. F. *RNA* **2006**, *12*, 163-176.

106 Ui-Tei, K.; Naito, Y.; Zenno, S.; Nishi, K.; Yamato, K.; Takahashi, F.; Juni, A.; Saigo, K. *Nucl. Acids Res.* **2008**, *36*, 2136-2151.

107 Chiu, Y. L.; Rana, T. M. *RNA* **2003**, *9*, 1034-1048.

108 Braasch, D. A.; Jensen, S.; Liu, Y.; Kaur, K.; Arar, K.; White, M. A.; Corey, D. R. *Biochemistry* **2003**, *42*, 7967-7975.

109 Elbashir, S. M.; Martinez, J.; Patkaniowska, A.; Lendeckel, W.; Tuschl, T. *EMBO J.* **2001**, *20*, 6877-6888.

110 Czauderna, F.; Fechtner, M.; Dames, S.; Aygun, H.; Klippel, A.; Pronk, G. J.; Giese, K.; Kaufmann, J. *Nucl. Acids Res.* **2003**, *31*, 2705-2716.

111 Dorn, G.; Patel, S.; Wotherspoon, G.; Hemmings-Mieszczak, M.; Barclay, J.; Natt, F. J. C.; Martin, P.; Bevan, S.; Fox, A.; Ganju, P.; Wishart, W.; Hall, J. *Nucl. Acids Res.* **2004**, *32*, e49.

112 Prakash, T. P.; Allerson, C. R.; Dande, P.; Vickers, T. A.; Sioufi, N.; Jarres, R.; Baker, B. F.; Swayze, E. E.; Griffey, R. H.; Bhat, B. *J. Med. Chem.* **2005**, *48*, 4247-4253.

113 Amarzguioui, M.; Holen, T.; Babaie, E.; Prydz, H. *Nucl. Acids Res.* **2003**, *31*, 589-595.

114 Chen, X. L.; Shen, L.; Wang, J. H. *Oligonucleotides* **2004**, *14*, 90-99.

115 Harborth, J.; Elbashir, S. M.; Vandenburgh, K.; Manninga, H.; Scaringe, S. A.; Weber, K.; Tuschl, T. *Antisense Nucleic Acid Drug Dev.* **2003**, *13*, 83-105.

116 Blidner, R. A.; Hammer, R. P.; Lopez, M. J.; Robinson, S. O.; Monroe, W. T. *Chem. Biol. Drug Des.* **2007**, *70*, 113-122.

117 Layzer, J. M.; McCaffrey, A. P.; Tanner, A. K.; Huang, Z. A. N.; Kay, M. A.; Sullenger, B. A. *RNA* **2004**, *10*, 766-771.

118 Damha, M. J.; Wilds, C. J.; Noronha, A.; Brukner, I.; Borkow, G.; Arion, D.; Parniak, M. A. *J. Am. Chem. Soc.* **1998**, *120*, 12976-12977.

119 Wilds, C. J.; Damha, M. J. *Nucl. Acids Res.* **2000**, *28*, 3625-3635.

120 Dowler, T.; Bergeron, D.; Tedeschi, A.-L.; Paquet, L.; Ferrari, N.; Damha, M. J. *Nucl. Acids Res.* **2006**, *34*, 1669-1675.

121 Watts, J. K.; Choubdar, N.; Sadalapure, K.; Robert, F.; Wahba, A. S.; Pelletier, J.; Pinto, B. M.; Damha, M. J. *Nucl. Acids Res.* **2007**, *35*, 1441-1451.

122 Hoshika, S.; Minakawa, N.; Kamiya, H.; Harashima, H.; Matsuda, A. *FEBS Lett.* **2005**, *579*, 3115-3118.

123 Dande, P.; Prakash, T. P.; Sioufi, N.; Gaus, H.; Jarres, R.; Berdeja, A.; Swayze, E. E.; Griffey, R. H.; Bhat, B. *J. Med. Chem.* **2006**, *49*, 1624-1634.

124 Hoshika, S.; Minakawa, N.; Shionoya, A.; Imada, K.; Ogawa, N.; Matsuda, A. *ChemBioChem* **2007**, *8*, 2133-2138.

125 Petersen, M.; Wengel, J. *Trends Biotechnol.* **2003**, *21*, 74-81.

126 Elmen, J.; Thonberg, H.; Ljungberg, K.; Frieden, M.; Westergaard, M.; Xu, Y.; Wahren, B.; Liang, Z.; Urum, H.; Koch, T.; Wahlestedt, C. *Nucl. Acids Res.* **2005**, *33*, 439-447.

127 Bramsen, J. B.; Laursen, M. B.; Damgaard, C. K.; Lena, S. W.; Ravindra Babu, B.; Wengel, J.; Kjems, J. *Nucl. Acids Res.* **2007**, *35*, 5886-5897.

128 Mook, O. R.; Baas, F.; de Wissel, M. B.; Fluiter, K. *Mol. Cancer Therap.* **2007**, *6*, 833-843.

129 Hornung, V.; Guenthner-Biller, M.; Bourquin, C.; Ablasser, A.; Schlee, M.; Uematsu, S.; Noronha, A.; Manoharan, M.; Akira, S.; de Fougerolles, A.; Endres, S.; Hartmann, G. *Nat. Med.* **2005**, *11*, 263-270.

130 Hall, A. H. S.; Wan, J.; Shaughnessy, E. E.; Shaw, B. R.; Alexander, K. A. *Nucl. Acids Res.* **2004**, *32*, 5991-6000.

131 Schwarz, D. S.; Tomari, Y.; Zamore, P. D. *Curr. Biol.* **2004**, *14*, 787-791.

132 Braasch, D. A.; Paroo, Z.; Constantinescu, A.; Ren, G.; Oz, O. K.; Mason, R. P.; Corey, D. R. *Bioorg. Med. Chem. Lett.* **2004**, *14*, 1139-1143.

133 Prakash, T. P.; Kraynack, B.; Baker, B. F.; Swayze, E. E.; Bhat, B. *Bioorg. Med. Chem. Lett.* **2006**, *16*, 3238-3240.

134 Iwase, R.; Toyama, T.; Nishimori, K. *Nucleosides Nucleotides Nucleic Acids* **2007**, *26*, 1451 - 1454.

135 Sipa, K.; Sochacka, E.; Kazmierczak-Baranska, J.; Maszewska, M.; Janicka, M.; Nowak, G.; Nawrot, B. *RNA* **2007**, *13*, 1301-1316.

136 Hornung, V.; Ellegast, J.; Kim, S.; Brzozka, K.; Jung, A.; Kato, H.; Poeck, H.; Akira, S.; Conzelmann, K.-K.; Schlee, M.; Endres, S.; Hartmann, G. *Science* **2006**, *314*, 994-997.

137 Xia, J.; Noronha, A.; Toudjarska, I.; Li, F.; Akinc, A.; Braich, R.; Frank-Kamenetsky, M.; Rajeev, K. G.; Egli, M.; Manoharan, M. *ACS Chem. Biol.* **2006**, *1*, 176-183.

138 Holen, T.; Amarzguioui, M.; Wiiger, M. T.; Babaie, E.; Prydz, H. *Nucl. Acids Res.* **2002**, *30*, 1757-1766.

139 Marques, J. T.; Devosse, T.; Wang, D.; Zamanian-Daryoush, M.; Serbinowski, P.; Hartmann, R.; Fujita, T.; Behlke, M. A.; Williams, B. R. G. *Nat. Biotech.* **2006**, *24*, 559-565.

140 Nykanen, A.; Haley, B.; Zamore, P. D. *Cell* **2001**, *107*, 309-321.

141 Chen, P. Y.; Weinmann, L.; Gaidatzis, D.; Pei, Y.; Zavolan, M.; Tuschl, T.; Meister, G. *RNA* **2008**, *14*, 263-274.

142 Morrissey, D. V.; Lockridge, J. A.; Shaw, L.; Blanchard, K.; Jensen, K.; Breen, W.; Hartsough, K.; Machemer, L.; Radka, S.; Jadhav, V.; Vaish, N.; Zinnen, S.; Vargeese, C.; Bowman, K.; Shaffer, C. S.; Jeffs, L. B.; Judge, A.; MacLachlan, I.; Polisky, B. *Nat. Biotech.* **2005**, *23*, 1002-1007.

143 Morrissey, D. V.; Blanchard, K.; Shaw, L.; Jensen, K.; Lockridge, J. A.; Dickinson, B.; McSwiggen, J. A.; Vargeese, C.; Bowman, K.; Shaffer, C. S.; Polisky, B. A.; Zinnen, S. *Hepatology* **2005**, *41*, 1349-1356.

144 Chiu, Y.-L.; Rana, T. M. *Mol. Cell* **2002**, *10*, 549-561.

145 Muratovska, A.; Eccles, M. R. *FEBS Lett.* **2004**, *558*, 63-68.

146 Lorenz, C.; Hadwiger, P.; John, M.; Vornlocher, H.-P.; Unverzagt, C. *Bioorg. Med. Chem. Lett.* **2004**, *14*, 4975-4977.

147 Bolcato-Bellemin, A.-L.; Bonnet, M.-E.; Creusat, G.; Erbacher, P.; Behr, J.-P. *Proc. Natl. Acad. Sci. USA* **2007**, *104*, 16050-16055.

148 Martinez, J.; Patkaniowska, A.; Urlaub, H.; Luhrmann, R.; Tuschl, T. *Cell* **2002**, *110*, 563-574.

149 Schwarz, D. S.; Hutvágner, G.; Haley, B.; Zamore, P. D. *Mol. Cell* **2002**, *10*, 537-548.

150 Siolas, D.; Lerner, C.; Burchard, J.; Ge, W.; Linsley, P. S.; Paddison, P. J.; Hannon, G. J.; Cleary, M. A. *Nat. Biotech.* **205**, *23*, 227-231.

151 Brummelkamp, T. R.; Bernards, R.; Agami, R. *Science* **2002**, *296*, 550-553.

152 Banan, N.; Puri, M. *Curr. Pharm. Biotech.* **2004**, *5*, 441-450.

153 Abe, N.; Abe, H.; Ito, Y. *J. Am. Chem. Soc.* **2007**, *129*, 15108 -15109.

154 Holen, T.; Amarzguioui, M.; Babaie, E.; Prydz, H. *Nucl. Acids Res.* **2003**, *31*, 2401-2407.

155 Kim, D.-H.; Behlke, M. A.; Rose, S. D.; Chang, M.-S.; Choi, S.; Rossi, J. J. *Nat. Biotech.* **2005**, *23*, 222-226.

156 Minks, M. A.; West, D. K.; Benvin, S.; Baglioni, C. *J. Biol. Chem.* **1979**, *254*, 180-183.

157 Kennedy, S.; Wang, D.; Ruvkun, G. *Nature* **2004**, *427*, 645-649.

158 Takabatake, Y.; Isaka, Y.; Mizui, M.; Kawachi, H.; Takahara, S.; Imai, E. *Biochem. Biophys. Res. Commun.* **2007**, *363*, 432-437.

159 Allerson, C. R.; Sioufi, N.; Jarres, R.; Prakash, T. P.; Naik, N.; Berdeja, A.; Wanders, L.; Griffey, R. H.; Swayze, E. E.; Bhat, B. *J. Med. Chem.* **2005**, *48*, 901-904.

160 Turner, J. J.; Jones, S. W.; Moschos, S. A.; Lindsay, M. A.; Gait, M. J. *Molecular BioSystems* **2007**, *3*, 43-50.

161 de Fougerolles, A.; Vornlocher, H.-P.; Maraganore, J.; Lieberman, J. *Nat. Rev. Drug Discov.* **2007**, *6*, 443-453.

162 Manoharan, M., "RNA interference and chemical modifications: Conformational and stereochemical aspects," Abstracts of Papers, 231st ACS National Meeting, Atlanta, USA, March 26-30, 2006.

163 Koller, E.; Propp, S.; Murray, H.; Lima, W.; Bhat, B.; Prakash, T. P.; Allerson, C. R.; Swayze, E. E.; Marcusson, E. G.; Dean, N. M. *Nucl. Acids Res.* **2006**, *34*, 4467-4476.

164 Schlee, M.; Hornung, V.; Hartmann, G. *Mol. Ther.* **2006**, *14*, 463-470.

165 Marques, J. T.; Williams, B. R. G. *Nat. Biotech.* **2005**, *23*, 1399-1405.

166 Judge, A. D.; Sood, V.; Shaw, J. R.; Fang, D.; McClintock, K.; MacLachlan, I. *Nat. Biotech.* **2005**, *23*, 457-462.

167 Kim, D.-H.; Longo, M.; Han, Y.; Lundberg, P.; Cantin, E.; Rossi, J. J. *Nat. Biotech.* **2004**, *22*, 321-325.

168 Reynolds, A.; Anderson, E. M.; Vermeulen, A.; Fedorov, Y.; Robinson, K.; Leake, D.; Karpilow, J.; Marshall, W. S.; Khvorova, A. *RNA* **2006**, *12*, 988-993.

169 Kleinman, M. E.; Yamada, K.; Takeda, A.; Chandrasekaran, V.; Nozaki, M.; Baffi, J. Z.; Albuquerque, R. J. C.; Yamasaki, S.; Itaya, M.; Pan, Y.; Appukuttan, B.; Gibbs, D.; Yang, Z.; Karikó, K.; Ambati, B. K.; Wilgus, T. A.; DiPietro, L. A.; Sakurai, E.; Zhang, K.; Smith, J. R.; Taylor, E. W.; Ambati, J. *Nature* **2008**, *452*, 591-597.

170 Takeda, K.; Akira, S. *Int. Immunol.* **2005**, *17*, 1-14.

171 Judge, A.; MacLachlan, I. *Hum. Gene Ther.* **2008**, *19*, 111-124.

172 Zamanian-Daryoush, M.; Marques, J. T.; Gantier, M. P.; Behlke, M. A.; John, M.; Rayman, P.; Finke, J.; Williams, B. R. G. *J. Interferon Cytokine Res.* **2008**, *28*, 221-233.

173 Diebold, Sandra S.; Massacrier, C.; Akira, S.; Paturel, C.; Morel, Y.; Reis e Sousa, C. *Eur. J. Immunol.* **2006**, *36*, 3256-3267.

174 Judge, A. D.; Bola, G.; Lee, A. C. H.; MacLachlan, I. *Mol. Ther.* **2006**, *13*, 494-505.

175 Cekaite, L.; Furset, G.; Hovig, E.; Sioud, M. *J. Mol. Biol.* **2007**, *365*, 90-108.

176 Robbins, M.; Judge, A.; Liang, L.; McClintock, K.; Yaworski, E.; MacLachlan, I. *Mol. Ther.* **2007**, *15*, 1663-1669.

177 Karikó, K.; Buckstein, M.; Ni, H.; Weissman, D. *Immunity* **2005**, *23*, 165-175.

178 Jackson, A. L.; Bartz, S. R.; Schelter, J.; Kobayashi, S. V.; Burchard, J.; Mao, M.; Li, B.; Cavet, G.; Linsley, P. S. *Nat. Biotech.* **2003**, *21*, 635-637.

179 Jackson, A. L.; Burchard, J.; Schelter, J.; Chau, B. N.; Cleary, M.; Lim, L.; Linsley, P. S. *RNA* **2006**, *12*, 1179-1187.

180 Birmingham, A.; Anderson, E. M.; Reynolds, A.; Ilsley-Tyree, D.; Leake, D.; Fedorov, Y.; Baskerville, S.; Maksimova, E.; Robinson, K.; Karpilow, J.; Marshall, W. S.; Khvorova, A. *Nat. Meth.* **2006**, *3*, 199-204.

181 Zeng, Y.; Yi, R.; Cullen, B. R. *Proc. Natl. Acad. Sci. U. S. A.* **2003**, *100*, 9779-9784.

182 Doench, J. G.; Petersen, C. P.; Sharp, P. A. *Genes Dev.* **2003**, *17*, 438-442.

183 Fedorov, Y.; Anderson, E. M.; Birmingham, A.; Reynolds, A.; Karpilow, J.; Robinson, K.; Leake, D.; Marshall, W. S.; Khvorova, A. *RNA* **2006**, *12*, 1188-1196.

184 Jackson, A. L.; Burchard, J.; Leake, D.; Reynolds, A.; Schelter, J.; Guo, J.; Johnson, J. M.; Lim, L.; Karpilow, J.; Nichols, K.; Marshall, W.; Khvorova, A.; Linsley, P. S. *RNA* **2006**, *12*, 1197-1205.

185 Gilmore, I. R.; Fox, S. P.; Hollins, A. J.; Sohail, M.; Akhtar, S. *J. Drug Target.* **2004**, *12*, 315-340.

186 Palliser, D.; Chowdhury, D.; Wang, Q.-Y.; Lee, S. J.; Bronson, R. T.; Knipe, D. M.; Lieberman, J. *Nature* **2006**, *439*, 89-94.

187 Xie, F. Y.; Woodle, M. C.; Lu, P. Y. *Drug Discov. Today* **2006**, *11*, 67-73.

188 Aigner, A. *Appl. Microbiol. Biotechnol.* **2007**, *76*, 9-21.

189 De Paula, D.; Bentley, M. V. L. B.; Mahato, R. I. *RNA* **2007**, *13*, 431-456.

190 Ikeda, Y.; Taira, K. *Pharm. Res.* **2006**, *23*, 1631-1640.

191 Wolfrum, C.; Shi, S.; Jayaprakash, K. N.; Jayaraman, M.; Wang, G.; Pandey, R. K.; Rajeev, K. G.; Nakayama, T.; Charrise, K.; Ndungo, E. M.; Zimmermann, T.; Koteliansky, V.; Manoharan, M.; Stoffel, M. *Nat. Biotech.* **2007**, *25*, 1149-1157.

192 Heyes, J.; Palmer, L.; Bremner, K.; MacLachlan, I. *J. Controlled Release* **2005**, *107*, 276-287.

193 Zimmermann, T. S.; Lee, A. C. H.; Akinc, A.; Bramlage, B.; Bumcrot, D.; Fedoruk, M. N.; Harborth, J.; Heyes, J. A.; Jeffs, L. B.; John, M.; Judge, A. D.; Lam, K.; McClintock, K.; Nechev, L. V.; Palmer, L. R.; Racie, T.; Rohl, I.; Seiffert, S.; Shanmugam, S.; Sood, V.; Soutschek, J.; Toudjarska, I.; Wheat, A. J.; Yaworski, E.; Zedalis, W.; Koteliansky, V.; Manoharan, M.; Vornlocher, H. P.; MacLachlan, I. *Nature* **2006**, *441*, 111-114.

194 Peer, D.; Park, E. J.; Morishita, Y.; Carman, C. V.; Shimaoka, M. *Science* **2008**, *319*, 627-630.

195 Hu-Lieskovan, S.; Heidel, J. D.; Bartlett, D. W.; Davis, M. E.; Triche, T. J. *Cancer Res.* **2005**, *65*, 8984-8992.

196 Oishi, M.; Nagasaki, Y.; Itaka, K.; Nishiyama, N.; Kataoka, K. *J. Am. Chem. Soc.* **2005**, *127*, 1624-1625.

197 Heidel, J. D.; Yu, Z.; Liu, J. Y.-C.; Rele, S. M.; Liang, Y.; Zeidan, R. K.; Kornbrust, D. J.; Davis, M. E. *Proc. Natl. Acad. Sci. USA* **2007**, *104*, 5715-5721.

198 Shah, S.; Rangarajan, S.; Friedman, S. H. *Angew. Chem. Int. Ed.* **2005**, *44*, 1328-1332.

199 Nguyen, Q. N.; Chavli, R. V.; Marques, J. T.; Conrad, P. G.; Wang, D.; He, W. H.; Belisle, B. E.; Zhang, A. G.; Pastor, L. M.; Witney, F. R.; Morris, M.; Heitz, F.; Divita, G.; Williams, B. R. G.; McMaster, G. K. *BBA – Biomembranes* **2006**, *1758*, 394-403.

200 Shah, S.; Friedman, S. H. *Oligonucleotides* **2007**, *17*, 35-43.

201 Mikat, V.; Heckel, A. *RNA* **2007**, *13*, 2341-2347.

202 Wright, J. A.; Taylor, N. F.; Fox, J. J. *J. Org. Chem.* **1969**, *34*, 2632-2636.

203 Wright, J. A.; Wilson, D. P.; Fox, J. J. *J. Med. Chem.* **1970**, *13*, 269-272.

204 See the excellent review by K.W. Pankiewicz, *Carbohydr. Res.* **2000**, *327*, 87, and references therein.

205 Hertel, L. W.; Boder, G. B.; Kroin, J. S.; Rinzel, S. M.; Poore, G. A.; Todd, G. C.; Grindey, G. B. *Cancer Res.* **1990**, *50*, 4417-4422.

206 Masood, R.; Ahluwalia, G. S.; Cooney, D. A.; Fridland, A.; Marquez, V. E.; Driscoll, J. S.; Hao, Z.; Mitsuya, H.; Perno, C. F.; Broder, S. *Mol. Pharmacol.* **1990**, *37*, 590-596.

207 Graul, A.; Silvestre, J.; Castaner, J. *Drugs Future* **1998**, *23*, 1176-1189.

208 Marquez, V. E.; Tseng, C. K. H.; Mitsuya, H.; Aoki, S.; Kelley, J. A.; Ford, H.; Roth, J. S.; Broder, S.; Johns, D. G.; Driscoll, J. S. *J. Med. Chem.* **1990**, *33*, 978-985.

209 Stoeckler, J. D.; Bell, C. A.; Parks, J., Robert E.; Chu, C. K.; Fox, J. J.; Ikehara, M. *Biochem. Pharmacol.* **1982**, *31*, 1723-1728.

210 Watanabe, K. A.; Reichman, U.; Hirota, K.; Lopez, C.; Fox, J. J. *J. Med. Chem.* **1979**, *22*, 21-24.

211 Schinazi, R. F.; Peters, J.; Sokol, M. K.; Nahmias, A. J. *Antimicrob. Agents Chemother.* **1983**, *24*, 95-103.

212 Trousdale, M. D.; Nesburn, A. B.; Su, T. L.; Lopez, C.; Watanabe, K. A.; Fox, J. J. *Antimicrob. Agents Chemother.* **1983**, *23*, 808-813.

213 Burchenal, J. H.; Chou, T.-C.; Lokys, L.; Smith, R. S.; Watanabe, K. A.; Su, T.-L.; Fox, J. J. *Cancer Res.* **1982**, *42*, 2598-2600.

214 Abbruzzese, J. L.; Schmidt, S.; Raber, M. N.; Levy, J. K.; Castellanos, A. M.; Legha, S. S.; Krakoff, I. H. *Invest. New Drugs* **1989**, *7*, 195-201.

215 Kong, X.-B.; Scheck, A. C.; Price, R. W.; Vidal, P. M.; Fanucchi, M. P.; Watanabe, K. A.; Fox, J. J.; Chou, T.-C. *Antiviral Res.* **1988**, *10*, 153-166.

216 Ruth, J. L.; Cheng, Y.-C. *Mol. Pharmacol.* **1981**, *20*, 415-422.

217 Chu, C.; Ma, T.; Shanmuganathan, K.; Wang, C.; Xiang, Y.; Pai, S.; Yao, G.; Sommadossi, J.; Cheng, Y. *Antimicrob. Agents Chemother.* **1995**, *39*, 979-981.

218 Balakrishna Pai, S.; Liu, S.; Zhu, Y.; Chu, C.; Cheng, Y. *Antimicrob. Agents Chemother.* **1996**, *40*, 380-386.

219 Yao, G.-Q.; Liu, S.-H.; Chou, E.; Kukhanova, M.; Chu, C. K.; Cheng, Y.-C. *Biochem. Pharmacol.* **1996**, *51*, 941-947.

220 Marcellin, P.; Mommeja-Marin, H.; Sacks, S. L.; Lau, G. K. K.; Sereni, D.; Bronowicki, J.-P.; Conway, B.; Trepo, C.; Blum, M. R.; Yoo, B. C.; Mondou, E.; Sorbel, J.; Snow, A.; Rousseau, F.; Lee, H.-S. *Hepatology* **2004**, *40*, 140-148.

221 Lopez, C.; Watanabe, K. A.; Fox, J. J. *Antimicrob. Agents Chemother.* **1980**, *17*, 803-806.

222 Bowsher, R. R.; Compton, J. A.; Kirkwood, J. A.; Place, G. D.; Jones, C. D.; Mabry, T. E.; Hyslop, D. L.; Hatcher, B. L.; DeSante, K. A. *Antimicrob. Agents Chemother.* **1994**, *38*, 2134-2142.

223 R. McKenzie, M.W. Fried, R. Sallie, H. Conjeevaram, A.M. Di Bisceglie, Y. Park, B. Savarese, D. Kleiner, M. Tsokos, C. Luciano, T. Pruett, J.L. Stotka, S.E. Straus, and J.H. Hoofnagle. *N. Engl. J. Med.* **1995**, *333*, 1099. Also see the helpful editorial by M.N. Swartz. *N. Engl. J. Med.* **1995**, *333*, 1146, and commentary by A. Bari, L. Josephson, A.M. Prince, W. Lewis, F.W. Perrino, M. Gordon, J. Hoofnagle, R. McKenzie, S. Straus, M.N. Swartz, and J.L. Stotka. *N. Engl. J. Med.* **1996**, *334*, 1135.

224 *Review of the fialuridine (FIAU) clinical trials*; Manning, F.; Swartz, M., Eds.; National Academy Press: Washington, DC, 1995.

225 Fox, J. J.; Watanabe, K. A.; Chou, T. C.; Schinazi, R. F.; Soike, K. F.; Fourel, I.; Hantz, G.; Trepo, C. In *Fluorinated carbohydrates: chemical and biochemical aspects*; Taylor, N. F., Ed.; American Chemical Society: Washington, DC, 1988, pp. 176-190.

226 Leyland-Jones, B.; Donnelly, H.; Groshen, S.; Myskowski, P.; Donner, A. L.; Fanucchi, M.; Fox, J. *J. Infect. Dis.* **1986**, *154*, 430-436.

227 McKenzie, R.; Fried, M. W.; Sallie, R.; Conjeevaram, H.; Di Bisceglie, A. M.; Park, Y.; Savarese, B.; Kleiner, D.; Tsokos, M.; Luciano, C.; Pruett, T.; Stotka, J. L.; Straus, S. E.; Hoofnagle, J. H. *N. Engl. J. Med.* **1995**, *333*, 1099-1105.

228 Pui, C.-H.; Jeha, S.; Kirkpatrick, P. *Nat. Rev. Drug Discov.* **2005**, *4*, 369-370.

229 Bonate, P. L.; Arthaud, L.; Cantrell, W. R.; Stephenson, K.; Secrist, J. A.; Weitman, S. *Nat. Rev. Drug Discov.* **2006**, *5*, 855-863.

230 Chou, T. C.; Kong, X. B.; Fanucchi, M. P.; Cheng, Y. C.; Takahashi, K.; Watanabe, K. A.; Fox, J. J. *Antimicrob. Agents Chemother.* **1987**, *31*, 1355-1358.

231 Mansuri, M. M.; Ghazzouli, I.; Chen, M. S.; Howell, H. G.; Brodfuehrer, P. R.; Benigni, D. A.; Martin, J. C. *J. Med. Chem.* **1987**, *30*, 867-871.

232 Gambhir, S. S. *Nat. Rev. Cancer* **2002**, *2*, 683-693.

233 Buursma, A. R.; Rutgers, V.; Hospers, G. A. P.; Mulder, N. H.; Vaalburg, W.; de Vries, E. F. J. *Nucl. Med. Commun.* **2006**, *27*, 25-30.

234 Bettegowda, C.; Foss, C. A.; Cheong, I.; Wang, Y.; Diaz, L.; Agrawal, N.; Fox, J.; Dick, J.; Dang, L. H.; Zhou, S.; Kinzler, K. W.; Vogelstein, B.; Pomper, M. G. *Proc. Natl. Acad. Sci. USA* **2005**, *102*, 1145-1150.

235 Sun, H.; Mangner, T. J.; Collins, J. M.; Muzik, O.; Douglas, K.; Shields, A. F. *J. Nucl. Med.* **2005**, *46*, 292-296.

236 Chu, C. K.; Matulicadamic, J.; Huang, J. T.; Chou, T. C.; Burchenal, J. H.; Fox, J. J.; Watanabe, K. A. *Chem. Pharm. Bull.* **1989**, *37*, 336-339.

237 Shewach, D. S.; Daddona, P. E.; Ashcraft, E.; Mitchell, B. S. *Cancer Res.* **1985**, *45*, 1008-1014.

238 Verhoef, V.; Fridland, A. *Cancer Res.* **1985**, *45*, 3646-3650.

239 Faderl, S.; Gandhi, V.; Keating, M. J.; Jeha, S.; Plunkett, W.; Kantarjian, H. M. *Cancer* **2005**, *103*, 1985-1995.

240 Montgomery, J. A.; Shortnacy-Fowler, A. T.; Clayton, S. D.; Riordan, J. M.; Secrist, J. A. *J. Med. Chem.* **1992**, *35*, 397-401.

241 Carson, D.; Wasson, D.; Esparza, L.; Carrera, C.; Kipps, T.; Cottam, H. *Proc. Natl. Acad. Sci. USA* **1992**, *89*, 2970-2974.

242 Parker, W. B.; Shaddix, S. C.; Chang, C.-H.; White, E. L.; Rose, L. M.; Brockman, R. W.; Shortnacy, A. T.; Montgomery, J. A.; Secrist, J. A., III; Bennett, L. L., Jr. *Cancer Res.* **1991**, *51*, 2386-2394.

243 Reichman, U.; Watanabe, K. A.; Fox, J. J. *Carbohydr. Res.* **1975**, *42*, 233-240.

244 Anderson, C. D.; Goodman, L.; Baker, B. R. *J. Am. Chem. Soc.* **1958**, *80*, 5247-5252.

245 Tann, C. H.; Brodfuehrer, P. R.; Brundidge, S. P.; Sapino, C.; Howell, H. G. *J. Org. Chem.* **1985**, *50*, 3644-3647.

246 Brodfuehrer, P. R.; Sapino, C.; Howell, H. G. *J. Org. Chem.* **1985**, *50*, 2597-2598.

247 Schaerer, O. D.; Verdine, G. L. *J. Am. Chem. Soc.* **1995**, *117*, 10781-10782.

248 Yin, J.; Zarkowsky, D. S.; Thomas, D. W.; Zhao, M. M.; Huffman, M. A. *Org. Lett.* **2004**, *6*, 1465-1468.

249 Chou, T. S.; Becke, L. M.; O'Toole, J. C.; Carr, M. A.; Parker, B. E. *Tetrahedron Lett.* **1996**, *37*, 17-20.

250 Ma, T.; Pai, S. B.; Zhu, Y. L.; Lin, J. S.; Shanmuganathan, K.; Du, J.; Wang, C.; Kim, H.; Newton, M. G.; Cheng, Y. C.; Chu, C. K. *J. Med. Chem.* **1996**, *39*, 2835-2843.

251 Rubira, M.-J.; Jimeno, M.-L.; Balzarini, J.; Camarasa, M.-J.; Perez-Perez, M.-J. *Tetrahedron* **1998**, *54*, 8223-8240.

252 Alauddin, M. M.; Conti, P. S.; Mathew, T.; Fissekis, J. D.; Surya Prakash, G. K.; Watanabe, K. A. *J. Fluorine Chem.* **2000**, *106*, 87-91.

253 Middleton, W. J. *J. Org. Chem.* **1975**, *40*, 574-578.

254 Wilkinson, J. A. *Chem. Rev.* **1992**, *92*, 505-519.

255 Chambers, R. D. *Fluorine in Organic Chemistry*; Blackwell Publishing Ltd.: Oxford, 2004.

256 Sznaidman, M. L.; Almond, M. R.; Pesyan, A. *Nucleosides Nucleotides Nucleic Acids* **2002**, *21*, 155-163.

257 Howell, H. G.; Brodfuehrer, P. R.; Brundidge, S. P.; Benigni, D. A.; Sapino, C., Jr. *J. Org. Chem.* **1988**, *53*, 85-8.

258 Garcia, J.; Diaz-Rodriguez, A.; Fernandez, S.; Sanghvi, Y. S.; Ferrero, M.; Gotor, V. *J. Org. Chem.* **2006**, *71*, 9765-9771.

259 Pankiewicz, K. W.; Watanabe, K. A. *J. Fluorine Chem.* **1993**, *64*, 15-36.

260 Maruyama, T.; Takamatsu, S.; Kozai, S.; Satoh, Y.; Izawa, K. *Chem. Pharm. Bull.* **1999**, *47*, 966-970.

261 Montgomery, J. A.; Shortnacy, A. T.; Carson, D. A.; Secrist, J. A. *J. Med. Chem.* **1986**, *29*, 2389-2392.

262 Ma, T.; Lin, J.-S.; Newton, M. G.; Cheng, Y.-C.; Chu, C. K. *J. Med. Chem.* **1997**, *40*, 2750-2754.

263 Tennila, T.; Azhayeva, E.; Vepsalainen, J.; Laatikainen, R.; Azhayev, A.; Mikhailopulo, I. A. *Nucleosides Nucleotides Nucleic Acids* **2000**, *19*, 1861-1884.

264 Elzagheid, M. I.; Viazovkina, E.; Damha, M. J. In *Current Protocols in Nucleic Acid Chemistry*; Beaucage, S., Ed. 2002, p. Unit 1.7.

265 Elzagheid, M. I.; Viazovkina, E.; Damha, M. J. *Nucleosides Nucleotides Nucleic Acids* **2003**, *22*, 1339-1342.

266 Rosenberg, I.; Soler, J. F.; Tocik, Z.; Ren, W. Y.; Ciszewski, L. A.; Kois, P.; Pankiewicz, K. W.; Spassova, M.; Watanabe, K. A. *Nucleosides Nucleotides* **1993**, *12*, 381-401.

267 Kois, P.; Tocik, Z.; Spassova, M.; Ren, W. Y.; Rosenberg, I.; Soler, J. F.; Watanabe, K. A. *Nucleosides Nucleotides* **1993**, *12*, 1093-1109.

268 Ikeda, H.; Fernandez, R.; Wilk, A.; Barchi, J. J.; Huang, X. L.; Marquez, V. E. *Nucl. Acids Res.* **1998**, *26*, 2237-2244.

269 Berger, I.; Tereshko, V.; Ikeda, H.; Marquez, V. E.; Egli, M. *Nucl. Acids Res.* **1998**, *26*, 2473-2480.

270 Damha, M. J.; Usman, N.; Ogilvie, K. K. *Tetrahedron Lett.* **1987**, *28*, 1633-1636.

271 Damha, M. J.; Usman, N.; Ogilvie, K. K. *Can. J. Chem.* **1989**, *67*, 831-9.

272 Resmini, M.; Pfleiderer, W. *Helv. Chim. Acta* **1993**, *76*, 158-167.

273 Mikita, T.; Beardsley, G. P. *Biochemistry* **1994**, *33*, 9195-9208.

274 Gao, Y. G.; Van der Marel, G. A.; Van Boom, J. H.; Wang, A. H. J. *Biochemistry* **1991**, *30*, 9922-9931.

275 Pieters, J. M. L.; De Vroom, E.; Van der Marel, G. A.; Van Boom, J. H.; Koning, T. M. G.; Kaptein, R.; Altona, C. *Biochemistry* **1990**, *29*, 788-799.

276 Giannaris, P. A.; Damha, M. J. *Can. J. Chem.* **1994**, *72*, 909-918.

277 Noronha, A. M.; Wilds, C. J.; Lok, C.-N.; Viazovkina, K.; Arion, D.; Parniak, M. A.; Damha, M. J. *Biochemistry* **2000**, *39*, 7050-7062.

278 Viazovkina, E.; Mangos, M. M.; Elzagheid, M. I.; Damha, M. J. In *Current Protocols in Nucleic Acid Chemistry*; Beaucage, S., Ed. 2002, p. Unit 4.15.

279 Wang, S.; Kool, E. T. *Biochemistry* **1995**, *34*, 4125-4132.

280 Min, K.-L.; Viazovkina, E.; Galarneau, A.; Parniak, M. A.; Damha, M. J. *Bioorg. Med. Chem. Lett.* **2002**, *12*, 2651-2654.

281 Martin-Pintado, N.; Watts, J. K.; Gonzalez, C.; Damha, M. J. *Manuscript in preparation*.

282 Wilds, C. J. *Synthesis, Physicochemical and Biological Properties of Oligonucleotides Containing 2-Fluoro-2-deoxy-β-D-arabinose*; PhD Thesis, McGill University, 1999.

283 Stein, C. A.; Subasinghe, C.; Shinozuka, K.; Cohen, J. S. *Nucl. Acids Res.* **1988**, *16*, 3209-3221.

284 Lok, C.-N.; Viazovkina, E.; Min, K.-L.; Nagy, E.; Wilds, C. J.; Damha, M. J.; Parniak, M. A. *Biochemistry* **2002**, *41*, 3457-3467.

285 Lacombe, J.; Viazovkina, E.; Bernatchez, P. N.; Galarneau, A.; Damha, M. J.; Sirois, M. G. *Can. J. Physiol. Pharmacol.* **2002**, *80*, 951-961.

286 Noronha, A. M. *Synthesis, physicochemical and biological studies on oligonucleotides containing D-arabinose*; PhD Thesis, McGill University, 1999.

287 The potential of 2'F-ANA as an AON, in the context of other sugar-modified AONs, has been reviewed in M.M. Mangos and M.J. Damha. *Curr. Top. Med. Chem.* **2002**, *2*, 1147.

288 Mangos, M. M.; Min, K.-L.; Viazovkina, E.; Galarneau, A.; Elzagheid, M. I.; Parniak, M. A.; Damha, M. J. *J. Am. Chem. Soc.* **2003**, *125*, 654-661.

289 Patureau, B. M.; Hudson, R. H. E.; Damha, M. J. *Bioconjugate Chem.* **2007**, *18*, 421-430.

290 Kalota, A.; Karabon, L.; Swider, C. R.; Viazovkina, E.; Elzagheid, M.; Damha, M. J.; Gewirtz, A. M. *Nucl. Acids Res.* **2006**, *34*, 451-461.

291 Ferrari, N., "TPI ASM8 and TPI 1100 – Multi-targeted antisense oligonucleotide approaches for the treatment of lung inflammatory diseases," Eurotides 2007, Berlin, Germany, 2007.

292 Wilds, C. J.; Damha, M. J. *Bioconjugate Chem.* **1999**, *10*, 299-305.

293 Ellington, A. D.; Szostak, J. W. *Nature* **1990**, *346*, 818-822.

294 Joyce, G. F. *Gene* **1989**, *82*, 83-87.

295 Tuerk, C.; Gold, L. *Science* **1990**, *249*, 505-510.

296 Ng, E. W. M.; Shima, D. T.; Calias, P.; Cunningham, E. T.; Guyer, D. R.; Adamis, A. P. *Nat. Rev. Drug Discov.* **2006**, *5*, 123-132.

297 Peng, C. G.; Damha, M. J. *Nucl. Acids Res.* **2007**, *35*, 4977-4988.

298 Gehring, K.; Leroy, J.-L.; Gueron, M. *Nature* **1993**, *363*, 561-565.

299 Robidoux, S.; Damha, M. J. *J. Biomol. Struct. Dyn.* **1997**, *15*, 529-535.

300 Peng, C. G.; Damha, M. J. *J. Am. Chem. Soc.* **2007**, *129*, 5310-5311.

301 Peng, C. G.; Damha, M. J. *Can. J. Chem.* **2008**, in press.

302 Viazovkina, E.; Min, K.-L.; Galarneau, A.; Damha, M. J. *Nucleosides Nucleotides Nucleic Acids* **2003**, *22*, 1335-1338.

303 Schultz, R. G.; Gryaznov, S. M. *Tetrahedron Lett.* **2000**, *41*, 1895-1899.

304 Elzagheid, M. I.; Tedeschi, A. L.; Damha, M. J. *Nucleosides Nucleotides Nucleic Acids* **2003**, *22*, 1343-1346.

305 Tedeschi, A.-L. *Synthesis and Biological Evaluation of Oligonucleotides Containing 3'- and 5'-S-Phosphorothiolate Internucleotide Linkages*; MSc, McGill University, 2004.

306 Monia, B. P.; Johnston, J. F.; Geiger, T.; Muller, M.; Fabbro, D. *Nat. Med.* **1996**, *2*, 668-675.

307 For reviews, see A.A. Levin. *Biochimica et Biophysica Acta (BBA) - Gene Structure and Expression* **1999**, *1489*, 69; and T.L.H. Jason, J. Koropatnick, and R.W. Berg. *Toxicol. Appl. Pharmacol.* **2004**, *201*, 66.

308 Tinoco, I. *J. Am. Chem. Soc.* **1960**, *82*, 4785-4790.

309 Marky, L. A.; Breslauer, K. J. *Biopolymers* **1987**, *26*, 1601-1620.

310 Martin, R. *Gel Electrophesis: Nucleic Acids*; Bios Scientific Publishers: Oxford, UK, 1996.

311 Crowther, J. B.; Hartwick, R. A. In *HPLC in Nucleic Acid Research*; Brown, P. R., Ed.; Marcel Dekker: New York, 1984, pp. 195-213.

312 Crain, P. F. In *Electrospray Ionization Mass Spectrometry*; Cole, R. B., Ed.; John Wiley & Sons: New York, 1997, pp. 421-457.

313 Limbach, P. A.; McCloskey, P. F. C. J. A. *Curr. Opin. Biotechnol.* **1995**, *6*, 96-102.

314 Johnson, W. C. In *Circular Dichroism: Principles and Applications*; Nakanishi, K., Berova, N., Woody, R. W., Eds.; VCH: New York, 1994, pp. 523-540.

315 Evans, J. N. S. In *Biomolecular NMR Spectroscopy*; Oxford University Press: Oxford, 1995, pp. 343-391.

316 Karplus, M. *J. Am. Chem. Soc.* **1963**, *85*, 2870-2871.

317 Bhattacharya, P. K.; Cha, J.; Barton, J. K. *Nucl. Acids Res.* **2002**, *30*, 4740-4750.

318 *Computational Studies of RNA and DNA*; Sponer, J.; Lankas, F., Eds.; Springer: Dordrecht, 2006; Vol. 2.

319 Cheatham III, T. E.; Case, D. A. In *Computational Studies of RNA and DNA*; Sponer, J., Lankas, F., Eds.; Springer: Dordrecht, 2006, pp. 45-71.

320 Pearlman, D. A.; Case, D. A.; Caldwell, J. W.; Ross, W. S.; Cheatham III, T. E.; DeBolt, S.; Ferguson, D.; Seibel, G.; Kollman, P. *Comput. Phys. Commun.* **1995**, *91*, 1-41.

321 MacKerell Jr., A. D.; Nilsson, L. In *Computational Studies of RNA and DNA*; Sponer, J., Lankas, F., Eds.; Springer: Dordrecht, 2006, pp. 73-94.

322 Brooks, B. R.; Bruccoleri, R. E.; Olafson, B. D.; States, D. J.; Swaminathan, S.; Karplus, M. *J. Comput. Chem.* **1983**, *4*, 187-217.

323 Cheatham, T. E.; Kollman, P. A. *Annu. Rev. Phys. Chem.* **2000**, *51*, 435-471.

324 Parsegian, V. A.; Rand, R. P.; Rau, D. C. *Methods Enzymol.* **1995**, *259*, 43-94.

325 Spink, C. H.; Chaires, J. B. *Biochemistry* **1999**, *38*, 496-508.

326 Rozners, E.; Moulder, J. *Nucl. Acids Res.* **2004**, *32*, 248-254.

327 Spink, C. H.; Garbett, N.; Chaires, J. B. *Biophys. Chem.* **2007**, *126*, 176-185.

328 Trempe, J.-F.; Wilds, C. J.; Denisov, A. Y.; Pon, R. T.; Damha, M. J.; Gehring, K. *J. Am. Chem. Soc.* **2001**, *123*, 4896-4903.

329 Denisov, A. Y.; Noronha, A. M.; Wilds, C. J.; Trempe, J.-F.; Pon, R. T.; Gehring, K.; Damha, M. J. *Nucl. Acids Res.* **2001**, *29*, 4284-4293.

330 Marquez, V. E.; Tseng, C. K. H.; Kelley, J. A.; Mitsuya, H.; Broder, S.; Roth, J. S.; Driscoll, J. S. *Biochem. Pharmacol.* **1987**, *36*, 2719-2722.

331 Martin, F. H.; Tinoco, I., Jr. *Nucl. Acids Res.* **1980**, *8*, 2295-2300.

332 Venkateswarlu, D.; Ferguson, D. M. *J. Am. Chem. Soc.* **1999**, *121*, 5609-5610.

333 Minasov, G.; Teplova, M.; Nielsen, P.; Wengel, J.; Egli, M. *Biochemistry* **2000**, *39*, 3525-3532.

334 Christensen, N. K.; Petersen, M.; Nielsen, P.; Jacobsen, J. P.; Olsen, C. E.; Wengel, J. *J. Am. Chem. Soc.* **1998**, *120*, 5458-5463.

335 Noy, A.; Luque, F. J.; Orozco, M. *J. Am. Chem. Soc.* **2008**, *130*, 3486-3496.

336 Li, F.; Sarkhel, S.; Wilds, C. J.; Wawrzak, Z.; Prakash, T. P.; Manoharan, M.; Egli, M. *Biochemistry* **2006**, *45*, 4141-4152.

337 Gonzalez, C.; Stec, W.; Kobylanska, A.; Hogrefe, R. I.; Reynolds, M.; James, T. L. *Biochemistry* **1994**, *33*, 11062-11072.

338 Gonzalez, C.; Stec, W.; Reynolds, M. A.; James, T. L. *Biochemistry* **1995**, *34*, 4969-4982.

339 Auffinger, P.; Westhof, E. *J. Mol. Biol.* **2001**, *305*, 1057-1072.

340 Auffinger, P.; Westhof, E. *Angew. Chem. Int. Ed.* **2001**, *40*, 4648-4650.

341 Kaur, H.; Arora, A.; Wengel, J.; Maiti, S. *Biochemistry* **2006**, *45*, 7347-7355.

342 Cupane, A.; Vitrano, E.; Sanbiago, P. L.; Madonia, F.; Palma, M. U. *Nucl. Acids Res.* **1980**, *8*, 4283-4303.

343 *CRC Handbook of Chemistry and Physics*; Lide, D. R., Ed.; CRC Press: Boca Raton, RL, 1996.

344 Glasoe, P. K.; Long, F. A. *J. Phys. Chem.* **1960**, *64*, 188-190.

345 Von Hippel, P. H.; Wong, K.-Y. *Science* **1964**, *145*, 577-80.

346 Hatefi, Y.; Hanstein, W. G. *Proc. Natl. Acad. Sci. USA* **1969**, *62*, 1129-1136.

347 von Hippel, P. H.; Wong, K.-Y. *Biochemistry* **1962**, *1*, 664-674.

348 von Hippel, P. H.; Wong, K.-Y. *Biochemistry* **1963**, *2*, 1387-1398.

349 Hamaguchi, K.; Geiduschek, E. P. *J. Am. Chem. Soc.* **1962**, *84*, 1329-1338.

350 Ninham, B. W. In *Smart Colloidal Materials*; Springer: Berlin, 2006.

351 Courtenay, E. S.; Capp, M. W.; Anderson, C. F.; Record, M. T. *Biochemistry* **2000**, *39*, 4455-4471.

352 Erdmann, R. M.; Pegram, L. M.; Record, M. T., "Salt effects on DNA melting," Abstracts of Papers, 235th ACS National Meeting, New Orleans, USA, April 6-10, 2008.

353 Liepinsh, E.; Otting, G.; Wuthrich, K. *Nucl. Acids Res.* **1992**, *20*, 6549-6553.

354 Liepinsh, E.; Leupin, W.; Otting, G. *Nucl. Acids Res.* **1994**, *22*, 2249-2254.

355 Johannesson, H.; Halle, B. *J. Am. Chem. Soc.* **1998**, *120*, 6859-6870.

356 Shui, X.; McFail-Isom, L.; Hu, G. G.; Williams, L. D. *Biochemistry* **1998**, *37*, 8341-8355.

357 Shui, X.; Sines, C. C.; McFail-Isom, L.; VanDerveer, D.; Williams, L. D. *Biochemistry* **1998**, *37*, 16877-16887.

358 McFail-Isom, L.; Sines, C. C.; Williams, L. D. *Curr. Opin. Struct. Biol.* **1999**, *9*, 298-304.

359 Tereshko, V.; Minasov, G.; Egli, M. *J. Am. Chem. Soc.* **1999**, *121*, 3590-3595.

360 Zoltewicz, J. A.; Clark, D. F.; Sharpless, T. W.; Grahe, G. *J. Am. Chem. Soc.* **1970**, *92*, 1741-1750.

361 Holmquist, G. *Chromosoma* **1979**, *72*, 203-224.

362 Pogocki, D.; Schöneich, C. *J. Pharm. Sci.* **2000**, *89*, 443-456.

363 Garrett, E. R.; Mehta, P. J. *J. Am. Chem. Soc.* **1972**, *94*, 8532-8541.

364 York, J. L. *J. Org. Chem.* **1981**, *46*, 2171-2173.

365 Schultz, R.; Gryaznov, S. *Nucl. Acids Res.* **1996**, *24*, 2966-2973.

366 Oivanen, M.; Kuusela, S.; Lonnberg, H. *Chem. Rev.* **1998**, *98*, 961-990.

367 Based on the United States Pharmacopeia recipe for simulated gastric fluid (USP 24-NF 19, 2000) but containing no pepsin: 0.20 g NaCl was dissolved in 99 mL water and autoclaved, then 0.70 mL HCl was added (pH ~1.2).

368 Oivanen, M.; Ora, M.; Almer, H.; Stromberg, R.; Lonnberg, H. *J. Org. Chem.* **1995**, *60*, 5620-7.

369 Ora, M.; Oivanen, M.; Lonnberg, H. *J. Org. Chem.* **1997**, *62*, 3246-3253.

370 Liu, X.; Reese, C. B. *Tetrahedron Lett.* **1995**, *36*, 3413-3416.

371 Kuimelis, R. G.; McLaughlin, L. W. *Nucl. Acids Res.* **1995**, *23*, 4753-4760.

372 Reviewed in Akhtar, S.; Hughes, M. D.; Khan, A.; Bibby, M.; Hussain, M.; Nawaz, Q.; Double, J.; Sayyed, P. *Adv. Drug Deliver. Rev.* **2000**, *44*, 3-21.

373 Mellman, I.; Fuchs, R.; Helenius, A. *Annu. Rev. Biochem.* **1986**, *55*, 663-700.

374 Schmid, S. L.; Fuchs, R.; Male, P.; Mellman, I. *Cell* **1988**, *52*, 73-83.

375 Tolstrup, N.; Nielsen, P. S.; Kolberg, J. G.; Frankel, A. M.; Vissing, H.; Kauppinen, S. *Nucl. Acids Res.* **2003**, *31*, 3758-3762.

376 Castoldi, M.; Schmidt, S.; Benes, V.; Noerholm, M.; Kulozik, A. E.; Hentze, M. W.; Muckenthaler, M. U. *RNA* **2006**, *12*, 913-920.

377 Calin, G. A.; Croce, C. M. *Cancer Res.* **2006**, *66*, 7390-7394.

378 Eckstein, F. *Antisense Nucleic Acid Drug Dev.* **2000**, *10*, 117-121.

379 Burgers, P. M. J.; Eckstein, F. *Biochemistry* **1979**, *18*, 592-596.

380 Burgers, P. M.; Eckstein, F.; Hunneman, D. H. *J. Biol. Chem.* **1979**, *254*, 7476-7478.

381 Damha, M. J.; Giannaris, P. A.; Marfey, P. *Biochemistry* **1994**, *33*, 7877-7885, and references therein.

382 Birks, J. B. In *Photophysics of Aromatic Molecules*; Wiley-Interscience: London, 1970, pp. 403-491.

383 Birks, J. B. *Rep. Prog. Phys.* **1975**, *38*, 903-974.

384 Paris, P. L.; Langenhan, J. M.; Kool, E. T. *Nucl. Acids Res.* **1998**, *26*, 3789-3793.

385 Bichenkova, E. V.; Savage, H. E.; Sardarian, A. R.; Douglas, K. T. *Biochem. Biophys. Res. Commun.* **2005**, *332*, 956-964.

386 Masuko, M.; Ohtani, H.; Ebata, K.; Shimadzu, A. *Nucl. Acids Res.* **1998**, *26*, 5409-5416.

387 Bichenkova, E. V.; Sardarian, A. R.; Wilton, A. N.; Bonnet, P.; Bryce, R. A.; Douglas, K. T. *Org. Biomol. Chem.* **2006**, *4*, 367-378.

388 Bichenkova, E. V.; Marks, D.; Dobrikov, M. I.; Vlassov, V. V.; Morris, G. A.; Douglas, K. T. *J. Biomol. Struct. Dyn.* **1999**, *17*, 193-211.

389 Vorlíckova, M.; Minyat, E. E.; Kypr, J. *Biopolymers* **1984**, *23*, 1-4.

390 Brahms, J.; Mommaerts, W. F. H. *J. Mol. Biol.* **1964**, *10*, 73-88.

391 Zimmerman, S. B.; Pheiffer, B. H. *J. Mol. Biol.* **1979**, *135*, 1023-1027.

392 Vorlickova, M. *Biophys. J.* **1995**, *69*, 2033-2043.

393 Ivanov, V. I.; Minyat, E. E. *Nucl. Acids Res.* **1981**, *9*, 4783-4798.

394 Krylov, D. Y.; Makarov, V. L.; lvanov, V. l. *Nucl. Acids Res.* **1990**, *18*, 759-761.

395 Kypr, J.; Chladkova, J.; Zimulova, M.; Vorlickova, M. *Nucl. Acids Res.* **1999**, *27*, 3466-3473.

396 Vorlickova, M.; Khudyakov, I. Y.; Hejtmankova, I.; Kypr, J. *J. Biomol. Struct. Dyn.* **1991**, *9*, 81-85.

397 Geacintov, N. E.; Prusik, T.; Khosrofian, J. M. *J. Am. Chem. Soc.* **1976**, *98*, 6444-6452.

398 Petersen, M.; Nielsen, C. B.; Nielsen, K. E.; Jensen, G. A.; Bondensgaard, K.; Singh, S. K.; Rajwanshi, V. K.; Koshkin, A. A.; Dahl, B. M.; Wengel, J.; Jacobsen, J. P. *J. Mol. Recognit.* **2000**, *13*, 44-53.

399 Marquez, V. E.; Siddiqui, M. A.; Ezzitouni, A.; Russ, P.; Wang, J.; Wagner, R. W.; Matteucci, M. D. *J. Med. Chem.* **1996**, *39*, 3739-3747.

400 Damha, M. J.; Wilds, C. J.; Noronha, A.; Brukner, I.; Borkow, G.; Arion, D.; Parniak, M. A. *J. Am. Chem. Soc.* **1998**, *120*, 12976-12977.

401 Wilds, C. J.; Damha, M. J. *Nucleic Acids Res.* **2000**, *28*, 3625-3635.

402 Yoshimura, Y.; Kitano, K.; Yamada, K.; Satoh, H.; Watanabe, M.; Miura, S.; Sakata, S.; Sasaki, T.; Matsuda, A. *J. Org. Chem.* **1997**, *62*, 3140-3152.

403 Yoshimura, Y.; Endo, M.; Miura, S.; Sakata, S. *J. Org. Chem.* **1999**, *64*, 7912-7920.

404 Yoshimura, Y.; Endo, M.; Sakata, S. *Tetrahedron Lett.* **1999**, *40*, 1937-1940.

405 Yoshimura, Y.; Kitano, K.; Yamada, K.; Sakata, S.; Miura, S.; Ashida, N.; Machida, H. *Bioorg. Med. Chem.* **2000**, *8*, 1545-1558.

406 Sapse, A. M.; Snyder, G. *Cancer Invest.* **1985**, *3*, 115-21.

407 Hicks, N.; Howarth, O. W.; Hutchinson, D. W. *Carbohydr. Res.* **1991**, *216*, 1-9.

408 PSEUROT 6.3; van Wijk, J.; Haasnoot, C. A. G.; de Leeuw, F. A. A. M.; Huckriede, B. D.; Hoekzema, A. W.; Altona, C.; Leiden Institute of Chemistry, Leiden University: Leiden, The Netherlands, 1999.

409 He, J.; Mikhailopulo, I. A.; Seela, F. *J. Org. Chem.* **2003**, *68*, 5519-5524.

410 Sivets, G. G.; Kalinichenko, E. N.; Mikhailopulo, I. A. *Lett Org Chem* **2006**, *3*, 402-408.

411 Ford, H.; Dai, F.; Mu, L.; Siddiqui, M. A.; Nicklaus, M. C.; Anderson, L.; Marquez, V. E.; Barchi, J. J. *Biochemistry* **2000**, *39*, 2581-2592.

412 Peng, X.; Seela, F. *Org. Biomol. Chem.* **2004**, *2*, 2838-2846.

413 Seela, F.; Chittepu, P.; He, J.; Eickmeier, H. *Acta Crystallogr., Sect. C* **2004**, *c60*, o884-o886.

414 Satoh, H.; Yoshimura, Y.; Sakata, S.; Miura, S.; Machida, H.; Matsuda, A. *Bioorg. Med. Chem. Lett.* **1998**, *8*, 989-992.

415 Yuasa, H.; Kajimoto, T.; Wong, C. H. *Tetrahedron Lett.* **1994**, *35*, 8243-8246.

416 Naka, T.; Minakawa, N.; Abe, H.; Kaga, D.; Matsuda, A. *J. Am. Chem. Soc.* **2000**, *122*, 7233-7243.

417 Yuasa, H.; Tamura, J.; Hashimoto, H. *J. Chem. Soc., Perkin Trans. 1* **1990**, 2763-2769.

418 Jeong, L. S.; Nicklaus, M. C.; George, C.; Marquez, V. E. *Tetrahedron Lett.* **1994**, *35*, 7569-7572.

419 Young, Robert J.; Shaw-Ponter, S.; Hardy, G. W.; Mills, G. *Tetrahedron Lett.* **1994**, *35*, 8687-8690.

420 Shaw-Ponter, S.; Mills, G.; Robertson, M.; Bostwick, R. D.; Hardy, G. W.; Young, R. J. *Tetrahedron Lett.* **1996**, *37*, 1867-70.

421 Wang, Y.; Inguaggiato, G.; Jasamai, M.; Shah, M.; Hughes, D.; Slater, M.; Simons, C. *Bioorg. Med. Chem.* **1999**, *7*, 481-487.

422 Inguaggiato, G.; Jasamai, M.; Smith, J. E.; Slater, M.; Simons, C. *Nucleosides Nucleotides* **1999**, *18*, 457-467.

423 Lide, D. R., ed. *CRC Handbook of Chemistry and Physics*; 71st ed.; CRC Press: Boca Raton, 1990.

424 Trempe, J. F.; Wilds, C. J.; Denisov, A. Y.; Pon, R. T.; Damha, M. J.; Gehring, K. *J. Am. Chem. Soc.* **2001**, *123*, 4896-4903.

425 Chong, Y.; Chu, C. K. *Bioorg. Med. Chem. Lett.* **2002**, *12*, 3459-62.

426 Becke, A. D. *J. Chem. Phys.* **1986**, *84*, 4524-4529.

427 de Leeuw, F. A. A. M.; Vankampen, P. N.; Altona, C.; Diez, E.; Esteban, A. L. *J. Mol. Struct.* **1984**, *125*, 67-88.

428 Diez, E.; Esteban, A. L.; Bermejo, F. J.; Altona, C.; de Leeuw, F. A. A. M. *J. Mol. Struct.* **1984**, *125*, 49-65.

429 Diez, E.; Esteban, A. L.; Guilleme, J.; Bermejo, F. L. *J. Mol. Struct.* **1981**, *70*, 61-64.

430 Koole, L. H.; Plavec, J.; Liu, H. Y.; Vincent, B. R.; Dyson, M. R.; Coe, P. L.; Walker, R. T.; Hardy, G. W.; Rahim, S. G.; Chattopadhyaya, J. *J. Am. Chem. Soc.* **1992**, *114*, 9936-9943.

431 FOURDIEZ is a part of the PSEUROT 6.3 suite of programs.

432 Thibaudeau, C.; Plavec, J.; Chattopadhyaya, J. *J. Org. Chem.* **1998**, *63*, 4967-4984.

433 Thibaudeau, C.; Chattopadhyaya, J. *Stereoelectronic Effects in Nucleosides and Nucleotides and their Structural Implications*; PhD, Uppsala University, 1999.

434 The DFT calculations undertaken for the parametrization of PSEUROT confirmed that the replacement of O4' by S causes the value of ϕ_{max} to increase by 10-15º.

435 Pinto, B. M.; Leung, R. Y. N. In *The Anomeric Effect and Associated Stereoelectronic Effects*; Thatcher, G. R. J., Ed.; American Chemical Society: Washington, DC, 1993, pp. 126-155.

436 Wolfe, S.; Pinto, B. M.; Varma, V.; Leung, R. Y. N. *Can. J. Chem.* **1990**, *68*, 1051-1062.

437 Schleyer, P. V.; Jemmis, E. D.; Spitznagel, G. W. *J. Am. Chem. Soc.* **1985**, *107*, 6393-6394.

438 Wirsching, J.; Voss, J.; Adiwidjaja, G.; Balzarini, J.; De Clercq, E. D. *Bioorg. Med. Chem. Lett.* **2001**, *11*, 1049-1051.

439 Watts, J. K.; Sadalapure, K.; Choubdar, N.; Pinto, B. M.; Damha, M. J. *J. Org. Chem.* **2006**, *71*, 921-925.

440 Houseknecht, J. B.; Altona, C.; Hadad, C. M.; Lowary, T. L. *J. Org. Chem.* **2002**, *67*, 4647-4651.

441 Gaussian 03W, Revision C.02; Frisch, M. J.; Trucks, G. W.; Schlegel, H. B.; Scuseria, G. E.; Robb, M. A.; Cheeseman, J. R.; Montgomery, J., J. A.; Vreven, T.; Kudin, K. N.; Burant, J. C.; Millam, J. M.; Iyengar, S. S.; Tomasi, J.; Barone, V.; Mennucci, B.; Cossi, M.; Scalmani, G.; Rega, N.; Petersson, G. A.; Nakatsuji, H.; Hada, M.; Ehara, M.; Toyota, K.; Fukuda, R.; Hasegawa, J.; Ishida, M.; Nakajima, T.; Honda, Y.; Kitao, O.; Nakai, H.; Klene, M.; Li, X.; Knox, J. E.; Hratchian, H. P.; Cross, J. B.; Bakken, V.; Adamo, C.; Jaramillo, J.; Gomperts, R.; Stratmann, R. E.; Yazyev, O.; Austin, A. J.; Cammi, R.; Pomelli, C.; Ochterski, J. W.; Ayala, P. Y.; Morokuma, K.; Voth, G. A.; Salvador, P.; Dannenberg, J. J.; Zakrzewski, V. G.; Dapprich, S.; Daniels, A. D.; Strain, M. C.; Farkas, O.; Malick, D. K.; Rabuck, A. D.; Raghavachari, K.; Foresman, J. B.; Ortiz, J. V.; Cui, Q.; Baboul, A. G.; Clifford, S.; Cioslowski, J.; Stefanov, B. B.; Liu, G.; Liashenko, A.; Piskorz, P.; Komaromi, I.; Martin, R. L.; Fox, D. J.; Keith, T.; Al-Laham, M. A.; Peng, C. Y.; Nanayakkara, A.; Challacombe, M.; Gill, P. M. W.; Johnson, B.; Chen, W.; Wong, M. W.; Gonzalez, C.; Pople, J. A.; Gaussian, Inc.: Wallingford, CT, 2004.

442 Altona, C.; Francke, R.; Dehaan, R.; Ippel, J. H.; Daalmans, G. J.; Hoekzema, A.; Vanwijk, J. *Magn. Reson. Chem.* **1994**, *32*, 670-678.

443 Altona, C.; Ippel, J. H.; Hoekzema, A.; Erkelens, C.; Groesbeek, M.; Donders, L. A. *Magn. Reson. Chem.* **1989**, *27*, 564-576.

444 Mikhailopulo, I. A.; Pricota, T. I.; Sivets, G. G.; Altona, C. *J. Org. Chem.* **2003**, *68*, 5897-5908.

445 Braasch, D. A.; Corey, D. R. *Biochemistry* **2002**, *41*, 4503-4510.

446 Opalinska, J. B.; Gewirtz, A. M. *Nat. Rev. Drug Discov.* **2002**, *1*, 503-514.

447 Dorsett, Y.; Tuschl, T. *Nat. Rev. Drug Discov.* **2004**, *3*, 318-329.

448 Stein, C. A.; Cheng, Y. C. *Science* **1993**, *261*, 1004-1012.

449 Verbeure, B.; Lescrinier, E.; Wang, J.; Herdewijn, P. *Nucl. Acids Res.* **2001**, *29*, 4941-4947.

450 Wahlestedt, C.; Salmi, P.; Good, L.; Kela, J.; Johnsson, T.; Hokfelt, T.; Broberger, C.; Porreca, F.; Lai, J.; Ren, K.; Ossipov, M.; Koshkin, A.; Jakobsen, N.; Skouv, J.; Oerum, H.; Jacobsen, M. H.; Wengel, J. *Proc. Natl. Acad. Sci. U. S. A.* **2000**, *97*, 5633-5638.

451 Fedoroff, O. Y.; Salazar, M.; Reid, B. R. *J. Mol. Biol.* **1993**, *233*, 509-523.

452 Salazar, M.; Fedoroff, O. Y.; Miller, J. M.; Ribeiro, N. S.; Reid, B. R. *Biochemistry* **1993**, *32*, 4207-4215.

453 Bellon, L.; Barascut, J. L.; Maury, G.; Divita, G.; Goody, R.; Imbach, J. L. *Nucl. Acids Res.* **1993**, *21*, 1587-1593.

454 Leydier, C.; Bellon, L.; Barascut, J. L.; Morvan, F.; Rayner, B.; Imbach, J. L. *Antisense Res. Dev.* **1995**, *5*, 167-174.

455 Jones, G. D.; Lesnik, E. A.; Owens, S. R.; Risen, L. M.; Walker, R. T. *Nucl. Acids Res.* **1996**, *24*, 4117-4122.

456 Hoshika, S.; Minakawa, N.; Matsuda, A. *Nucl. Acids Res.* **2004**, *32*, 3815-3825.

457 Inoue, N.; Minakawa, N.; Matsuda, A. *Nucl. Acids Res.* **2006**, *34*, 3476-3483.

458 Yoshimura, Y.; Endo, M.; Miura, S.; Sakata, S. *J. Org. Chem.* **1999**, *64*, 7912-7920.

459 Baker, B. F.; Lot, S. S.; Condon, T. P.; Cheng-Flournoy, S.; Lesnik, E. A.; Sasmor, H. M.; Bennett, C. F. *J. Biol. Chem.* **1997**, *272*, 11994-12000.

460 Freier, S. M.; Altmann, K.-H. *Nucl. Acids Res.* **1997**, *25*, 4429-4443.

461 Nishizaki, T.; Iwai, S.; Ohtsuka, E.; Nakamura, H. *Biochemistry* **1997**, *36*, 2577-2585.

462 Ratmeyer, L.; Vinayak, R.; Zhong, Y. Y.; Zon, G.; Wilson, W. D. *Biochemistry* **1994**, *33*, 5298-5304.

463 Rose, S. D.; Kim, D.-H.; Amarzguioui, M.; Heidel, J. D.; Collingwood, M. A.; Davis, M. E.; Rossi, J. J.; Behlke, M. A. *Nucl. Acids Res.* **2005**, *33*, 4140-4156.

464 Schwarz, D. S.; Hutvagner, G.; Du, T.; Xu, Z.; Aronin, N.; Zamore, P. D. *Cell* **2003**, *115*, 199-208.

465 Khvorova, A.; Reynolds, A.; Jayasena, S. D. *Cell* **2003**, *115*, 209-216.

466 Hohjoh, H. *FEBS Lett.* **2004**, *557*, 193-198.

467 This lower cost is because of a facile synthetic route through the 2,2'-anhydronucleoside in the case of pyrimidine nucleosides, which can be ring-opened by nucleophilic fluoride ions to yield 2'-fluoro-RNA.

468 Wu, H.; Lima, W. F.; Crooke, S. T. *J. Biol. Chem.* **1999**, *274*, 28270-28278.

469 Novac, O.; Guenier, A.-S.; Pelletier, J. *Nucl. Acids Res.* **2004**, *32*, 902-915.

470 Pillai, R. S.; Bhattacharyya, S. N.; Artus, C. G.; Zoller, T.; Cougot, N.; Basyuk, E.; Bertrand, E.; Filipowicz, W. *Science* **2005**, *309*, 1573-1576.

471 Inoue, N.; Shionoya, A.; Minakawa, N.; Kawakami, A.; Ogawa, N.; Matsuda, A. *J. Am. Chem. Soc.* **2007**, *129*, 15424-15425.

472 Nemer, M. J.; Ogilvie, K. K. *Tetrahedron Lett.* **1980**, *21*, 4149-4152.

473 Wilds, C. J.; Pattanayek, R.; Pan, C.; Wawrzak, Z.; Egli, M. *J. Am. Chem. Soc.* **2002**, *124*, 14910-14916.

474 Carrasco, N.; Huang, Z. *J. Am. Chem. Soc.* **2004**, *126*, 448-449.

475 Carrasco, N.; Caton-Williams, J.; Brandt, G.; Wang, S.; Huang, Z. *Angew. Chem. Int. Ed.* **2006**, *45*, 94-97.

476 Tram, K.; Wang, X.; Yan, H. *Org. Lett.* **2007**, *9*, 5103-5106.

477 Carrasco, N.; Ginsburg, D.; Du, Q.; Huang, Z. *Nucleosides Nucleotides Nucleic Acids* **2001**, *20*, 1723 - 1734.

478 Brandt, G.; Carrasco, N.; Huang, Z. *Biochemistry* **2006**, *45*, 8972-8977.

479 Du, Q.; Carrasco, N.; Teplova, M.; Wilds, C. J.; Egli, M.; Huang, Z. *J. Am. Chem. Soc.* **2002**, *124*, 24-25.

480 Teplova, M.; Wilds, C. J.; Wawrzak, Z.; Tereshko, V.; Du, Q.; Carrasco, N.; Huang, Z.; Egli, M. *Biochimie* **2002**, *84*, 849-858.

481 Buzin, Y.; Carrasco, N.; Huang, Z. *Org. Lett.* **2004**, *6*, 1099-1102.

482 Carrasco, N.; Buzin, Y.; Tyson, E.; Halpert, E.; Huang, Z. *Nucl. Acids Res.* **2004**, *32*, 1638-1646.

483 Hobartner, C.; Micura, R. *J. Am. Chem. Soc.* **2004**, *126*, 1141-1149.

484 Hobartner, C.; Rieder, R.; Kreutz, C.; Puffer, B.; Lang, K.; Polonskaia, A.; Serganov, A.; Micura, R. *J. Am. Chem. Soc.* **2005**, *127*, 12035-12045.

485 Moroder, H.; Kreutz, C.; Lang, K.; Serganov, A.; Micura, R. *J. Am. Chem. Soc.* **2006**, *128*, 9909-9918.

486 Sheng, J.; Jiang, J.; Salon, J.; Huang, Z. *Org. Lett.* **2007**, *9*, 749-752.

487 Salon, J.; Sheng, J.; Jiang, J.; Chen, G.; Caton-Williams, J.; Huang, Z. *J. Am. Chem. Soc.* **2007**, *129*, 4862-4863.

488 Serganov, A.; Keiper, S.; Malinina, L.; Tereshko, V.; Skripkin, E.; Höbartner, C.; Polonskaia, A.; Phan, A. T.; Wombacher, R.; Micura, R.; Dauter, Z.; Jäschke, A.; Patel, D. J. *Nat. Struct. Mol. Biol.* **2005**, *12*, 218-224.

489 Egli, M.; Pallan, P. S.; Pattanayek, R.; Wilds, C. J.; Lubini, P.; Minasov, G.; Dobler, M.; Leumann, C. J.; Eschenmoser, A. *J. Am. Chem. Soc.* **2006**, *128*, 10847-10856.

490 Ennifar, E.; Carpentier, P.; Ferrer, J. L.; Walter, P.; Dumas, P. *Acta Crystallogr D* **2002**, *58*, 1262-1268.

491 Jayakanthan, K.; Johnston, B. D.; Pinto, B. M. *Carbohydr. Res.* **2008**, in press; doi: 10.1016/j.carres.2008.02.014

492 Inagaki, Y.; Minakawa, N.; Matsuda, A. *Nucl. Acids Symp. Ser.* **2007**, *51*, 139-140.

493 Jeong, L. S.; Tosh, D. K.; Kim, H. O.; Wang, T.; Hou, X.; Yun, H. S.; Kwon, Y.; Lee, S. K.; Choi, J.; Zhao, L. X. *Org. Lett.* **2007**, *10*, 209-212.

494 Ogilvie, K. K.; Sadana, K. L.; Thompson, E. A.; Quilliam, M. A.; Westmore, J. B. *Tetrahedron Lett.* **1974**, *15*, 2861-2863.

495 Lubini, P.; Zürcher, W.; Egli, M. *Chem. Biol.* **1994**, *1*, 39-45.

496 Krotz, A. H.; Klopchin, P. G.; Walker, K. L.; Srivatsa, G. S.; Cole, D. L.; Ravikumar, V. T. *Tetrahedron Lett.* **1997**, *38*, 3875-3878.

497 Sambrook, J.; Fritsch, E. F.; Maniatis, T. *Molecular Cloning: A Laboratory Manual*; Cold Spring Harbor Laboratory Press: Plainview, NY, 1989.

Appendix: Research compliance certificates

This thesis has presented research involving both radioactivity and living cells.

All work with living cells was carried out by our collaborators, so no certificate is attached (it is available from our collaborators if desired.)

As for radiation safety, a certificate confirming my training is provided on the following page.